Trinity College Dublin
Coláiste na Tríonóide, Baile Átha Cliath
The University of Dublin

The development of brain markers for conscious awareness in infancy

Huiqing Hu

School of Psychology and Trinity College Institute of Neuroscience

Trinity College Dublin, University of Dublin

A thesis submitted to

Trinity College Dublin, University of Dublin

For the degree of

Doctor of Philosophy

2024

Declaration

I declare that this thesis has not been submitted as an exercise for a degree at this or any other university and it is entirely my own work.

I agree to deposit this thesis in the University's open access institutional repository or allow the Library to do so on my behalf, subject to Irish Copyright Legislation and Trinity College Library conditions of use and acknowledgement.

I consent to the examiner retaining a copy of the thesis beyond the examining period, should they so wish (EU GDPR May 2018).

Signed: 

Date: 25/04/2024

Summary

One of the great frontiers of consciousness science is understanding how early consciousness arises in the development of the human infant. Although each of us was once a baby, infant consciousness remains mysterious, not least because of uncertainty regarding how best to measure consciousness. Accounts of the ontogeny of consciousness can be divided into two broad camps: 'early-onset' views, which locate the emergence of consciousness at, or shortly after, birth, and 'late-onset' views, which locate the emergence of consciousness significantly after birth. The lack of language and the very limited motor function preclude self-report or behavioural responses and, thus, prevent the empirical assessment of consciousness in neonates at birth. We sidestepped these limitations by asking a foundational question for understanding the capacity for conscious experience in neonates: Are the brain mechanisms of consciousness instantiated in infants from birth? To answer this question, I investigated brain markers that have been developed to test the presence of conscious awareness in behaviourally non-responsive adult populations in full-term neonates (gestational age at birth > 37 weeks) at birth. Additionally, I investigated the effects of premature birth and early neonate age on the development of these brain markers. I used resting-state functional MRI data of full-term neonates (N = 278) from the developing Human Connectome Project and of adults (N = 176) from the Human Connectome Project. The effect of neonate age at the time of assessment was disentangled from the effect of premature birth by the inclusion of two groups: the first (N = 70) born before, but scanned at term-equivalent age (TEA), and the second (N = 70) born and scanned before TEA.

In Chapter 2, I investigated whether the reciprocal relationship between the default mode (DMN) and fronto-parietal networks (the dorsal attention and executive control

networks)—a neural circuitry that enables information integration across diverse sensory and high-order functional modules in healthy adults— has emerged in neonates at birth. Additionally, I tested how premature birth and early neonate age affected its development. Results showed that the reciprocal relationship between the DMN and dorsal attention network (DAN) was present in neonates at full-term birth or TEA. Although different from the adult networks, the DMN, DAN, and executive control network (ECN) were present as distinct networks at full-term birth or TEA. However, premature birth was associated with lower network coherence in DMN and DAN in neonates at TEA. Before TEA, neonates showed dramatic underdevelopment of these high-order networks and their relationships.

In Chapter 3, I investigated the development of the brain's functional small-world architecture, which has been shown to enable efficient information differentiation and integration at local and global brain scales in healthy adults. The global scale network efficiency was measured using small-world propensity, and nodal scale communication efficiency was measured using nodal efficiency. Although less pronounced than that in adults, small-world architecture was already present in neonates at full-term birth or TEA. By contrast, premature neonates before TEA showed underdevelopment of small-world architecture and regional communication in 9/11 networks (including DMN, DAN, and ECN), with disruption in 32% of brain nodes. By TEA, premature neonates showed large-scale recuperation of regional communication, with only 1.4% of nodes remaining significantly underdeveloped.

In Chapter 4, I investigated the development of neural entropy, which the uncertainty and informational richness of conscious states. Neural entropy decreases when consciousness fades, i.e., during sleep or general anaesthesia, as well as in the minimally conscious state or the unresponsive wakefulness syndrome. By contrast, neural entropy was found to increase in altered states of consciousness, such as during hallucinatory or the

psychological state elicited by classic psychedelic drugs (i.e., LSD and psilocybin). Neural entropy was measured by the sample entropy of network configuration, by using graph theoretical analysis combined with a sliding-window approach. I found that neonates exhibited higher neural entropy relative to adults. In addition, premature birth was associated with higher neural entropy in neonates at TEA. Lastly, I found neural entropy decreases with increasing age in preterm neonates from birth to TEA.

Taken together, these findings shed light on the ontogeny of brain markers that support conscious awareness and provide evidence for 'early-onset' views of conscious awareness. Furthermore, they highlight the importance of the third trimester of pregnancy, the typical period of premature birth, for the development of the brain markers that support conscious awareness.

List of Publications and Presentations

This thesis incorporates material already published or currently under review in the following manuscripts:

Hu, H., Cusack, R., & Naci, L. (2022). Typical and disrupted brain circuitry for conscious awareness in full-term and preterm infants. *Brain communications*, 4(2), fcac071. https://academic.oup.com/braincomms/article/4/2/fcac071/6553686

Hu, H., Coppola, P., Stamatakis, E. A., & Naci, L. (2023). Typical and disrupted small-world architecture and regional communication in full-term and preterm infants. *bioRxiv*, 2023-06. https://doi.org/10.1101/2023.06.12.544595

The following are presentations arising from this work:

Hu, H., Coppola, P., Stamatakis, E., Naci, L., Typical and disrupted neural entropy in human neonates, Poster presentation at *Lifespan MRI Meeting, The Royal Irish Academy, Dublin, Ireland, October 2023*

Hu, H., Coppola, P., Stamatakis, E., Naci, L., Typical and disrupted brain mechanism for conscious awareness in full-term and preterm infants, Oral presentation at *the 26th annual meeting of the Association for the Scientific Study of Consciousness, New York, USA, June 2023*

Hu, H., Coppola, P., Stamatakis, E., Naci, L., Typical and disrupted brain dynamic complexity in human neonates. Poster presentation at *School of Psychology Research Symposium, Trinity College Dublin, Dublin, Ireland, March 2023*

Hu, H., Coppola, P., Stamatakis, E., Naci, L., The development of functional small-world architecture in infancy., Poster presentation at *Annual Meeting of Organisation for Human Brain Mapping, Glasgow, Scotland. June 2022*

Hu, H., Cusack, C., Naci, L., Typical and disrupted brain circuitry for conscious awareness in full-term and preterm infants., Poster presentation at *Neuroscience Ireland Meeting, Virtual, September 2021*

Hu H., Cusack R, Naci L., The ontogeny of the brain circuitry for conscious awareness, Poster presentation at *Annual Meeting of Organisation for Human Brain Mapping, Virtual, June 2021*

Hu, H., Cusack R, Naci L., The development of brain circuitry supporting conscious awareness in infancy, Oral presentation at *Neuromatch Conference., Virtual, October 2020*

Acknowledgement

This thesis would not have been possible without the support of many people and institutions. First, I would like to thank my supervisor, Prof. Lorina Naci, for your academic guidance, encouragement, and patience during my PhD. I truly appreciate the time and dedication you invested in reviewing my work, which significantly improved the overall quality of my thesis.

I would like to thank Prof. Rhodri Cusack for all your help with infant imaging processing and expertise in infant development. Thank you, Dr. Peter Coppola, for your guidance and feedback on data analysis and writing in general. Thank you to Prof. Emmanuel A Stamatakis for your expertise in the field of consciousness. Thank you to Prof. Redmond O'Connell and Prof. Nixon Elizbeth for serving as my examination appraisers. Thank you to Sharon Chi Tak Lee for proofreading my thesis. I would like to thank the Developing Human Connectome Project and the Human Connectome Project for kindly sharing the valuable datasets. Thank you to the China Scholarship Council – Trinity College Dublin Joint Scholarship Programme for funding this degree.

I would like to thank all past and present members of Naci's lab, Feng Deng, Qing Qi, Bolin Cao, Peter Gorman, Amy Heneghan, Nicola Taylor, Ines Jani, Lou Angey and Sandra El-Sherbiny, for their valuable advice and emotional support. I would also like to thank my friends, Yihe Weng, Mengdi Wang, Elliot Quinn, Sharon Chi Tak Lee, Anusha Yasoda-Mohan, and Thomas McGrath for generously sharing their time and care, making my time in Dublin so special and precious.

A special thank you to my parents and my sister for their love and support. Thank you to my boyfriend, Guang, for always being by my side throughout this journey. Your company and support have been a source of strength and comfort.

List of Figures

List of Tables

List of Abbreviations

DAN	Dorsal attention network
DCH	Dynamic Core Hypothesis
dHCP	Developing Human Connectome Project
DMN	Default mode network
DVARS	The root mean square intensity difference between successive volumes
ECN	Executive control network
EEG	Electroencephalography
EPI	Echo-planar imaging
FC	Functional connectivity
FD	Framewise displacement
fMRI	Functional Magnetic Resonance Imaging
FPN	Frontoparietal network
FOV	Field of view
GA	Gestational age
GLM	General linear model
GNWT	Global Neuronal Workspace Theory
HCP	The Human Connectome Project
ICA	Independent component analysis
IIT	Integrated Information theory
MDS	Multidimensional scaling
NREM	Non-rapid-eye-movement sleep
PMA	Postmenstrual age
REM	Rapid-eye-movement sleep

ROIs	Regions of interest
Rs-fMRI	Resting-state functional Magnetic Resonance Imaging
sMRI	Structural Magnetic Resonance Imaging
TEA	Term-equivalent age
SW	Small worldness

Table of Contents

1. Chapter 1: General introduction

1.1 Conscious awareness

1.1.1 Arousal and awareness

One of the great frontiers of consciousness science is understanding how early consciousness arises in the development of the human infant. It remains unknown how infants and children acquire the capacity for conscious awareness, and whether this capacity is present from birth or emerges through development in the early years of life. The notion of consciousness, which this thesis is concerned with in the broadest sense, involves the possession of an experiential point of view. An organism is conscious if (and only if) it has a subjective perspective—if there is 'something that it is like' to be that organism (Nagel, 1974, 1980). Different kinds of conscious states are distinguished from each other in terms of what it is like to be in them. What it is like to see a face is distinct from what it is like to hear a melody, and each of those experiences is itself distinct from what it is like to feel pain. Experiential aspects of consciousness can be hard to assess experimentally. In recent years, great progress has been made in the empirical measurement of consciousness through clinical neuroscience studies that investigate states of reduced/altered consciousness in adults. Clinically, consciousness is defined and measured by examining two distinct dimensions: arousal and awareness (Laureys et al., 2004). Arousal is measured by assessing spontaneous eye opening, sleep-wake cycles, and other tonic, systemic fluctuations in the ability to engage with the environment. Clinically, awareness is primarily assessed by examining the ability to wilfully respond to commands behaviourally and/or through language, as well as the ability to provide self-report on mental states that relate to oneself or the environment (Clare et al., 2005; Mehling et al., 2009; Naci et al., 2014). For example, coma is characterised by the absence of arousal and

awareness. Patients in a coma state lie with their eyes closed and show no responses to stimuli (Plum & Posner, 1982). Patients in a vegetative state (Ashwal et al., 1994) can be awake for long periods of time and show a considerable range of reflex activities, such as 'looking' toward a bright light and turning toward a loud sound (Naci & Owen, 2022). However, they cannot show visual fixation or track an object/person in their visual field, suggesting a lack of awareness (Jennett & Plum, 1972).

Infants display clear signs of arousal from birth. Their eyes open wide, glancing around the surroundings. Newborns, though distinct from adults, have sleep-wake cycles (Carter & Wrede, 2017). Most importantly, they cry to convey discomfort, hunger, fatigue, or any other form of distress. However, the extent to which infants can consciously process information about themselves and their environment remains unknown. There is some evidence suggesting at least minimal awareness in neonates at birth. A few studies have found that infants perform some forms of stimuli discrimination from early hours-days after birth, including distinguishing one's body as different from the body of others (12 to 103 hours after birth) (Filippetti et al., 2013), their own cry from those of other newborns (within one day after birth) (Martin & Clark, 1982; Simner, 1971), their mother's voice from a stranger's (within 12 hours – 3 days after birth) (Decasper & Fifer, 1980; Ockleford et al., 1988; Querleu et al., 1984), and discriminating facial expressions of happiness from disgust (2 days after birth) (Addabbo et al., 2018). Prima facia, these studies suggest some forms of 'minimal' awareness in infants. However, these behaviours could be due to certain stimuli being primed in the early days of life or even in the womb, or the physical properties of stimuli themselves. For example, the mother's voice is very familiar to the infant, so any preferential responses (i.e., longer looking time or more head turns) could be due to the familiarity rather than the understanding of the meaning and significance of the mother figure. Similarly, the response to the crying of another infant, or facial expressions

of disgust, could be pre-conscious reactions to aversive stimuli (Ruffman et al., 2019). It is well established from adult studies that some forms of stimulus processing, such as unconscious priming (where unconscious exposure to a stimulus influences on a response to a later stimulus) (Dehaene et al., 1998; Schacter, 1992), and "blindsight" (Poppel et al., 1973; Weiskrantz et al., 1974), can occur without consciousness, and thus, caution must be exercised when interpreting the aforementioned studies to infer infant conscious processing.

1.1.2 Core awareness and extended awareness

Damasio (2000) proposed that consciousness could be divided into two aspects, a 'core awareness', or a basic integrated experience of the current moment, and an 'extended awareness', made possible by the accumulation of autobiographical memories that allow the creation of an internal world and projection beyond the present. Seeley and Sturm (2007) have made a similar distinction between a 'minimal' self and a 'longitudinal' self. The 'minimal' self refers to a self that is immediate (Gallagher, 2000) and comprises awareness of body boundaries and position, facial features and body size, visceral states, agency, mental states, and online behaviour (Sturm et al., 2018). By contrast, the presence of episodic autobiographical memory (i.e., memories of past events) and semantic self-knowledge (i.e., knowledge of one's own traits) allows for the construction of the 'longitudinal' self, that is extended across time. Given that the extended awareness requires experience over time and the formation of memories over periods of time, the time-course of 'core' (Parvizi & Damasio, 2001) or 'primary' (Edelman, 2003) consciousness development, and not the development of forms of consciousness that require reflection, self-consciousness, or off-line cognition (Goupil & Kouider, 2019; Rochat, 2003), is the

most pressing and relevant question related to the emergence of consciousness in young infants.

1.2 Behavioural evidence of infant consciousness

Previous behavioural studies have attempted to answer when infant consciousness emerges. Some studies observed some potential behavioural markers of conscious processing of external stimuli in neonates at birth or even earlier. As early as 28 weeks postmenstrual age, preterm infants show a series of reactions in response to noxious stimuli, like increased heart rate (Waxman et al., 2016) and skin conductance (Eriksson et al., 2008), limb withdrawal (Hartley et al., 2016), and facial grimacing (DiLorenzo et al., 2018). In addition, day-old infants exhibit the capacity for visual pursuit and fixation. Their eye movements are not random and aimless; instead, they can fixate on and follow a series of targets with their eyes closely coordinated, behaving as a single unit (Bidet-Ildei et al., 2014; Dayton Jr & Jones, 1964). By assessing their eye gaze behaviour, previous studies have found that newborns perform some forms of stimuli discrimination (Addabbo et al., 2018; Bidet-Ildei et al., 2014; Reid et al., 2018; Rigato et al., 2011). For instance, they look longer and exhibit more orienting responses toward happy facial expressions compared to neutral facial expressions (Rigato et al., 2011), as well as toward novel emotional facial expressions (Addabbo et al., 2018).

Beyond discriminative behavioural responses to external stimuli, neonates have been found to exhibit preferential responses to stimuli related to themselves, potentially implying a certain level of self-awareness from birth. Newborns exhibit the ability to distinguish between self-touch and touch from others, as demonstrated in the study by Rochat and Hespos (1997). In that experiment, newborns' cheeks were touched by an experimenter's

hand, or their own hand guided by the experimenter. The newborns were observed to have more rooting responses toward the experimenter compared to themselves. Another line of evidence for self-awareness in neonates at birth comes from research on multisensory integration and proprioception (Filippetti et al., 2013). Filippetti et al. (2013) found that newborn infants preferred to look at the videotape of another newborn's face being stroked by a brush when their own face is brushed synchronously, rather than asynchronously. This finding suggested that newborns can integrate visual and tactile information and detect inter-sensory synchrony when related to their own bodies. However, as mentioned above, behavioural studies do not definitively show evidence of consciousness awareness in infants, due to newborns' very limited motor/behavioural control and the lack of language abilities – faculties that provide the gold standard measures for assessment of consciousness.

An important caveat of previous studies is that they did not observe any intentional or goal-directed behaviours toward external stimuli in infants until they reached the age of 1 year old or later, which would otherwise provide stronger evidence of conscious awareness. Infants between the age of 13 and 15 months were observed exhibiting a particular gesture that indicated they may be able to guide an adult's attention toward a specific object and check whether the adult is attending to it (Bates et al., 1979; Bates et al., 1975). Fenson et al., (1994) observed that 13 months old infants started to use referential words referring to objects or activities. By about 1 and a half years old, infants can successfully take into account others' false beliefs when attempting to determine their goals and help them achieve their goals (Buttelmann et al., 2009; Southgate et al., 2010). Thus, infants older than 1-year-old seem to represent themselves as a goal-directed agent and are aware of other people's mental states. Conversely, infants appear unable to identify themselves in a mirror self-recognition task (the Rouge test) until they are 12 months old

(Amsterdam, 1972; Nielsen & Dissanayake, 2004), which has been identified as a hallmark of the development of adult-like self-awareness in childhood (Rochat, 2003). In this task, infants are typically presented with a mirror while a dot of rouge is applied to their face/neck. If individuals reach toward the dot, they are identified as having mirror self-recognition. To pass this test, infants need to detect the discrepancy between the mental representation of their own body and the observed marked mirror image. Similarly, previous studies (Amsterdam, 1972; Kristen-Antonow et al., 2015; Nielsen & Dissanayake, 2004) found that infants cannot recognize that the mirror reflects their self-experienced "Me", rather than another individual staring and mimicking them until 1 year old. The remaining question, however, is to what extent is our understanding on the emergence of consciousness in infants limited by these pre-existing paradigms and assessment tools, which rely on motoric and linguistic output for determining the presence of conscious awareness.

1.3 Early vs late onset views on infant awareness

Indeed, there is an ongoing debate on when conscious awareness emerges in infancy between proponents of the 'late onset' account and the 'early onset' account (Bayne et al., 2023). Researchers who espouse a 'late onset' view think conscious awareness requires abilities that are almost certainly not available to infants until the age of 1. For example, according to higher-order consciousness theories (Brown, 2015; Lau & Rosenthal, 2011; Rosenthal, 2005), conscious awareness requires the abilities to represent oneself as being in a particular mental state, i.e. 'I see an apple', or other people being in a particular mental state, e.g., 'someone sees an apple'. The earliest indications of the ability to represent others' mental states were observed in neonates at 7 months (Kovacs et al., 2010). Kovacs

and colleagues (2010) found that infants' eye movements demonstrated a capacity to monitor other people's beliefs at 7 months in a visual object detection task. Perhaps the most stringent 'late onset' proposal was made by Carruthers (2003), who argues that conscious awareness does not emerge until the age of three. His argument is based on the grounds that this is when children first become capable of second-order recognition judgments of experience (i.e., "appears" and "seems"), a capability he deems fundamental to consciousness.

Researchers who espouse an 'early-onset' view posit that high order capacities are not necessarily a prerequisite for conscious awareness and that conscious awareness may appear as early as birth, or even during the third trimester of pregnancy. As mentioned above, many potential markers of conscious awareness have been found in early days of life. Newborns show a series of reactions in response to noxious stimuli (DiLorenzo et al., 2018; Eriksson et al., 2008; Waxman et al., 2016), perform some forms of stimulus discrimination early after birth (Addabbo et al., 2018; Bidet-Ildei et al., 2014; Reid et al., 2018; Rigato et al., 2011), and discriminate their self-related from other-related stimuli (Filippetti et al., 2013; Rochat & Hespos, 1997).

The lack of consensus on when conscious awareness emerges is driven at least in part by methodological differences in assessments across studies. The application of the so-called 'gold standard' assessment for studying conscious awareness in healthy adults and older children —such as verbal reporting or executing commands—to neonates during their initial months of life, can lead to a 'late onset' perspective. However, it is plausible that young infants indeed possess conscious awareness, but their inability to provide overt responses is limited by language and motor constraints. Another contributing factor to the absence of behavioural indicators of conscious awareness in early life could be the utilization of cognitively demanding measures, in paradigms derived from the assessment

of consciousness in adults. Such measures require the development of memory (LeDoux & Lau, 2020) and cognitive abilities, like executive control, inhibition, and reasoning (Baker, 2010; Nelson, 1996; Perner et al., 2023). For instance, the so-called "false-belief tasks" have often been used to assess one's "theory of mind" ability (Bennett, 1978; Wimmer & Perner, 1983). In such tasks, participants are typically required to predict a person's behaviour based on the person's false beliefs. To make correct predictions, participants not only need to have a mental representation of the person's belief but also need to reason about the person's false belief and inhibit their own (true) belief. Conversely, findings of studies that use relatively cognitively undemanding measures tend to align with the 'early onset' view. However, simple behavioural responses, like visual fixation and orienting responses, might be unintentional or involuntary and lack reliability to indicate conscious awareness (Baumeister et al., 2011; Giacino et al., 2009). As I mentioned above, preferential responses, like longer looking time or more frequent head orientation, could be due to familiarity or physical properties of stimuli. Therefore, whether those behavioural markers truly reflect conscious awareness is in question.

1.4 Brain markers of conscious awareness in infancy

Given these limitations in behavioural markers of consciousness, recent studies have underscored the significance of detecting brain markers that can indicate the presence or absence of conscious awareness in any behaviourally non-responsive population (Bayne et al., 2023), such as those with disorders of consciousness (DoC), clinically diagnosed to be in a coma or vegetative state.

DoC studies to date have established that brain activity can be used as a proxy for conscious awareness in the absence of overt behavioural responses (Boly et al., 2007;

Monti et al., 2010; Naci et al., 2014; Naci et al., 2017; Owen et al., 2006). A small but significant proportion (17–24%; Monti et al., 2010) of DoC patients, who entirely lack any behavioural signs of consciousness and fulfil the international agreed criteria for coma or vegetative state (Ashwal et al., 1994), can nevertheless indicate their conscious awareness by performing mental imagery tasks in full accordance with verbal instructions (Bardin et al., 2011; Boly et al., 2007; Monti et al., 2010; Owen et al., 2006), or following and understanding complex narratives (Naci et al., 2014; Naci et al., 2018; Naci et al., 2017) while lying inside the MRI scanner (for a review see Naci & Owen, 2022). While these paradigms appear promising to measuring consciousness in other populations with behavioural limitations such as infants, they are not applicable to the population of young infants in their current form. Due to the absence of language ability, neonates cannot comprehend and follow experimenters' instructions or complex narratives.

Another recently developed analytical approach, based on resting-state fMRI (rs-fMRI) may provide a complementary route for assessing the emergence of conscious awareness in early infancy. Rs-fMRI is acquired as participants lie quiet in the scanner, unengaged in an active experimental task. Participants do not need to produce any overt responses (either motor or verbal responses) or understand study instructions. Importantly, resting-state blood-oxygen-level-dependent (BOLD) signal correlation has been found to recapitulate the topography of task-evoked responses. Since Biswal and colleagues (1995) first found that resting-state BOLD signals at low frequency band were temporally correlated within the somatomotor system, accumulating studies (Beckmann et al., 2005; Cordes et al., 2000; Greicius et al., 2003; Gusnard & Raichle, 2001; Lowe et al., 1998; Seeley et al., 2007) have demonstrated similar patterns of resting-state coherence, which are so-called 'functional networks', in most cortical and subcortical systems in human brain, such as DMN, ECN, salience networks, etc. Thus, rs-fMRI can be used to investigate brain

networks that are known to underlie high-order cognition, such as executive function (i.e., the fronto-parietal network), or self-referential and integrative processes (i.e., DMN). Because of these reasons mentioned above, rs-fMRI has been widely and successfully applied to study behaviourally unresponsive populations (Barttfeld et al., 2015; Coppola et al., 2022; Demertzi et al., 2019; Huang et al., 2016; Liu et al., 2017). However, the ontogeny of brain network development in infants is poorly understood, and previous studies have provided conflicting results. Furthermore, insights gained from DoC studies on the link between conscious awareness and brain network dynamics have not been applied to newborn infants, an important gap that I will address in this thesis.

Some might question the legitimacy of using brain markers developed in human adults to probe conscious awareness in neonates, given the neuroanatomical and functional differences between infant brain and adult brain (Johnson, 2001; Johnson, 2003). However, several studies to date have suggested that neonate's brain at full-term birth is surprisingly more mature than expected. Some fundamental prerequisites for the emergence of complex brain function were found to be present in neonates by full-term birth. The first one is the growth of the cortex. Although different from that in adults, the cortical plate appears in foetuses around 15–22 weeks of gestation, and gets thicker and more diverse during the second and third trimesters of pregnancy with proliferative processes, synaptic formation, and dendritic arborization (Rakic, 1988). Second, regional specialisation (cortical gyrification), a key component in the development of complex brain function, starts from around 14 weeks gestation, develops dramatically between 25 and 35 weeks of gestation, and becomes mature by full-term birth (Burkhalter et al., 1993; Kostovic & Judas, 2006; Kostovic et al., 2019). Third, the vertical brain stem, diencephalic, and thalamocortical pathways, all of which are essential for arousal and consciousness, emerge around 24 weeks of gestation (Plum, 1991). During 24 to 32 weeks of gestation, thalamocortical

fibres grow from the subplate into the cortical plate of various regions, including the somatosensory, visual, auditory, and frontal cortex (Kostovic et al., 2002; Krsnik et al., 2017). The number of synapses increases, along with the development of thalamocortical fibres, which have been suggested to be of paramount significance for consideration of the interaction of human foetus with the environment. Indeed, we view the development of thalamocortical connectivity−generally regarded as necessary for consciousness–as providing a lower bound of 24 - 26 weeks gestation (Kostovic & Jovanov-Milosevic, 2006; Lagercrantz, 2014) on the emergence of consciousness. Fourth, similar structural connectomes have been observed in neonates and adults. During the late prenatal period (after 34 weeks gestation), long interhemispheric and interhemispheric cortico-cortical afferents start to grow (Eyre et al., 2000; Kostovic & Judas, 2010; Vanhatalo & Kaila, 2006). By 30 weeks, adult-like structural network topology was observed in preterm neonates. van de Heuvel et al. (2015) demonstrated a large similarity between neonatal and adult structural connectomes, comprising 85% overlap of connections. Firth, primary motor and sensory networks observed in adults have been consistently observed in early infancy (Cao, Huang, et al., 2017; Doria et al., 2010; Eyre et al., 2021; Fransson et al., 2007). By contrast, however, the literature on the development of higher-order networks in neonates is very inconclusive, a gap that I will address in this thesis. Taken together, the aforementioned studies suggest that the brain markers observed in human adults can be effectively utilized to explore the development of conscious awareness in neonates. A couple of caveats are important to note. First, while the aforementioned lower bound or 24–26 gestation weeks is placed at a stage of typical intrauterine foetal development in healthy foetuses, this thesis focuses on the development of extrauterine conscious awareness, or in neonates from/shortly after birth. It is also important to recognize that at least some (and perhaps all) of these markers are experience-dependent, and their emergence can be delayed/altered by a variety of factors, most notably, premature birth.

For example, Emberson et al. (2017) found no evidence of cortical omission responses in 6-month-old infants who had been born preterm. Given that premature infants present a key population both in terms of early infant age manipulation and potential alterations to their brain development and brain markers of consciousness due to prematurity itself, I have included this population in my studies as an important comparison group to full-term born infants.

In the following sections, I review some of the markers that have emerged from consciousness science as being key to the brain mechanisms of conscious awareness in adult humans.

1.4.1 The reciprocal relationship between FPN and DMN

One of the key properties of consciousness is integration (or unity): the conscious experience the one has at a particular time is an integrated whole (Bayne, 2012). For instance, when you see a red dot, you would have a single experience of it rather than two separate experiences—one of the colour red and the other of the dot. Two of the most influential theories of consciousness, the Integrated Information Theory (IIT) (Tononi, 2004; Tononi, 2008; Tononi et al., 2016) and the Global Neuronal Workspace Theory (GNWT) (Dehaene et al., 2011; Mashour et al., 2020) (though they place different degrees of importance on the unity of consciousness), postulates that consciousness requires integration of information from discrete but interconnected modules across the brain. According to IIT, consciousness is generated by a distributed functional cluster that specifies a maximum of irreducible integrated information. GNWT suggested that consciousness arises from the broadcasting of information within a widely distributed but functionally integrated workspace.

Adult functional neuroimaging studies have identified the FPN and DMN as two such distinct cortical systems that support consciousness and play complementary roles in information integration. Myriad neuro-psychological and neuroscientific studies show that fronto-parietal regions — comprising the DAN and ECN — are critical for stimulus-driven high-order cognition (Duncan, 2010; Elliott, 2003; Ptak, 2012; Shallice, 1988; Woolgar et al., 2010), and recent work suggests they facilitate awareness of external stimuli (Demertzi et al., 2013; Huang et al., 2020; Vanhaudenhuyse et al., 2011). By contrast, the DMN has been primarily implicated in self-referential and self-awareness processing (Andrews-Hanna et al., 2010; Beer, 2007; Buckner & Carroll, 2007; D'Argembeau et al., 2005; Demertzi et al., 2013; Gusnard & Raichle, 2001; Qin & Northoff, 2011; Schneider et al., 2008; Vanhaudenhuyse et al., 2011; Wicker et al., 2003), and more recently in context processing (Margulies et al., 2016; Smith et al., 2018; Vatansever et al., 2018). Importantly, the fronto-parietal network and DMN share a reciprocal relationship, where they are not simultaneously active, i.e., are anti-correlated or exhibit a low correlation of functional time-courses relative to other brain network pairings (Fox et al., 2005; Fransson, 2005; Josipovic et al., 2012; Kelly et al., 2008; Yeo et al., 2015). This reciprocal relationship is suggested to sustain an ongoing interaction between internally directed thoughts and engagement with the external environment, thereby contributing to consciousness (Carhart-Harris & Friston, 2010). This relationship is abolished when consciousness is extinguished, irrespective of condition, e.g., whether during deep anaesthesia under various pharmacological manipulations or after severe brain injury (Bonhomme et al., 2012; Boveroux et al., 2010; Haugg et al., 2018; Huang et al., 2020). In addition, this reciprocal relationship has been found to be weaker in other conditions where the state of consciousness is altered, such as psychedelic states (Carhart-Harris et al., 2013; Dai et al., 2023), in experienced meditators during rest and meditation (which share some phenomenological similarities with the psychedelic state) (Brewer et al., 2011; Froeliger et

al., 2012; Josipovic et al., 2012). These findings suggest that the reciprocal relationship between DMN and FPNs tracks the presence of conscious awareness. Therefore, the investigation of the development of DMN, DAN and ECN and their reciprocal relationship has the potential to provide valuable insights into the emergency of conscious awareness in early infancy.

Previous studies have yielded inconsistent findings on whether the DMN, DAN and ECN, are present as distinct networks from birth. Some found no evidence for the presence of these networks until the end of the first year (Fransson et al., 2007; Gao, Alcauter, Elton, et al., 2015; Gao et al., 2009; Smyser et al., 2010). By contrast, other rs-fMRI studies support the idea that these networks have already emerged in neonates (Doria et al., 2010; He & Parikh, 2015, 2016; Linke et al., 2018). Several factors may contribute to these divergent results. Due to methodological and technical challenges, the incipient field of infant neuroimaging has, to date, not adhered to unified testing protocols. The aforementioned studies employed vastly different sample sizes (e.g. ranging from n = 11 to 143), different MR field strengths (e.g. 1.5T versus 3T) yielding different spatial and temporal resolutions (Triantafyllou et al., 2005; Weiskopf et al., 2006), different motion artefact control methods and lack age-specific structural brain templates for neonates. The multitude of different methodologies across previous studies renders it impossible to conclude, in light of inconsistent results, whether the DMN, DAN and ECN are already present at birth or not. Furthermore, to the best of our knowledge, only one study (Gao et al., 2013) to date has investigated whether the reciprocal relationship between these three high-order networks is developed in early infancy. They reported that the anticorrelated interaction between the DMN and DAN was absent at birth, but became apparent at one year of age. However, this study investigated a small neonate cohort (n= 51), which may have reduced the statistical power to detect the effects of interest (Button et al., 2013). In summary, key

gaps remain on whether the DAN, ECN and DMN and their reciprocal relationship are present in neonates at birth, and will be the focus of the work described in Chapter 2.

1.4.2 Functional small-world architecture

Another fundamental property of conscious experiences is differentiation (Cooney & Gazzaniga, 2003; Deco et al., 2015; Seth, 2009; Seth et al., 2006; Tononi & Edelman, 1998). While each conscious experience is unified, at the same time, it is of remarkable differentiation. Consider a typical daily scenario: upon entering a room, one's consciousness may register various sensory inputs such as the colour of the walls, the scent of flowers on the table, and the sounds emanating from the television. It has been postulated that the balance of differentiating and integrative processes, which appear prima facia to be opposed, is a key feature of consciousness (Seth et al., 2006; Tononi & Edelman, 1998). Therefore, the neural processes underpinning conscious experience must demonstrate both functional integration and differentiation.

Recent scientific theories of consciousness have proposed that a neural system characterized by the coexistence of functional segregation and integration is essential for the emergence of consciousness. For instance, according to the Dynamic Core Hypothesis (DCH), consciousness requires a functional cluster characterized by high statistical dependence within each subset and relatively lower dependence with elements outside the subset (Tononi & Edelman, 1998). Although starting from different premises, the GNWT also links consciousness to coexistence of functional segregation and integration (Dehaene et al., 2011; Mashour et al., 2020). It proposed that information becomes conscious when it is 'broadcasted' within an anatomically widely distributed neuronal workspace. Brain regions within the workspace are functionally specialised and segregated, yet the

communication between them is extensive and rapid so any information available to one is quickly available to others.

Graph theoretical analyses of brain activity have shown that functional brain networks display a so-called ‘small-world’ organization, comprised of dense within-network connections that facilitate specialized processes and sparse between-network connections that enhance global information integration (Bassett & Bullmore, 2006; Bassett & Bullmore, 2017). Small-world brain organization is, thus, an important feature of the healthy adult brain that plausibly facilitates the optimal balance of information segregation and integration required for conscious processing.

Some empirical studies have suggested that the small-world organization facilitates conscious information processing. Consciousness state manipulations that abolish consciousness, i.e., by sleep or anaesthesia (Barttfeld et al., 2015; Luppi, Golkowski, et al., 2021), and by consciousness perturbations after brain injury (Luppi et al., 2019; Pandit et al., 2013), modulate small-world organization. For example, Luppi et al. (2019) observed that DoC patients displayed reduced small-world characteristics in DoC patients as well as in participants under deep propofol anaesthesia relative to awake healthy volunteers. In patients exhibiting cognitive impairments after traumatic brain injury, functional brain networks shifted away from a small-world organization and displayed reduced efficiency and decreased integration compared to healthy controls (Pandit et al., 2013). These studies have led to a broad consensus that small-word organization is related to processes that support complex cognition and consciousness in human adults (see Coppola et al., 2022; Monti et al., 2013; also Schröter et al., 2012 for a divergent view). Given the foregoing, small-world architecture should be expected to track both healthy neurodevelopment and the emergence of conscious awareness in early infancy.

However, it remains poorly understood whether functional small-world architecture is present in neonates. A handful of previous studies have suggested that small-world architecture is present in full-term born neonates (Bouyssi-Kobar et al., 2019; De Asis-Cruz et al., 2015; Fransson et al., 2011; Omidvarnia et al., 2014), but several limitations undermine their conclusions. Particularly, the index (σ) (Humphries & Gurney, 2008) that has been used to quantify small-world properties in these studies has been criticised (Bassett & Bullmore, 2017; Papo et al., 2016; Telesford et al., 2011) because it can result in a high false-positive rate (Telesford et al., 2011). In addition, the small sample size (N = 10 to 66) and low temporal and spatial resolution limit their results' reliability (Button et al., 2013). Therefore, more rigorous measures of small-world architecture are needed and their application in large neonate rs-fMRI cohorts is required to definitively answer the question of whether small-world architecture is present in neonates at birth. Addressing this gap is the focus of the work described in Chapter 3.

1.4.3 Neural entropy

Subjective experience is not fixed but rather ever changing and unfold and develop over time. Each conscious experience is specific, differing from a vast array of conscious states at any given time. According to the DCH (Tononi & Edelman, 1998), a spatially distributed and highly integrated functional clustering is necessary but not sufficient for consciousness. The brain must be capable of a large repertoire of different activity patterns or neural states to produce the stream of consciousness. Different theories of consciousness also align in suggesting that the dynamic complexity/richness of possible brain states is a fundamental hallmark of consciousness (Carhart-Harris et al., 2014; Cooney & Gazzaniga, 2003; Dehaene et al., 2011; Mashour et al., 2020; Northoff & Huang, 2017).

The entropic brain hypothesis (Carhart-Harris, 2018; Carhart-Harris et al., 2014) proposes that the dynamic complexity of spontaneous brain activity reflects the uncertainty and informational richness of conscious states. Consciousness arises within a critical zone where the entropy or dynamic complexity of brain activity is neither excessively ordered nor disordered. Compared to states where consciousness is diminished or abolished (e.g., disorders of consciousness, general anesthesia, sedation), normal waking consciousness is characterized by richer conscious content and greater flexibility of possible states. Psychedelic compounds shift the brain (in normal waking conscious states) towards a higher entropic state, yielding richer conscious contents and higher flexibility of mind (Schartner et al., 2017). Yet, this shift comes at the cost of other functions, such as a diminished sense of self and associated metacognitive functions, such as an ability to reflect on one's own thoughts and behaviour (Fleming et al., 2012; Shimamura, 2000), theory of mind (Bennett, 1978; Wimmer & Perner, 1983), and mental time-travel (Fleming et al., 2012).

Indeed, neural entropy, which captures dynamic complexity of of brain activity patterns, has been found to be an accurate and experimentally tractable measure for quantifying different conscious states (i.e., psychedelic states, general anaesthesia, disorders of consciousness) (Cai et al., 2020; Cavanna et al., 2018; Coppola et al., 2022; Crone et al., 2020; Golkowski et al., 2019; Toker et al., 2022; Varley, Carhart-Harris, et al., 2020; Varley, Luppi, et al., 2020). Convergent evidence from neuroimaging studies has shown that neural entropy fluctuates among states of reduced or altered consciousness. Neural entropy decreases when consciousness fades, i.e., during sleep (Miskovic et al., 2019) or general anaesthesia (Dasilva et al., 2021; Schartner et al., 2015; Varley, Luppi, et al., 2020), as well as in the minimally conscious state (MCS) or the unresponsive wakefulness syndrome (UWS) (Coppola et al., 2022; Demertzi et al., 2019; Li et al., 2022b; Sitt et al.,

2014). By contrast, neural entropy was found to increase in altered states of consciousness, such as during hallucinatory or the psychological state elicited by classic psychedelic drugs (i.e., LSD and psilocybin) (Herzog et al., 2023a; Luppi, Carhart-Harris, et al., 2021a; Schartner et al., 2017; Varley, Carhart-Harris, et al., 2020) and lucid dreaming (Baird et al., 2022). Importantly, a recent paper by Coppola et al., (2022) measured neural entropy based on dynamic fluctuations observed in the small-world architecture in individuals who were awake, under propofol sedation, in MCS or in UWS patients. They found that neural entropy consistently scaled down with decreasing levels of consciousness (awake > propofol sedation > MCS > UWS). Furthermore, this result was robustly replicated using another independent propofol sedation dataset, as well as different brain parcellations.

Whether neonates exhibit different levels of neural entropy relative to adults remains unknown. One EEG study to date (Lippé et al., 2009) compared neural entropy in 1- to 2-month-old neonates and adults and reported lower sample entropy in neonates. However, the very small sample of neonates (7 neonates and 20 adults) limits the reliability of their result. Furthermore, it is well established that neural entropy is best computed by using the temporospatial activity pattern (Hoel et al., 2013; Oizumi et al., 2014), whereas Lippe and colleagues (2009) averaged entropy across all electrodes, resulting in a loss of information regarding the spatial complexity of connections between regions. Therefore, there is a clear need to investigate neural entropy in neonates relative to adults by assessing temporospatial activity patterns with large fMRI datasets in order to obtain robust and reliable results. Addressing this important gap is the focus of the work described in Chapter 4.

1.5 The effect of premature birth on brain markers of conscious awareness in early infancy

Knowledge of the impact of premature birth on the development of the three aforementioned brain markers of conscious awareness is extremely scarce. To our best knowledge, no study has investigated the effects of premature birth on the relationship between FPNs and DMN in neonates. Only three small studies (N = 10 to 66) have examined small-world organization in neonates born at full term or at term-equivalent age (postmenstrual age of 37 weeks) (Bouyssi-Kobar et al., 2019; Gozdas et al., 2018; Omidvarnia et al., 2014), and only two studies (Cao, He, et al., 2017; Omidvarnia et al., 2014) have focused on neonates before TEA, both with very small samples (N = 10 to 23). For example, Bouyssi-Kobar et al. (2019) used rs-fMRI and reported lower segregation and higher integration in neonates at TEA relative to full-term born, but no significant difference in small-worldness. Gozdas et al. (2018) used rs-fMRI and found significantly higher small-worldness in preterm neonates compared with full-term born neonates. Omidvarnia et al. (2014) used EEG and reported lower segregation in preterm neonates before TEA (N = 11), but no significant difference in either small-worldness or integration, relative to full-term born (N = 10). In terms of the effect of premature birth on neural entropy, only three EEG studies (Janjarasjitt et al., 2008; Kaffashi et al., 2013b; Scher et al., 2005) have investigated this question, reporting inconsistent results. While Scher et al. (2005) and Kaffashi et al. (2013b) observed higher neural entropy in full-term neonates relative to preterm neonates at the same age, Janjarasjitt et al. (2008) did not observe any significant difference between them. As is the case with other literature on infant brain development, primarily due to the incipient state of this field, the inconsistencies are likely due to small sample sizes and methodological differences, e.g., different brain parcellations and different methods to define brain networks. Therefore, there is an urgent need to use

large infant datasets to ensure adequate statistical power as well as reliability and generalizability of findings. In addition, validation analyses that use different brain parcellations and different data analysis operations are very important to assess the reproducibility of the results.

In this thesis, I use a large dataset of full-term and prematurely born infants. I look at prematurely but healthy-born neonates as a group which allows us to examine the effect of early neonate age, and prematurity itself, on the development of each of the above brain markers of conscious awareness.

1.6 Addressing limitations of previous studies in this thesis

1.6.1 Large open-source rs-fMRI datasets of infants and adults

To address the limitations of previous studies and fill in the delineated research gaps, I used rs-fMRI data from the largest open-source neonate dataset, the developing Human Connectome Project (dHCP, http://www.developingconnectome.org/). The dHCP is an open science study, which aims to map the structural and functional development across the perinatal period. The dataset conferred several advantages, which improve the reliability of results based on this dataset. First, 3T MRI multiband echo-planar imaging technique employed in the study significantly improves temporal resolution (TE/TR = 38/392 ms) and signal-to-noise ratio relative to sequences used in previous studies (Zhang et al., 2019). Second, the rs-fMRI data are of adequate acquisition duration (15 min, 2300 volumes) (Nakamura et al., 2022), and of large sample size (Termenon et al., 2016), which ensure adequate statistical power and reliability of results. Lastly, the dHCP group provides more accurate week-to-week neonate structural templates (Schuh et al., 2018) for

registration between rs-fMRI and T1 images. This approach takes into consideration the rapid anatomical development of the neonatal brain during early infancy and enhances the accuracy of registration.

The infant data used in my thesis were from the second (2019) dHCP public data release (N = 511). To fully leverage this large number dataset, I did not exclude participants based on the head movement of all time points. Instead, I first applied a scrubbing procedure to retain a continuous sub-sample of the data (~70%, 1600 time points) with the lowest motion for each participant. I then excluded participants who still had more than 160 motion-outlier volumes (equivalent to 10% of the cropped dataset) or whose mean framewise displacement (FD) exceeded 0.5 mm. Thus, in this thesis, I used a subset of lower motion rs-fMRI data (N = 420), including 278 scans from full-term neonates (gestational age at birth = 39.9 weeks ± 8.6 days; postmenstrual age at scan = 41.2 weeks ± 12.2 days; 119 females) and 72 scans from preterm neonates at TEA (GA at birth = 32.1 weeks ± 25.5 days; PMA at scan = 40.9 weeks ± 14.6 days; 32 females) and 70 scans from preterm neonates before TEA (GA at birth = 32.5 weeks ± 20.7 days; PMA at scan = 34.7 weeks ± 12.7 days; 22 females).

As a reference adult group, I used a subset (N = 176; mean age = 29 years old; range = 22 – 36 years old; 77 males) of high-quality data from the final release of the Washington University-Minnesota Consortium of Human Connectome Project (HCP) selected by Ito et al. (2020) (https://github.com/ito-takuya/corrQuench). The subject exclusion criteria were as follows: participants with 1) focal anatomical anomalies, 2) focal segmentation or surface errors, 3) data collected during period of known problems with the head coil, 4) with high head motion (more than 50% of time points showing greater than 0.25 framewise displacement), 5) family relation with another participant, or 6) no genotyping testing.

1.7 Validation analyses

There are rising concerns regarding the reproducibility of results of fMRI studies (Laumann et al., 2017; Poldrack et al., 2017; Power et al., 2018). One of the attributing factors concerns the researcher's degree of freedom in data analysis, such as using different pre-processing workflows (Carp, 2012) and data analysis operations (Shen et al., 2013). In this thesis, I used pre-processed rs-fMRI data from the dHCP and HCP, both of which used similar pre-processing workflow (See Chapter 2 Methods for detailed descriptions on pre-processing procedures). In addition, I applied identical data analysis operations to the neonate and adult data for all three projects. To ensure that our results were not driven by the use of arbitrary data analysis operations (particularly for graph theoretical analysis) (Shen et al., 2013), I performed several validation analyses. In Chapter 3, I employed different parcellations (the Power atlas or UNC-0-1-2 atlas), edge-definition methods (binary or weighted), multiple thresholds (to get sparse connections), and various algorithms to assess small-world architecture, all aimed at ensuring the reproducibility of the results. In chapter 4, I also checked the reproducibility of the results using two different brain parcellations (the Power atlas and UNC-0-1-2 atlas).

1.8 Overview of the thesis

Based on the research reviewed in this chapter, there is a clear need to investigate the development of a) the reciprocal relationship between FPNs and DMN, b) functional small-world architecture, and c) neural entropy in full-term neonates and how the development of these markers is affected by premature birth and early infant age prior to full-term birth. Each finding chapter aims to investigate the development of each brain marker. The neonates delivered and scanned at full-term (N = 278) from the second (2019)

dHCP public data release (http://www.developingconnectome.org/seconddata-release/) and a reference adult group (N = 176) from the HCP dataset were used to investigate the typical development of the brain markers in early infancy in the three empirical chapters.

We considered the effect of neonate age at the time of assessment separately from the effect of premature birth, by including two groups: the first (n = 72) born prior to but scanned at TEA, and the second (n = 70) born and scanned before TEA. A subset of paired scans collected from the same infants (n = 33, GA at birth = 32.2 weeks ± 20.1 days) before TEA (PMA at scan = 34.5 weeks ± 11.5 days) and at TEA (PMA at scan = 41.0 weeks ± 10.16 days) was also included. I reasoned that any differences between neonates born and scanned at full-term and preterm neonates scanned at TEA would reflect effects of premature birth, while controlling for neonate age. Conversely, any differences between preterm neonates scanned at TEA and those scanned before TEA would reflect the effects of neonate age.

Chapter 2 investigated the development of the DMN, DAN and ECN, as well as their reciprocal relationship in neonates relative to adults, and the effects of premature birth and early neonate age on network development. I first generated FC matrices based on the nineteen regions of interest (ROI) for the DMN, DAN and ECN defined in Raichle (2011) for each participant. I investigated the presence of the three networks and their reciprocal relationship by exploring within and between-group differences. Then, to probe any differences in network development in neonates relative to adults, I compared the within- and between-network FC in the DMN, DAN or ECN between each neonate group and adults. In addition, hierarchical clustering analyses and non-metric multidimensional scaling were used to capture network structural differences and to visualize the similarity of ROI responses in neonates and adults. To investigate the effect of premature birth while controlling for age at scan on network development, I compared the FC within each

network and between each pair of networks, between preterm neonates scanned at TEA and full-term neonates. To investigate the effects of neonate age while controlling for prematurity, the same preterm neonates scanned before and at TEA were used. My hypothesis was that DMN, DAN, ECN and their relationship would be less developed in neonates relative to adults. In addition, I expected that premature birth and early neonate age would be associated with altered network development.

Chapter 3 first investigated whether the functional small-world architecture was developed in neonates at birth and how it was affected by premature birth and early neonate age. As brain regions develop at different rates, I also investigated the effects of premature birth and neonate age on the balance of integration and segregation at the regional level. Whole-brain functional network properties and nodal-level communication efficiency were assessed using graph theoretical analyses. To investigate the development of small-world architecture in early infancy, I compared the whole-brain functional architecture in neonates and adults. To investigate the effects of premature birth, I compared both global functional brain architecture and regional communication efficiency between full-term and preterm neonates scanned at TEA. Lastly, I compared functional brain architecture at both global and regional level between preterm neonates scanned twice to investigate the effects of neonate age. My hypothesis was that (a) neonates exhibit less developed functional small-world architecture relative to adults, (b) relative to full-term birth, premature birth would be associated with altered small-world architecture and nodal efficiency, and (c) some alterations in these measures would persist as preterm neonates reached TEA.

Chapter 4 first investigated whether the neural entropy in neonates is different from that of adults. I then asked how premature birth and neonate age affected the development of neural entropy. The development of neural entropy in neonates was assessed by the entropy of network configuration of whole brain (except cerebellum), using graph

theoretical analysis combined with a sliding-window approach. To answer the first research question, I compared the neural entropy in different neonate groups relative to adults. To investigate the effects of premature birth, I compared neural entropy in full-term neonates and preterm neonates scanned at the same age. In addition, I treated neonate age as a continuous variable and assessed the association between neonate age and neural entropy in preterm neonates scanned before TEA. I hypothesized that: (a) neural entropy in neonates would be different from that in adults, (b) premature birth would be associated with altered neural entropy, and (c) premature birth would be associated with abnormal development trajectory of neural entropy in the early days to weeks of life.

2. Chapter 2: Typical and disrupted brain circuitry for conscious awareness in full-term and preterm infants

2.1 Introduction

One of the key properties of consciousness is integration (or unity): the conscious experience the one has at a particular time is an integrated whole (Bayne, 2012). For instance, when you see a red dot, you would have a single experience of it rather than two separate experiences—one of the red colour and the other of the dot. Two of the most influential theories of consciousness, the IIT (Tononi, 2004; Tononi, 2008; Tononi et al., 2016) and GNWT (Dehaene et al., 2011; Mashour et al., 2020) (though they place different degrees of importance on the unity of consciousness), postulates that consciousness requires integration of information from discrete but interconnected modules across the brain. According to IIT, consciousness is generated by a distributed functional clustering that specifies a maximum of irreducible integrated information. GNWT suggested that consciousness arises from the broadcasting of information within a widely distributed but functionally integrated workspace.

Adult functional neuroimaging studies have identified the FPN and DMN as two such distinct cortical systems that support consciousness and play complementary roles in information integration. Myriad neuro-psychological and neuroscientific studies show that fronto-parietal regions — comprising the DAN and ECN — are critical for stimulus-driven high-order cognition (Duncan, 2010; Elliott, 2003; Ptak, 2012; Shallice, 1988; Woolgar et al., 2010), and recent work suggests they facilitate awareness of external stimuli (Demertzi et al., 2013; Huang et al., 2020; Vanhaudenhuyse et al., 2011). By contrast, the DMN has been primarily implicated in self-referential and self-awareness processing (Andrews-Hanna et al., 2010; Beer, 2007; Buckner & Carroll, 2007; D'Argembeau et al., 2005;

Demertzi et al., 2013; Gusnard & Raichle, 2001; Qin & Northoff, 2011; Schneider et al., 2008; Vanhaudenhuyse et al., 2011; Wicker et al., 2003), and more recently in context processing (Margulies et al., 2016; Smith et al., 2018; Vatansever et al., 2018).

Importantly, the fronto-parietal network and DMN share a reciprocal relationship, where they are not simultaneously active, i.e., are anti-correlated or exhibit a low correlation of functional time-courses relative to other brain network pairings. This relationship is abolished when consciousness is extinguished, irrespective of condition, e.g., whether during deep anaesthesia under various pharmacological manipulations or after severe brain injury (Bonhomme et al., 2012; Haugg et al., 2018; Huang et al., 2020), suggesting that it tracks the presence of conscious awareness, as dissociable from arousal (such as, in the case of wakeful brain injured patients in the vegetative state) (Haugg et al., 2018). Therefore, the investigation of the development of DMN, DAN and ECN and their reciprocal relationship has the potential to provide valuable insights into the emergency of conscious awareness in early infancy.

Previous structural studies suggested that the structural connections underlying the DMN and FPNs are present in neonates at birth. For example, the cingulum bundle, a key tract that interconnects the anterior and posterior core midline regions of the DMN (Hagmann et al., 2008; van den Heuvel et al., 2008), was already present at full-term birth (Kumpulainen et al., 2023) or even earlier (Dubois et al., 2006). The superior longitudinal fasciculus, a primary and direct tract that connects frontal and parietal cortices (Petrides & Pandya, 1984; Schmahmann et al., 2009), has been identified in full-term neonates (Geng et al., 2012; Liang et al., 2022; Uda et al., 2015) and preterm neonates at TEA (Rose et al., 2014). However, whether the DMN, DAN and ECN and their reciprocal relationship are developed by birth and whether they are affected by premature birth and neonate age, remain poorly understood and are the focus of this chapter.

To assess the literature, I conducted a literature search with keywords, ‘functional network’ or ‘functional connectivity’, ‘infant’ or ‘newborn’ or ‘neonatal’, and “fMRI” that resulted in 20 neonate studies summarized in Appendix A, Table 6.1. While the three primary sensory and motor networks were consistently reported in neonates (Cui et al., 2017; Doria et al., 2010; Fransson et al., 2007; Gao, Alcauter, Elton, et al., 2015; Gao, Alcauter, Smith, et al., 2015), findings were inconsistent on the presence of high-order networks, including the DMN, DAN, ECN. Some rs-fMRI studies found no evidence for the presence of these networks until the end of the first year (Fransson et al., 2007; Gao, Alcauter, Elton, et al., 2015; Gao et al., 2009; Smyser et al., 2010). Fransson et al. (2007) found that the DMN in preterm neonates was fragmented into an anterior and posterior part. Similarly, Gao et al. (2009) reported that although the two main hubs of DMN (i.e., the ventral/dorsal medial prefrontal cortex and posterior cingulate/retrosplenial cortex) were consistently observed in 2-week-olds, 1-year-old and 2-year-olds, other aspects of the DMN (i.e., the inferior parietal lobule, lateral temporal cortex, and hippocampus regions) were not found in 2-week-olds. A similar pattern was also reported for the DAN and ECN (Fransson et al., 2009; Gao, Alcauter, Smith, et al., 2015). By contrast, other rs-fMRI studies support the idea that these networks have already emerged in neonates (Doria et al., 2010; He & Parikh, 2015, 2016; Linke et al., 2018). For instance, Doria et al. (2010) found that both primary and high-order networks were present in full-term and preterm neonates scanned at term-equivalent age (TEA: 37 – 42 weeks of postmenstrual age). He and Parikh (2015) detected a fronto-parietal network, comprising the frontal gyrus and inferior parietal cortex, and a second one, comprising the anterior cingulate cortex, medial prefrontal cortex, superior/middle frontal gyrus, in preterm neonates. Linke et al. (2018) found that both the ECN and DMN were present even in neonates with perinatal brain injuries, both full-term and preterm neonates scanned at TEA. Eyre et al. (2021), the largest study of newborn brain network topography to date, used the dHCP dataset and reported an adult-

like topography in six high-order networks, including a frontoparietal network similar to the DAN distribution, but did not find evidence for the DMN. This study did not investigate the reciprocal relationship between these networks. The extant evidence for the emergence of the DMN, DAN and ECN at birth is summarized in Appendix A, Table 6.2.

Several factors may contribute to these divergent results. Due to methodological and technical challenges, the incipient field of infant neuroimaging has, to date, not adhered to unified testing protocols. The aforementioned studies employ vastly different sample sizes (e.g., ranging from N = 11 to 143), different MR field strengths (e.g., 1.5T vs 3T) yielding different spatial and temporal resolutions (Triantafyllou et al., 2005; Weiskopf et al., 2006), different motion artifact control methods, and lack age-specific structural brain templates for neonates. The multitude of different methodologies across previous studies renders it impossible to conclude, in light of inconsistent results, whether the DMN, DAN and ECN are already present at birth or not. Moreover, to the best of our knowledge, only one study to date has investigated whether the reciprocal relationship between these three high-order networks is developed in early infancy (Gao et al., 2013). Gao et al. (2013) reported that the anticorrelated interaction between the DMN and DAN was absent at birth, but became apparent at one year of age. However, this study had a relatively small number of full-term neonates (N = 51) and no preterm neonates, which may have reduced the power to detect effects of interest.

To address these two research gaps, the first aim of this study was to investigate whether the DMN, DAN, and ECN, and their reciprocal relationship were present in neonates at full-term birth. To answer this question, I used a large full-term neonate cohort (N = 282) from the open source dHCP dataset, and a reference adult group (N = 176) from the HCP. The second aim was to investigate the effect of neonate age on these networks and their relationship. The effect of chronological age at the time of assessment was deconfounded

from the effect of premature birth (Bhutta et al., 2002), by the inclusion of two groups: the first (N = 73) born before but scanned at TEA, and the second (N = 73) born and scanned before TEA. A subset of paired scans collected from the same infants (N = 37) before and at TEA was also included. I reasoned that any differences between neonates born and scanned at full-term and preterm neonates scanned at TEA would reflect the effects of premature birth, while controlling for neonate age. Conversely, any differences between preterm neonates scanned at TEA and those scanned before TEA would reflect the effects of neonate age. My prediction was that premature birth and early neonate age are associated with altered network development.

2.2 Materials and methods

2.2.1 Participants

Neonates. The neonate data were from the second (2019) dHCP public data release (http://www.developingconnectome.org/data-release/second-data-release/). All neonates were scanned at the Evelina Newborn Imaging Centre, Evelina London Children's Hospital. Ethical approval was obtained from the UK's National Research Ethics Committee and parental informed consent was obtained before imaging. Full details of dHCP data acquisition can be found at Fitzgibbon et al. (2020). Prior to scanning, neonates were fed, swaddled, and comfortably positioned in a vacuum jacket to promote natural sleep. The effect size for the difference between adults and neonates could not be estimated directly from previous work, since no studies have compared FC in DMN and FPNs between them. Therefore, I conducted sensitivity power analyses for all the comparisons between adults and neonates in G*Power 3.1 (Faul et al., 2009). Again, since the effect

size could not be estimated directly from previous works, I conducted sensitivity power analyses for all the comparisons between neonate groups.

Full-term neonates 342 full-term neonates were available in the dHCP dataset. Only one subject was scanned twice, at 37 weeks PMA and after 37 weeks PMA, but I only used the later one for the full-term group. I used 282 scans in the full-term neonates (GA at birth = 40.0 weeks ± 8.6 days; PMA at scan = 41.2 weeks ± 12.0 days; 122 females) after quality control procedures (for details see Data acquisition and pre-processing section below).

Preterm neonates 121 preterm neonates had fMRI data in the second dHCP public data release. 74 of them were scanned once: 40 participants scanned at TEA and 34 participants scanned before TEA. 47 of the 121 preterm neonates were scanned twice, at and before TEA. Thus, for preterm neonates, we have 87 scans obtained at TEA and 81 scans obtained before TEA. I used 73 scans from preterm neonates scanned at TEA (GA at birth = 32.0 weeks ± 25.6 days; PMA at scan = 40.9 weeks ± 14.5 days; 31 females) and preterm neonates scanned before TEA (GA at birth = 32.5 weeks ± 13.4 days; PMA at scan = 34.6 weeks ± 13.4 days; 23 females) after quality control. Of the 47 preterm neonates scanned both at and before TEA, 10 were discarded because of excessive movement of either one of the two scans, resulting in 37 paired scans (GA at birth = 31 weeks ± 6.8 days; PMA at first scan = 34 weeks ± 1.3 days; PMA at second scan: 40 weeks ± 6.9 days; 13 females). Further details on demographic information can be found in Table 2.1.

Table 2.1 Information obtained from the Developing Human Connectome Project for scans used in the present study.

Group	Sex	Birth age (GA, weeks ± days)	Scan age (PMA, weeks ± days)	Birth weight (Kg)
Full-term neonates	160M/122F	40.0 ± 8.6	41.2 ± 12.0	3.35 ± 0.54
Preterm neonates scanned at TEA	41M/32F	32.0 ± 25.6	40.9 ± 14.5	1.76 ± 0.79
Preterm neonates scanned before TEA	50M/23F	32.5 ± 13.4	34.6 ± 13.4	1.78 ± 0.61

Abbreviations: GA, gestational age; PMA, postmenstrual age; TEA, term-equivalent age; M, male; F, female.

Adults. As a reference adult group, I used a subset (N = 176; 22 – 36 years; 99 females) of high-quality rs-fMRI data from the final release of the HCP selected by Ito et al. (2020) (https://github.com/ito-takuya/corrQuench). The subject exclusion criteria used by Ito et al. (2020) were as follows: participants with 1) focal anatomical anomalies, 2) focal segmentation or surface errors, 3) data collected during periods of known problems with the head coil, 4) high head motion (more than 50% of time points showing greater than 0.25 framewise displacement), 5) family relation with another participant, or 6) no genotyping testing. For details of study procedures see Van Essen et al. (2013).

2.2.2 Data acquisition and pre-processing

dHCP. Data were acquired on a 3T Philips Achieva with a dedicated neonatal imaging system including a neonatal 32-channel phased-array head coil. Fifteen minutes of high temporal and spatial resolution rs-fMRI data were acquired using a multislice gradient-echo echo planar imaging (EPI) sequence with multiband excitation (TE = 38 ms; TR = 392 ms; MB factor = 9x; 2.15 mm isotropic, 2300 volumes). In addition, single-band EPI reference (sbref) scans were also acquired with bandwidth-matched readout, along with additional spin echo EPI acquisitions with 4xAP and 4xPA phase-encoding directions. To correct susceptibility distortion in rs-fMRI data, field maps were also obtained from an interleaved (dual TE) spoiled gradient-echo sequence (TR = 10 ms; TE1 = 4.6 ms; TE2 = 6.9 ms; flip angle = 10°; 3 mm isotropic in-plane resolution, 6mm slice thickness). High-resolution T1- and T2-weighted anatomical imaging were also acquired in the same scan session, with a spatial resolution of 0.8 mm isotropic. For T1w image: TR = 4795 ms and the field of view (FOV) = 145 × 122 × 100 mm. For T2w image: TR = 12000 ms, TE = 156 ms and the FOV = 145 × 122 × 100 mm.

The dHCP rs-fMRI data were pre-processed by dHCP group using the project's in-house pipeline optimized for neonatal imaging. In brief, this pipeline includes: 1) motion and distortion correction: corrects for intra-volume movement artefacts and for artefacts associated with susceptibility-induced off-resonance field changes (susceptibility-by-movement artefacts), and estimates motion nuisance regressors; 2) registration: aligns all functional images with the native T2 space and the neonatal template space, which refers to the week-specific 40-week template from the dHCP volumetric atlas (Schuh et al., 2018); 3) temporal high-pass filter: 150s high-pass cut-off; 4) denoising: estimates artefact nuisance regressors and regresses all nuisance regressors from the functional data obtained from the first step. See SI and Fitzgibbon et al. (2020) for full details.

To further reduce the effect of motion on FC measures, motion-outlier volumes were identified, and a scrubbing procedure was applied to retain a continuous sub-sample of the data (~70%) with the lowest motion for each participant. The subjects who still had a high level of motion after the scrubbing procedure were excluded from further analyses. I discarded the first 5 volumes to allow for adaptation to the environment and equilibrium of the MR signal at first. Then, motion outliers were identified from the remaining 2295 volumes. Volumes with DVARS (the root mean square intensity difference between successive volumes) higher than the 1.5 interquartile range above the 75th centile, after motion and distortion correction, were considered motion outliers. Then, a continuous sub-sample of 1600 volumes with the minimum number of motion outliers was retained for each subject. Subjects with more than 160 motion-outlier volumes (10% of the cropped dataset) in the continuous subset were labelled 'high level of motion' and excluded entirely. Thus, 8 preterm neonates scanned before TEA, 14 preterm neonates scanned at TEA and 61 full-term neonates were excluded (Figure 2.1). In addition, I performed a temporal low-pass filter (0.08 Hz low-pass cutoff) on the pre-processed dHCP rs-fMRI to conduct FC analyses, as previous studies found that oscillations were primarily detected within grey matter in 0.01 – 0.08 Hz (Salvador et al., 2008; Zuo et al., 2010). Figure 2.2a provides a schematic of the processing steps for dHCP fMRI data.

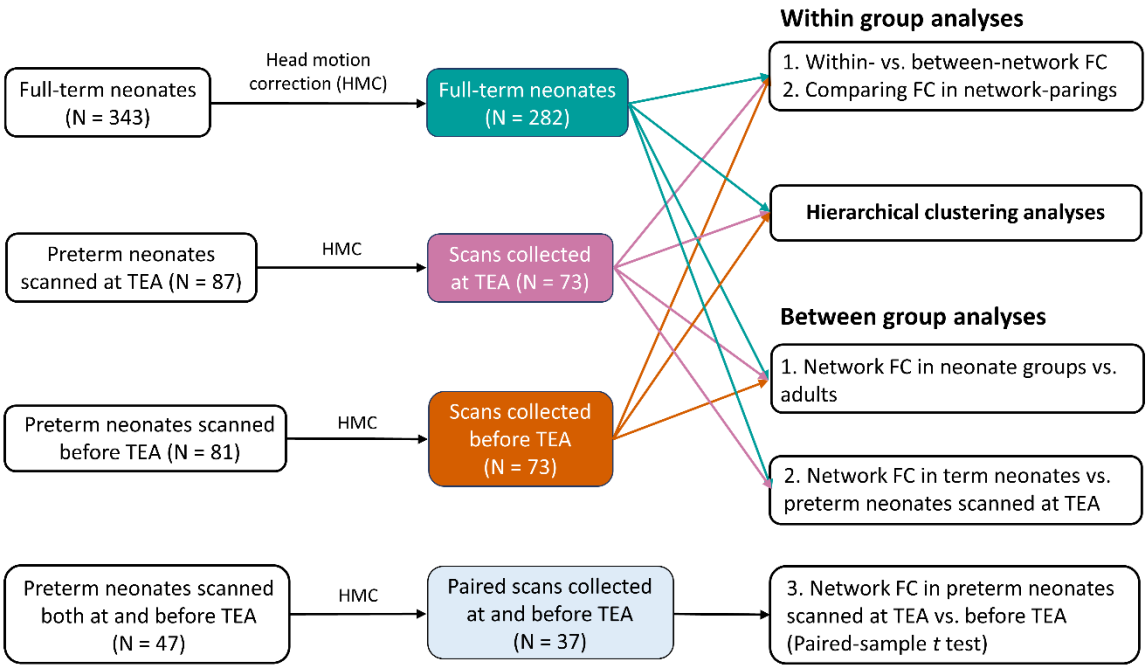

Figure 2.1 The number of scans included in data analyses. The frames in green/pink/brown indicate the scans collected from full-term neonates/preterm neonates at/before term-equivalent age that passed head motion criteria. The frame in light blue indicates the scans collected at and before term-equivalent age from the same preterm neonates. Abbreviations: TEA, term-equivalent age; vs., versus; FC, functional connectivity.

HCP. Data were acquired on a customized 3T Siemens "Connectome Skyra" with a 32-channel head coil. Resting-state images were collected using gradient-echo EPI sequence: TR = 720 ms; TE = 33.1 ms; flip angle = 52°; FOV = 208 × 180 mm (RO × PE), slice thickness = 2 mm, 72 slices, 2.0 mm isotropic voxels, 1200 volumes per run. Rs-fMRI data were collected in four runs of 14.4 minutes each, two runs in one session and two in another session. The two sessions were conducted in two days separately and we only used the data collected in the first session. Within each session, oblique axial acquisitions alternated between phase encoding in a right-to-left (RL) direction in one run and phase

encoding in a left-to-right (LR) direction in the other run. Full details of HCP data acquisition can be found at Van Essen et al. (2013).

The rs-fMRI data of HCP were pre-processed by HCP group using the following pipeline: 1) Distortion correction: correction of gradient-nonlinearity-induced distortion and phase-encoding-direction-induced distortion; 2) Motion correction: realigns the timeseries to correct for subject motion by using a 6 DOF FLIRT (Oxford Centre for Functional MRI of the Brain Fs Linear Registration Tool) registration of each frame to the single-band reference image; 3) Aligns the original EPI data (rs-fMRI data) to Montreal Neurological Institute (MNI) template space: EPI to T1w from FLIRT BBR, fine tuning of EPI to T1w with BBR-register, nonlinear T1w to MNI template; 4) Intensity normalization to mean of 10000 and bias field removal; 5) Temporal high-pass filter: 150s high-pass cut-off; 6) Denoising: removes artefactual or "bad" components using ICA-FIX to automatically. Detailed pre-processing procedure can be found in Glasser et al. (2013). Additionally, we performed a temporal low-pass filter (0.08 Hz low-pass cut-off) on the denoised rs-fMRI data and removed the first five volumes. As the selection of the subset of HCP had controlled head motion (i.e., exclusion of participants that had any fMRI run in which more than 50% of TRs had greater than 0.25mm framewise displacement), and adults generally have smaller maximal head motion than neonates (Cusack et al., 2017), we did not apply the same scrubbing method used in the dHCP dataset to adult data. Figure 2.2b provides a schematic of the processing steps for HCP fMRI data.

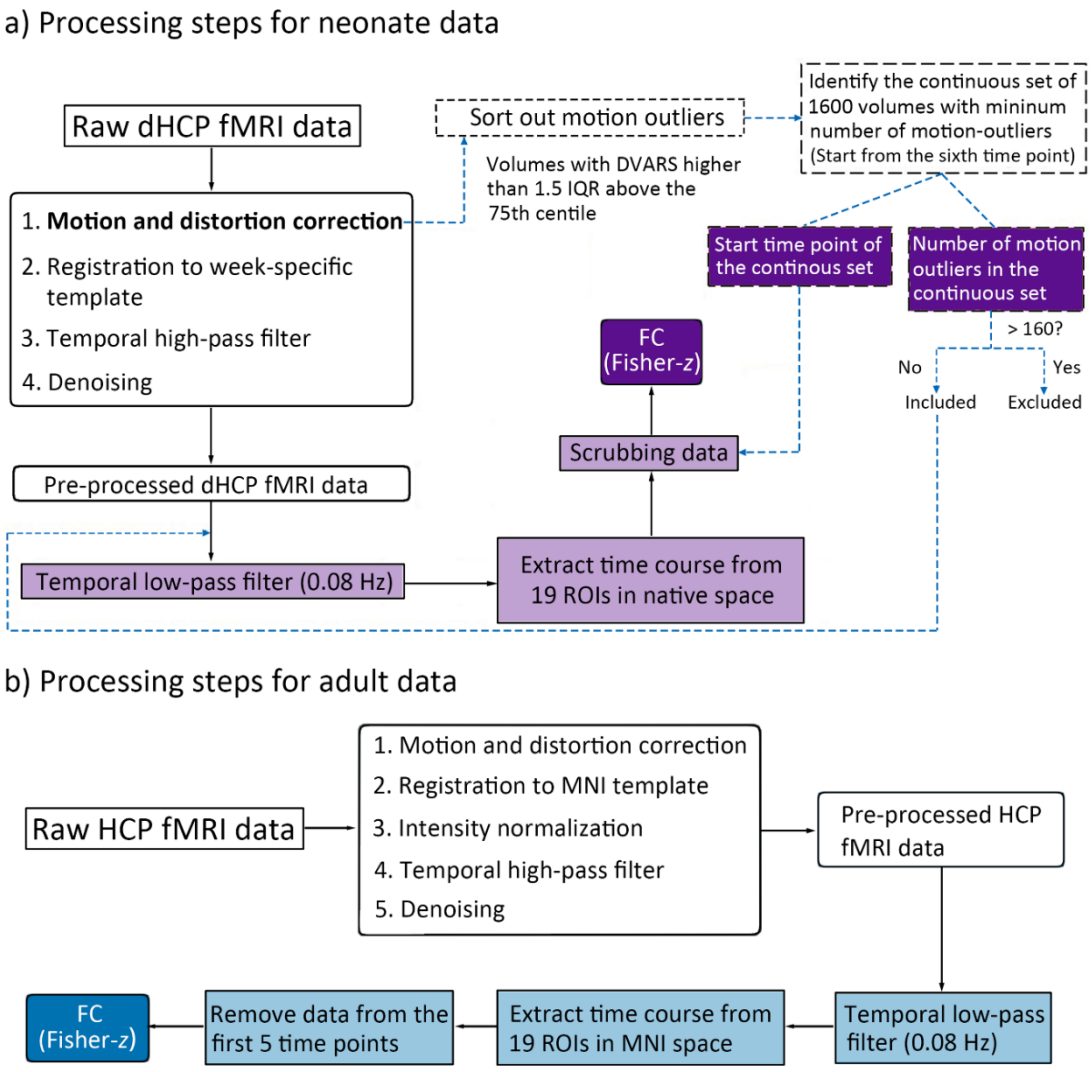

Figure 2.2 Data processing steps for neonate and adult data. a) Processing steps for the neonate rs-fMRI data. The rectangles with rounded corners indicate the steps in the fMRI neonatal pre-processing pipeline of the Developing Human Connectome Project. The frames in light purple indicate additional processing steps in this study, and the dotted black line rectangles represent the steps for correcting motion outliers. The frames in dark purple represent the data that I obtained. b) Processing steps for the adult fMRI data. The rectangles with rounded corners indicate the steps in the fMRI pre-processing pipeline of the Human Connectome Project. The frames in light blue indicate additional processing steps in this study, and the frame in dark blue represents data that I obtained. Abbreviations: dHCP, Developing Human Connectome Project; DVARS, D referring to temporal derivative of time courses and VARS referring to root mean squared variance over voxels; ROI, regions of interest; IQR, Inter Quartile Range; FC, functional connectivity; HCP, Human Connectome Project.

2.2.3 Data analyses

Network definition. I used a theory and meta-analyses-driven node-based approach to network mapping. Nineteen ROI (8-mm radius spheres) for the three networks (Table 6.3 in Appendix A), DMN, DAN and ECN, were created based on well-established landmark regions defined in Raichle (2011). These ROIs, created in MNI space, were registered to neonates' native space according to the following steps. I first aligned these ROIs with 40-week dHCP T1w template (Schuh et al., 2018). This involved: 1) trimming the dura from the 40-week dHCP T1w template, and the cerebellum from both the 40-week dHCP T1w template and MNI T1w template; 2) aligning the 40-week dHCP T1w template to MNI T1w template using non-linear registration (ANTs SyN) (See Figure 6.1 in Appendix A for the registration accuracy between them); 3) applying the warp file generated in the last step to the ROIs in MNI space with 40-week dHCP T1w template as a reference. In the next step, we needed to align these ROIs in 40-week dHCP T1w template space with neonate native space (See Figure 2.3 for ROIs in infant template space and Figure 2.4 for ROIs in infant native space). I inverted the func-to-template warp provided by dHCP group and applied this inverted warp to ROIs in the 40-week dHCP T1w template space. Thus, I obtained ROIs in each neonate native functional space (Figure 6.2 in Appendix A). For adults, as the denoised HCP data had been aligned to MNI space, I used these ROIs in MNI space directly.

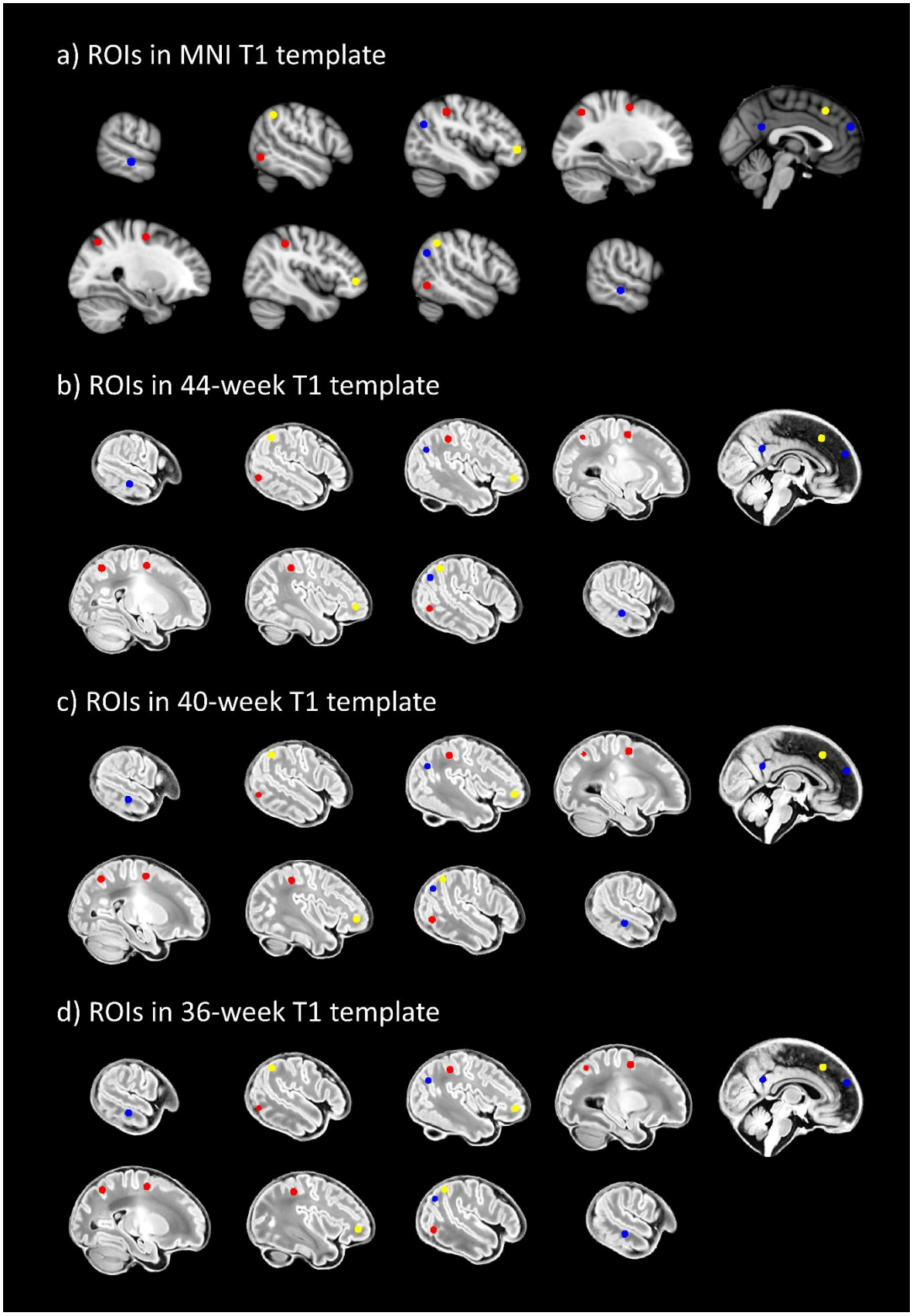

Figure 2.3 Regions of interest in MNI152 T1 template space and week-specific neonate T1 template spaces. Regions of interest (ROIs) in the MNI152 template, as well as the 44-

week, 40-week, and 36-week T1 template spaces (prior to term-equivalent age), are presented here to visually assess any differences in ROI locations due to infant age (8-week difference) or premature birth. Visual inspection of the ROIs suggests similar locations in both the MNI152 template spaces and all neonate template spaces. Blue spheres represent regions of the default mode network, red spheres represent regions of the dorsal attention network, and yellow spheres represent regions of the executive control network.

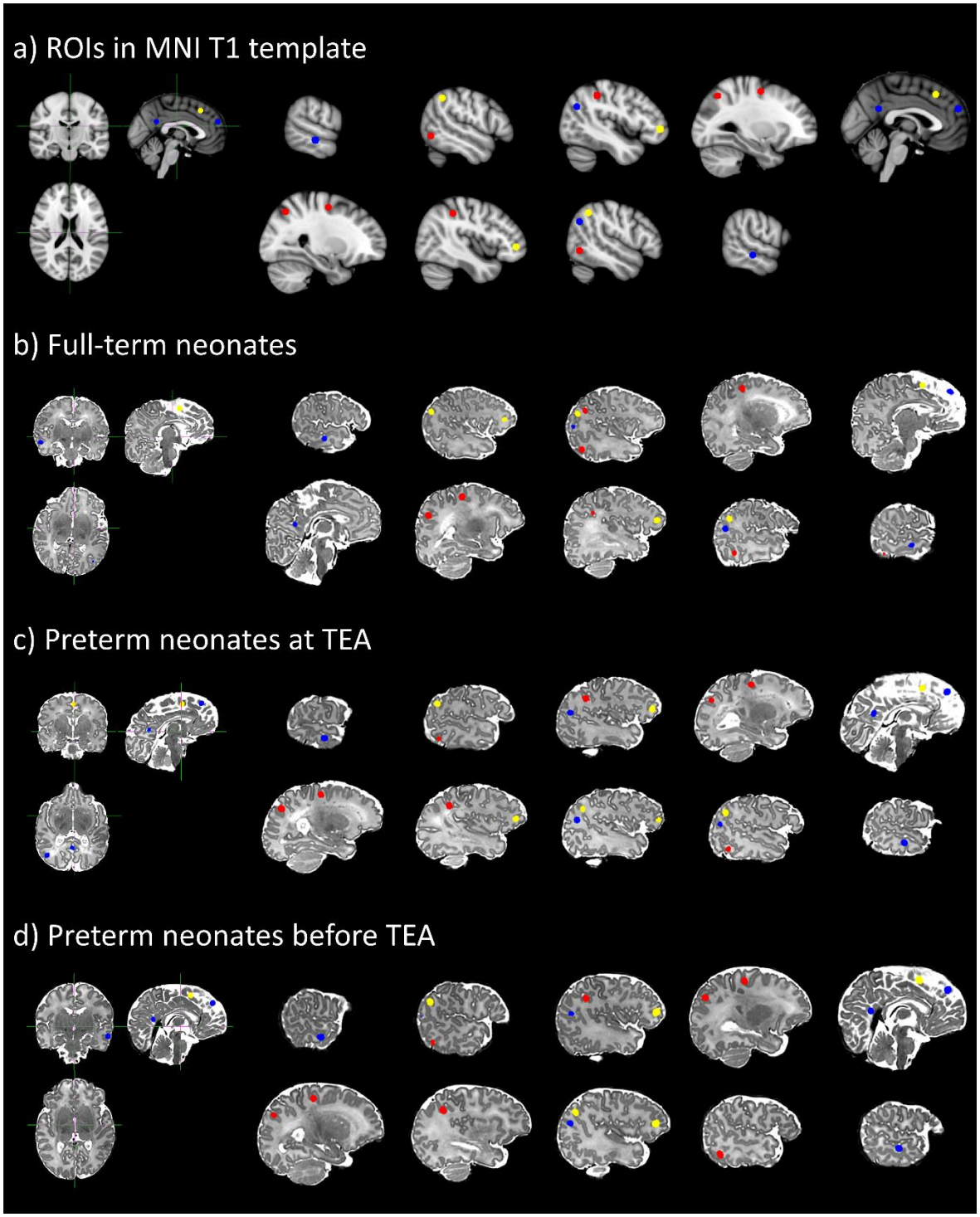

Figure 2.4 Regions of interest in MNI152 T1 template space and neonate native space. Regions of interest (ROIs) in the MNI152 template space, full-term neonates (for example, using sub-CC00810XX10 with age at scan = 40 weeks 5 days and age at birth = 38 weeks 4 days), preterm neonates at term-equivalent age (TEA; for example, using sub-CC00689XX22 with age at scan = 40 weeks 0 days and age at birth = 34 weeks 3 days), and preterm neonates before TEA (for example, using sub-CC00284AN13 with age at scan

= 32 weeks 1 day and age at birth = 30 weeks 5 days) are presented here to visually check for any differences ROI locations among different infant groups. Visual inspection of the ROIs suggests fairly similar locations in both MNI152 template space and infant native spaces. The differences in ROI locations observed here are partially attributed to the orientation of images in the native space. Blue spheres represent regions of the default mode network, red spheres represent regions of the dorsal attention network, and yellow spheres represent regions of the executive control network.

Functional connectivity. FC between ROIs was assessed by calculating the Pearson correlation of pre-processed time courses, and z scored using the Fisher-z transformation. At the individual level, within-network FC was obtained by averaging the FC between ROIs belonging to the same network and between-network FC by averaging the FC between ROIs of each network to the others. For all between-group comparisons, the ROI-level FC within each subject was normalized to facilitate a focus on the FC patterns between groups rather than potentially differing FC strength between the groups (Eyre et al., 2021; Smyser et al., 2016).

2.2.4 Statistical analysis

ANOVAs and *t*-tests were used to explore within and between group differences. Bonferroni correction for multiple comparisons was applied to all statistical results.

Comparison of neonates and adults. General linear models (GLM) were used to test for group differences in FC within DMN, DAN or ECN while controlling for head motion, as I found neonates had significantly higher head motion than adults (Figure 6.3 and 6.4 in Appendix A). Hierarchical clustering analysis and non-metric multidimensional scaling were used to capture network structure, and visualize the similarity of ROI responses in neonates and adults (Frakes & Baeza-Yates, 1992; Ripley, 2007). See Section 2.2.5 and 2.2.6 for further details.

Comparison of neonate groups. To investigate the effect of premature birth, while controlling for neonate age at scan, on network development, I compared the FC within each network and between each pair of networks, between preterm neonates scanned at TEA and full-term neonates. Head motion was not included as a covariate, since I did not

observe any significant difference between the two groups (Figure 6.4 in Appendix A). To investigate the effect of neonate age, while controlling for prematurity, the same preterm neonates scanned before and at TEA (N = 37) were used.

2.2.5 Hierarchical clustering analyses

We captured the structure of the three networks in different groups with hierarchical clustering analysis (Rasmussen, 1992; Ripley, 2007), which has proven informative in prior studies (Blumensath et al., 2013; Cusack et al., 2018). This hierarchical clustering algorithm builds up an entire cluster tree in which neighbouring regions are joined if their similarity is maximal among all pairs of neighbouring regions. Here, we used the time-course extracted from the 19 ROIs as input to access the hierarchical relationship among the ROIs. For the neonate data, we first calculated initial pairwise distance between ROIs using one minus the linear correlation between the scrubbed time-courses extracted from the 19 ROIs at the individual level. For adults, the initial pairwise distance between ROIs was calculated using one minus the linear correlation between the time-courses of 1195 time points extracted from the 19 ROIs at the individual level. Then, we averaged the pairwise distances between ROIs within each group to get the group-level pairwise distances, which were submitted to hierarchical clustering analysis to create a hierarchical cluster tree of the 19 ROIs for each group respectively. The cophenetic correlation coefficient was used to create a dendrogram for each group. The length of each C link in the dendrogram represents the distance between regions/clusters.

2.2.6 Multidimensional scaling analysis

Non-metric multidimensional scaling (MDS) was also used to facilitate visualizing the similarity of ROIs functional response for adults and neonate groups. The non-metric MDS performs non-metric multidimensional scaling on the dissimilarity matrix of item−item (i.e., ROI−ROI dissimilarity matrix) to compute a configuration (Kruskal, 1964). Then, the Euclidean distances between items (i.e., ROIs) in the configuration were obtained. The difference between the monotonic transformed dissimilarities in the item−item (i.e., ROI−ROI) matrix and the Euclidean distances between items (i.e., ROIs) in this configuration were minimized and items (ROIs) were represented in a low-dimensional space (i.e., a 2-D space). The ROI−ROI dissimilarity matrix (one minus the linear correlation between the time-courses) for each group from the hierarchical clustering analysis was submitted to non-metric MDS analysis implemented in MATLAB.

2.3 Results

2.3.1 The development of high-order networks in neonates

For full-term neonates, a 2 × 3 repeated measure ANOVA [type of FC (within-network, between-network) × network (DMN, DAN, ECN)] showed a significant main effect of type of FC (F (1, 281) = 766.14, $p < 0.001$), which was driven by higher overall connectivity for the within- relative to between-network connectivity (t (281) = 27.63, $p < 0.001$) (Figure 2.5A). I also found a main effect of network (F (2, 562) = 16.29, $p < 0.001$), which was driven by lower overall connectivity for the ECN relative to the DMN (t (281) = -3.06, $p < 0.005$) and DAN (t (281) = -5.84, $p < 0.001$). A significant interaction effect of type of FC by network (F (1.96, 550.18) = 81.44, $p < 0.001$) was driven by smaller

difference between within- and between-network connectivity in the DMN relative to the DAN (t (281) = -4.41, $p < 0.001$), and in the ECN relative to the DMN (t (281) = -8.88, $p < 0.001$), and the DAN (t (281) = -11.86, $p < 0.001$). Paired-t tests showed significantly higher within- to between-network FC for each network (DMN: t (281) = 17.32, $p < 0.001$; DAN: t (281) = 21.05, $p < 0.001$; ECN: t (281) = 5.51, $p < 0.001$) (Figure 2.5A). A sensitivity power analysis with $\alpha = 0.05$, a power of 0.8 and a sample size of 282 revealed an effect size of Cohen's $d = 0.17$. This suggested that the coherence of nodes within each network was stronger than with the other networks' nodes, in other words, each of the three networks was differentiated as a cohesive unit, distinct from the other networks.

For preterm neonates scanned at TEA, a similar 2 x 3 repeated measure ANOVA showed a significant main effect of FC type (F (1, 72) = 87.04, $p < 0.001$), which was driven by higher overall connectivity within- relative to between-network connectivity (t (72) = 9.35, $p < 0.001$) (Figure 2.5B). A significant interaction effect of type of FC by network (F (1.81, 130.23) = 6.03, $p < 0.005$), was driven by a smaller difference between within- and between-network connectivity in ECN relative to the DAN (t (72) = -2.96, $p < 0.005$). Paired-t tests showed significantly higher within- relative to between-network FC for each network (DMN: t (72) = 6.20, $p < 0.001$; DAN: t (72) = 8.05, $p < 0.001$; ECN: t (72) = 3.46, $p < 0.001$) (Figure 2.5B), suggesting that the DMN, DAN, and ECN were distinct from the one another in preterm neonates scanned at TEA. A sensitivity power analysis with $\alpha = 0.05$, a power of 0.8 and a sample size of 73 revealed an effect size of Cohen's $d = 0.33$.

For preterm neonates scanned before TEA, a similar 2 x 3 repeated measure ANOVA showed a significant main effect of type of FC (F (1, 72) = 16.80, $p < 0.001$), which was driven by higher overall connectivity for the within- relative to between-network connectivity (t (72) = 4.12, $p < 0.001$) (Figure 2.5C). A main effect of network (F

(1.83,131.64) = 22.15, $p < 0.001$) was driven by lower overall connectivity for the DMN (t (72) = -3.98, $p < 0.001$) and ECN (t (72) = -6.45, $p < 0.001$) relative to the DAN (Figure 2.4C). A significant interaction effect of type of FC by network (F (2, 144) = 33.78, $p < 0.001$) was driven by smaller difference between within- and between-network connectivity in DMN relative to that in DAN (t (72) = -3.93, $p < 0.001$), and in ECN relative to that in DMN (t (72) = -4.32, $p < 0.001$) and DAN (t (72) = -8.21, $p < 0.001$). Paired-t tests showed significantly higher within- relative to between-network FC for DAN (t (72) = 7.73, $p < 0.001$), but significantly lower within-network FC compared to between-network FC for ECN (t (36) = -3.86, $p < 0.001$) (Figure 2.5C), suggesting that only the DAN was distinct from the other two networks in preterm neonates scanned before TEA. The sample size of 73 allows for the detection of significant difference with an effect size of d = 0.33 ($\alpha = 0.05$ and a power of 0.8).

In summary, these results suggested that the DMN, DAN and ECN were present in full-term and preterm neonates scanned at TEA, but only the DAN was formed as a distinct network in the preterm neonates scanned before TEA. Furthermore, the DAN was the most cohesive network in all three neonate groups.

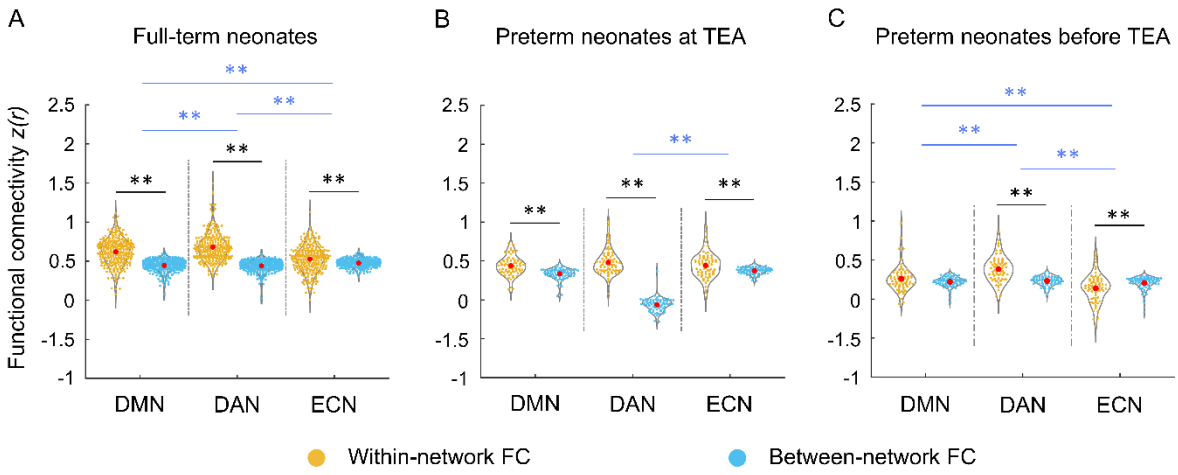

*Figure 2.5 Within-network and between-network functional connectivity across DMN, DAN and ECN in the neonate groups. A) full-term neonates; B) preterm neonates scanned at term-equivalent age (TEA); C) preterm neonates scanned before TEA. The black lines/asterisks indicate significant differences between functional connectivity (FC) measures for each network (Paired-t tests), and the blue lines/asterisks indicate significant differences in FC measures of different networks (Paired-t tests). The FC values were Fisher-z transformed and inter-subject variability was removed for display purposes. Abbreviations: TEA, term-equivalent age; DMN, default mode network; DAN, dorsal attention network; ECN, executive control network; FC, functional connectivity; ** = $p < 0.005$.*

2.3.2 The development of the reciprocal relationship between the DMN and fronto-parietal networks in neonates

In full-term neonates, a one-way ANOVA with repeated measures for between-network FC (DMN−DAN, DMN−ECN, DAN−ECN) showed a significant main effect (F (1.98, 555.60) = 27.11, $p < 0.001$), which was driven by significantly lower FC in the DMN−DAN relative to DMN−ECN (t (281) = -7.79, $p < 0.001$) and DAN−ECN (t (281) = -4.64, $p < 0.001$) pairings (Figure 2.6A). Similarly, to the adult data (Figure 6.6 in

Appendix A), the lower DMN−DAN FC relative to the other pairings suggested that the reciprocal relationship between the DMN and DAN was present in full-term neonates. In preterm neonates scanned at TEA, a similar main effect (F (1.87, 134.45) = 11.93, p < 0.001) was driven by significantly lower FC in the DMN–DAN compared to DMN–ECN (t (72) = -4.78, p < 0.001) and DAN–ECN (t (72) = -4.20, p < 0.001) pairings (Figure 2.6B), and suggested that the reciprocal relationship between the two networks was present in preterm neonates scanned at TEA. In preterm neonates scanned before TEA, a significant main effect (F (2, 144) = 4.86, p = 0.009) was driven by lower FC in DMN−ECN relative to DMN−DAN (t (72) = -2.88, p = 0.005) and DAN−ECN (t (72) = -2.94, p < 0.005) pairings (Figure 2.6C). This is consistent with aforementioned results suggesting that the DMN and ECN are not yet developed as distinct networks in this group (Figure 2.6C). Furthermore, these results suggested that, by contrast to the full-term and preterm neonates scanned at TEA, the relationships between the three networks in preterm neonates scanned before TEA do not yet resemble the adult pattern (see Figure 6.6 in Appendix A). In summary, these results suggested that the reciprocal relationship between the DMN and DAN has started to develop in full-term neonates and preterm neonates scanned at TEA, but not in preterm neonates scanned before TEA.

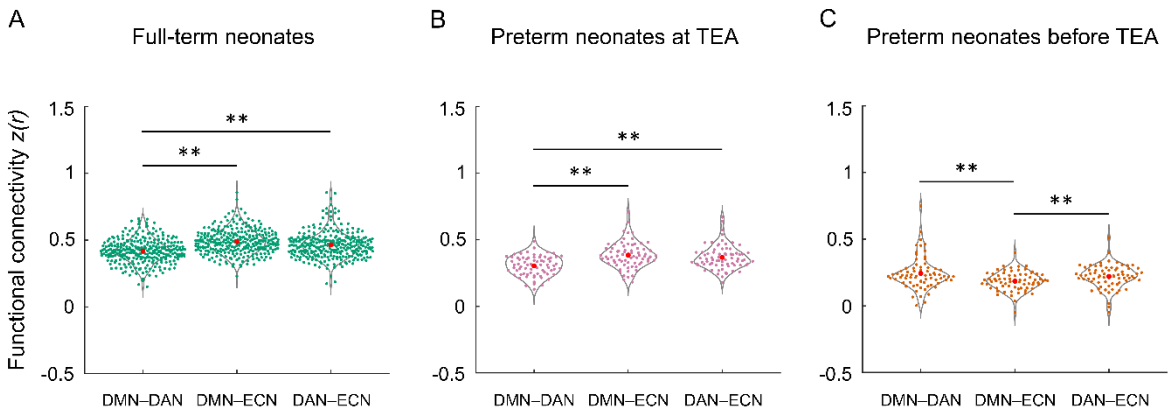

*Figure 2.6 Between-network functional connectivity in neonate groups. a) full-term neonates; b) preterm neonates scanned at term-equivalent age (TEA); c) preterm neonates scanned before TEA. One-way ANOVAs with repeated measures and Paired-t tests were used here. The FC values were Fisher-z transformed and inter-subject variability was removed for display purposes. Abbreviations: TEA, term-equivalent age; DMN−DAN, FC between the default mode network and dorsal attention network; DMN−ECN, FC between the default mode network and executive control network; DAN−ECN, FC between the dorsal attention network and executive control network; ** = p < 0.005.*

2.3.3 Comparison of neonate and adult networks

Visual inspection of the connectivity matrices (Figure 2.7) suggested that each neonate group had less cohesive networks (lower within-network relative to between-network connectivity) than the adult group. To investigate specifically how the three networks in neonates differed from those of adults, I compared the within- (Figures 2.8 and 2.9) and between-network (Figure 2.10) connectivity in the neonate and adult groups.

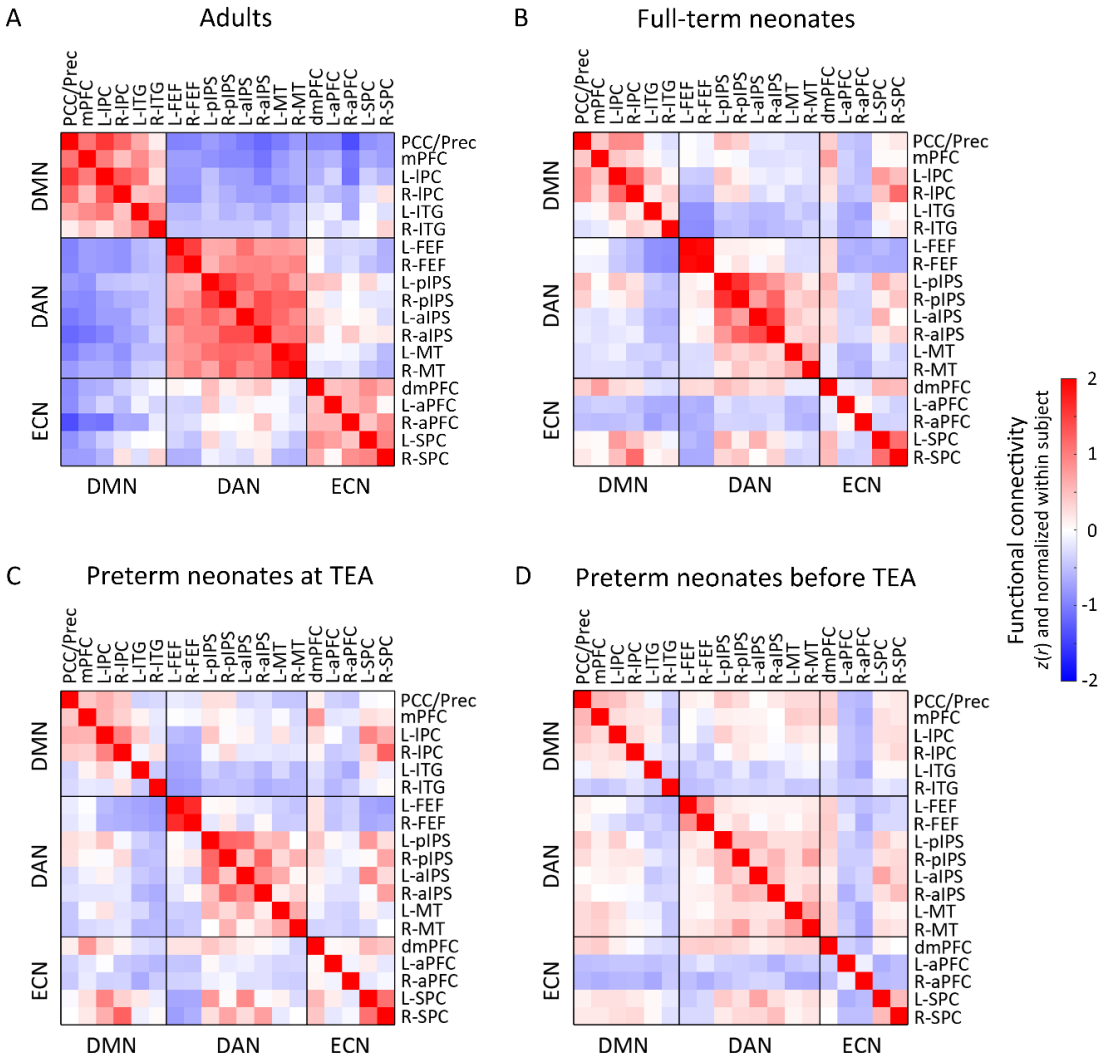

Figure 2.7 Functional connectivity (FC) in adults and neonate groups. a) adults, b) full-term neonates, c) preterm neonates scanned at term-equivalent age (TEA) and d) preterm neonates scanned before TEA. The FC value presents here was Fisher-z transformed and normalized within each subject before being averaged within each group. Blue–red indicates low–high values. Abbreviations: TEA, term-equivalent age; DMN, default mode network; DAN, dorsal attention network; ECN, executive control network; R, right; L, left; PCC/Prec, posterior cingulate cortex/precuneus; mPFC, medial prefrontal cortex; lPC, lateral parietal cortex; ITG, inferior temporal gyrus; FEF, frontal eye field; pIPS, posterior intraparietal sulcus; aIPS, anterior intraparietal sulcus; MT, middle temporal area; dmPFC, dorsal medial prefrontal cortex; aPFC, anterior prefrontal cortex; SPC, superior parietal cortex.

A GLM comparing adults and full-term neonates, including head motion as a covariate, showed a significant main effects of group for all of the three networks (DMN: F (1, 455) = 75.62, $p < 0.001$); DAN: F (1, 455) = 333.33, $p < 0.001$); ECN: F (1, 455) = 135.88, $p < 0.001$); Figure 2.8A), which was driven by significantly higher within-network FC in the adults relative to full-term neonates. A sensitivity power analysis revealed that a total sample size of 458 is sensitive enough to detect significant difference with an effect size of Cohen's $d = 0.26$ ($\alpha = 0.05$ and a power of 0.8). Hierarchical clustering analyses showed that, the adults' network nodes grouped neatly into the a-priory postulated three distinct clusters (Raichle, 2011), each comprising all the ROIs belonging to that network (See Table 6.3 in Appendix A). By contrast, in the full-term neonates, the ROIs clustered into groups that were inter-mixed between the three networks (Figure 2.8A). Similarly, for the preterm neonates scanned at TEA, I found significant main effects of group for all of the three networks (DMN: F (1, 246) = 90.16, $p < 0.001$); DAN: F (1, 246) = 252.32, $p < 0.001$); ECN: F (1, 246) = 42.40, $p < 0.001$); Figure 2.8B), again driven by significantly higher within-network FC in the adult group. Unlike the adult group, preterm ROIs clustered into groups inter-mixed between the three networks (Figure 2.8B). Consistent with the other two groups' results, for the preterm neonates scanned before TEA, I found significant main effects of group for all of the three networks (DMN: F (1, 246) = 145.15, $p < 0.001$; DAN: F (1, 246) = 276.15, $p < 0.001$; ECN: F (1, 246) = 218.91, $p < 0.001$; Figure 2.8C), which were driven by significantly higher within-network FC in adults, and ROI clusters that did not adhere to network identity (Figure 2.8C).

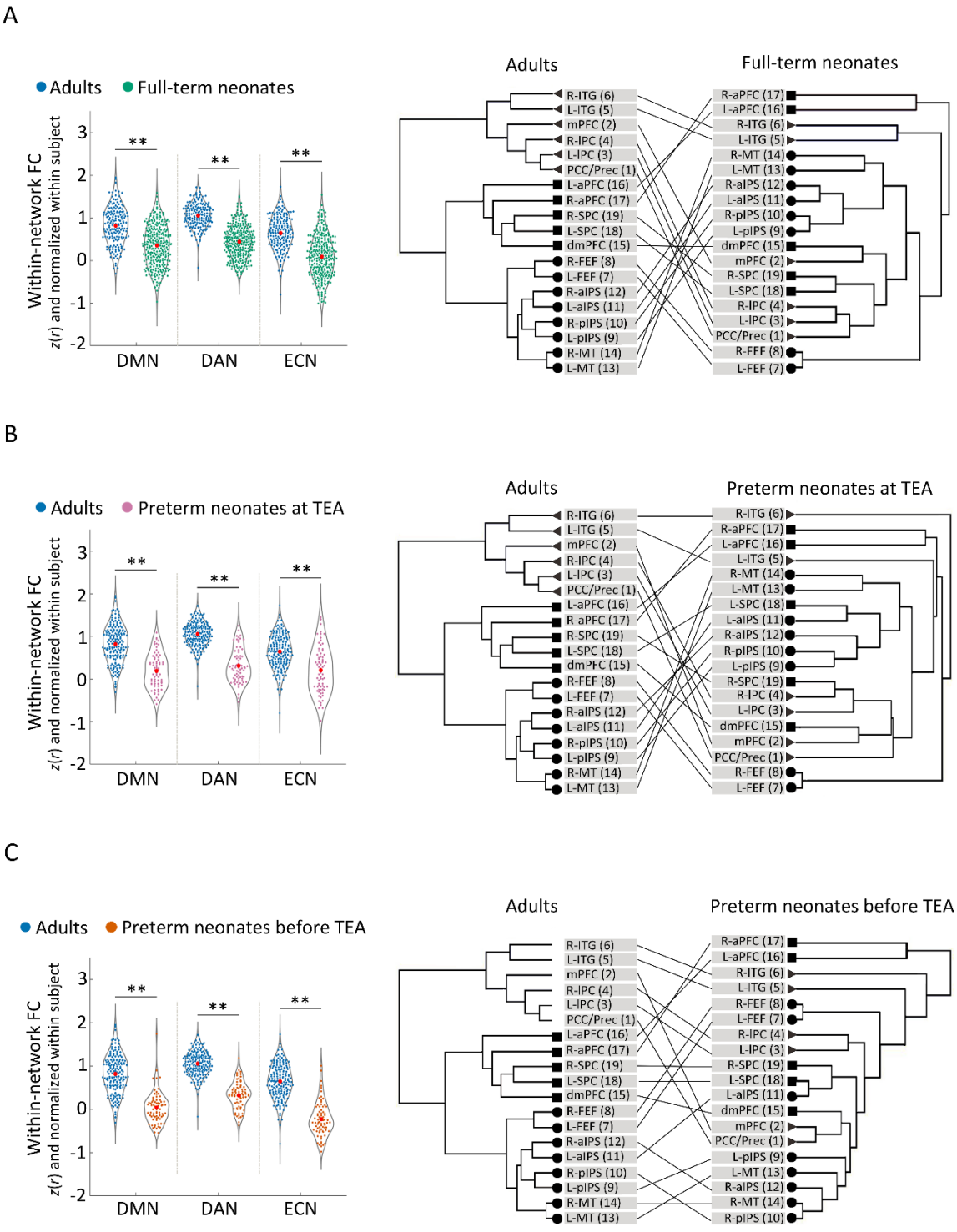

Figure 2.8 The development of the DMN, DAN and ECN in neonates relative to adults. (A) full-term neonates, (B) preterm neonates scanned at TEA and (C) preterm neonates scanned before TEA relative to the adults. The left panels of (A), (B) and (C) depict the comparison of within-network FC between each neonate group and the adults. GLMs were used to test for group differences while controlling for head motion. The FC values were Fisher-z transformed and normalized within each subject before being averaged within

*each group. The right panels of (A), (B) and (C) depict the network structure of each neonate group relative to adults. Triangles/circles/squares represent the nodes of the DMN/DAN/ECN. R, right; L, left; PCC/Prec, posterior cingulate cortex/precuneus; mPFC, medial prefrontal cortex; lPC, lateral parietal cortex; ITG, inferior temporal gyrus; FEF, frontal eye field; pIPS, posterior intraparietal sulcus; aIPS, anterior intraparietal sulcus; MT, middle temporal area; dmPFC, dorsal medial prefrontal cortex; aPFC, anterior prefrontal cortex; SPC, superior parietal cortex. **, p <0.005.*

Multidimensional scaling analyses further confirmed these results, by showing that the adult ROIs formed three distinct clusters conforming to network identify (Figure 2.9A), distanced from one another in representational space. By contrast, each network's ROIs in the neonate groups formed less distinct clusters, i.e., clusters were more closely grouped together, and their separability as distinct clusters was reduced with neonate age. The preterm neonates scanned before TEA showed the most intermingling of ROIs across the three networks in this two-dimensional manifold (Figure 2.9D).

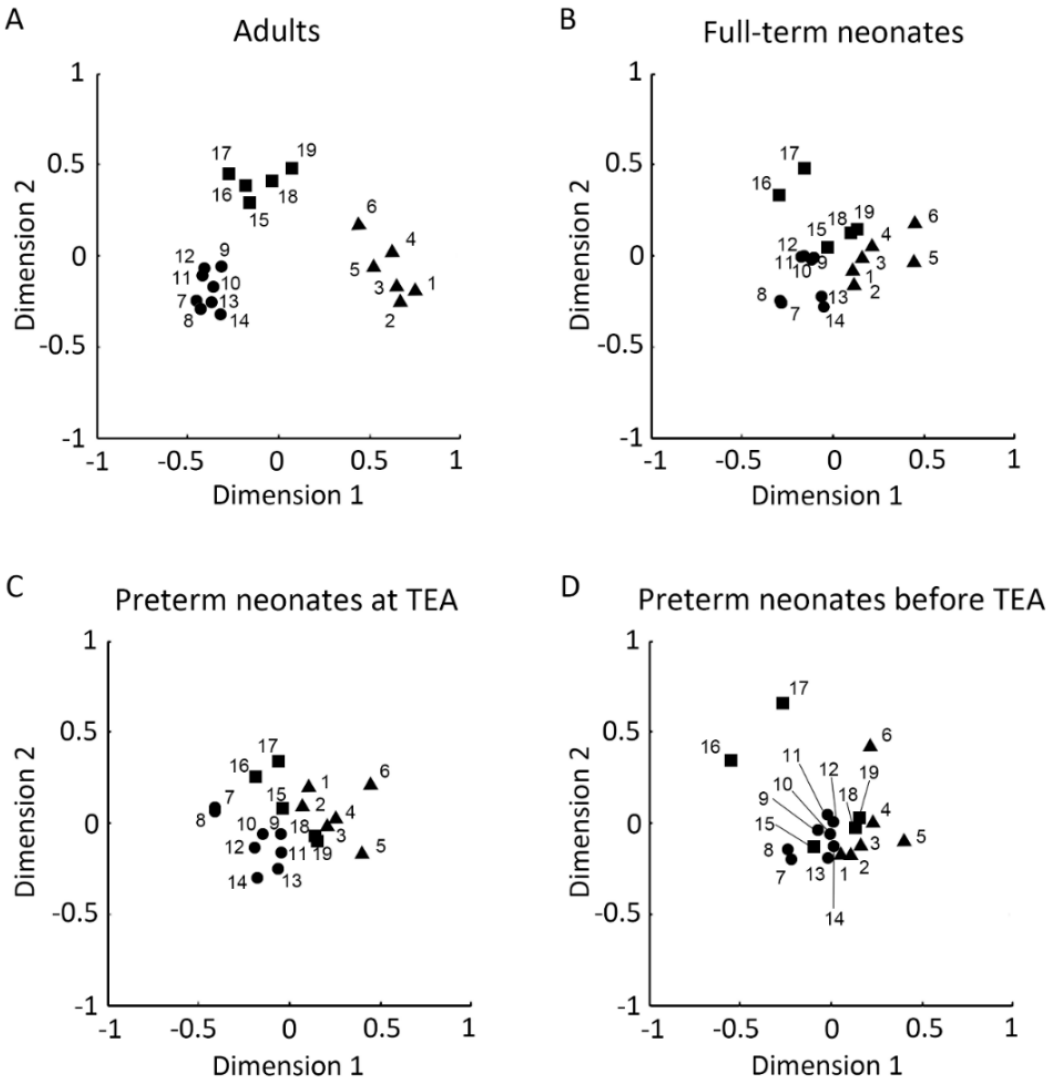

Figure 2.9 Multidimensional scaling (MDS) plots of regions in adults and neonates. a) adults, b) full-term neonates, c) preterm neonates scanned at term-equivalent age (TEA) and d) preterm neonates scanned before TEA. The 2-D plots were created using nonmetric MDS based on node's similarity. Here triangles/circles/squares indicate nodes of the default mode/dorsal attention/executive control network. Abbreviations: 1, posterior cingulate cortex/precuneus; 2, medial prefrontal cortex; 3, left lateral parietal cortex; 4, right lateral parietal cortex; 5, left inferior temporal gyrus; 6, right inferior temporal gyrus; 7, left frontal eye field; 8, right frontal eye field; 9, left posterior intraparietal sulcus; 10, right posterior intraparietal sulcus; 11, left anterior intraparietal sulcus; 12, right anterior intraparietal sulcus; 13, left middle temporal area; 14, right middle temporal area; 15, dorsal medial prefrontal cortex; 16, left anterior prefrontal cortex; 17, right anterior prefrontal cortex; 18, left superior parietal cortex; 19, right superior parietal cortex; TEA, term-equivalent age.

In summary, these results suggested that although the three networks were present in full-term and preterm neonates scanned at TEA, and the DAN in preterm neonates scanned before TEA, their coherence was lower and structure less well-organised than the canonical adult networks. This is consistent with previous studies showing that brain networks continue to develop from birth onwards (Cusack et al., 2016; Doria et al., 2010; Keunen et al., 2017; Limperopoulos et al., 2005; Turk et al., 2019).

As expected, the reciprocal relationship between the DMN and fronto-parietal networks was also weaker in neonates relative to adults (Figure 2.10). For full-term neonates, we found significant main effects of group for all of the pairings (DMN−DAN: F (1, 455) = 278.77, $p < 0.001$; DMN−ECN: F (1, 455) = 195.83, $p < 0.001$; DAN−ECN: F (1, 455) = 15.59, $p < 0.001$), which was driven by significantly lower FC in DMN−DAN and DMN−ECN, and higher FC in DAN−ECN in the adults related to full-term neonates (Figure 2.10A). These results suggested that the DMN was more functionally differentiated from the DAN and ECN, and thus, suggesting a stronger reciprocal relationship in adults relative to full-term neonates. For preterm neonates scanned at TEA, we found a significant main effect of group for DMN−DAN (F (1, 246) = 105.83, $p < 0.001$), DMN−ECN (F (1, 246) = 91.39, $p < 0.001$), which was driven by significantly lower FC in DMN−DAN and DMN−ECN in the adults related to preterm neonates scanned at TEA (Figure 2.10B). A sensitivity power analysis revealed that a total sample size of 355 is sensitive enough to detect significant difference with an effect size of Cohen's d = 0.30 (α = 0.05 and a power of 0.8). Similarly, to full-term neonates, these results demonstrated that the DMN was more functionally differentiated from DAN and ECN, suggesting a stronger reciprocal relationship in adults relative to preterm neonates scanned at TEA. We also compared between-network connectivity in preterm neonates scanned before TEA and adults using a GLM that controlled for head motion, although we did not observe a

reciprocal relationship between DMN and frontoparietal network in that neonate group. We found a significant main effect of group for DMN−DAN (F (1, 246) = 257.78, p < 0.001) and DMN−ECN (F (1, 246) = 45.54, p < 0.001), which was driven by significantly lower FC in DMN−DAN and DMN−ECN in the adults relative to the preterm neonates scanned before TEA (Figure 2.10C). A sensitivity power analysis revealed that a total sample size of 355 is sensitive enough to detect significant difference with an effect size of Cohen's d = 0.30 (α = 0.05 and a power of 0.8).

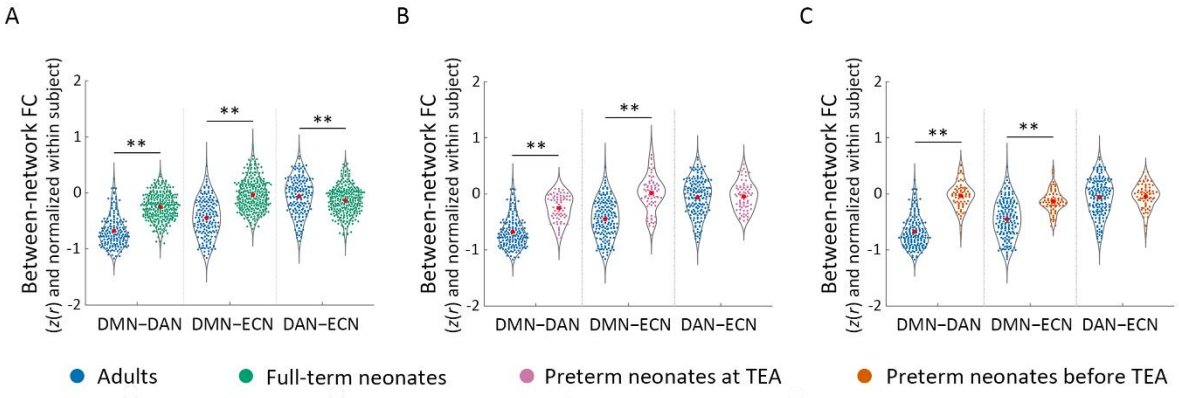

*Figure 2.10 The development of the between-network functional connectivity (FC) in neonates relative to adults. a) full-term neonates, b) preterm neonates scanned at term-equivalent age (TEA) and c) preterm neonates scanned before TEA relative to the adults. General linear models were used to test for group differences while controlling for head motion. The FC values were Fisher-z transformed and normalized within each subject before averaging within each group. Abbreviations: FC, functional connectivity; DMN−DAN, FC between DMN and DAN; DMN−ECN, FC between DMN and ECN; DAN−ECN, FC between DAN and ECN; ** = p < 0.005.*

2.3.4 The effect of premature birth on network development and their relationship

Comparison of network FC in full-term relative to preterm neonates scanned at TEA showed significantly lower FC within the DMN (t (353) = -2.64, p = 0.009) and the DAN (t (353) = -2.63, p = 0.009) in the preterm group (Figure 2.11A). In addition, I observed higher FC between the DAN and ECN (t (353) = 2.83, p = 0.005) in preterm neonates (Figure 2.11A). A sensitivity power analysis revealed that this analysis is sensitive enough to detect significant difference with an effect size of Cohen's d = 0.37 (α = 0.05 and a power of 0.8). These results suggested that, by term-equivalent age, premature birth is associated with lower DMN and DAN network coherence, and lower differentiation of the DAN and ECN from one another, relative to full-term birth.

2.3.5 The effect of neonate age on network development and their relationship

I found significantly lower FC within the ECN (t (36) = -4.28, $p < 0.001$) and higher DMN–DAN FC (t (36) = 4.39, $p < 0.001$), suggesting lower ECN network coherence and lower functional differentiation between the DMN and DAN, for preterm neonates scanned before TEA relative to this same group of infants scanned once they reached TEA (Figure 2.11B). A sensitivity power analysis revealed that this analysis is sensitive enough to detect significant difference with an effect size of Cohen's d = 0.47 (α = 0.05 and a power of 0.8). Thus, these results suggested that neonate age, and particularly, development up to term-equivalent age, is a significant factor for the maturation of the ECN and of the development of the reciprocal relationship between the DMN and the DAN.

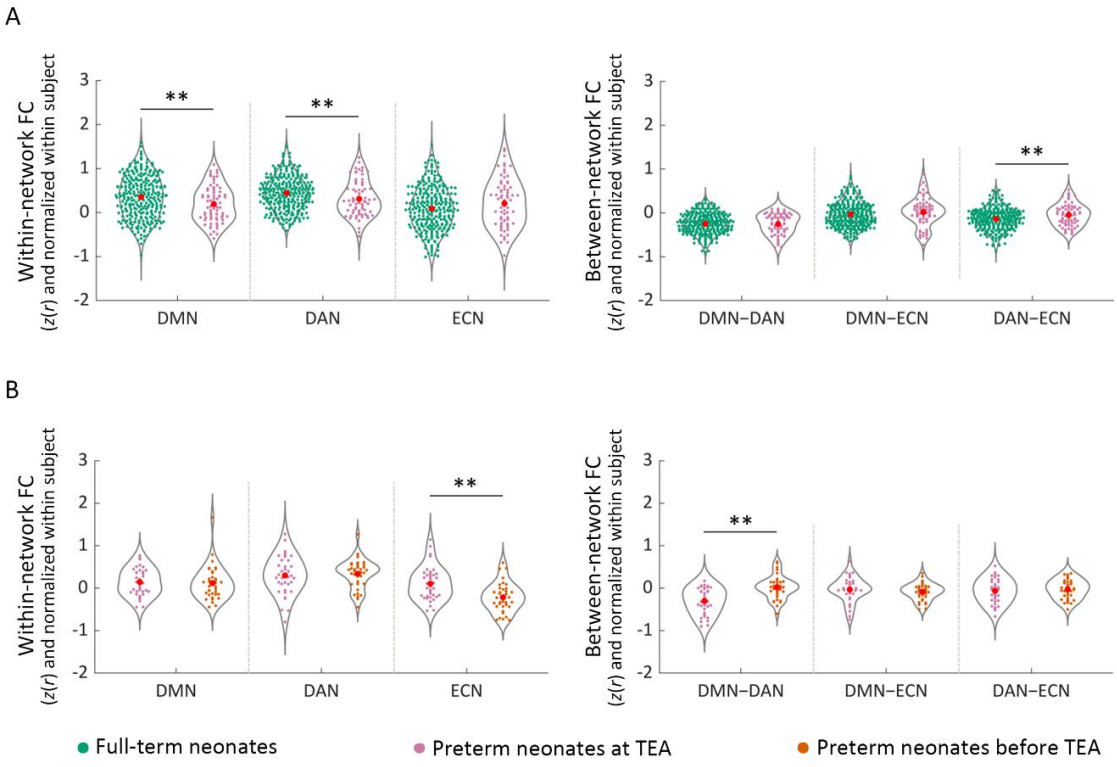

*Figure 2.11 The effect of premature birth and early neonate age on the development of network functional connectivity (FC). a) The effect of premature birth on a-i) within-network FC and a-ii) between-network FC. The FC values represented in a-i) and a-ii) were Fisher-z transformed and normalized within each subject before averaging within each group. Independent-sample t-tests were applied to detect the effect of premature birth here. b) The effect of early neonate age on b-i) within-network FC and b-ii) between-network FC. The FC values represented in b-i) and b-ii) were Fisher-z transformed, normalized within each subject, and inter-subject variability was removed for display purposes. Paired-t tests were applied to detect the effect of early neonate age here. Abbreviations: DMN, default mode network; DAN, dorsal attention network; ECN, executive control network; DMN−DAN, FC between DMN and DAN; DMN−ECN, FC between DMN and ECN; DAN−ECN, FC between DAN and ECN; ** = $p < 0.005$.*

2.4 Discussion

In this study, I examined whether or not the brain circuitry of conscious awareness is developed at birth. In particular, I focused on the impact of premature birth and early neonate age on the development of the default mode and fronto-parietal networks, and of their reciprocal relationship. The critical novel contribution of this study is showing that the DAN, ECN and DMN are already present in neonates by full-term or term-equivalent age, and furthermore, that the reciprocal relationship between the DMN and the DAN, is already instantiated by this age. By contrast, this relationship is not present in preterm neonates before term-equivalent age.

2.4.1 Effect of premature birth

I found that the three networks were present in preterm neonates at TEA. Furthermore, for the first time, I showed that the reciprocal relationship between the DAN and DMN was instantiated in preterm neonates at TEA. Previous rs-fMRI neonate studies that have investigated the effect of premature birth have mainly focused on disrupted within-network coherence or topological organization (Cao, Huang, et al., 2017; Eyre et al., 2021; Smyser et al., 2016; van den Heuvel et al., 2015), and knowledge of the impact of premature birth on the relationship between high-order brain networks remains scarce. It is, therefore, striking to see that this key functional relationship develops in healthy-born premature neonates by term-equivalent age, according to a pre-programmed developmental trajectory despite prematurity.

However, premature birth had a negative impact on network development. Preterm neonates at TEA had significantly lower within-network connectivity in the DMN and DAN, suggesting that these networks were less developed relative to full-term neonates despite the matched age. Furthermore, the DAN–ECN connectivity was higher in preterm neonates at TEA, likely due to weaker within-network connectivity in the DAN. My results are consistent with Smyser et al. (2016) and Eyre et al. (2021) findings of lower within-network connectivity in preterm relative to full-term neonates. Bouyssi-Kobar et al. (2019) showed decreased density of connections in parietal-temporal and frontal areas in preterm neonates scanned at TEA relative to full-term neonates, using graph theoretical modelling. Previous structural MRI studies also found widespread deficiencies in grey and white matter (Bouyssi-Kobar et al., 2018; Pandit et al., 2014), including in the DMN regions, in preterms scanned at TEA relative to full-term neonates (Bouyssi-Kobar et al., 2018). Consistent with a growing literature, my results shed light on disrupted brain mechanisms that may underlie the significant risks for neurodevelopmental and psychiatric problems in later life (Bhutta et al., 2002; Marlow et al., 2005; Nosarti et al., 2012; Saigal & Doyle, 2008), that are associated with premature birth.

2.4.2 Impact of neonate age on network development

In contrast to preterm neonates assessed at TEA, neonates who were assessed before TEA showed dramatic underdevelopment of networks and their relationships. Only the DAN, but not the ECN and DMN, was present as a discrete network. Strengthening of within-network connectivity in fronto-parietal regions has been reported in previous studies that assessed preterm neonates longitudinally (He & Parikh, 2016). These findings suggest that relative to other high-order networks, e.g., the DMN, the ECN aspect of the fronto-parietal

networks is the least developed in preterms and most liable to undergo developmental change in the early weeks post-birth. Furthermore, the reciprocal relationship between the fronto-parietal and DMN networks also strengthened in the weeks up to term-equivalent age. It was not formed before TEA, but appeared once preterms reached TEA. These results present a novel finding for premature neonates. They resonate with fetal studies showing that coactivation from the posterior cingulate cortex (node of the DMN) to areas of dorsal attention/executive networks became more negatively coupled with increasing fetal age (Thomason et al., 2014; Thomason et al., 2015).

2.4.3 Comparison of neonate and adult networks

On the one hand, it is important to note that although the DAN, ECN and DMN were already present at full-term and term-equivalent age, they were significantly different from the adult networks. The neonate networks had significantly lower within-network connectivity and were atypical in their nodal structure, suggesting less within-network cohesiveness compared to the adults'. Similarly, the reciprocal relationship between the DMN and DAN was less developed in neonates relative to adults. These findings are consistent with previous studies showing that the functional organization of the brain rapidly develops from birth onwards (Fair et al., 2007; Gao et al., 2009; Sherman et al., 2014). For example, Gao et al. (2009) reported that the DMN becomes adultlike by 2 years of age. A developmental shift towards the adult pattern of high functional connectivity variability in high-order networks has been reported for the DAN and frontoparietal networks, which can be predicted by developmental cortical expansion (Stoecklein et al., 2020). Studies have also reported significant differences in segregation and integration,

indicators of functional network maturation, in the DMN and ECN between childhood and adulthood (Fair et al., 2008; Fair et al., 2007; Sherman et al., 2014).

Of the three high-order networks, the ECN was the least developed in premature neonates, whereas the DAN was the most well-formed across all neonate groups. These results suggest different ontogenesis trajectories for the two fronto-parietal networks, likely explained by their differing functions. The DAN serves to orient and modulate attention to the saliency of incoming sensory inputs (Corbetta & Shulman, 2002), a capacity that probably emerges early in fetal development, as foetuses start to perceive sounds inside the womb. By contrast, behavioural response planning and monitoring, subserved by the ECN (Kroger et al., 2002), is a mental faculty that relies heavily on the increasingly complex interactions with their environment that neonates engage in as they mature from the first weeks and months after birth.

On the other hand, my results show a strikingly similar patterning of the neonatal brain to the adult brain, with three key high-order brain networks and the reciprocal relationship between them being present by term-equivalent age. My results in full-term neonates resonate with previous studies that observed high-order networks in this group (Doria et al., 2010; He & Parikh, 2015, 2016; Linke et al., 2018; Rajasilta et al., 2020). My results are also consistent with some brain structural studies, suggesting that fundamental structural features of the adult brain are already present in neonates from birth. For example, the white matter microstructure, a putative neural basis for information processing speed and intelligence in adults, is present in very early life (Telford et al., 2017). Furthermore, distinct hierarchical tiers of network nodes resembling those of the adult brain have been found in neonates (Blesa et al., 2021), and graph theoretical measures have shown an efficient rich club organization of the neonatal brain structure similar to that observed in adults (Ball et al., 2014).

2.4.4 Summary

In summary, for the first time, I showed that the reciprocal relationship between the DMN and DAN was present at full-term birth or term-equivalent age. Although different from the adult networks, the DMN, DAN and ECN were present as distinct networks at full-term birth or term-equivalent age, but premature birth was associated with network disruption. By contrast, prior to TEA, neonates showed dramatic underdevelopment of high-order networks. These results suggest that, by TEA, but not before, infants possess key features of the neural circuitry that enables integration of information across diverse sensory and high-order functional modules, giving rise to conscious awareness. These findings shed light on the ontogeny of high-order brain networks and their relationship.

2.4.5 Methodological consideration

Although some previous studies have observed high-order networks in neonates (Doria et al., 2010; He & Parikh, 2015, 2016; Linke et al., 2018; Rajasilta et al., 2020), others have not (Fransson et al., 2007; Gao, Alcauter, Elton, et al., 2015; Gao, Alcauter, Smith, et al., 2015). This inconsistency is likely due to methodological differences in the type of data acquired and the analyses method. By contrast to some previous studies (Fransson et al., 2007; Gao, Alcauter, Elton, et al., 2015; Gao, Alcauter, Smith, et al., 2015), here we were enabled by the high quality dHCP dataset to employ a uniquely large sample of high temporal and spatial resolution infant rs-fMRI data, and accurate week-by-week structural templates of the developing infant brain, which ensured higher sensitivity to detect brain networks in early infancy. Second, I used a theoretically motivated region-of-interest

analysis rather than a data-driven independent component analysis (ICA) for network definition. While ICA is a convenient data-driven tool to extract networks, it requires a critical free parameter that determines how many will be extracted, and hence the degree to which brain networks are likely to be detected as whole versus broken into parts. For example, a recent paper by Eyre et al. (2021), that used the dHCP dataset, did not find a single network corresponding to the whole DMN, but it is possible that this result would have changed with a different parameter choice. Given these methodological strengths and clear results, we believe this study helps to resolve previous inconsistent findings on the development of high-order brain networks in neonates.

3. Chapter 3: Typical and disrupted small-world architecture and regional communication in full-term and preterm infants

3.1 Introduction

A fundamental property of conscious experiences is that they are both differentiated and integrated (Cooney & Gazzaniga, 2003; Deco et al., 2015; Seth, 2009; Seth et al., 2006; Tononi & Edelman, 1998). The balance of differentiation and integration, which prima facia appear to be opposed, is postulated to be a key feature of consciousness (Seth et al., 2006; Tononi & Edelman, 1998). Functional brain networks display a so-called 'small-world' organization, which can sustain this fine-tunned balance, through dense within-network connections that facilitate specialized processes, and sparse between-network connections that enhance global information integration (Bassett & Bullmore, 2006; Bassett & Bullmore, 2017). This network architecture is shown to increase the resistance to insult (Achard & Bullmore, 2007), and facilitate efficient and cost-effective information transfer (Papo et al., 2016; Takagi, 2018, 2020; Tan & Cheong, 2017). Studies have found that small-world organization is modulated by consciousness state manipulations i.e., by sleep or anaesthesia (Barttfeld et al., 2015; Luppi, Golkowski, et al., 2021), and by consciousness perturbations after brain injury (Duclos et al., 2021; Luppi et al., 2019), further providing empirical evidence that small-world organization facilitates conscious information processing. For example, Luppi et al. (2019) observed that patients with disorders of consciousness (i.e., in the unresponsive wakefulness syndrome/vegetative state, or the minimally conscious state) displayed reduced small-world characteristics relative to awake healthy volunteers. These studies have led to a broad consensus that small-word organization supports complex cognition and consciousness in human adults

(see Coppola et al., (2022); Monti et al., (2013); Schröter et al., (2012) for a divergent view).

It remains unknown how functional small-world architecture develops with young infant age at birth and how it is affected by prematurity. Understanding the development of small-world architecture can elucidate not only the ontogeny of brain development, but also whether the capacity for conscious awareness, that this architecture supports, is present at birth. A literature search in PubMed with keywords 'small-world architecture' or 'small worldness' or 'small-world propensity', 'infant' or 'newborn' or 'neonate' and 'fMRI' or 'functional imaging,' revealed very few studies delivering inconsistent findings (Table 3.1). A handful have suggested that the small-world architecture is present in full-term born neonates (Table 3.1: Bouyssi-Kobar et al., 2019; Gozdas et al., 2018; Asis-Cruz et al., 2015; Omidvarnia et al., 2014; Fransson et al., 2011), but the index (σ) (Humphries & Gurney, 2008) used to quantify small-world properties in these studies has been criticised (Bassett & Bullmore, 2017; Papo et al., 2016; Telesford et al., 2011), due to a high false-positive rate (Telesford et al., 2011). In addition, the small sample size (N = 10 to 66) and low temporal and spatial resolution limit their results' reliability. The effects of premature birth on small-world organization has, to the best of our knowledge, been investigated only in four studies examining neonates at term-equivalent age (TEA, postmenstrual age of 37 weeks) (Table 3.1: Bouyssi-Kobar et al., 2019; Gozdas et al., 2018), and two studies of neonates before TEA (Table 3.1: Cao, He et al., 2017; Omidvarnia et al., 2014), with very small samples (N = 11 to 66). These studies have offered inconsistent results, including stronger, weaker or no difference in small-worldness due to prematurity, likely due to different neuroimaging techniques, different brain atlases, and very small sample sizes.

Furthermore, a big gap remains in understanding of the effect of prematurity on integration and segregation at the brain regional level in neonates, especially given the varying developmental rates of different brain regions. For example, Doria et al., (2010) observed medial visual, auditory, somatosensory, motor, cerebellum, brainstem and thalami and default mode in neonates at 30 weeks of age, but not lateral visual, dorsal visual stream, executive control networks until 34 weeks of age. The interhemispheric connectivity in motor, somatosensory, default mode, and executive control networks increased with increasing age from 28 to 44 weeks of age, whereas that of the visual cortex decreased with increasing age. Before TEA, the dorsal attention network is present in preterm neonates, while the default mode network and executive network are dramatically underdeveloped at this time (Hu et al., 2022). Premature birth, in and of itself, has also been associated with differential atypical development of functional architecture within and across brain networks (Allievi et al., 2016; Fenn-Moltu et al., 2023; Hu et al., 2022). However, the effects of early age and prematurity have not been dissociated in previous studies.

To address these gaps, we first investigated whether small-world organization was developed at birth, and how it was affected by prematurity and neonate age across the brain. We then asked how the balance of segregation and integration at the regional level were affected by premature birth and neonate age. To address the limitations of previous studies, we used rs-fMRI data from the largest open-source neonate dataset, the Developing Human Connectome Project (dHCP), which conferred several advantages, including a large sample size (N = 278), 3T magnetic resonance imaging (MRI) multiband echo-planar imaging (EPI), that significantly improves temporal resolution and signal-to-noise ratio relative to sequences used in previous studies (Zhang et al., 2019), registration to more accurate week-to-week neonate structural templates, and significant improvements

in motion correction (see Methods for further details). We also included a large reference adult group (N = 176) from the Human Connectome Project. The effect of chronological age at the time of assessment was deconfounded from the effect of premature birth (Bhutta et al., 2002) by the inclusion of two groups: the first (N = 72) born before and scanned at TEA, and the second (N = 70) born and scanned before TEA. A subset of paired scans collected from the same infants (N = 33) both before, and at TEA, was also included. The balance of segregation and integration was assessed with rigorous measures of small-world architecture (Muldoon et al., 2016) across the brain, and with measures of nodal efficiency (Achard & Bullmore, 2007) at the regional level. Based on my findings on the effects of premature birth on the development of high-order brain networks in Chapter 2 (Hu et al., 2022), we tested the following hypotheses: (a) small-world organization would be developed at birth, (b) relative to full-term birth, premature birth would be associated with altered small-world architecture and nodal efficiency, and (c) that some alterations in these measures would persist as preterm neonates reached TEA.

Table 3.1 A summary of functional imaging studies that investigated the development of small-world architecture in neonates.

Technique	Studies	Age at scan (PMA, weeks) 25 35 45 55 65 75 85	Number of participants	State during scan	Scanner	Network type	Atlas	Thresholds	Main findings
fMRI	Argyropoulou et al., (2022)		10 10	Under sedation	1.5 T	B	UNC	0.15	σ > 1
	Bouyssi-Kobar et al., (2019)		66 66	Unsedated	3T	B	AAL	0.18:0.01:0.48	σ > 1 γ: full-term > preterm λ: full-term < preterm
	Gozdas et al., (2018)		24 51	Unsedated	3T	B	AAL	0.06:0.01:0.3	σ > 1 σ: preterm > full-term
	Cao et al., (2017)		40	Unsedated	3T	B & W	Voxelwise	0.05	σ > 1
	Asis-Cruz et al., (2015)		60	Unsedated	3T	B	UNC	0:0.025:0.45	σ > 1
	Fransson et al., (2011)		18	Unsedated	1.5 T	B	Voxelwise	0.2:0.05:0.4	σ > 1
	Gao et al., (2011)		51	Unsedated	3T	W	AAL	highest 1% – 50% according to *p*-value	σ > 1 γ increase with age λ decrease with age
EEG	Omidvarnia et al., (2014)		11 10	Unsedated	-	W	Data-specific atlas (Fransson et al., 2012)	0.05	σ > 1 σ: No difference γ: full-term > preterm

The first column shows what functional imaging technique the study used. The second column shows a reference to the study. The third column shows the neonates' age at scan in post-menstrual weeks for studies without an asterisk and post-birth weeks plus 40 for studies with an asterisk. Different colours label different groups. Green/pink/brown indicates full-term neonates/preterm neonates scanned at TEA/preterm neonates scanned before TEA, and grey indicates mixed neonates from more than one group. A "blurry" box with normally distributed transparency depicts the mean and standard deviation of the neonates' age, and a box with even transparency shows an age range. $\sigma > 1$ indicates that the neonate's brains exhibit a strong small-world architecture. Abbreviations: PMA, postmenstrual age in weeks; B, Binary; W, weighted; σ, small-worldness; γ, normalized clustering coefficient; λ, normalized characteristic path length.

3.2 Materials and methods

3.2.1 Participants

Neonates. The neonate data used in Chapter 2 were also used in the current Chapter. To further minimise the effects of head motion on my results, I additionally excluded neonates whose mean framewise displacement (after the scrubbing procedure) were larger than 0.5 mm. Thus, 4 full-term neonates, 1 preterm neonate scanned at TEA, and 3 preterm neonates scanned before TEA were excluded (Figure 3.1). The final analysis samples comprised 278 full-term neonates (GA at birth = 39.9 weeks ± 8.6 days; PMA at scan = 41.2 weeks ± 12.2 days; 119 females) after quality control procedures. 72 scans from the preterm neonates at TEA (GA at birth = 32.1 weeks ± 25.5 days; PMA at scan = 40.9 weeks ± 14.6 days; 32 females) and 70 scans from the preterm neonates before TEA (GA at birth = 32.5 weeks ± 20.7 days; PMA at scan = 34.7 weeks ± 12.7 days; 22 females) were included. I also included a subset of paired scans collected from the same preterm infants (N = 33, GA at birth = 32.2 weeks ± 20.1 days) at (PMA at scan = 41.0 weeks ± 10.16 days) and before TEA (PMA at scan = 34.5 weeks ± 11.5 days) to investigate the effects of neonate age. Further details on inclusion criteria are shown in Figure 3.1 and details on demographic information can be found in Table 3.2.

Adults. The same adult group used in the Chapter 2 was included in the current chapter. Details on inclusion criteria and demographic information can be found in Chapter 2 Section 2.2.1.

The effect size for the difference between adults and neonates could not be estimated directly from previous work, since no studies compared small-world architecture between them. Therefore, I conducted sensitivity power analyses for all the comparisons between adults and

neonates. A previously published work (Omidvarnia et al., 2014) has found an effect size of Cohen's $d = 1.26$ for the difference in small-world properties between full-term neonates and preterm neonates before TEA. A power analysis in G*Power (Faul et al., 2009) with Cohen's $d = 1.26$, $\alpha = 0.05$ and a power of 0.8 suggested that a total sample size of at least 34 (27 full-term neonates and 7 preterm neonates before TEA) was required to detect an existing difference between these two groups. Therefore, the sample size of the current study (278 full-term neonates and 70 preterm neonates before TEA) would have sufficient power. Nevertheless, sensitivity power analyses were applied to all the comparisons between full-term neonates and preterm neonates.

Table 3.2 Information obtained from the Developing Human Connectome Project for scans used in the present study.

Group	Sex	Birth age (GA, weeks ± days)	Scan age (PMA, weeks ± days)	Birth weight (Kg)
Full-term neonates	159M/119F	39.9 ± 8.6	41.2 ± 12.2	3.35 ± 0.54
Preterm neonates scanned at TEA	40M/32F	32.1 ± 25.5	40.9 ± 14.6	1.77 ± 0.79
Preterm neonates scanned before TEA	48M/22F	32.5 ± 20.7	34.7 ± 12.7	1.79 ± 0.58

Abbreviations: GA, gestational age; PMA, postmenstrual age; TEA, term-equivalent age; M, male; F, female.

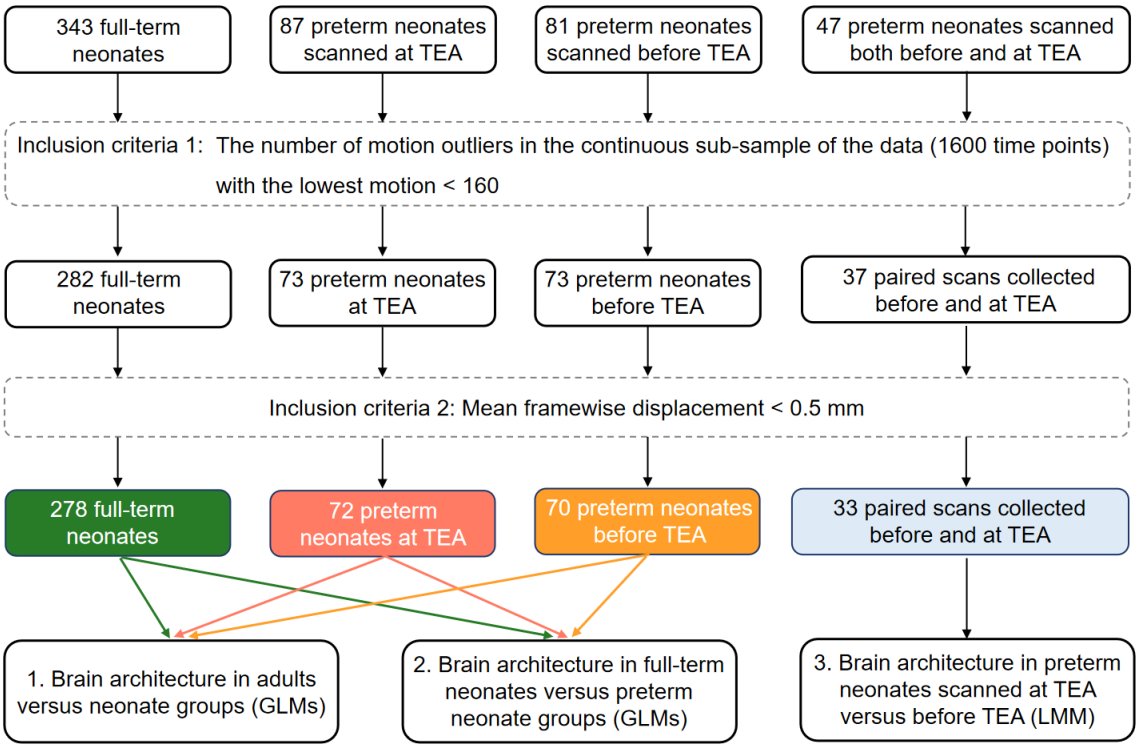

Figure 3.1 The number of scans included in data analyses. The frames in green/pink/brown indicate the scans collected from full-term neonates/preterm neonates at/before term-equivalent age that passed head motion criteria. The frame in light blue indicates the scans collected at and before term-equivalent age from the same preterm neonates. Abbreviations: TEA, term-equivalent age; GLMs, general linear models; LMM, linear mixed-effect model.

3.2.2 Data acquisition and Preprocessing

Details of the data acquisition and preprocessing for neonates and adults can be found in Chapter 2, Section 2.2.2.

3.2.3 Data analyses

Node definition

Using a meta-analytically derived functional brain atlas from Power et al. (2011), I defined 264 cortical and subcortical ROIs (8-mm radius spheres) in MNI space. 33 uncertain nodes (do not belong to any of the 11 networks) and 5 cerebellar nodes were excluded. Therefore, I included the remaining 226 nodes comprised 11 networks according to the network labels provided by Power et al. (2011): 1) sensory/somatomotor hand (30 nodes), 2) sensory/somatomotor mouth (5 nodes), 3) cingulo-opercular control (14 nodes), 4) auditory (13 nodes), 5) default mode (57 nodes), 6) visual (31 nodes); 7) frontoparietal control (25 nodes), 8) salience (18 nodes), 9) subcortical (13 nodes), 10, ventral attention (9 nodes), and dorsal attention (11 nodes) networks. For neonates, the 226 ROIs in MNI space were transformed into neonate native space using the same registration procedure used in Chapter 2. Details on the registration procedure can be found in Chapter 2, Section 2.2.3. Time courses were extracted from each neonate based on these ROIs in the native space and from adults based on ROIs in the MNI space.

To ensure that I used the same number of nodes/connections across groups, in the following graph construction, I checked the extracted time courses from adults, full-term neonates, preterm neonates at TEA, and preterm neonates before TEA. 9 nodes were further excluded because of low registration accuracy according to the following criteria: 1) over 5% of participants in any of the four groups missed time courses in that node; 2) node showed significant differences in the proportions of participants having missing time courses between the four groups. Thus, 4 nodes of DMN (node 83, 116, 119, 120), 4 nodes of the visual network (node 153, 165, 168, 172), and node 179 of the frontoparietal control network were excluded (Figure 3.2).

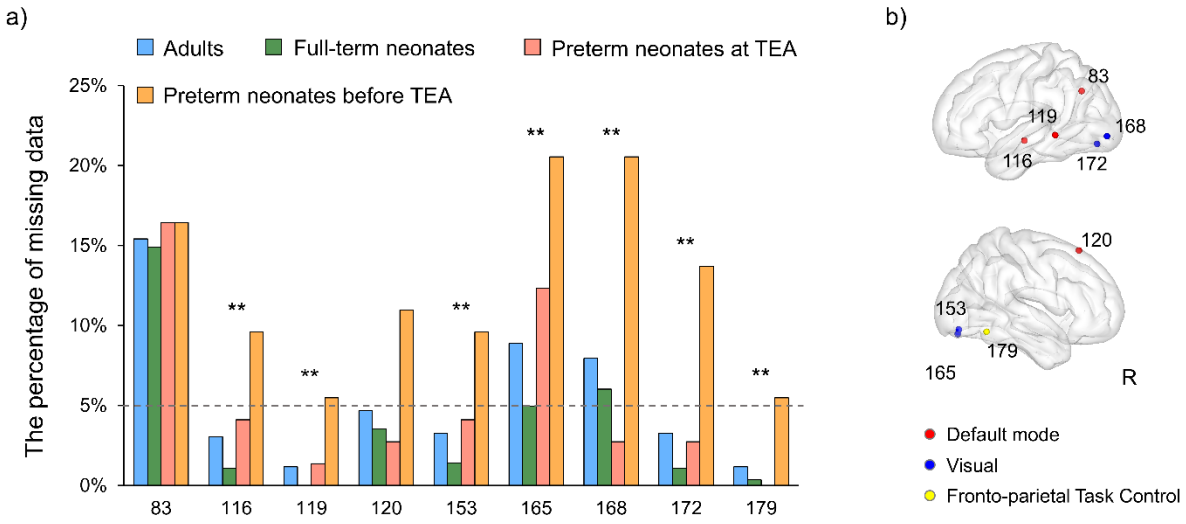

*Figure 3.2 Regions excluded from the Power-264 atlas. Abbreviations: R, right; ** = $p < 0.005$.*

Graph construction

The Pearson's correlation between time courses of any two pairs of nodes was calculated. Then, self-connections were set to 0, and NaNs and negative correlations were removed. 21 proportional thresholds, from 10% to 30% in 1% increments (Godwin et al., 2015; Monti et al., 2013), were used to threshold functional matrices (Figure 3.3) to ensure that results were not driven by specific connection densities (Hallquist & Hillary, 2018; Rubinov & Sporns, 2010; van den Heuvel et al., 2017).

Small-world properties

Nodal-level clustering coefficient and shortest path length were first calculated based on the FC matrices under each threshold for each participant. The clustering coefficient of a node captures the tendency to which the neighboring nodes of a node are interconnected (Watts & Strogatz, 1998), and it was computed as follows (Onnela et al., 2005)

$$C_i = \frac{1}{k_i(k_i-1)}\sum_{j,k}\left(\widehat{w}_{ij}\widehat{w}_{jk}\widehat{w}_{ik}\right)^{1/3}, \quad (1)$$

Where C_i corresponds to the clustering coefficient of node i, k_i is the number of edges connected to node i, w_{ij} corresponds to the strength of a connection between nodes i and j, and $\widehat{w}_{ij}$ represents the weight scaled by the highest weight in the network ($\widehat{w}_{ij} = w_{ij}/\max(w)$). Then, the global-level clustering coefficient was calculated by averaging the nodal-level clustering coefficient across all nodes.

The shortest path length represents the lowest cost of information moving between them. Thus, for weighted FC matrices, the nodal-level shortest path length is defined as

$$d_{ij} = 1/w_{ij} \quad (2)$$

The global-level characteristic path length is given by (Percha et al., 2005)

$$L = \frac{1}{N(N-1)}\sum_{i\neq j} d_{ij}\ , \quad (3)$$

The commonly used formula to quantify small-worldness was proposed by Humphries and Gurney (2008) (See Appendix B, Section 7.1.2 for detailed description), but it has been criticized (Bassett & Bullmore, 2017; Papo et al., 2016; Telesford et al., 2011) because it is strongly driven by network clustering and density of the graph. Recently, Telesford et al.

(2011) established a new small-worldness index separately comparing network clustering to a regular network and path length to a random network. In the present study, I used an alternative index (φ) proposed by Muldoon et al. (2016) to investigate whether or not neonates' brains at birth show a similar functional small-world architecture to the adult brain. That function follows Telesford and colleagues' measure (2011) and, at the same time, takes variations in network density and connection strengths into account. The φ is computed according to the following equation

$$\varphi = 1 - \sqrt{\frac{{\Delta_C}^2 + {\Delta_L}^2}{2}}, \tag{4}$$

where

$$\Delta_c = \frac{C_{\text{latt}} - C_{\text{obs}}}{C_{\text{latt}} - C_{\text{rand}}}, \tag{5}$$

and

$$\Delta_L = \frac{L_{\text{obs}} - L_{\text{rand}}}{L_{\text{latt}} - L_{\text{rand}}}, \tag{6}$$

where latt/obs/rand represent lattice/observed/random networks, the Δc and Δ_L represent the fractional deviation of the C_{obs} or L_{obs} from its respective lattice and random networks constructed with the same number of nodes and the same degree distribution (null model). Thus, Δc and Δ_L both range from 0 to 1, and a higher value means the observed networks have a lower clustering coefficient and a higher characteristic path length. The φ ranges from 0 to 1, and a higher φ value reflects the observed networks exhibiting stronger small-world architecture.

The normalized small-world properties, Δc, Δ_L and φ, were then averaged across all 21 thresholds for further statistical analyses. In addition, I also calculated the mean strength of FC, which can be a confound in between-group difference of small-world properties (van den Heuvel et al., 2017). The mean FC was calculated for each participant by averaging all positive edges.

Nodal efficiency

To quantify the communication efficiency at individual brain node, I used nodal efficiency (E_i), which is defined as follows (Achard & Bullmore, 2007):

$$E_i = \frac{1}{n-1}\sum_{j \in G}\frac{1}{d_{i,j}}\,, \tag{7}$$

where E_i is the mean of the inverse shortest path length from node i to the other nodes. Brain node having high E_i exhibits a high level of efficiency in communicating with the rest of the brain.

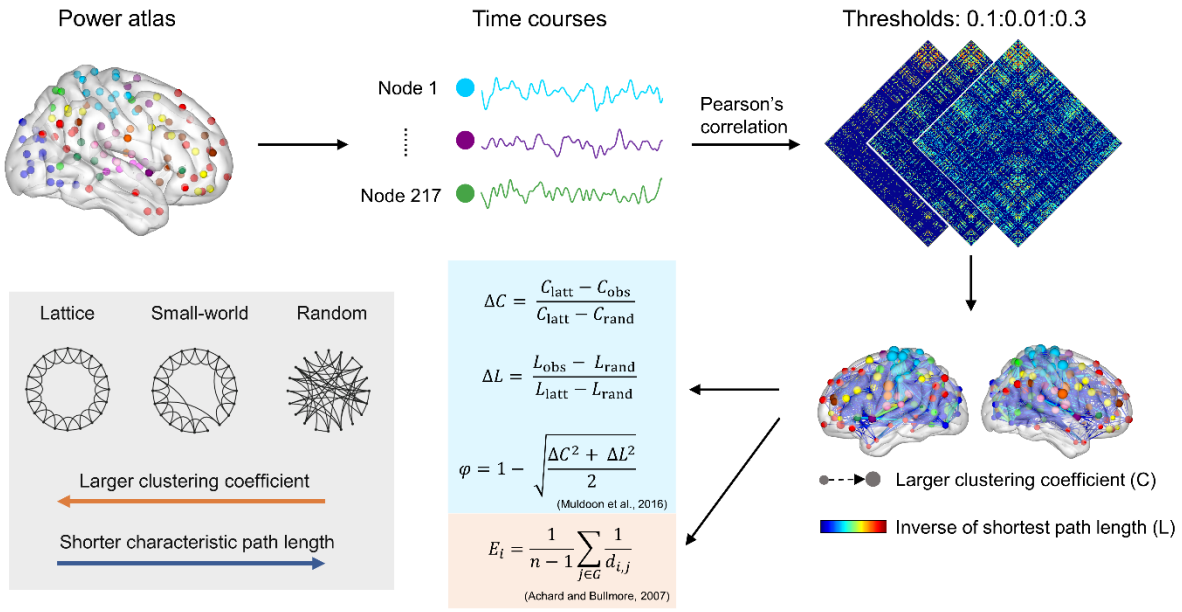

Figure 3.3 Schematic of the method. Time courses were extracted from each brain node, and Pearson's correlation was applied to obtain a weighted graph for each participant. 21 proportional thresholds from 10% to 30% in 1% increments were applied to threshold the weighted graphs. The local clustering coefficient for each node and the shortest path length between every two nodes were calculated based on weighted graphs at each cost function. Nodal efficiency for each node was calculated based on shorted path length at each cost function and then averaged. Then, small-world propensity, normalized clustering coefficient and normalized characteristic path length for each brain network were calculated (Muldoon et al., 2016) at each cost function and averaged.

3.2.4 Statistical analyses

Comparison in functional brain architecture at the global level

Adults versus neonates. To investigate how the functional brain architecture in neonates differs from that of adults, I compared small-world properties in the adults and neonate groups. GLMs were used to test the difference in φ, normalized clustering coefficient (Δc) or normalized characteristic path length (Δ_L) between adults and each neonate group while controlling for mean FD and FC, which are significantly different between the adults and neonate groups (Figure 7.1 and 7.2 in Appendix B).

Full-term versus preterm neonates. To investigate the effect of premature birth on the development of functional architecture at the global level, I compared the normalized small-world properties (φ, Δc or Δ_L) between the full-term neonates and preterm neonates at/before TEA. GLMs were used to detect the difference between full-term neonates and preterm neonates at or before TEA while controlling for mean FD and FC.

Preterm neonates scanned at TEA versus preterm neonates before TEA. A smaller sample of 33 preterm neonates scanned both before and at TEA was used to investigate how small-world architecture develops in preterm neonates from before to reaching TEA. Linear mixed-effect models were applied to detect the difference in small-world properties (φ, Δc or Δ_L) between preterm neonates scanned at and before TEA while controlling for mean FD and FC.

Comparison in nodal efficiency between full-term and preterm neonates

To investigate the effect of premature birth on efficiency of regional communication, GLMs were used to detect any differences in nodal efficiency between full-term neonates and

preterm neonates at or before TEA, while controlling for mean FD and FC. Correction for the false discovery rate (FDR) was applied to all statistical results at a threshold of $p < 0.05$.

3.2.5 Validation analyses

The main global-level network analyses in the current study were based on weighted FC matrices and the algorithms proposed by Muldoon et al. (2016). To ensure that my results were not driven by specific choice of network types and algorithms, I also calculated and compared small-world architecture using 1) binary FC matrices and algorithms proposed by Muldoon et al. (2016); 2) weighted FC matrices and algorithms proposed by Humphries and Gurney (2008); and 3) binary FC matrices and algorithms proposed by Humphries and Gurney (2008). In addition, given how graph theoretical analysis results may be driven by specific parcellations, I tested the reproducibility of my results using an anatomical parcellation, the UNC-0-1-2 atlas with 223 regions (Shi et al., 2018), as a recent study (Luppi & Stamatakis, 2021) showed a parcellation with about 200 regions may be the most representative for functional network (See Appendix B, Section 7.1.1 for details on the UNC-0-1-2 atlas).

3.3 Results

3.3.1 Comparison of neonate and adult functional small-world architecture

GLMs comparing the adults and full-term neonates, including head motion and mean FC as covariates, showed significant main effects of groups for φ (F (1, 450) = 74.69, $p < 0.0001$) and Δc (F (1, 450) = 167.78, $p < 0.0001$), which was driven by significantly higher φ and lower Δc in the adults relative to full-term neonates, respectively (Figure 3.4b). A sensitivity power analysis revealed that a total sample size of 454 is sensitive enough to detect significant difference with an effect size of Cohen's $d = 0.31$ ($\alpha = 0.05$ and a power of 0.8). I observed similar results when comparing the adults and preterm neonate groups. For preterm neonates scanned at TEA, I found significant main effects of group for φ (F (1, 244) = 184.98, $p < 0.0001$) and Δc (F (1, 244) = 141.69, $p < 0.0001$). The adults had significantly higher φ and lower Δc relative to preterm neonates at TEA (Figure 3.4b). A sensitivity power analysis revealed that a total sample size of 248 is sensitive enough to detect significant difference with an effect size of Cohen's $d = 0.42$ ($\alpha = 0.05$ and a power of 0.8). Similarly, for the preterm neonates before TEA, I found significant main effects of group for φ (F (1, 242) = 256.97, $p < 0.0001$), and Δc (F (1, 242) = 32.43, $p < 0.0001$), which were driven by significantly higher φ and lower Δc in the adults (Figure 3.4b). In addition, I observed a significant main effect for Δ_L (F (1, 242) = 53.78, $p < 0.0001$), which was driven by significantly lower Δ_L in the adults. A sensitivity power analysis revealed that a total sample size of 246 is sensitive enough to detect significant difference with an effect size of Cohen's $d = 0.42$ ($\alpha = 0.05$ and a power of 0.8). In summary, as expected, significantly higher small-world propensity/small-worldness and clustering coefficient were consistently observed in the adult relative to neonate groups using different algorithms and types of FC matrices,

which controlled for differences in FC and head motion between adult and infant groups (Figure 7.6 in Appendix B).

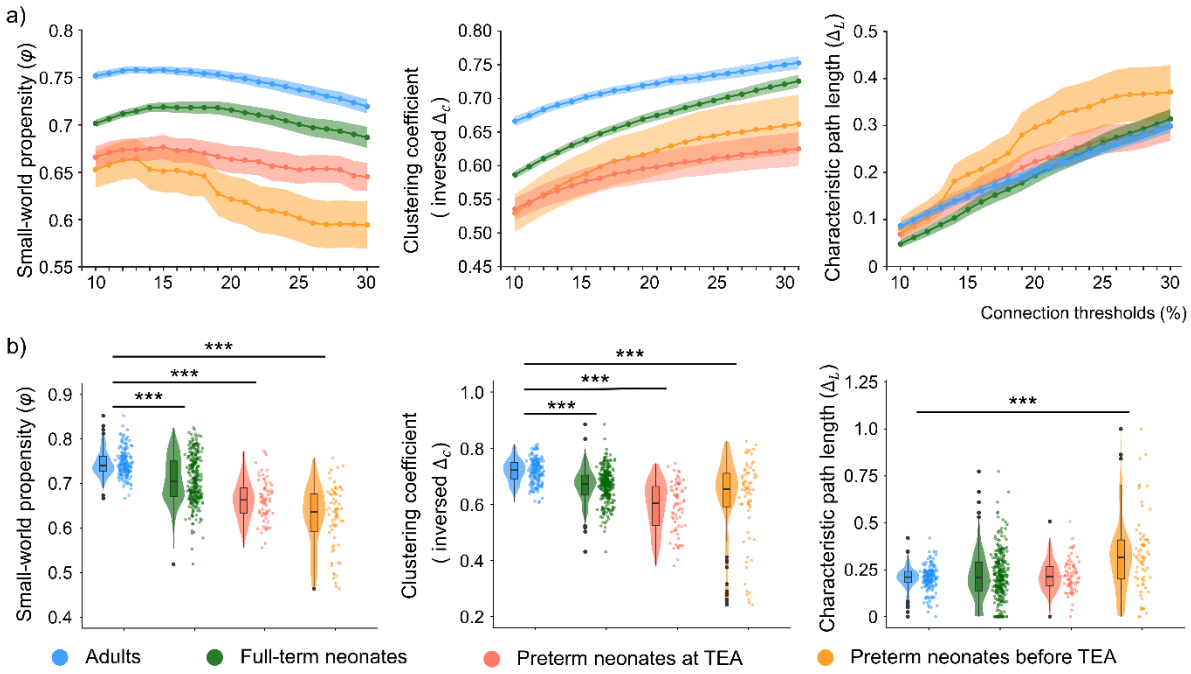

*Figure 3.4 The development of small-world architecture in the neonates relative to adults. a) small-world properties at all tested thresholds (from 10% to 30% in 1% increments) and b) small-world properties in the neonate groups relative to adults. The shaded areas shown in a) represent the 95% confidence intervals. The small-world propensity, clustering coefficient, and characteristic path length shown in b) were averaged across all thresholds. Higher φ/inversed ΔC/ΔL represent higher small-world propensity, higher clustering coefficient and longer characteristic path length. The inversed ΔC was calculated by 1 - ΔC and for visualization purposes only and the statistical analyses were conducted using ΔC. The violin plots show the distribution of the data. The line that divides the box into two parts represents the median of the data. The ends of the box represent the upper (Q3) and lower (Q1) quartiles of the data. The extreme lines of the boxplot show Q3 + 1.5 * interquartile to Q1 – 1.5 * interquartile range. The black dots beyond the extreme lines show potential outliers. Abbreviations: TEA, term-equivalent age. *** = p < 0.0005.*

3.3.2 Small-world organization in neonates

When a threshold value of $\varphi = 0.6$ (Muldoon et al., 2016) was applied to detect whether neonates exhibited small-world architecture or not, the threshold was met or surpassed in 100% of the adults, 97.8% of full-term neonates, 90.3% of preterm neonates at TEA and 72.9% of preterm neonates before TEA (Table 3.3). Although capturing only a summary level view, this result suggested that small-world organization is present in a large proportion of neonates before TEA, and in the majority/all preterm neonates at term equivalent age/born at full term age. In the next sections, I performed fine-grained analyses and group comparisons to unravel the effect of prematurity and early infant age on small-world organization.

Table 3.3 The percentages of participants exhibiting strong small-world architecture in the adults and neonate groups.

Groups	$\varphi > 0.6$		$\sigma > 1$	
	Weighted	Binary	Weighted	Binary
Adults	100.0%	100.0%	92.0%	94.3%
Full-term neonates	97.8%	97.8%	83.1%	90.3%
Preterm neonates at TEA	90.3%	94.4%	76.4%	93.1%
Preterm neonates before TEA	72.9%	71.4%	55.7%	74.3%

Abbreviations: PMA, postmenstrual age in weeks; φ, small-world propensity calculated according to Muldoon et al., (2016); σ, small-worldness calculated according to Humphries and Gurney (2008).

3.3.3 The effect of premature birth on the development of small-world architecture

When the effects prematurity and early infant age were collapsed, in the comparison between full-term neonates and preterm neonates before TEA, I found significant main effects of group for φ (F (1, 344) = 86.37, $p < 0.0001$) and Δ_L (F (1, 344) = 43.21, $p < 0.0001$), driven by significantly higher φ and lower Δ_L in the full-term neonates (Figure 3.5a). A sensitivity power analysis revealed that a total sample size of 348 is sensitive enough to detect significant difference with an effect size of Cohen's $d = 0.36$ ($\alpha = 0.05$ and a power of 0.8). These results suggested that functional architecture has higher small-worldness and higher integration in full-term neonates compared to preterm neonates before TEA at birth.

When the effects of prematurity were considered independently of early infant age, in the comparison between full-term neonates and preterm neonates at TEA, I found a trend main effect of group for φ (F (1, 346) = 5.69, $p = 0.018$), driven by higher φ in the full-term neonates (Figure 3.5b). However, this result did not survive multiple comparisons correction. In addition, I observed a significant main effect of group for Δ_C (F (1, 346) = 10.78, $p = 0.001$), driven by a significantly lower Δ_C in full-term neonates relative to preterm neonates at TEA (Figure 3.5b). A sensitivity power analysis revealed that a total sample size of 350 is sensitive enough to detect significant difference with an effect size of Cohen's $d = 0.36$ ($\alpha = 0.05$ and a power of 0.8). These results suggested that full-term born neonates had higher segregation relative to preterm neonates of the same age. Similar findings were observed using different algorithms and types of FC matrices (Figure 7.6 in Appendix B) and an anatomical parcellation (Section 7.2.4 and Figure 7.8b in Appendix B).

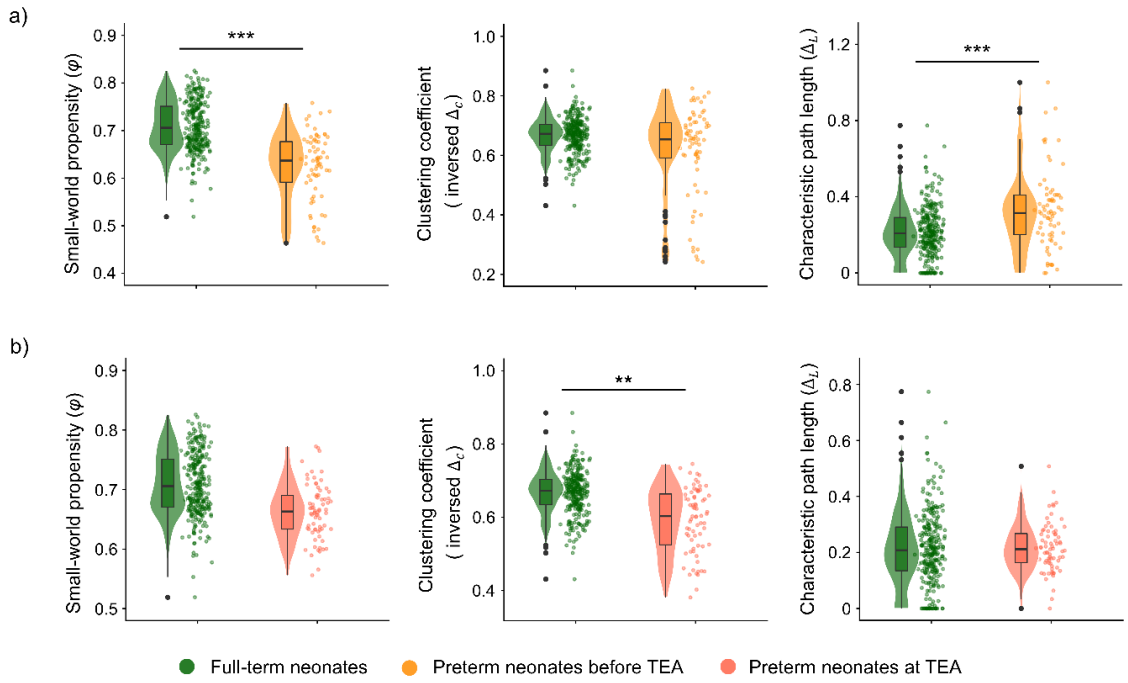

*Figure 3.5 Effects of premature birth on the development of small-world architecture. a) small-world properties in the full-term neonates relative to preterm neonates before TEA; b) small-world properties in the full-term neonates relative to preterm neonates at TEA. Full-term neonates had significantly higher small-world propensity and lower normalized path length relative to preterm neonates before TEA, independent of mean functional connectivity. Full-term neonates had significantly higher clustering coefficient relative to preterm neonates at TEA. Higher φ/inversed ΔC/ΔL represent higher small-world propensity, higher clustering coefficient and longer characteristic path length. The inversed ΔC was calculated by 1 - ΔC and for visualization purposes only and the statistical analyses were conducted using ΔC. The violin plots show the distribution of the data. The line that divides the box into two parts represents the median of the data. The ends of the box represent the upper (Q3) and lower (Q1) quartiles of the data. The extreme lines of the boxplot show Q3 + 1.5 * interquartile to Q1 – 1.5 * interquartile range. The black dots beyond the extreme lines show potential outliers. Abbreviations: TEA, term-equivalent age. *** = p < 0.0005; ** = p < 0.005.*

3.3.4 The effect of neonate age on the development of small-world architecture

When I investigated the effect of early infant age, independently of prematurity, by comparing the same preterm neonate group that was scanned twice – before and at TEA – I found a significant main effect of neonate age on φ (F (1, 40.21) = 13.23, p = 0.001), which was driven by significantly higher small-world propensity in preterm at TEA relative to the same group before TEA (Figure 3.6b). A sensitivity power analysis revealed that a sample size of 33 is sensitive enough to detect significant difference with an effect size of Cohen's d = 0.75 (α = 0.05 and a power of 0.8). In addition, I found that the percentage of neonates exhibiting small-world architecture increased from 66.7% (22 out of 33) to 90.9% (30 out of 33) when they reached TEA. These results suggested that functional small-world architecture develops significantly with early infant age as premature infants reach TEA. In summary, when small-world properties are considered at a fine-grain level, I see that significant effects of premature birth remain when infants reach term equivalent age.

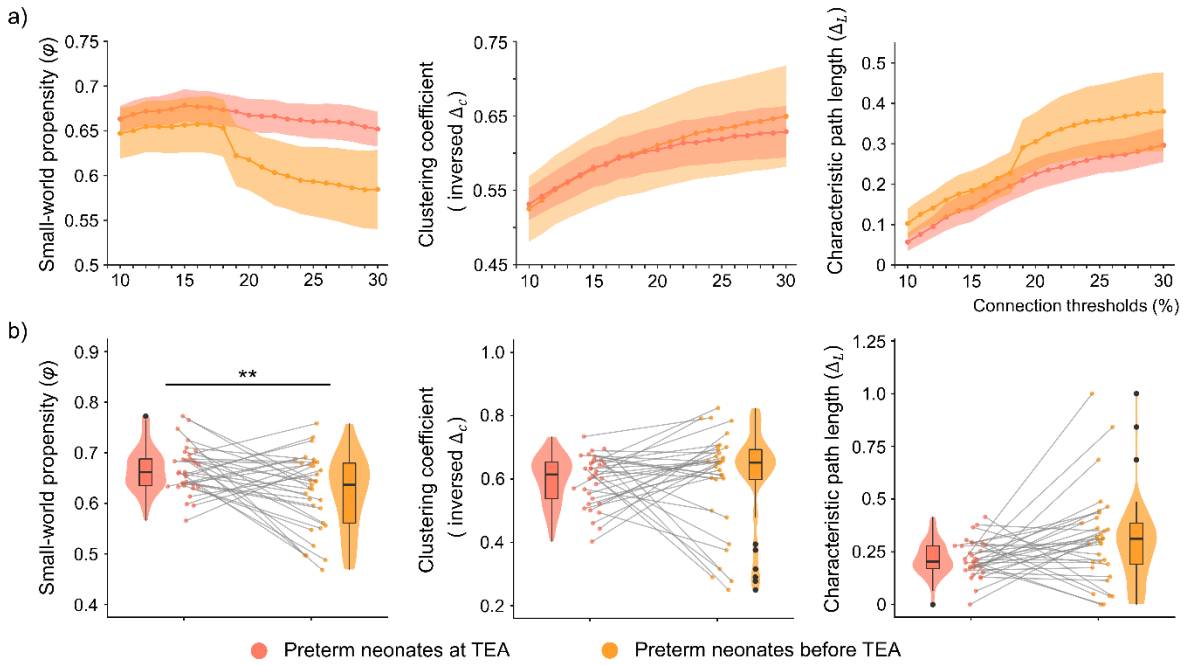

*Figure 3.6 The development of small-world architecture in preterm neonates up to term-equivalent age. a) small-world properties at all tested thresholds (from 10% to 30% in 1% increments) and b) small-world properties in the preterm neonates at TEA relative to the same neonates scanned before TEA. The shaded areas shown in a) represent the 95% confidence intervals. The small-world propensity, clustering coefficient and characteristic path length shown in b) were averaged across all thresholds. Higher φ/inversed ΔC/ΔL represent higher small-world propensity, higher clustering coefficient and longer characteristic path length. The inversed ΔC was calculated by 1 - ΔC and for visualization purposes only and the statistical analyses were conducted using ΔC. The violin plots show the distribution of the data. The line that divides the box into two parts represents the median of the data. The ends of the box represent the upper (Q3) and lower (Q1) quartiles of the data. The extreme lines of the boxplot show Q3 + 1.5 * interquartile to Q1 – 1.5 * interquartile range. The black dots beyond the extreme lines show potential outliers. Abbreviations: TEA, term-equivalent age. ** = p < 0.005.*

3.3.5 The effect of premature birth and early infant age on the development of nodal efficiency

The collapsed effects of premature birth and infant age were first considered. The GLMs comparing nodal efficiency between the full-term neonates and preterm neonates before TEA, while controlling mean FC and FD, showed the full-term neonates had significantly higher nodal efficiency in 9 networks: the sensorimotor mouth network (100% of nodes), sensorimotor hand network (56.67%), dorsal attention (45.45%), cingular opercular (42.86%), frontoparietal control (41.67%), salience (38.89%), auditory (23.08%), default mode (22.64%), and the visual network (18.52%) (Figure 3.7a and Table 3.4) (Please see Figure 7.4 in Appendix B for further supporting results).

Second, I considered the effect of premature birth independently of infant age. The GLMs comparing nodal efficiency between the full-term neonates and preterm neonates at TEA showed that the full-term neonates had higher nodal efficiency in the right angular gyrus (node 194, frontoparietal control network), the orbital part of right inferior frontal gyrus (node 210, salience network) and the right middle temporal gyrus (node 239, ventral attention network) (Figure 3.7b). Significant differences in these nodes were also observed relative to preterm neonates before TEA (above; Figure 3.7a). Third, when I considered the effects of infant age independently of prematurity by comparing nodal efficiency between the same preterm neonates scanned before and at TEA no significant main effects were found (Figure 3.7c).

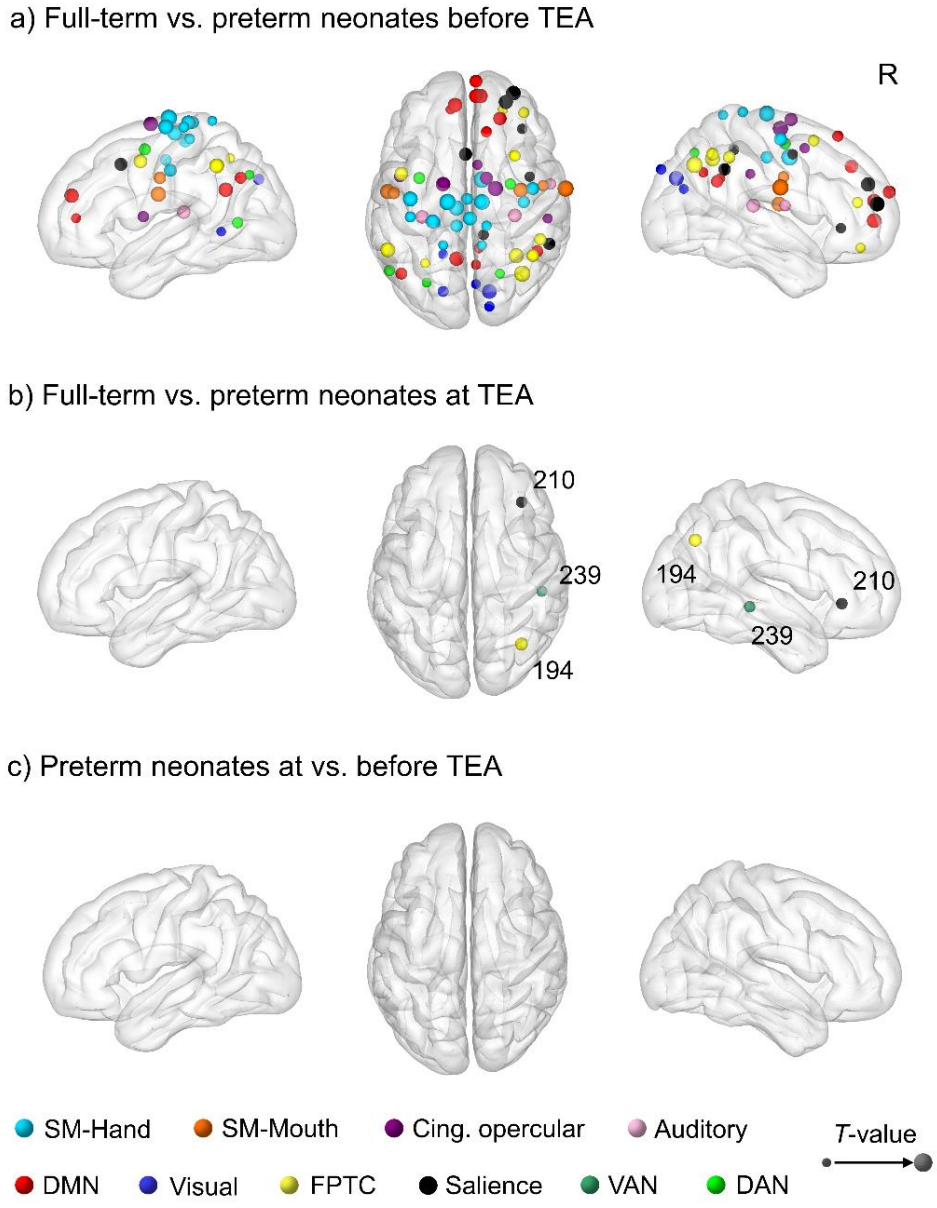

Figure 3.7 Effects of premature birth on nodal efficiency. a) nodes showing higher nodal efficiency in the full-term neonates relative to preterm neonates before TEA; b) nodes showing higher nodal efficiency in the full-term neonates relative to preterm neonates at TEA; and c) no significant difference between preterm neonates scanned at TEA and the same neonates scanned before TEA. The size of the node represents T-value. Abbreviations: SM-Hand, sensory/somatomotor hand network; SM-Mouth, sensory/somatomotor mouth network; Cing. opercular, cingulo-opercular task control network; DMN, Default mode network; FPTC, frontoparietal task control network; VAN, ventral attention network; DAN, dorsal attention network; R, right.

Table 3.4 The percentage of nodes showing significantly higher nodal efficiency in each network in the full-term neonates relative to preterm neonates before TEA.

Networks	Percentage of significant nodes
SM-Mouth	100.00% (5/5)
SM-Hand	56.67% (17/30)
DAN	45.45% (5/11)
Cing. opercular	42.86% (6/14)
FPTC	41.67% (10/24)
Salience	38.89% (7/18)
Auditory	23.08% (3/13)
DMN	22.64% (12/53)
Visual	18.52% (5/27)
Subcortical	0.00% (0/13)
VAN	0.00% (0/9)

Abbreviations: SM-Hand, sensory/somatomotor hand network; SM-Mouth, sensory/somatomotor mouth network; Cing. opercular, cingulo-opercular task control network; DMN, Default mode network; FPTC, frontoparietal task control network; VAN, ventral attention network; DAN, dorsal attention network.

3.4 Discussion

Although small-world organization is thought to be related to the brain mechanism of human consciousness in adults, it remains unknown whether it is developed in infants at birth. I investigated the development of functional small-world architecture in neonates and how this

architecture may be altered by premature birth and early infant age. I found that small-world architecture was developed in full-term born infants. To the best of our knowledge, this is the first fMRI study to investigate the effect of prematurity before term equivalent age (TEA), both on the global small-world properties and the efficiency of regional functional communication. The key novel finding was that premature neonates before TEA showed significant and widespread differences in small-world brain architecture and in the efficiency of regional communication, relative to full-term born neonates. These differences were driven by both sensory and higher-order networks, with the somatomotor, dorsal attention, cingulo-opercular, and frontoparietal control networks carrying the largest effects, and the visual network the smallest. In addition, I observed that, for the most part, global small-world properties and regional communication efficiency developed in healthy-born premature neonates as they reached TEA, suggesting a pre-programmed developmental trajectory of this functional architecture despite of prematurity. Nevertheless, significant prematurity-related disruption of small-world architecture persisted at TEA.

3.4.1 Comparison of neonate and adult functional architectures

As expected, adults had stronger small-worldness values, including higher clustering coefficient, than all neonate groups, suggesting more efficient and segregated functional brain architecture relative to neonates. It is worth noting that differences in functional architecture between adults and neonate groups and across neonate groups were independent of any differences in functional connectivity or head motion. Importantly, we found that small world architecture was developed in full-term born infants. My findings add robustness to earlier studies in small infant groups, suggesting that small-worldness is developed in full-term born neonates (Bouyssi-Kobar et al., 2019; De Asis-Cruz et al., 2015; Fransson et al., 2011;

Gozdas et al., 2018; Omidvarnia et al., 2014). These results suggest that the functional organization of the brain develops rapidly from birth onwards in the first years of life, with functional brain networks gradually becoming more cohesive (Gao et al., 2009; Sherman et al., 2014) and specialized (Fransson et al., 2011; Scheinost et al., 2016; Wen et al., 2019).

3.4.2 Impact of prematurity and young infant age

A dearth of studies on small-world architecture in premature infants before term equivalent age has led to lack of understanding on the effect of prematurity on small-world organization. The two studies in this area, that these authors are aware of, delivered inconsistent results from small infant cohorts. I address this gap by using the world's largest sample of neonatal functional MRI dataset (N = 420) with high temporal and spatial resolution. Our results show that premature neonates before TEA have significantly weaker small-world organization and higher path length, or lower neural integration, relative to full-term neonates. This finding differs from the two previous studies, which reported stronger small-world properties in preterm neonates before TEA (Cao, He, et al., 2017; Omidvarnia et al., 2014), a discrepancy likely due to the small sample sizes (N = 11 to 23) and the highly specific connectivity parameters (e.g., density 5% threshold) in these previous studies. Furthermore, preterm neonates before TEA showed lower efficiency of regional communication in 32% of 217 nodes, distributed across 9/11 brain networks, relative to full-term counterparts. Lower nodal efficiency was observed both in sensory and higher-order networks. The somatomotor network showed the most pronounced underdevelopment in nodal efficiency, with those involved in mouth and hand movements showing lower values in 100% and 57% of the relevant nodes, respectively, suggesting that functional communication in these regions undergoes dramatic developments during the 3rd trimester of pregnancy. Foetuses receive

somatomotor input from their muscles and limb movements in utero, which is key for early development of movement abilities before birth. My results suggest that movement of the mouth and hands by birth is a key priority of brain development in the 3rd trimester of pregnancy.

Following closely in the effect of prematurity were networks associated with higher cognition, i.e., the dorsal attention (45% of nodes), cingulo opercular (43% of nodes), and fronto-parietal control (42% of nodes) networks, suggesting that these undergo dramatic development in utero during the 3rd trimester as well, likely to prepare for the rapid development of high-level cognition from birth. By contrast, the ventral attention network showed no differences in nodal efficiency between preterms before TEA and full-term neonates, suggesting that regional communication in these networks does not change significantly during the 3rd trimester of pregnancy. As all preterm infants were scanned at or very shortly after birth, these neonates would have had very limited extra-uterine sensory visual experience. The ventral attention network has been implicated in visuospatial cognition (Corbetta & Shulman, 2002), and, thus, it likely undergoes experience-dependent changes post birth, once infants are exposed to visual information from their environment. Consistent with this interpretation is the finding the visual network showed reduced efficiency in the fewest nodes (< 20%), relative to the other networks in preterm infants before TEA. Taken together, these findings are consistent with the limited visuo-sensory experience of neonates and suggest that visually-driven brain networks develop at a lesser pace than others in the 3rd trimester of pregnancy, and pick up developmental pace post birth, once infants receive continuous visual input. Visual acuity is low in neonates and it is thought that this period of blurriness plays an adaptive role in enhancing the recognition of fine grained visual information, as the infant develops (Vogelsang et al., 2018). The aforementioned features of underdeveloped small-world architecture and regional communication efficiency observed in

preterm neonates before TEA are due both to prematurity and young infant age, relative to full-term born neonates.

When infant age was controlled for, in the comparison between preterms at TEA and full-term born neonates, prematurity-related disruptions of small-worldness persisted, but at a much lesser extent. This suggested a pre-programmed developmental trajectory of functional architecture despite of prematurity, as infants reach term equivalent age. Nevertheless, preterm neonates at TEA had significantly smaller clustering coefficient (lower neural segregation) relative to full-term born neonates, and significantly reduced communication efficiency in 3/217 nodes (i.e., 1.4%, compared to 32% in preterms before TEA). These nodes belonged to the salience, visual attention network, and frontoparietal control networks. In addition to partaking in networks that support attention and executive function, these nodes fall within the right angular, inferior frontal gyrus, and middle temporal gyrus, regions that are related to language processing (Friederici, 2011; Hickok & Poeppel, 2007; Perani et al., 2011). Therefore, disruption of nodal efficiency in these regions associated with prematurity in term equivalent neonates may underlie the significant risks for language development delays that are associated with premature birth. Children born prematurely are at risk for problems in language acquisition, word comprehension, and the development of receptive language skills (Guarini et al., 2009; Rushe, 2010; Vandormael et al., 2019).

The effect of infant age in and of itself, while controlling for prematurity, was investigated in the comparison of a small subset of preterm neonates (N=33) that were scanned twice, once before TEA and, subsequently, when they reached TEA. As they reached the TEA, these preterm infants showed significantly stronger small-world organization. In addition, the percentage of neonates exhibiting small-world architecture increased from 66.7% to 90.9%,

when they reached TEA. These results suggested that functional small-world architecture develops significantly with early infant age as premature infants reach TEA.

3.4.3 Summary

In summary, young premature infants showed the largest and extensive disruption to small-world organization and regional communication efficiency relative to full-term born neonates, underscoring the importance of the 3rd trimester of pregnancy for the development of the brain infrastructure that supports cognition and conscious awareness. This result is consistent with findings in Chapter 2 (Hu et al., 2022), where I showed that preterm neonates before TEA did not exhibit distinct high-order networks, particularly the default mode and fronto-parietal executive control networks, in stark contrast to their full-term born counterparts, who manifested these networks as distinct (Sylvester et al., 2023) and engaged in the complex anti-posed dynamical communication that is observed in the adult brain (Hu et al., 2022).

3.4.4 Methodological consideration

The comparisons between preterm neonates scanned twice were based on less than 40 participants and showed relatively lower reproducibility relative to other comparisons (Figure 7.6 in Appendix B). Future longitudinal studies with a large sample of preterm neonates will be important for tracing the effect of prematurity on the development of functional brain development in early infancy.

4. Chapter 4 Typical and atypical development of neural entropy in full-term and preterm neonates

4.1 Introduction

Our experiences are constantly evolving, unfolding, and developing over short periods of time (at a sub-second resolution). Each conscious experience is specific, differing from a vast array of conscious states at any given time. According to Dynamic Core Hypothesis (Tononi & Edelman, 1998), the brain must be capable of a large repertoire of different activity patterns or neural states to produce the stream of consciousness. Different theories of consciousness also align in suggesting that the dynamic complexity of possible brain states is a fundamental hallmark of consciousness (Carhart-Harris et al., 2014; Cooney & Gazzaniga, 2003; Dehaene et al., 2011; Mashour et al., 2020; Northoff & Huang, 2017).

The entropic brain hypothesis (Carhart-Harris, 2018; Carhart-Harris et al., 2014) proposes that the dynamic complexity of spontaneous brain activity reflects the uncertainty and informational richness of conscious states (Figure 4.1). Consciousness arises within a critical zone where the entropy or dynamic complexity of brain activity is neither excessively ordered nor disordered. Compared to states where consciousness is diminished or abolished (e.g., disorders of consciousness, general anesthesia, sedation), normal waking consciousness is characterized by richer conscious content and greater flexibility of possible states. Psychedelic compounds shift the brain (in normal waking conscious states) towards a higher entropic state, yielding richer conscious contents and higher flexibility of mind (Schartner et al., 2017). Yet, this shift comes at the cost of other functions, such as a diminished sense of self and associated metacognitive functions, such as an ability to reflect on one's own

thoughts and behaviour (Fleming et al., 2012; Shimamura, 2000), theory of mind (Bennett, 1978; Wimmer & Perner, 1983), and mental time-travel (Fleming et al., 2012).

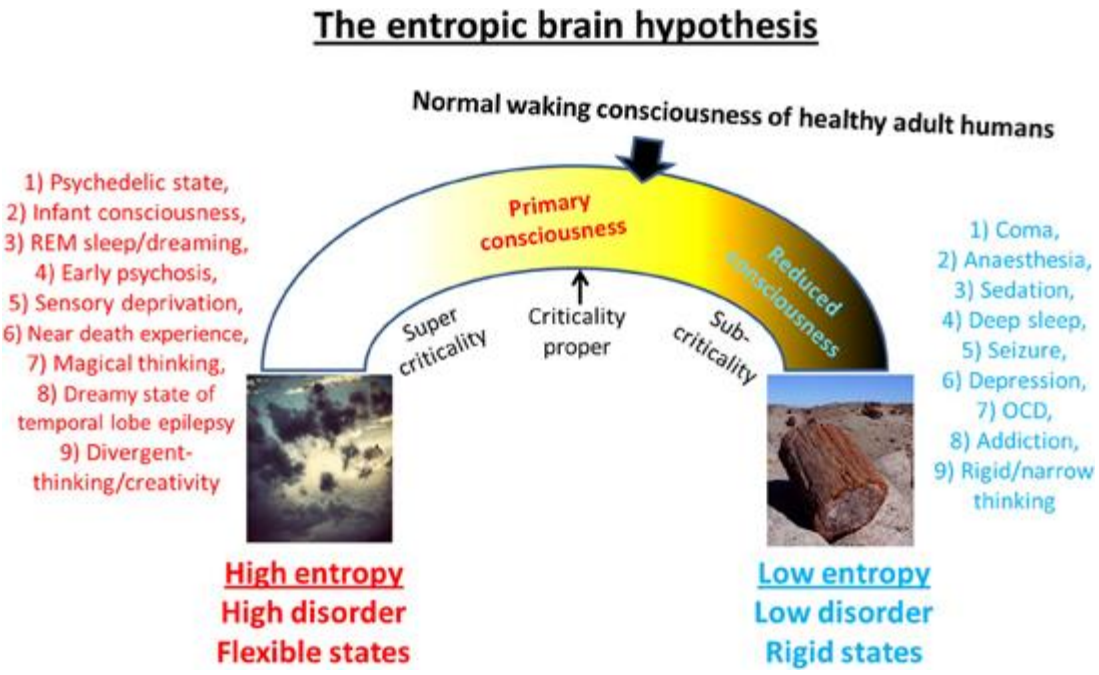

Figure 4.1 The entropic brain hypothesis (Carhart-Harris et al., 2014).

Indeed, neural entropy, which captures dynamic complexity of brain activity patterns, has been found to be an experimentally tractable and accurate measure for quantifying different conscious states (i.e., psychedelic states, general anaesthesia, disorders of consciousness) (Cavanna et al., 2018; Coppola et al., 2022; Crone et al., 2020; Toker et al., 2022; Varley, Carhart-Harris, et al., 2020; Varley, Luppi, et al., 2020). Convergent evidence from neuroimaging studies has shown that neural entropy fluctuates among states of reduced or

altered consciousness. Neural entropy decreases when consciousness fades, i.e., during sleep (Miskovic et al., 2019) or general anaesthesia (Dasilva et al., 2021; Schartner et al., 2015), as well as in the minimally conscious state or the unresponsive wakefulness syndrome (Coppola et al., 2022; Demertzi et al., 2019; Li et al., 2022a; Sitt et al., 2014). By contrast, neural entropy was found to increase in altered states of consciousness, such as during hallucinatory or the psychological state elicited by classic psychedelic drugs (i.e., LSD and psilocybin) (Herzog et al., 2023b; Luppi, Carhart-Harris, et al., 2021b; Varley, Carhart-Harris, et al., 2020). Importantly, a recent paper by Coppola et al., (2022) measured neural entropy based on dynamic fluctuations observed in the small-world architecture in individuals who were awake, under propofol sedation, in MCS or in UWS patients. They found that neural entropy consistently scaled down with decreasing levels of consciousness (awake > propofol sedation > MCS > UWS). Furthermore, this result was robustly replicated using another independent propofol sedation dataset, as well as different brain parcellations.

Newborn infants spend most of their time (about 16 to 18 hours per day) sleeping. Although different from the sleep structure in adults, a precursor of rapid eye movement (REM) sleep (active sleep) and non-REM (NREM) sleep (quiet sleep) have been observed in newborns (Dereymaeker et al., 2017; Scher, 2008). Both REM and NREM sleep are characterized by diminished arousal relative to wakefulness, but REM sleep is distinct from NREM by having rich conscious content (dreaming) (Carskadon & Dement, 2005). A typical neural entropy pattern has been found in healthy human adults during wakefulness and sleep cycles with the highest neural entropy during wakefulness, intermediate levels during REM, and the lowest during NREM (Bruce et al., 2009; Lee et al., 2013; Mateos et al., 2018). A recent study (Miskovic et al., 2019) found that this pattern is specific to short temporal scales (the time length used to get averaged time series < 100 ms), while the opposite pattern was observed at long temporal scales (> 250 ms). Previous electroencephalography (EEG) studies (Scher et

al., 2005; Wielek et al., 2019; Zhang et al., 2009) have observed partially similar neural entropy patterns in sleep/awake states in full-term neonates as that in adults. Scher et al. (2005) and Zhang et al. (2009) observed higher neural entropy in active sleep compared to quiet sleep in neonates at long temporal scales. Wielek et al. (2019) found neonates exhibited the highest neural entropy during wakefulness and the lowest neural entropy during quiet sleep at short time scale, and higher entropy in active sleep relative to quiet sleep or the awake state at long time scale. Nevertheless, on the whole, these findings have suggested that neural entropy is different between sleep stages in adults and broadly similar in infants. Based on this literature, there is good reason to believe that neural entropy can be expected to reflect conscious states in early infancy. However, none of those aforementioned studies directly compared neural entropy in neonates and adults.

However, whether neonates exhibit different levels of neural entropy relative to adults remains unknown. One EEG study to date (Lippé et al., 2009) compared neural entropy in 1- to 2-month-old neonates and adults and reported lower sample entropy in neonates. However, the very small sample of neonates (7 neonates and 20 adults) limits the reliability of their results. Furthermore, it is well established that neural entropy is best computed by using the temporospatial activity pattern (Hoel et al., 2013; Oizumi et al., 2014), whereas Lippe and colleagues (2009) averaged entropy across all electrodes, which resulted in a loss of information regarding spatial complexity. Therefore, there is a clear need to investigate neural entropy in neonates relative to adults by assessing temporospatial activity patterns and the employment of large fMRI datasets, in order to obtain robust and reliable results.

To our best knowledge, only three EEG studies (Janjarasjitt et al., 2008; Kaffashi et al., 2013a; Scher et al., 2005) have investigated the effects of premature birth on the neural entropy around birth, reporting inconsistent results. While Scher et al. (2005) and Kaffashi et

al. (2013a) observed higher neural entropy in full-term neonates relative to preterm neonates at the same age, Janjarasjitt et al. (2008) did not observe any significant difference between them. These inconsistent results are likely due to the small sample sizes of preterm neonates (N = 8 to 33). Critically, none of these studies has systematically examined the effect of premature birth and neonate age by comparing preterm neonates scanned at birth (before TEA), preterm neonates scanned at TEA, and the same neonate group born and scanned at full-term birth.

I address these limitations in the current study. I first asked whether the neural entropy in neonates is different from that in adults. I then asked how premature birth and early neonate age affect the development of neural entropy. The same neonate (N = 420) and adult rs-fMRI datasets (N = 176) used in Chapter 3 were used in the current chapter. I detected the development of neural entropy in neonates by measuring the entropy of network configuration of the whole brain (except the cerebellum) using graph theoretical analysis combined with a sliding-window approach. The effect of neonate age at the time of assessment was deconfounded from the effect of premature birth, by the inclusion of two preterm groups: the first (N = 72) born before and scanned at TEA, and the second (N = 70) born and scanned before TEA. I hypothesized that: (a) neural entropy in neonates is different from that in adults, (b) premature birth is associated with altered neural entropy, and (c) some alterations in neural entropy would persist as preterm neonates reached TEA.

4.2 Materials and methods

4.2.1 Participants

The same neonate (N = 420) and adult rs-fMRI datasets (N = 176) used in Chapter 3 were used in the current chapter. Details on participants' inclusion criteria and demographic information can be found in Chapter 3, Section 3.2.1. The effect size for the difference between adults and neonates could not be estimated directly from Lippé et al. (2009), so I conducted sensitivity power analyses for all the comparisons between adults and neonates using G*Power (Faul et al., 2009). A previously published work (Janjarasjitt et al., 2008) has found an effect size of Cohen's $d = 0.45$ for the difference in neural entropy between full-term neonates and preterm neonates at TEA. A priori power analysis in G*Power with Cohen's $d = 0.45$, $\alpha = 0.05$ and a power of 0.8 suggested that a total sample size of at least 240 (190 for full-term neonates and 50 for preterm neonates at TEA) was required to detect an existing effect of premature birth. Janjarasjitt et al. (2008) also found an effect size of Cohen's $d = 0.57$ for the difference in neural entropy between full-term neonates and preterm neonates before TEA. A priori power analysis with Cohen's $d = 0.57$, $\alpha = 0.05$ and a power of 0.8 suggested that a total sample size of at least 154 (123 for full-term neonates and 31 for preterm neonates before TEA) was required to detect an existing difference between full-term neonates and preterm neonates before TEA. Therefore, the sample size of the current study (278 full-term neonates, 72 preterm neonates at TEA and 70 preterm neonates before TEA) would have sufficient power to detect the differences between full-term neonates and preterm neonates.

4.2.2 Data acquisition and preprocessing

Details of the data acquisition and preprocessing for neonates and adults can be found in Chapter 2, Section 2.2.2.

4.2.3 Data analyses

Dynamic graph construction

Neonates. Time courses extracted from neonates using the Power atlas (2011) in Chapter 3 were used to construct dynamic graphs. A sliding-window approach was applied to create time-varying connectivity matrices (Figure 4.2). According to this method, the time series extracted from each node was split into a window comprising 90 time points (35.28 s) (Coppola et al., 2022; Luppi et al., 2019; Preti et al., 2017), and window sliding of 2 time points (784 ms) was chosen, resulting in 755 time windows for each neonate. Then, time series were tempered with a Gaussian window before calculating connectivity matrices to minimize the effect of time points at the edge of the window. Pearson's correlation between the time courses of any two pairs of nodes was calculated. Then, self-connections were set to 0, and NaNs and negative correlations were removed. 21 proportional thresholds, from 10% to 30% in 1% increases (Godwin et al., 2015; Monti et al., 2013), were used to threshold functional matrices to ensure that results were not driven by specific connection densities (Hallquist & Hillary, 2018; Rubinov & Sporns, 2010; van den Heuvel et al., 2017)

Adults. Time courses extracted from adults using the Power atlas (2011) in Chapter 3 were used. Additionally, to keep the length of time courses used for calculating neural entropy consistent in neonates and adults, I randomly selected a continuous sub-sample of time series (871 time points) from each adult for dynamic graph construction. The time series extracted

from each node was split into a window comprising 49 time points (the same time length as that in neonates), and window sliding of 1 time point (720 ms) was chosen, resulting in 822 time windows for each adult. Then, the same dynamic graph construction procedure as that used in neonates was applied to adults.

Network properties

Small world propensity, normalized clustering coefficient (network segregation), and normalized path length (network integration) were calculated based on the algorithms described in Section 3.2.3 of Chapter 3, using the thresholded FC matrix for each time window. Given how graph theoretical analysis results may be driven by specific parcellations, I tested the reproducibility of my results using a macroscopic anatomical parcellation, the UNC-0-1-2 atlas with 223 regions (Shi et al., 2018; Shi et al., 2011), as a recent study (Luppi & Stamatakis, 2021) showed a parcellation with about 200 regions may be the most representative for functional networks. Please see Section 7.1.1 in Appendix B for detailed information on the UNC-0-1-2 atlas.

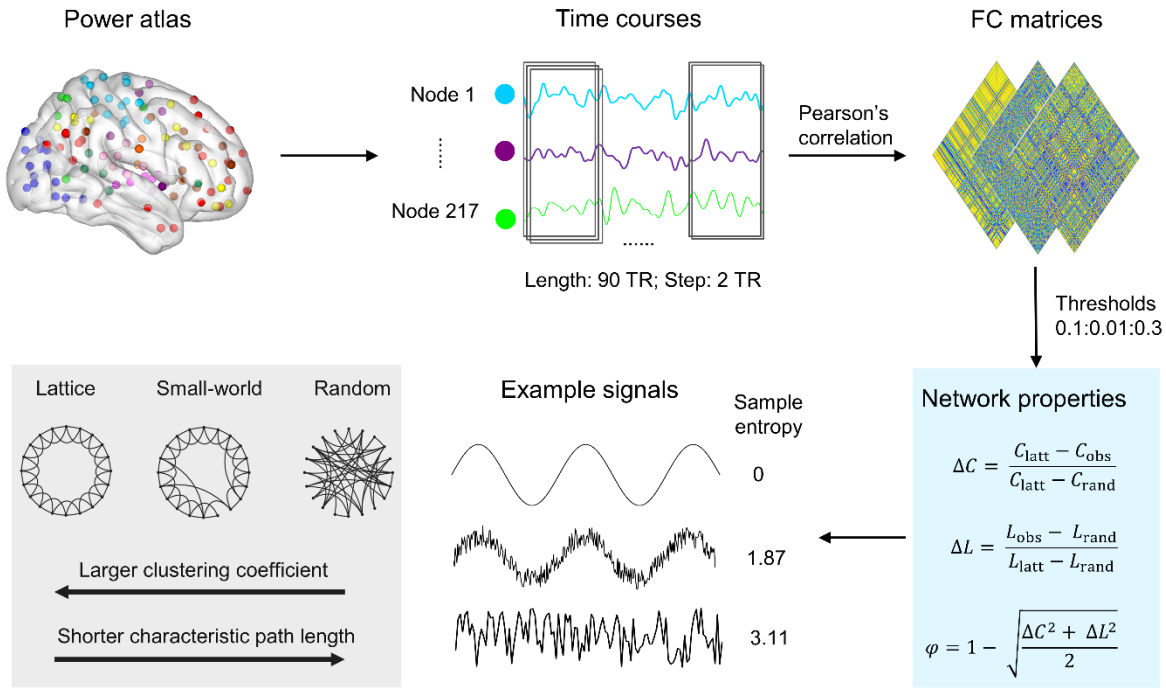

Figure 4.2 Schematic of the method. Time courses were extracted from each brain node first, and a time window approach (Neonates: length = 90 time points, step = 2 time points; Adults: length = 49 time points, step = 1 time point) was applied. For each time window, Pearson's correlation was applied to obtain weighted functional connectivity (FC) matrices. 21 proportional thresholds from 10% to 30% in 1% increases were applied to threshold the FC matrix. In the next step, I calculated small-world propensity (φ), normalized clustering coefficient (ΔC) and normalized characteristic path length (ΔL) (Muldoon et al., 2016) based on FC matrix at each cost function. Finally, sample entropy was calculated and averaged across thresholds. Abbreviations: FC, functional connectivity.

Sample entropy

I applied sample entropy (Richman & Moorman, 2000), an information-theory measure adapted to biological dynamical systems, to measure neural entropy. It is derived from approximate entropy (Kolmogorov, 1968), which measures the rate of information produced. A complex system shows high entropy and cannot be easily described, while a simple system

offers low entropy and can be quickly and briefly summarized. In other words, if a shorter segment explains the data better than a longer segment, the system is of lower self-similarity and higher complexity. It was computed as follows (Lake et al., 2002):

$$SampEn = -log\frac{A}{B}, \quad (4)$$

where A is how similar the shorter time-series segment (via Chebyshev distance) is to the rest of the time series, and B is how similar the longer time-series segment is to the rest of the time series. Larger sample entropy indicates lower self-similarity and higher dynamic complexity.

In the present study, to calculate the sample entropy of network properties across windows, I set the maximal length of the template (*M*, length of the window of the different vector comparisons) as two windows and the minimal length of the template as one window (Pedersen et al., 2017). A tolerance (*r*) for accepting similarity matches between the time-series segment and the rest of the time series was set to 0.2 times the standard deviation. The sample entropy of small worldness, normalized clustering coefficient or normalized path length were calculated at each threshold and then averaged across 21 thresholds for statistical analysis. I also calculated the sample entropy of positive functional connectivity to include it as a covariate in the following statistical analyses, as the difference in positive FC has confounding consequences for the between-group difference in network properties (van den Heuvel et al., 2017).

4.2.4 Statistical analysis

Sample entropy of network properties in adults versus neonates

To investigate the development of neural entropy in neonates, I compared the sample entropy of network properties between the adult and neonate groups using logistic regressions ('*glm*' function of R package 'aod'). The interpretable odds ratios provided by this regression model allow us to know the predictive power of factors to distinguish groups. Specifically, I used group ('1' = adults, '2' = full-term neonates/preterm neonates at TEA/before TEA) as the dependent variable, sample entropy of network properties as an independent variable, and sample entropy of positive FC, static network properties (small worldness/clustering coefficient/path length) and mean FD as covariates. As multiple independent variables were included in these models, I also assessed multicollinearity using 'vif' function of R package 'car'. All tests were two-sided given little knowledge is known about the neural entropy in neonates.

The effect of premature birth on sample entropy of network properties

To assess the effects of premature birth on neural entropy, I first conducted groupwise comparisons between the full-term neonates and preterm neonate groups in logistic regression models. Specifically, to detect the difference in sample entropy of small worldness, 'group' was set as the dependent variable ('1' = full-term neonates, '2' = preterm neonates at TEA/before TEA), sample entropy of small worldness as the independent variable, with sample entropy of positive FC, small worldness and mean FD as covariates. Similar logistic regression models were applied to detect the effects of premature birth on sample entropy of clustering coefficient or sample entropy of path length. All tests were again two-sided given little knowledge is known about the effects of premature birth on neural entropy in neonates.

The effect of neonate age on neural entropy before TEA

As the third trimester of pregnancy (after 24 weeks of gestational age) is crucial for infant brain development (Burkhalter et al., 1993; Kostovic & Judas, 2010; Kostovic et al., 2019; Rakic, 1988), I was interested in understanding how neural entropy evolves during this critical period. To investigate the effects of neonate age (at scan) on neural entropy up to TEA, I used regression models to look at the association between sample entropy of network properties and neonate age in preterm neonates before TEA. Specifically, I used sample entropy of network properties (small worldness/clustering coefficient/path length) as dependent variables, neonate age as independent variables, with sample entropy of positive FC, network properties (small worldness/clustering coefficient/path length), and mean FD as covariates.

4.3 Results

4.3.1 Higher neural entropy in neonates relative to adults

The logistic regression models comparing adults and full-term neonates showed significant predictive power of sample entropy of network properties, despite controlling for the underlying FC dynamics, small worldness, and head motion (Figure 4.3a and Table 4.1). The estimated odds of being full-term neonates versus adults are 111.95 times given one unit increase in sample entropy of small worldness (odds ratio (OR) = 111.95, 95% confidence interval (CI) = [21.90 654.51], $p < 0.0001$). A sensitivity power analysis revealed that a total sample size of 454 is sensitive enough to detect significant difference with an effect size of Cohen's d = 1.10 or odds ratio = 7.33 ($\alpha = 0.05$ and a power of 0.8). Similarly, full-term neonates showed significantly higher sample entropy of clustering coefficient (OR = 4.48,

95% CI = [1.71 12.11], p = 0.003, effect size of Cohen's d = 0.94 or odds ratio = 5.49 with 80% power) and sample entropy of path length (OR = 107.70, 95% CI = [19.15 678.35], p < 0.0001, effect size of Cohen's d = 1.42 or odds ratio = 13.19 with 80% power) relative to adults (Figure 4.3b, 4.3c and Table 4.1). For the preterm neonates scanned at TEA, I also found significantly higher sample entropy of network properties (small worldness: OR = 870.26, 95% CI = [33.01 35422.28], p < 0.0001; effect size of Cohen's d = 1.00 or odds ratio = 6.11 with 80% power; clustering coefficient: OR = 26.97, 95% CI = [4.70 202.10], p < 0.0001, effect size of Cohen's d = 1.10 or odds ratio = 7.34 with 80% power; path length: OR = 47618.99, 95% CI = [2583. 60 1526863.00], p < 0.0001, effect size of Cohen's d = 1.11 or odds ratio = 7.42 with 80% power) relative to the adults (Figure 4.3 and Table 4.1). Similarly to the other two infant groups', the preterm neonates before TEA showed significantly higher sample entropy of network properties relative to the adults (small worldness: OR = 1640.94, 95% CI = [26.72 260529.40], p = 0.001, effect size of Cohen's d = 0.52 or odds ratio = 2.58 with 80% power; clustering coefficient: OR = 19.13, 95% CI = [4.57 89.74], p < 0.0001, effect size of Cohen's d = 1.05 or odds ratio = 6.66 with 80% power; path length: OR = 252731.00, 95% CI = [3703.43 43362000.00], p < 0.0001, effect size of Cohen's d = 0.56 or odds ratio = 2.74 with 80% power) (Figure 4.3 and Table 4.1). Consistent findings of the comparisons in sample entropy of network properties between adults and neonate groups were observed with validation analyses that used an independent brain atlas (UNC-0-1-2 atlas) (Figure 8.4 and Table 8.7 in Appendix C). These findings strongly suggested that neonates exhibit higher neural entropy relative to adults.

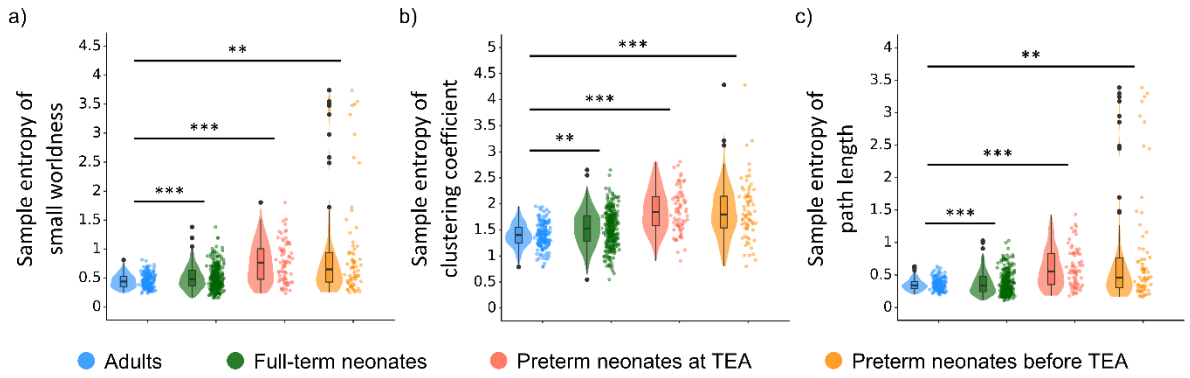

*Figure 4.3 Sample entropy of network properties in adults relative to neonates. Sample entropy of a) small worldness, b) clustering coefficient, and c) path length in neonates. Significantly higher sample entropy of network properties was found in neonates relative to adults. Abbreviations: TEA, term-equivalent age; ***, $p < 0.0005$; **, $p < 0.005$.*

Table 4.1 Sample entropy of network properties in neonates relative to adults.

Network properties	**Comparisons**	**SampEnt of network properties Odds ratios [CI]**	***p*-value**	**SampEnt of FC Odds ratios [CI]**	***p*-value**
Small worldness	Adults vs. Full-term neonates	111.95 [21.90 654.51]	< 0.0001 ***	0.17 [0.09 0.32]	< 0.0001 ***
	Adults vs. preterm neonates at TEA	870.26 [33.01 35422.28]	< 0.0001 ***	0.56 [0.17 1.69]	0.31
	Adults vs. preterm neonates before TEA	1640.94 [26.72 260529.40]	0.001 **	0.27 [0.06 1.04]	0.07
Clustering coefficient	Adults vs. Full-term neonates	4.48 [1.71 12.11]	0.003 **	0.20 [0.11 0.35]	< 0.0001 ***
	Adults vs. preterm neonates at TEA	26.97 [4.70 202.10]	< 0.0001 ***	0.84 [0.30 2.34]	0.73
	Adults vs. preterm neonates before TEA	19.13 [4.57 89.74]	< 0.0001 ***	0.50 [0.23 1.07]	0.07
Path length	Adults vs. Full-term neonates	107.70 [19.15 678.35]	< 0.0001 ***	0.44 [0.27 0.69]	< 0.0001 ***
	Adults vs. preterm neonates at TEA	47618.99 [2583. 60 1526863.00]	< 0.0001 ***	1.89 [0.80 4.59]	0.15
	Adults vs. preterm neonates before TEA	252731.00 [3703.43 43362000.00]	< 0.0001 ***	2.23 [0.71 7.68]	0.18

*Abbreviations: SampEnt, sample entropy; CI, confidence interval; FC, functional connectivity; TEA, term-equivalent age; ***, $p < 0.0005$; **, $p < 0.005$.*

4.3.2 Higher neural entropy in preterm neonates relative to full-term neonates

Logistic regression models were conducted to assess the association between premature birth and sample entropy of network properties (Figure 4.4 and Table 4.2). When the effects of prematurity were considered independently of early infant age, in the comparison between full-term neonates and preterm-born neonates at TEA, I found preterm neonates at TEA had significantly higher sample entropy of small worldness (OR = 19.98, 95% CI = [4.95 90.09], $p < 0.0001$) (Figure 4.4a and Table 4.2). In addition, I found preterm neonates at TEA had significantly higher sample entropy of clustering coefficient (OR = 6.31, 95% CI = [2.24 18.65], $p < 0.0001$) and higher sample entropy of path length (OR = 104.53, 95% CI = [19.47 646.64], $p < 0.0001$) relative to full-term neonates (Figure 4.4b, 4.4c, and Table 4.2). These results suggested that preterm-born neonates at TEA had significantly higher neural entropy relative to full-term neonates. Consistent findings were observed using the UNC-0-1-2 atlas (Figure 8.5 and Table 8.8 in Appendix C).

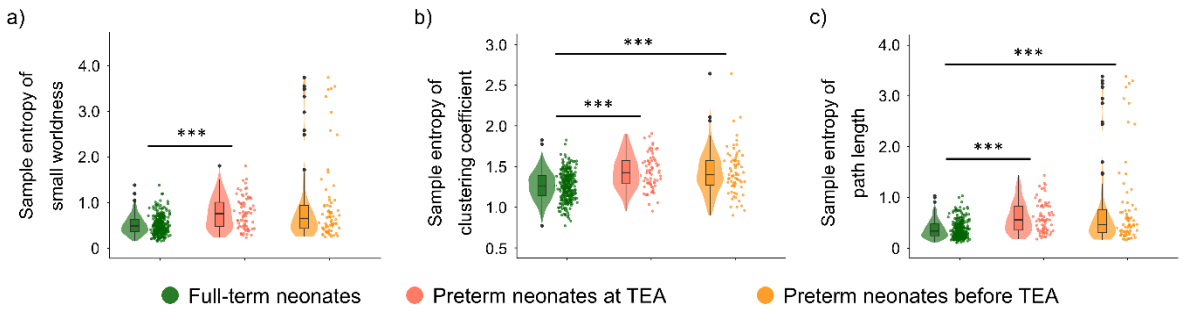

*Figure 4.4 Sample entropy of network properties in neonates. Sample entropy of a) small worldness, b) clustering coefficient, and c) path length in neonates. Significantly higher sample entropy of network properties was found in preterm neonate groups relative to full-term neonates. Abbreviations: TEA, term-equivalent age; ***, $p < 0.0005$.*

When the effects of prematurity and early infant age were collapsed, in the comparison between full-term neonates and preterm neonates before TEA, I found significantly higher sample entropy of clustering coefficient (OR = 6.23, 95% CI = [2.38 17.35], $p < 0.0001$) and higher sample entropy of path length (OR = 62.99, 95% CI = [11.29 480.89], $p < 0.0001$) in preterm neonates before TEA relative to full-term neonates (Figure 4.4b, 4.4c, and Table 4.2). These results suggested that preterm neonates before TEA at birth had higher neural entropy relative to full-term neonates. However, when using the UNC-0-1-2 atlas, I did not observe any significant difference in neural entropy between the two neonate groups (Figure 8.5 and Table 8.8 in Appendix C). Thus, caution should be exercised when interpreting this result.

Table 4.2 Sample entropy of network properties in preterm neonates relative to full-term neonates

Network properties	**Comparisons**	**SampEnt of network properties Odds ratios (CI)**	***p*-value**	**SampEnt of FC Odds ratios (CI)**	***p*-value**
Small worldness	Full-term vs. preterm neonates at TEA	19.98 [4.95 90.09]	< 0.0001 ***	1.72 [0.88 3.43]	0.12
	Full-term vs. preterm neonates before TEA	3.83 [1.03 17.32]	0.07	1.02 [0.51 2.03]	0.95
Clustering coefficient	Full-term vs. preterm neonates at TEA	6.31 [2.24 18.65]	< 0.0001 ***	1.97 [0.97 4.03]	0.06
	Full-term vs. preterm neonates before TEA	6.23 [2.38 17.35]	< 0.0001 ***	2.28 [1.21 4.36]	0.01 *
Path length	Full-term vs. preterm neonates at TEA	104.53 [19.47 646.64]	< 0.0001 ***	2.13 [1.12 4.14]	0.02 *
	Full-term vs. preterm neonates before TEA	62.99 [11.29 480.89]	< 0.0001 ***	2.34 [1.08 5.27]	0.03 *

*Abbreviations: SampEnt, sample entropy; CI, confidence interval; FC, functional connectivity; TEA, term-equivalent age; ***, $p < 0.0005$, *, $p < 0.05$.*

4.3.3 Association between neonate age and neural entropy in neonates before TEA

To investigate how neural entropy develops in preterm neonates when they are reaching TEA, I applied regression models to look at the contribution of neonate age at scan on sample entropy of network properties. I found a significant negative association between sample entropy of path length and neonate age (Figure 4.5c and Table 4.3), with sample entropy of path length decreasing with increasing neonate age (β(SE) = -0.110 (0.039), p = 0.006). A sensitivity power analysis revealed that a total sample size of 70 is sensitive enough to detect significant difference with an effect size of Cohen's d = 0.86 (α = 0.05 and a power of 0.8). A similar negative association was observed between sample entropy of small worldness and neonate age (β(SE) = -0.077 (0.037), p = 0.039) (Figure 4.5a, and Table 8.1 in Appendix C), but this result did not survive multiple comparisons correction. No significant association was observed between sample entropy of clustering coefficient and neonate age (Figure 4.5b, and Table 8.2 in Appendix C). Consistent findings were observed while using the UNC-0-1-2 atlas (Table 8.9 – 8.11 in Appendix C). These findings suggested that neural entropy decreases with age as preterm-born neonates reach TEA.

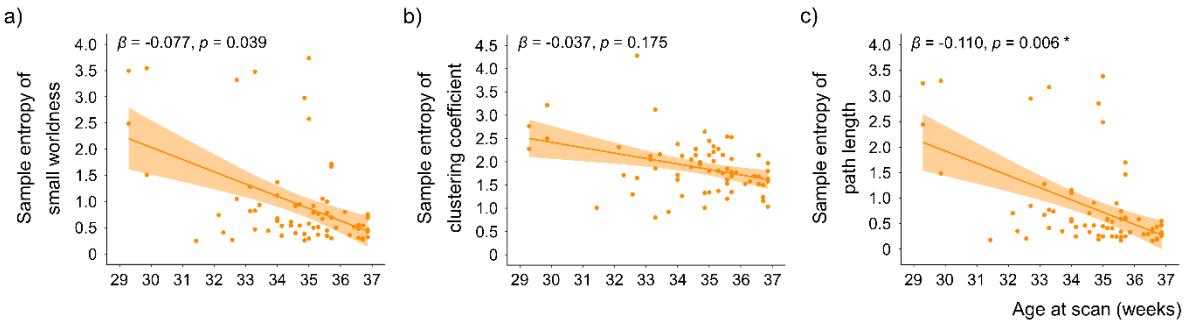

Figure 4.5 Association of neonate age with sample entropy of network properties in neonates before term-equivalent age. The x-axis displays neonates' postmenstrual age at scan, and the y-axis displays sample entropy of a) small worldness, b) clustering coefficient, and c) path length. Negative associations between neonate age and sample entropy of small worldness and of path length were observed in preterm neonates before TEA.

Table 4.3 Association between neonate age and sample entropy of path length in preterm neonate before term-equivalent age

Model summary	R^2	F	p
	0.65	29.50	< 0.0001 ***
DV	**IV**	β**(SE)**	p
Sample entropy of path length	Age at scan	-0.110 (0.039)	0.006 *
	Sample entropy of FC	0.456 (0.135)	0.001 **
	Path length	-1.030 (0.465)	0.030
	Mean FD	2.352 (0.931)	0.014 *

*Note: Unstandardized coefficient (β) and standard error (SE) were reported. DV, dependent variable; IV, independent variable; FC, functional connectivity; FD, frame-wised displacement; ***, $p < 0.0005$; **, $p < 0.005$; *, $p < 0.05$.*

4.4 Discussion

This study is the first neuroimaging study to investigate the development of entropy of network architecture in human neonates and how it may be altered by premature birth and early infant age. I showed that neonates had higher neural entropy relative to adults. Specifically, the dynamic reconfigurations of network architecture in neonates are more disordered and less predictable compared to adults. Premature birth was associated with higher neural entropy as neonates who were born prematurely but scanned at TEA showed higher neural entropy compared to full-term neonates. In addition, we found a negative association between neural entropy and neonate age as preterm neonates reached TEA.

4.4.1 Higher neural entropy in neonates relative to adults

I showed that neonates exhibit higher neural entropy compared to adults, indicating that the dynamic reconfigurations of brain networks are more random and unpredictable in neonates. Importantly, the higher neural entropy in neonates cannot be easily attributed to less-developed (static) functional architecture in comparison to adults, as I included static network properties as covariates in the statistical analyses. To our best knowledge, only one EEG study (Lippé et al., 2009) compared neural entropy in neonates around birth and in adults and reported the opposite finding. Lippé et al. (2009) found that term-born neonates showed lower neural entropy in response to visual and auditory stimuli than adults. The discrepancy is likely due to the small sample size (7 neonates and 20 adults), short acquisition time (less than 30 seconds), and importantly, the measure used to capture neural entropy lacking information on spatial entropy, as they averaged sample entropy (of time course) across channels in Lippé et al., (2009). This interpretation is further supported by my supplementary results showing lower sample entropy of time courses in full-term neonates relative to adults (Figure 8.1 and Table 8.3 in Appendix C). These findings provide further evidence for the idea that neural entropy is best computed by using the temporospatial activity pattern (Hoel et al., 2013; Oizumi et al., 2014).

The higher neural entropy in neonates may be attributed to weaker function-structure coupling in neonates relative to adults (Baum et al., 2020; van den Heuvel et al., 2015). Previous studies have shown that temporal changes in functional connectivity are, in part, determined by anatomical architecture (Batista-García-Ramó & Fernández-Verdecia, 2018; Deco et al., 2011; Fukushima et al., 2018; Liu et al., 2022). The structure-function coupling increases with age from the early weeks of life to adulthood (Baum et al., 2020; Soman et al., 2023; van den Heuvel et al., 2015). In neonates, temporal changes in

functional connections are likely less constrained by the underlying white-matter pathways relative to adults, which may partially explain the higher neural entropy in neonates.

4.4.2 Higher neural entropy associated with premature birth

I found, despite the matched age, preterm neonates at TEA exhibited higher neural entropy than full-term neonates. A consistent finding was observed while assessing neural entropy using sample entropy of time course (Figure 8.2 and Table 8.4 in Appendix C). My findings are different from previous EEG studies showing no differences (Janjarasjitt et al., 2008) or decreased neural entropy related to premature birth at TEA (Scher et al., 2005). This inconsistency is likely due to methodological differences in the type of data acquired, measures used to capture neural entropy, and relatively small sample sizes (n = 50 to 55) in these studies. For the first time, my findings suggested that prematurity was associated with less predictable brain network reconfigurations in neonates at term-equivalent age. These results are consonant with previous studies which showed that prematurity was associated with abnormal dynamic brain connectivity (Baranger et al., 2021; França et al., 2022; Ma et al., 2020). Specifically, Baranger et al. (2021) showed that a state showing thalamocortical disconnection is more predominant in preterm neonates compared to full-term neonates. The higher neural entropy observed in preterm neonates is likely due to early exposure to ex-utero environments and developmental risk factors associated with premature birth, such as intrauterine infection, inflammation, and maternal stress (Robert L Goldenberg et al., 2008).

4.4.3 Association between neonate age and neural entropy

We found that neural entropy decreased with increasing age in preterm neonates up to TEA. This result is corroborated by Frohlich et al. (2022), who measured neural entropy (of time course in cortical areas) in 41 foetuses showing evidence of perceptual consciousness in an auditory oddball paradigm (Moser et al., 2021). Frohlich and colleagues (2022) found that cortical entropy decreased with age in foetuses aged from 25 to 40 weeks of gestational age. Similarly, my supplementary analysis showed a significantly negative association between sample entropy of time course and neonate age in preterm neonates before TEA (Figure 8.3 and Table 8.5 in Appendix C). Therefore, the present study extends the findings of Frohlich et al. (2022) by demonstrating that neural entropy decreases with age even in neonates born prematurely and outside the womb. The dynamic reconfigurations of functional networks became more predictable with increasing age when preterm neonates approached TEA.

4.4.4 Summary

In summary, the findings of the current study showed that neonates at birth exhibit higher neural entropy relative to adults, suggesting more complex/less predictable network dynamics in neonates. In addition, preterm neonates before term-equivalent age show higher neural entropy relative to full-term born neonates. Although neural entropy decreases with neonatal age during the third trimester, preterm neonates do not ‘catch up’ at term-equivalent age and exhibit higher neural entropy relative to their term-born peers, suggesting persistent effects of premature birth. Overall, my results demonstrate that infants at birth exhibit distinct dynamic changes in brain networks compared to adulthood, possibly associated with different conscious experiences during infancy. In addition, my

findings emphasize the importance of the third trimester in the development of brain network dynamics. These findings improve understanding of the ontogeny of functional brain network dynamics in infancy.

4.4.5 Methodological consideration

Although some previous EEG/Magnetoencephalography (MEG) studies (Frohlich et al., 2022; Isler et al., 2018; Scher et al., 2005; Wielek et al., 2019; Zhang et al., 2009) have investigated the development of neural entropy in neonates at birth, due to the limited spatial resolution of EEG/MEG recordings, those studies did not consider the information on spatial entropy. My findings further supported the idea that neural entropy is better computed using the temporospatial activity pattern (Hoel et al., 2013; Oizumi et al., 2014). It is worth noting that the neonate rs-fMRI data have a higher temporal resolution (TR = 392 ms) relative to the adult data (TR = 720 ms). To ensure that the higher neural entropy observed in neonates was not a result of a higher resampling rate, I resampled the infant data by omitting one time point for every two time points. I then repeated all the comparisons between neonates and adults, which yielded consistent results (Table 8.6 in Appendix C). Given these methodological strengths and clear results, I believe this study improves our understanding of development of neural entropy in early infancy.

5. Chapter 5: General Discussion

One of the great frontiers of consciousness science is understanding how early consciousness arises in the development of human infants. The lack of language and wilful motoric output presents major barriers to consciousness science in neonates. These limitations can be sidestepped by asking a foundational question to the understanding of the capacity for conscious experience: whether or not the brain mechanisms of conscious awareness are instantiated in neonates. I investigated the development of brain markers indicative of conscious awareness (observed in behaviourally non-responsive adult populations) in neonates at birth. These brain markers are a) the reciprocal relationship between DMN and FPNs, b) functional small-world architecture and c) neural entropy. In addition, I investigated the effects of premature birth and early neonate age on the development of these brain markers. Below, I first review the main and novel findings of this thesis. I then discuss the implications of my results for the understanding of infant consciousness. Lastly, I discuss the limitations of the current work and future directions.

5.1 Summary of findings

The aim of Chapter 2 was to investigate the development of DMN, FPNs (DAN and ECN) and the reciprocal relationship between the DMN and FPN in neonates at birth. This relationship is thought to facilitate the integration of information across the brain. A handful of neonatal neuroimaging studies have investigated the development of DMN and FPNs in neonates. However, due to methodological differences and relatively small sample sizes in previous neonatal rs-fMRI studies, it is impossible to conclude, in light of inconsistent results, whether the three networks are already present at birth or not. Here, I used a large open-source neonate dataset, the dHCP dataset (n = 282). The high temporal

and spatial resolution infant rs-fMRI data, along with accurate week-by-week structural templates of the developing infant brain, ensured higher sensitivity to detect the presence of discrete brain networks in early infancy. The key novel finding of Chapter 2 was the presence of the DMN and FPNs and their reciprocal relationship at full-term birth or TEA. This suggests that neonates possess key features of the brain infrastructure that enables the integration of information across diverse sensory and higher order functional modules by full-term birth or TEA. However, relative to adults, all neonates exhibited less developed DMN, FPNs, and their reciprocal relationship, suggesting that this system is yet to undergo substantial change before it resembles that of the adults. By contrast, I did not observe the DMN, ECN aspect of the FPNs, or the reciprocal relationship between DMN and FPNs in preterm neonates before TEA. This suggests that the 3rd trimester of pregnancy is a key period for their development. In addition, preterm neonates showed less cohesive DMN and DAN at TEA relative to their term-born peers, suggesting a negative impact of premature birth on the development of these high-order networks.

In Chapter 3, I took the whole brain into consideration and investigated the development in infancy of the functional small-world architecture, which enables efficient differentiated and integrated information at local and global brain scales, in the healthy adult brain. However, whether this efficient functional brain architecture is developed in neonates at birth, and how it is affected by premature birth and early neonate age remain unclear. Here I used large neonate rs-fMRI cohorts to answer whether small-world architecture is present in neonates at birth. In addition, as choices of brain parcellations and data processing procedure affect network topological architecture, I devoted particular attention to the reproducibility of my results using different parcellations (the Power atlas or UNC-0-1-2 atlas), edge-definition methods (binary or weighted), multiple thresholds (0.1:0.01:0.3), and various algorithms to assess small-world architecture. I found robust evidence that neonates possess the small-world architecture that supports the balance of information

integration and segregation at full-term birth or TEA. Nevertheless, brain architecture in neonates is closer to that of a random network, exhibiting weaker small-worldness and lower network segregation compared to adults. This finding suggests that neonates have less efficient differentiating and integrative processes compared to adults. For the first time, I showed that preterm neonates before TEA were less likely to exhibit small-world architecture and had widely underdeveloped nodal efficiency in 9 out of 11 networks across the brain relative to full-term counterparts. These differences were driven by both sensory and higher-order networks. In addition, we observed that, for the most part, global small-world properties and regional communication efficiency developed in healthy-born premature neonates as they reached TEA, suggesting a pre-programmed developmental trajectory of this functional architecture despite of prematurity. Nevertheless, significant prematurity-related disruption of small-world architecture persisted at TEA.

In Chapter 4, I investigated the development of neural entropy, which is believed to reflect the uncertainty and richness of brain states. Adult studies suggest that neural entropy is an experimentally tractable and accurate measure for quantifying different conscious states. Neural entropy decreases when consciousness fades, i.e., during sleep or general anaesthesia, as well as in the minimally conscious state or the unresponsive wakefulness syndrome. By contrast, neural entropy was found to increase in altered states of consciousness, such as during hallucinatory or the psychological state elicited by classic psychedelic drugs (i.e., LSD and psilocybin). It remains unknown whether neural entropy in neonates is different from that of adults, and how premature birth and early neonate age affect that development. I assessed neural entropy by the sample entropy of network configuration of the whole brain (except the cerebellum), using graph theoretical analysis combined with a sliding-window approach, in neonates and adults. The first novel finding of Chapter 4 is that neonates had higher neural entropy relative to adults, indicating that the dynamic reconfiguration of brain networks are more complex and unpredictable in

neonates. The second novel finding is that preterm neonates exhibited higher neural entropy relative to full-term neonates, regardless of matched age of assessment. This result suggested that premature birth was associated with more complex and less predictable brain network reconfigurations. In addition, I found that neural entropy decreases with increasing age in preterm neonates from birth to TEA, suggesting the brain dynamics become more orderly and predictable as infants grow in the early days of life.

5.2 Implications

5.2.1 Brain markers for conscious awareness are present in neonates at full-term birth

Two key properties of conscious experiences are integration (unity) and differentiation (Deco et al., 2015; Seth, 2009; Seth, et al., 2006; Cooney & Gazzaniga, 2003; Tononi & Edelman, 1998). A conscious brain can integrate distinct experiential features (e.g., sights, sounds, smells, visceral sensations, etc.) into a unified conscious experience. At the same time, each conscious experience is unique, differing from a vast array of conscious states at any given time. It has been postulated that these key properties of conscious experience rely on the capacity of widely distributed and functionally specialized regions of the thalamocortical system to interact rapidly and effectively to form an integrated whole (Dehaene & Changeux, 2011; Friston, 2002; Laureys, 2005; Tononi & Koch, 2008). In this thesis, I investigated the development of three functional brain markers that support the differentiation and integration properties of conscious experiences in neonates at birth. The reciprocal relationship between the DMN and FPNs is believed to facilitate information integration. The functional small-world architecture contributes to efficient information integration and segregation. Neural entropy quantifies the uncertainty and richness of possible brain states within the brain system.

Some structural prerequisites for the emergence of these functional brain markers were already present in neonates by full-term birth. The structural connections underlying the DMN and FPNs are present in neonates at birth. For example, the cingulum bundle, a key tract that interconnects the anterior and posterior core midline regions of the DMN (Hagmann et al., 2008; van den Heuvel et al., 2008), was already present at full-term birth (Kumpulainen et al., 2023) or even earlier (Dubois et al., 2006). The superior longitudinal fasciculus, a primary and direct tract that connects frontal and parietal cortices (Petrides & Pandya, 1984; Schmahmann et al., 2009), has been identified in full-term neonates (Geng et al., 2012; Liang et al., 2022; Uda et al., 2015) and preterm neonates at TEA (Rose et al., 2014). Similarly, neonate's structural networks exhibited a small-world architecture at full-term birth (Huang et al., 2015; Ratnarajah et al., 2013; Shi et al., 2012).However, whether the DMN, FPNs (Doria et al., 2010; Gao, Alcauter, Elton, et al., 2015; Gao et al., 2009; He & Parikh, 2015, 2016; Linke et al., 2018; Smyser et al., 2010) and functional small-world architecture (Bouyssi-Kobar et al., 2019; De Asis-Cruz et al., 2015; Fransson et al., 2011; Omidvarnia et al., 2014) are present in neonates at birth remain unclear.

Here I used the largest neonate rs-fMRI cohorts and week-specific neonate templates to answer whether these functional brain markers are present in neonates at birth. I found that the DMN and FPNs were already present in full-term neonates. In addition, for the first time, I observed the reciprocal relationship between DMN and FPNs in full-term neonates at birth. My findings suggested that those distributed high-order networks were more developed at birth than would be expected. Besides, I also found robust evidence that functional small world architecture was also present at full-term birth. Taken together, these findings suggest that at full-term birth, infants possess key features of the brain infrastructure that support efficient information integration and differentiation. Accounts of the ontogeny of consciousness can be divided into two broad camps: 'early-onset' views, which posit the emergence of consciousness at, or shortly after, birth, and 'late-onset'

views, which propose the emergence of consciousness at least by the age of one. My findings in full-term neonates therefore provide evidence for ‘early-onset’ views of conscious awareness.

Highly relevant to understanding neonate awareness is Damasio’s (2000) distinction between a ‘core awareness’, or a basic integrated experience of the current moment, and an ‘extended awareness’, made possible by the accumulation of autobiographical memories that allow the creation of an internal world and projection beyond the present. This is echoed in the distinction between a ‘minimal’ self and a ‘longitudinal’ self (Seeley & Sturm, 2007). The ‘minimal’ self refers to a self that is immediate (Gallagher, 2000) and comprises awareness of body boundaries and position, facial features and body size, visceral states, agency, mental states, and online behaviour (Sturm et al., 2018). By contrast, the presence of episodic autobiographical memory (i.e., memories of past events) and semantic self-knowledge (i.e., knowledge of one’s own traits) allows for the construction of the ‘longitudinal’ self, that is extended across time. My results suggest that, at birth, the infant brain infrastructure likely supports the development of ‘core’ consciousness (Edelman, 2003; Parvizi & Damasio, 2001) and a ‘minimal’ self , and not the forms of consciousness that require reflection, self-consciousness, or off-line cognition (Goupil & Kouider, 2019; Rochat, 2003). These features can be absent even in adult states of consciousness (Metzinger, 2020; Nour et al., 2016), and are unlikely to be present in the earliest stages of experience (Bayne et al., 2023).

It is important to note that my findings suggest that functional brain networks and their organization are yet to undergo substantial change before they resemble that of adults. In Chapter 2, I found that all neonate groups had less cohesive DMN and FPNs (lower within relative to between-network connectivity) and these networks’ nodal structure were atypical compared to adults. Importantly, for the first time, I showed that the reciprocal

relationship between DMN and FPNs was weaker in neonates relative to adults (Chapter 2), suggesting less efficient information integration in neonates. Similarly, I found that neonates were less likely to exhibit strong small-world architecture and had lower network segregation compared to adults (Chapter 3), suggesting that network architecture in neonates are closer to that of a random network. Therefore, while my findings suggest that the capacity for conscious experience is present at birth, coupled with previous evidence, they suggest that such experiences are likely limited and rapidly to become more fully fledged from the first days and months of life. The frontal cortex, a nexus of the frontoparietal and DMN networks, undergoes dramatic maturation and reorganization by the end of the first year of life, resulting in big improvements in several cognitive abilities, and in sophistication of related mental content at that age (Diamond & Goldman-Rakic, 1989). Kouider et al. (2013) found an electrophysiological signature of perceptual consciousness which was present albeit weak and delayed in 5-month-olds, became stronger and faster in 12−15-month-old infants. Kovács et al. (2010) found that infants' eye movements demonstrated a capacity to monitor other people's beliefs at 7 months, and to make predictions about visual scenes at 12 months. Critically, at birth, neonates are largely bereft of the wealth of prior experiences that inform episodic memory and semantic knowledge, which allow for the construction of longitudinal awareness (Damasio, 2000; Seeley & Sturm, 2007), and the creation of an internal world that projects beyond the present and is extended across time. Nevertheless, even from the first days of life, neonates encode, store, and retrieve information about events in their world (Ellis et al., 2021; Howe & Courage, 2004; Howe et al., 2003). They start to integrate sensory, kinesthetic and proprioceptive stimulus response contingencies (Dall'Orso et al., 2021), in order to understand the actions of others and generate models for producing similar actions. Our results suggest that from birth neonates possess the capacity to integrate sensory and

incipient cognitive experiences into coherent conscious experiences about their core self and the developing relationship to their environment.

In addition, I found that not only the static functional brain architecture (Chapter 3), but also the temporal reconfigurations of brain architecture were more random and unpredictable in neonates compared to adults (Chapter 4). It is plausible that network configurations at each "microstate" (in short temporal sliding window) are less likely to follow the 'small world' rule and are more random in neonates relative to adults. At the same time, neonates' brain might be more sensitive to intrinsic or extrinsic perturbations and rapidly visit different states. Our finding of higher neural entropy in neonates compared to adults aligns with the 'entropic brain' hypothesis proposed by Carhart-Harris and colleagues (2014). According to this hypothesis, infant consciousness might serve as an exemplar of altered states of consciousness, where the brain operates closer to the super-critical end of a critical zone. In this regard, brain system is likely to prioritize flexibility over preservation and exploration over exploitation (Cohen et al., 2007). This prioritization allows the brain to explore a broader repertoire of transient states than during normal waking consciousness. It is intriguing to note that this proposal is agreed with Gopnik's (2007, 2009) idea that infant consciousness is like a 'lantern', to be contrasted with adult consciousness, which is like a 'spotlight'. Adults typically take a goal-directed exploitation strategy to explore the world (Frankenhuis & Gopnik, 2023). They are good at focusing their attention on a specific goal-related event and being less conscious of other unattended events. In contrast, infants' attention is less focused, and they explore their environment more actively and randomly. Due to their lack of experience, all stimuli in the environment are novel for infants, easily capturing their attention. Thus, they are less likely to fixate within a specific state and can easily traverse a variety of states. The broader attention makes babies aware of a broader range (though weaker and less vivid) of information than adults. For example, 6- to 8-month-old infants raised in English-speaking

households were able to discriminate 2 pairs of natural Hindi speech contrasts (/ta/ /Ta/ and /T^h//d^h/), while monolingual adult English speakers failed to do so (Werker et al., 1981). Similar developmental trajectories have also been observed in face perception, whereby a broad non-specific system becomes gradually tuned for processing species-specific faces (Nelson, 2001; Pascalis et al., 2020). Therefore, the higher neural entropy observed in neonates in the current thesis, coupled with previous evidence, suggested that infant consciousness should not be regarded as inherently less advanced or inferior to that of adults.

5.2.2 The third trimester of pregnancy is important for the development of these brain markers

The third trimester of pregnancy (after 24 weeks of GA) has been found to be an important period for infant brain development. During this period, the cortical plate gets thicker and more diverse (Rakic, 1988), cortical gyrification develops dramatically (Burkhalter et al., 1993; Kostovic & Judas, 2006; Kostovic et al., 2019), and long interhemispheric and interhemispheric cortico-cortical afferents start to grow (Eyre et al., 2000; Kostovic & Judas, 2010; Vanhatalo & Kaila, 2006). Some previous functional MRI studies in preterm neonates also showed that some canonical functional networks, especially primary motor and sensory networks, develop rapidly when they reach TEA (Cao, He, et al., 2017). Importantly, premature birth commonly happens during this critical period of brain development.

Several limitations in previous studies prevent us from understanding the functional brain development in preterm neonates, in the early days to weeks of life and the effect of premature birth on such development. First, previous rs-fMRI neonate studies that have

investigated the effect of premature birth have mainly focused on disrupted within-network coherence or topological organization (Cao, Huang, et al., 2017; Eyre et al., 2021; Smyser et al., 2016; van den Heuvel et al., 2015), and knowledge of the impact of premature birth on the relationship between high-order brain networks and brain dynamics remains scarce. Second, there is a lack of studies systematically investigating the effects of prematurity and early neonate age by including full-term neonates and preterm neonates scanned at different ages (both before and at TEA). Third, most of the previous studies are of small sample size and of low spatial and temporal resolution. My studies address these limitations to deliver novel findings that address the impact of prematurity in the development of brain markers that support consciousness.

For the first time, in Chapter 2, I showed that the DMN and FPNs were developed in healthy-born premature neonates by TEA, but not before that age (except for DAN). These findings suggest that relative to other high-order networks, e.g., the DMN, the ECN aspect of the fronto-parietal networks is the least developed in preterms and most liable to undergo developmental change in the early weeks post-birth. Furthermore, the reciprocal relationship between the FPNs and DMN also showed underdevelopments in preterms before TEA, but appeared to develop once infants reached TEA. Similarly, I found that although the functional small-world architecture was present in both preterm neonates at TEA and before TEA, the functional architecture was dramatically underdeveloped in neonates before TEA (Chapter 3). Premature neonates before TEA showed weaker small-world brain architecture and widely disrupted nodal efficiency across 217 nodes comprising 11 brain networks, including both primary networks and high-order networks (i.e., dorsal attention and frontoparietal control networks). By contrast, the global small-world properties and long-range regional communication normalised as preterm neonates approached term-equivalent age, suggesting a pre-programmed developmental trajectory of functional architecture despite prematurity. Taken together, the findings in preterm

neonates suggested that the third trimester of pregnancy is a critical period for the development of the DMN, FPNs and their relationship.

In addition, I found that although premature neonates showed large-scale recuperation of functional network development by TEA, some effects of premature birth persisted at that age. In preterm-born neonates at TEA, prematurity was associated with less cohesive/developed DMN and DAN (Chapter 2), disrupted small-world architecture and reduced efficiency of regional communication in networks related to high-order cognition, including language (Chapter 3). Similarly, I found that the effects of premature birth on temporal reconfigurations of brain architecture persist at term-equivalent age. Despite the matched age, preterm neonates at TEA exhibited higher neural entropy than full-term neonates (Chapter 4). This result is consonant with Baranger et al. (2021), which showed that prematurity was associated with abnormal dynamic brain connectivity, particularly a thalamocortical disconnection. These disrupted static and dynamic functional network development in preterm neonates may be due to early exposure to ex-utero environments and developmental risk factors associated with premature birth, such as intrauterine infection, inflammation, and maternal stress (R. L. Goldenberg et al., 2008). My results shed light on disrupted brain mechanisms that may underlie the significant risks for neurodevelopmental and psychiatric problems in later life (Bhutta et al., 2002; Marlow et al., 2005; Nosarti et al., 2012; Saigal & Doyle, 2008), that are associated with premature birth. It is important to note that the findings showing delayed or altered brain markers of conscious awareness do not imply that conscious awareness itself is delayed. The brain markers used in this thesis are one-way markers, which are of high specificity but low or unknown sensitivity. The presence of these markers corresponds with the presence of the capacity for conscious awareness, but their absence does not correspond with the absence of that capacity.

5.2.3 How do these findings relate to the theoretical understanding of consciousness

In this thesis, I took a cluster-based approach, investigating the presence of three brain markers that were found to indicate the presence of conscious awareness in adults' populations, rather than relying on a specific theory of consciousness. This is partially because different theories of consciousness have differing perspectives on when consciousness begins (Bayne et al., 2023). The IIT (Tononi, 2004; Tononi et al., 2016) is likely to hold an 'early-onset' view, while the higher-order theories (Brown, 2015; Lau & Rosenthal, 2011) and local re-entry theory suggest a late-onset of consciousness (Lamme, 2006; Lamme & Roelfsema, 2000). Nevertheless, some of my findings can be related to two theories of consciousness, the GNWT and IIT (a direct evolution of the Dynamic Core Hypothesis).

According to the GNWT (Dehaene et al., 2011; Dehaene et al., 1998; Mashour et al., 2020), information becomes conscious when it is 'broadcasted' within an anatomically widely distributed neuronal workspace, and becomes available to a wide range of cognitive processes, such as attention, memory, evaluation, and verbal reports. The global neuronal workspace is suggested to consist of widely distributed high-order cortical association areas, with the fronto-parietal areas playing a key role in the integration and broadcasting of information for conscious access (Dehaene & Changeux, 2005; Dehaene et al., 2003). Additionally, other cortical areas, such as the anterior temporal, anterior and posterior cingulate cortex, and precuneus (which are key nodes of the DMN), as described above may be equally important for consciousness (Dehaene & Changeux, 2005; Mashour et al., 2020). Therefore, my finding of the presence of FPNs and DMN, especially FPNs, as distinct networks in full-term or term-equivalent young infants suggests some kind of parietal/prefrontal workspace is in place from birth. However, it remains unclear whether this workspace fulfils the criteria for being considered a 'global' workspace, partly due to

the lack of a precise specification of the criteria that a workspace must satisfy to be truly 'global'. In addition, according to GNWT, brain regions within the global neuronal workspace are functionally specialised and segregated, yet the communication between them is extensive and rapid so any information available to one is quickly available to others (Boly et al., 2007; Mashour et al., 2020; Odegaard et al., 2017). In Chapter 3, I found that the functional small-world architecture, which facilitates efficient information transformation both within each module and between modules, was present in neonates at full-term birth or term-equivalent age. This finding suggested that a potential functional brain architecture supporting efficient information transformation is already present in neonates at full-term birth.

Another theory of consciousness relevant to my results is the IIT (Tononi, 2004; Tononi et al., 2016). The IIT holds that consciousness should be understood in terms of "cause-effect power" that reflects the amount of maximally irreducible integrated information generated by a physical system, which can be quantified by Φ (Tononi, 2004; Tononi & Sporns, 2003). According to IIT, any system that generates non-zero integrated information (at least to some extent) is conscious. However, IIT has been criticized, because Φ is intractable and cannot be directly measured in the brain (Barrett & Mediano, 2019; Northoff et al., 2019). A weak version of IIT (Mediano et al., 2022) circumvents the tractability issues and aims to offer empirically measurable and powerful explanatory neural correlates of various aspects of consciousness, such as differentiation, information, and/or integration. The week IIT proposed that brain must have access to and spontaneously visit a large and different repertoire of states to have rich conscious experience. The dynamic complexity in neural systems (neural entropy) accounts for the differentiation aspect of consciousness (Canales-Johnson et al., 2020; Casali et al., 2013; Coppola et al., 2022; Luppi et al., 2019), which is necessary for the system to be informative. The high neural entropy observed in neonates in Chapter 4 suggests that

infants may be capable of experiencing various states. However, it is important to note that the richness of brain states does not necessarily imply the richness of mental content. This limitation will be discussed further in the future direction section.

5.3 Limitations

The rs-fMRI data used in the current thesis were collected from neonates and adults in different sleep and awake conditions. The neonates were scanned during sleep without sedation, while adults were scanned during wakefulness with eyes open. This difference in sleep/awake state might have influenced the results. Although resting-state functional networks have been found to be grossly preserved during sleep (Boly et al., 2012; Boly et al., 2008; Samann et al., 2011; Tagliazucchi, von Wegner, Morzelewski, Brodbeck, Jahnke, et al., 2013), they were different from those in awake (Stevner et al., 2019; Tagliazucchi & Laufs, 2014; Yates et al., 2023). Importantly, reduced coupling of components of DMN (Horovitz et al., 2009) and the reciprocal relationship between DMN and FPNs (Samann et al., 2011) were observed during sleep compared to wakefulness in human adults. These considerations notwithstanding, in Chapter 2, I observed the FPNs, DMN, and their reciprocal relationship (Chapter 2) in neonates at full-term birth or TEA scanned during sleep (Chapter 3). It is shown that adult brains exhibit increased network segregation and decreased network integration (Tagliazucchi, Von Wegner, Morzelewski, Brodbeck, Borisov, et al., 2013) and shift toward a regular network during sleep (Spoormaker et al., 2010). Nevertheless, I found functional small-world architecture in both full-term and preterm neonates. These results were reproduced across different analysis procedures and different parcellations. Though sleep was found to be associated with lower neural entropy (Acharya et al., 2005; Bruce et al., 2009; Miskovic et al., 2019) in human adults, I found that neonates scanned during sleep exhibited higher neural

entropy compared to adults scanned during normal wakefulness (Chapter 4). Thus, the differences between neonates and adults observed in the current thesis can still be attributable, even if not entirely, to development.

The preterm groups in this thesis are not well representative of extreme prematurity (< 28 weeks)/very low birth weight (< 1500 g), because the mean gestational age of the preterm groups was 32 weeks. Extreme prematurity could be associated with different functional brain development at TEA, as well as during the preterm period, compared with infants with higher gestational ages, and will be investigated in future studies. Second, though the sample sizes of preterm neonates scanned at (n = 72), or before TEA (n = 70), are large for infant neuroimaging studies, the causes and outcomes of premature birth are highly heterogeneous (Romero et al., 2014). Thus, the size of the effects of premature birth and neonate age may not reflect a broader population of preterm neonates.

Although I used a few procedures to minimize the effects of head motion on my results, I acknowledge that it remains an unavoidable higher head motion in neonates relative to adults. I partially address this issue by conducting the statistical analyses with the head motion as a covariate, but it may still benefit from further investigation. The comparisons between preterm neonates scanned twice were based on less than 40 participants, which lacks statistical power and is of low reliability, as I already highlighted. Future longitudinal studies with a large sample of preterm neonates will be important for tracing the effect of prematurity on the development of functional brain development in early infancy.

5.4 Future directions

This thesis showed that the functional brain networks and their neural entropy were different in neonates and adults. However, how they develop beyond the newborn period

and when they reach the same level as that in adults remain unknown. Larger and older cohorts of infants and toddlers, followed up longitudinally, are needed to answer these research questions.

In Chapter 4, I measured neural entropy in neonates and adults using resting-state fMRI data. The results showed that neonates had richer repertoire of brain activity patterns relative to adults. However, we cannot tell whether the richer repertoire is driven by consciously processing internal and external stimulus or noise. An optimal way to approach this issue is to perturb the system in a controlled way and measure the perturbational complexity. In doing so, we can assess the causal relationships between the dynamic complexity and correlated inputs/perturbation and minimise the influence of noise. Casali et al. (2013) proposed that the complexity of cortical EEG responses to a transcranial magnetic stimulation (TMS) induced pulse or "perturbation", known as Perturbational Complexity Index (PCI) (Casali et al., 2013), might be a promising measure to tackles this problem. The PCI gauges the amount of information contained in the cortical responses to a direct perturbation. PCI decreases when consciousness fades (Bai et al., 2016; Casali et al., 2013; Lee et al., 2022; Sarasso et al., 2015; Sitt et al., 2014), i.e., during non-rapid eye movement sleep, general anaesthesia, as well as in the minimally conscious state or the unresponsive wakefulness syndrome. Conversely, PCI has been found to increase in altered states of consciousness, such as during hallucinatory or psychedelic states (Sarasso et al., 2015; Schartner et al., 2017). However, because the risk profile of TMS in developing brains is not well understood, its application in infants is considered unethical unless medically justified (Pridmore et al., 2021; Rossi et al., 2021). The sensory version of the PCI (sPCI) approach, perturbing cortical responses with sensory stimuli like visual, auditory, or olfactory stimuli, could be a potentially useful tool for detecting levels or states of conscious awareness in infants. Some previous studies (Frohlich et al., 2022; Shuffrey et al., 2022) have measured sPCI in response to audio

oddball stimuli using MEG/EEG in foetuses and infants. For instance, Frohlich et al. (2022) applied a "local-global" paradigm with pure tones to foetuses and newborns and collected cortical responses using MEG scans. They hypothesised that local and global deviants might produce different sizes of cortical perturbations, given that detection of global regularity is highly correlated with consciousness, while detection of local regularity can occur without consciousness (Bekinschtein et al., 2009; Engemann et al., 2018; Naccache et al., 2015). However, they did not observe any difference in complexity of cortical responses between the two conditions. One of the plausible interpretations is that the limited spatial resolution of MEG signals prevents the full capture the spatiotemporal patterns of perinatal cortical activity. Future studies that detect sPCI using neuroimaging techniques of higher spatial resolution, i.e., advanced MEG source localization techniques or fMRI, combined with sensory stimuli might provide valuable insight into the development of conscious awareness in infancy.

This thesis primarily relied on resting-state fMRI data for understanding conscious awareness in infants at very early age. Indeed, it can offer insight into the capacity for conscious awareness in infants, such as in our study we found infants possess the brain infrastructure for conscious awareness at full-term birth or TEA. However, it remains unknown how infant conscious experience differs from that of adults, since I did not measure the content of consciousness. Naturalistic paradigms (such as movies and audio clips) may be particularly suited to assess conscious experience in neonates, who cannot understand or follow study instructions and have a short attention span (Richards & Casey, 2014). First, this approach does not require compliance with task instructions. Second, it engages attention naturally through meaningful stimuli that are similar to real-world sensory information. Third, it has been demonstrated that naturalistic paradigm reduces head motion (Frew et al., 2022; Vanderwal et al., 2015), and improves test-retest reliability of functional connectivity (Wang et al., 2017; Zhang et al., 2022). Naturalistic paradigms

have been successfully used to investigate conscious experience in behaviourally unresponsive patients (Deng et al., 2023; Kandeepan et al., 2020; Laforge et al., 2020; Naci et al., 2014; Naci et al., 2017). For instance, Naci and colleagues (2014) found that a patient, who had remained largely behaviourally unresponsive for 16 years, demonstrated a highly similar brain response (in frontal and parietal cortical areas that support executive function) to that of healthy participants while viewing a highly engaging movie clip. The patient's brain activity suggested that he could consciously and continuously engage in complex thoughts about real-world events. Indeed, some recent studies have used movie stimuli to investigate cognition (Lloyd-Fox et al., 2017; Yates et al., 2022; Zhou et al., 2022), face perception (Bahrick & Newell, 2008; Farroni et al., 2013; Kelly et al., 2019) and audio perception (Cristia et al., 2014; Kotilahti et al., 2010; Wild et al., 2017) in infants from the first few days to the first year of life. For example, Wild et al., (2017) used a series of sung lullabies to investigate whether the immature auditory cortex of young infants (3 and 9 months) has similar responses as that in adults. They found that the temporal activity patterns observed in the infant auditory cortex show similarities to those found in adults. While some of these shared responses can be attributed to basic acoustic characteristics like frequency and pitch envelope, others cannot. This suggests that even more complex, adult-like features are represented in the auditory cortex during early infancy. Yates et al. (2022) collected fMRI data from awake infants (3-12 months) and adults watching a cartoon and applied a hidden Markov model to investigate even segmentation in infants and how it differs from adults. They found that infant tend to integrate sensory information over longer temporal windows and segment continuous experience into fewer events compared to adults. Therefore, naturalistic paradigms might be a useful tool for investigating the development of conscious experiences in neonates.

One potential approach is to collect neuroimaging data (e.g., fMRI, EEG, and MEG) from neonates (and adults, for comparison) while they watch/listen to intact and scrambled

movie/audio clips. We can then assess the dynamic complexity of cortical responses at the voxel level for each condition. The rationale behind this approach is that intact naturalistic stimuli carry more information, such as the causal relationship between actions and goals (Liu et al., 2019), compared to scrambled movies. If neonates are capable of encoding more complex features that require integrating information across time, beyond basic visual or acoustic features, they would exhibit higher dynamic complexity of cortical responses to intact stimuli relative to scrambled stimuli.

Nevertheless, selecting naturalistic stimuli that are both developmentally appropriate and highly engaging for young infants can pose challenges. Due to limited perception, cognition, attention, and memory abilities in the early days of life, the number of features that infants can register is limited. Moreover, previous studies found that infants prefer some types of stimuli or experimental designs over others. For example, infant prefer infant-directed over adult-directed speech (Pegg et al., 1992) and perform better in tasks involving goal-directed action (Liu et al., 2019; Woodward, 1998) and memory (Howard & Woodward, 2019) when an agent is involved. In addition, recent studies (Truzzi & Cusack, 2023; Yates et al., 2022) found that infants tend to integrate information over longer timescales relative to adults. Future studies should experimentally manipulate the content and timescales of naturalistic stimuli to make them more suitable for infants.

5.5 Conclusion

In summary, the aim of this thesis was to investigate the development of brain markers for conscious awareness in full-term neonates at birth. Additionally, I investigated the effects of premature birth and early neonate age on the development of these brain markers. I found that at full-term birth or TEA, the brain markers that support information integration

(the DMN, FPNs, and their reciprocal relationship), and efficient information processing (small-world architecture) were present. These findings provided some evidence to support the early-onset views of consciousness, which locate the emergence of consciousness at, or shortly after, birth. On the other hand, these brain markers in full-term neonates are still significantly different from those in adults, implicating a different conscious experience in neonates. The lower within-network cohesiveness in DMN, and FPNs, weaker reciprocal relationship between DMN and FPNs, and weaker small-world architecture suggested that conscious experiences may be limited in neonates compared to adults. The higher neural entropy observed in neonates, coupled with previous evidence, suggests that infant conscious experience might be less focused compared to that of adults. Furthermore, I found that the DMN, ECN, and the reciprocal relationship were not present in neonates before TEA. They were less likely to exhibit the small-world architecture and showed less efficient regional communication due to early neonate age. These findings emphasized the importance of the third trimester of pregnancy, the typical period of premature birth, for the development of the brain markers that support conscious awareness. Lastly, although I found that large-scale recuperation of functional brain development at TEA, some effects of premature birth persist, which might be associated with abnormal neurodevelopmental and higher risk for neurodevelopmental disorders. Taken together, these findings improve our understanding of the ontogeny of the brain markers that support conscious awareness in early infancy.

6. Appendix A – Supplementary materials in Chapter 2

6.1 Methods and Materials

6.1.1 Comparison of head motion in neonates and adults

To assess the differences in head motion between neonates and adults, we compared the mean FD value in adults and neonates before/after the scrubbing procedure (Power et al., 2012; Power et al., 2014). The FD value indexes the movement of the head from one volume to the next and is defined as the sum of the absolute values of the differential realignment estimates (the six realignment parameters). It has been widely used to index head movement and exclude subjects of high motion.(Gu et al., 2015; Hoptman et al., 2012; Sripada et al., 2020)

6.2 Results

6.2.1 Higher head motion in neonates relative to adults

Independent-samples *t*-tests showed that adults had significantly lower head motion compared to neonates before (t (491.45) = -12.49, $p < 0.001$) and even after scrubbing (t (580.56) = -9.92, $p < 0.001$; Figure 6.3). A paired-*t* test was applied to detect the difference in head motion in neonates before and after the scrubbing procedure. Results showed that neonates had significantly lower head motion after scrubbing relative to before scrubbing (t (427) = -9.69, $p < 0.001$) (Figure 6.3). Bonferroni correction for multiple comparisons was applied to statistical results.

Figure 6.3 about here please

6.2.2 Higher head motion in neonate groups after scrubbing relative to adults

We conducted a one-way ANOVA to compare the difference in head motion between the adults and neonate groups after the scrubbing procedure and found a significant main effect of group (F (3, 600) = 16.46, $p < 0.001$). Independent-sample t-tests were applied to compare head motion between every two groups. We found that adults had significantly lower head motion relative to the full-term neonates (t (368.44) = -8.67, $p < 0.001$), preterm neonates scanned at TEA (t (79.69) = -4.14, $p < 0.001$), and preterm neonates scanned before TEA (t (76.97) = -4.16, $p < 0.001$) (Figure 6.4). Bonferroni correction for multiple comparisons was applied to statistical results.

Figure 6.4 about here please

6.2.3 High-order networks functional connectivity in adults

In adults, a 2 × 3 repeated measure ANOVA [*type of FC* (within-network, between-network) × *network* (DMN, DAN, ECN)] showed a significant main effect of type of FC (F (1, 175) = 2323.00, $p < 0.001$), which was driven by higher overall connectivity for the within- relative to between-network (t (175) = 48.11, $p < 0.001$). We also found a main effect of network (F (1.93, 337.773) = 37.50, $p < 0.001$), that was driven by lower overall connectivity for the DMN relative to the DAN (t(175) = -8.72, $p < 0.001$) and ECN (t (175) = -3.71, $p < 0.001$) and lower overall connectivity for the ECN relative to DAN (t (175) = -5.10, $p < 0.001$). Finally, a significant interaction effect of type of FC by network (F (2, 350) = 96.49, $p < 0.001$) was driven by a smaller within- vs between-network FC difference in ECN relative to DMN (t (175) = -11.20, $p < 0.001$) and DAN (t (175) = -13.03, $p < 0.001$). Paired-t tests showed significantly higher within- to between-network FC for each network (DMN:

t (175) = 30.69, p < 0.001; DAN: t (175) = 42.00, p < 0.001; ECN: t (175) = 27.40, p < 0.001) (Figure 6.5), confirming that each of the three networks was differentiated as a cohesive unit in adults. Bonferroni correction for multiple comparison was applied to statistical results.

Figure 6.5 about here please

6.2.4 The reciprocal relationship between the DMN and prefrontal networks in adults

A one-way ANOVA with repeated measures for between-network FC (DMN−DAN, DMN−ECN, DAN−ECN) showed a significant main effect (F (1.93, 337.22) = 118.92, p < 0.001), which was driven by significantly lower FC in the DMN−DAN relative to the DMN−ECN (t (175) = -6.19, p < 0.001) and DAN−ECN pairings (t (175) = -14.01, p < 0.001), and significantly lower FC in the DMN−ECN relative to DAN−ECN pairing (t (175) = -9.61, p < 0.001) (Figure 6.6). Bonferroni correction for multiple comparisons was applied to statistical results. The lower FC between the DMN and DAN relative to the other pairings suggested a reciprocal relationship between the two networks in adults.

Figure 6.6 about here please

6.3 Supplementary Figures and Legends

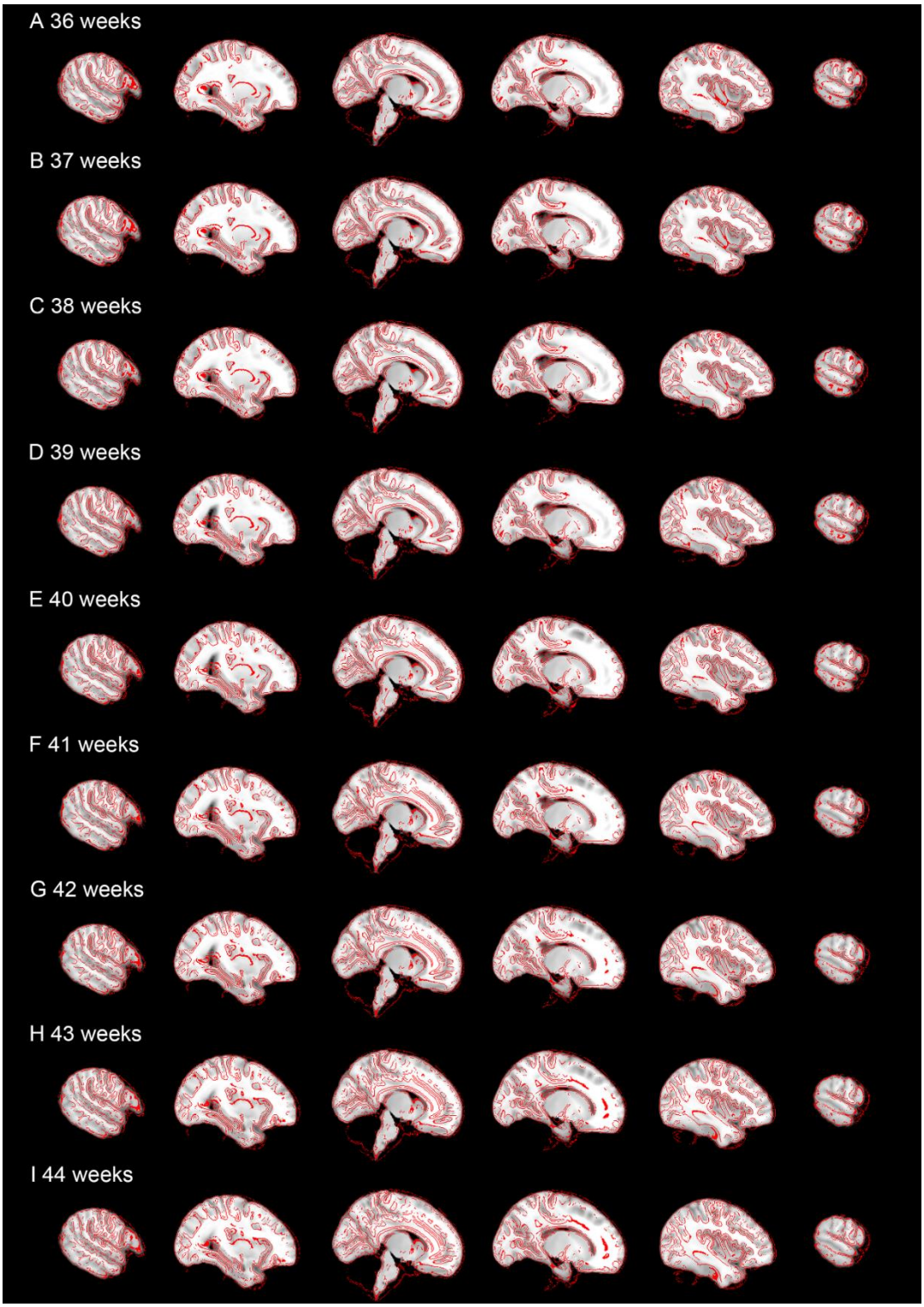

Figure 6.1. Registration of the MNI T1 template to the 40-week dHCP T1w template. The 40-week dHCP T1w templates shown in red lines were overlaid on the MNI T1 template registered to the 40-week dHCP T1w template spaces.

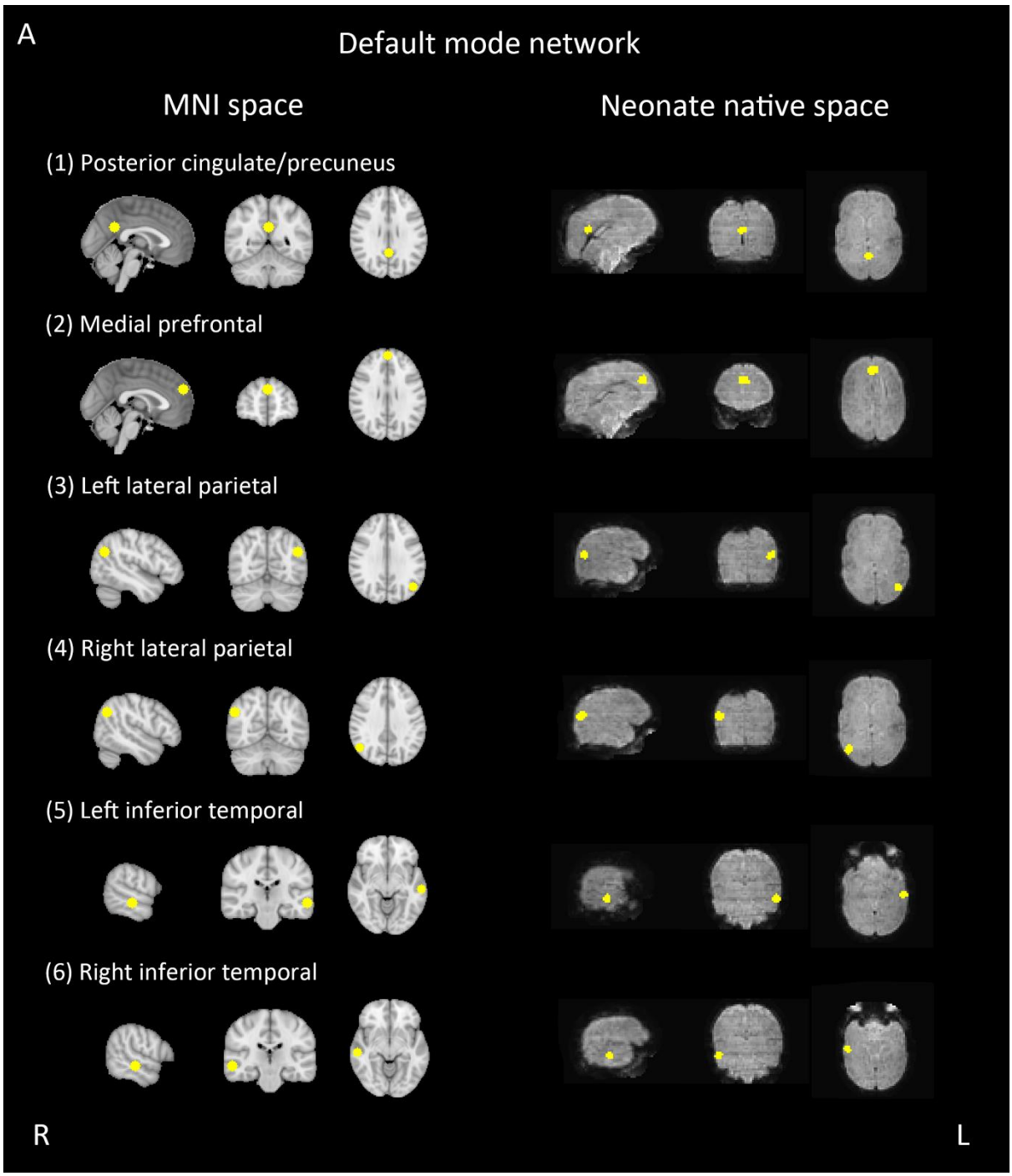
A
Default mode network
MNI space
Neonate native space
(1) Posterior cingulate/precuneus
(2) Medial prefrontal
(3) Left lateral parietal
(4) Right lateral parietal
(5) Left inferior temporal
(6) Right inferior temporal
R
L

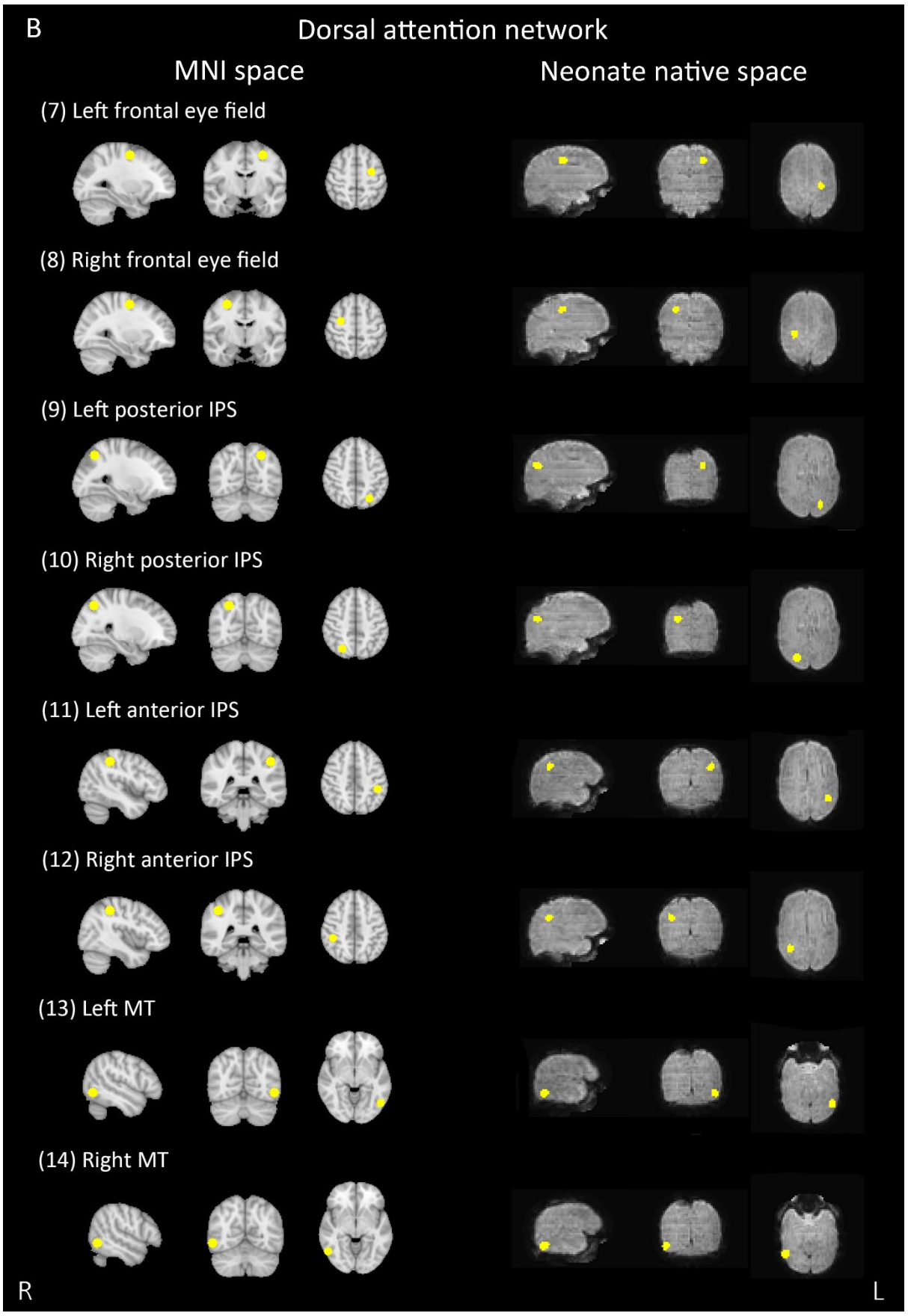
B
Dorsal attention network
MNI space
Neonate native space
(7) Left frontal eye field
(8) Right frontal eye field
(9) Left posterior IPS
(10) Right posterior IPS
(11) Left anterior IPS
(12) Right anterior IPS
(13) Left MT
(14) Right MT
R
L

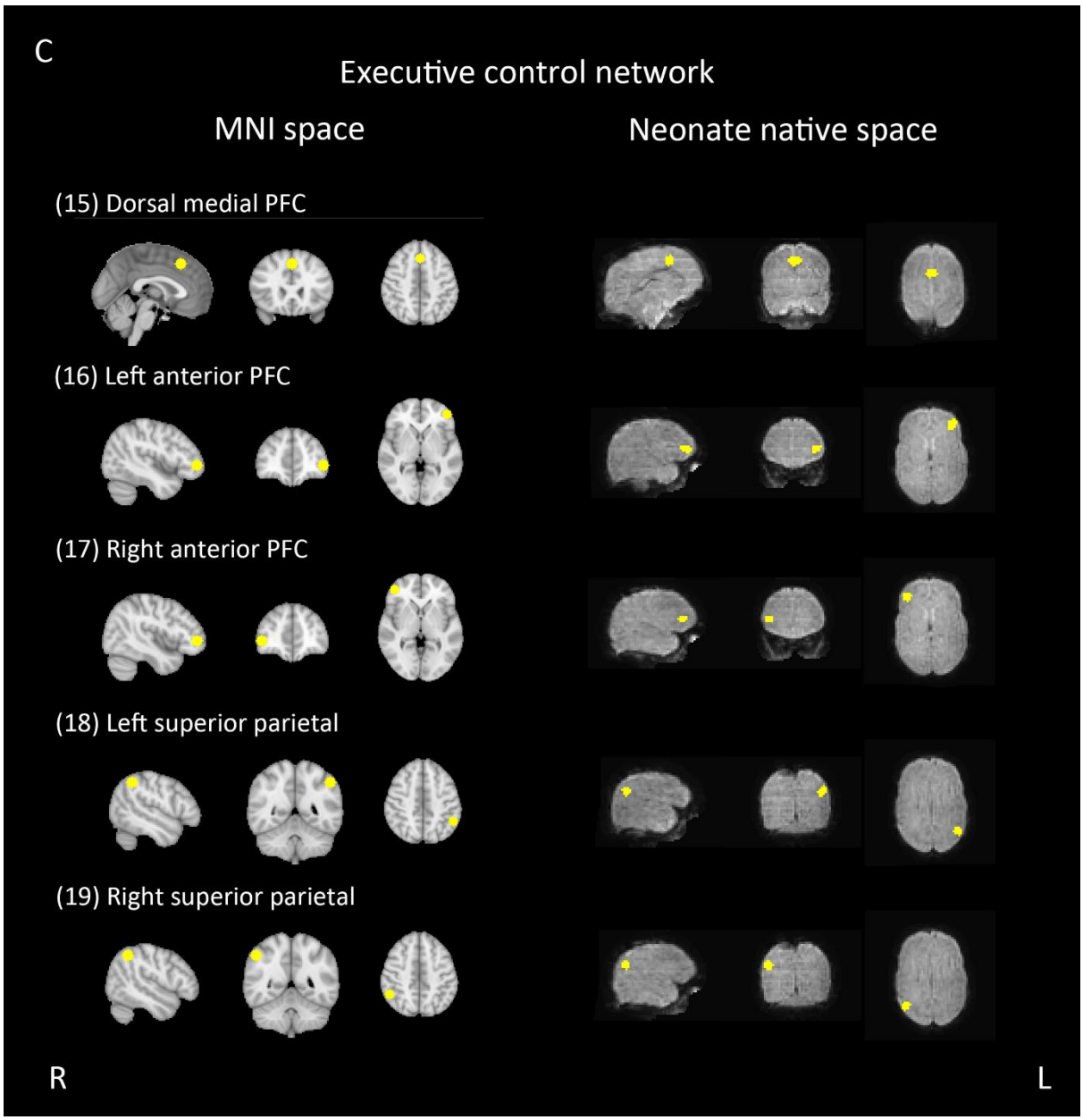

Figure 6.2 The three networks in the MNI space and neonate native space. The functional images represented here were from one neonate (sub-CC00518XX15), which was randomly chosen. (A) default mode network, (B) dorsal attention network, and (C) executive control network. Abbreviations: IPS: Intraparietal sulcus, MT: Middle temporal area, PFC: Prefrontal cortex; R, right; L, left.

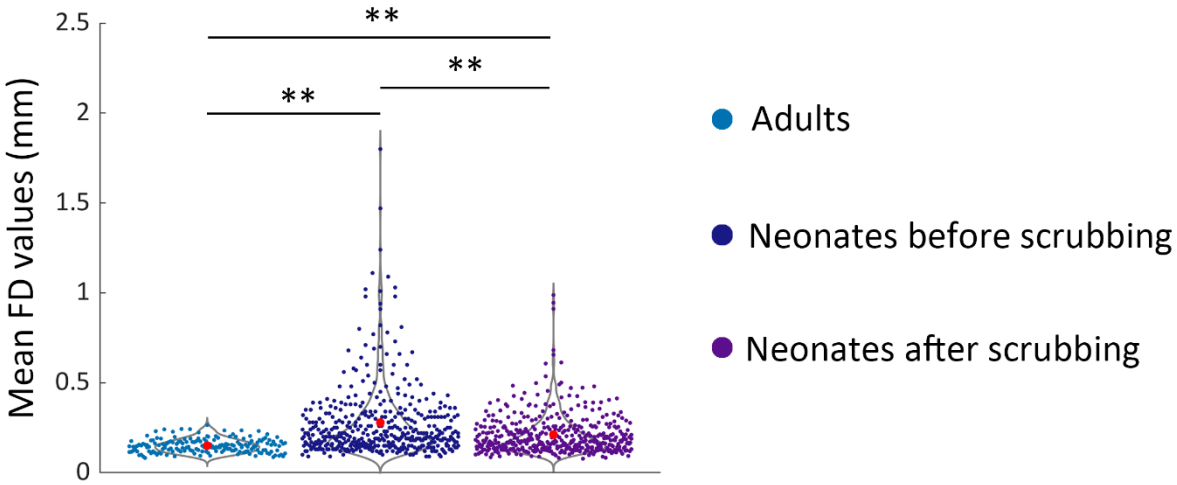

*Figure 6.3 Head motion in neonates and adults. The red dot indicates the mean framewise displacement value in each group. Independent-samples t-tests were applied to detect the difference between the adults and neonates. A paired-t test was applied to detect the difference between the neonates before and after scrubbing procedure. Abbreviations: FD, framewise displacement; ** = $p < 0.005$.*

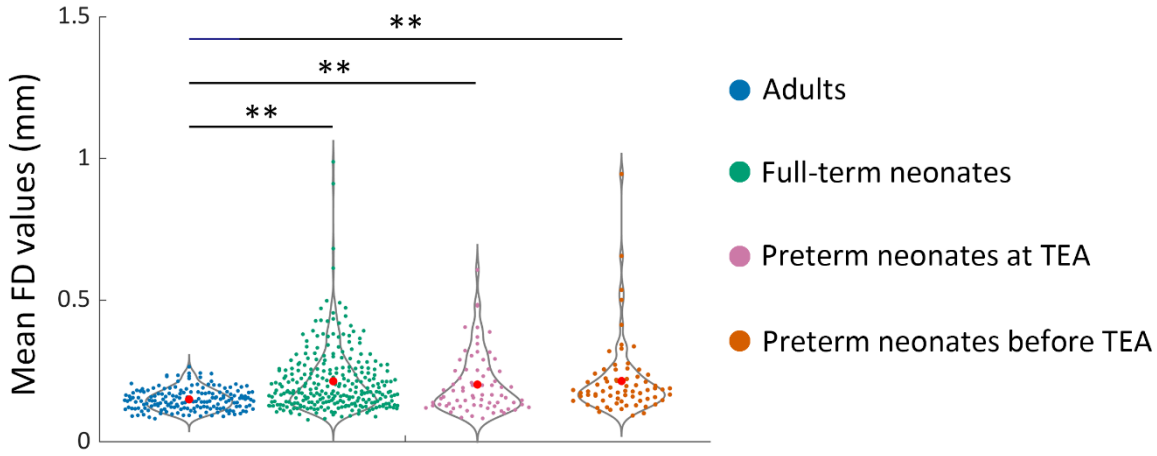

*Figure 6.4 Head motion in the neonate groups after censoring and the adults. The red dot indicates the mean framewise displacement value in each group. Independent-sample t-tests were applied to detect the difference between every two groups. Abbreviations: FD, framewise displacement; TEA, term-equivalent age; ** = p < 0.005.*

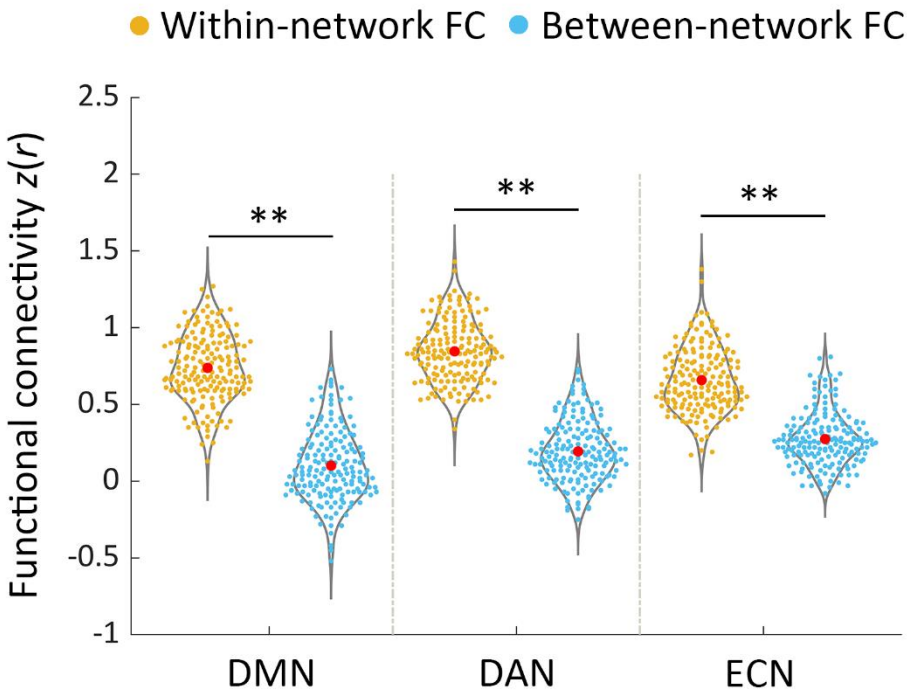

*Figure 6.5 Network functional connectivity in adults. The between-network connectivity depicts the average FC of each network with the other two. The red dot indicates the mean within/between-network functional connectivity of each network. Paired-t tests were applied to detect the difference between within-network and between-network FC for each network. Abbreviations: DMN, default mode network; DAN, dorsal attention network; ECN, executive control network; FC, functional connectivity; ** = $p < 0.005$.*

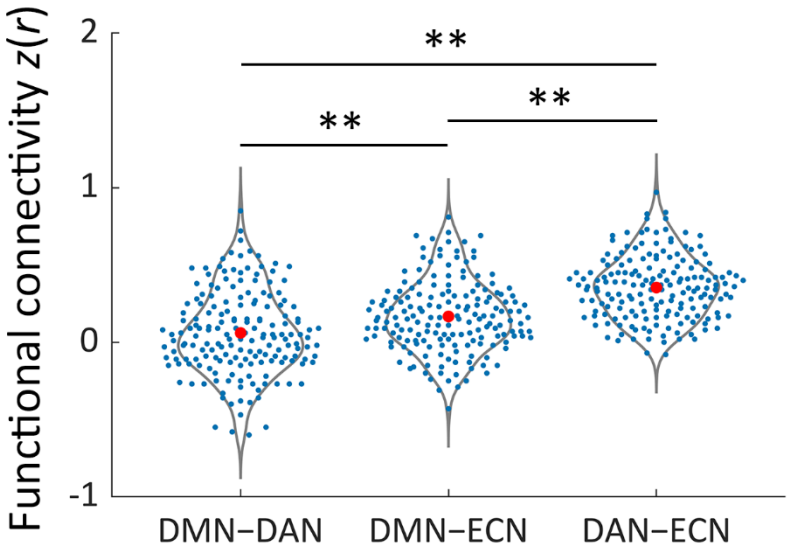

*Figure 6.6. Between-network functional connectivity (FC) in adults. FC values were Fisher-z transformed. The red dot indicates the mean functional connectivity in each network-pairing. Paired-t tests were applied to detect the difference between every two between-network FCs. Abbreviations: DMN−DAN, FC between the default mode network and dorsal attention network; DMN−ECN, FC between the default mode network and executive control network; DAN−ECN, FC between the dorsal attention network and executive control network; ** = $p < 0.005$.*

6.4 Supplementary Tables

Table 6.1. Previous rs-MRI studies of brain network development in neonates

No.	Article	Subjects	GA at birth	Age at scan	State at scan	Scanner	TR (ms)	voxel size (mm^3)	Duration (min)	Head motion control	Template	Analysis method	Neural network identified
1	Fransson et al. (2007)	12 preterm neonates scanned at TEA	25 weeks 6 days (24 weeks 4 days –27 weeks 5 days)	41 weeks 0 days PMA (39 weeks 1 day – 44 weeks 3 days)	under sedation	1.5 T	2000	2.8 × 2.8 × 4.5	10	scrubbing	neonate brain template (Dehaene-Lambertz et al., 2002)	ICA	1) VIS; 2) SMN; 3) AUD; 4) a network including the precuneus area, lateral parietal cortex, and the cerebellum; 5) an anterior network that incorporated the medial and dorsolateral prefrontal cortex.
2	Fransson et al. (2009)	19 full-term neonates	38 weeks 4 days (37 weeks 4 days – 39 weeks 1 day)	40 weeks 2 days PMA (39 weeks 2 days – 41 weeks 6 days)	natural sleep	1.5 T	2000	2.8 × 2.8 × 4.5	10	scrubbing	neonate brain template (Dehaene-Lambertz et al., 2002)	ICA	1) VIS; 2) SMN; 3) bilateral temporal/inferior parietal cortex including the primary auditory cortex, 4)posterior lateral and midline aspects of the parietal cortex; 5) medial and lateral parts of the prefrontal cortex and 6) the bilateral basal ganglia.

3	Lin et al. (2008)	38 preterm and full-term neonates	35 – 42 weeks	2 − 4 weeks after birth	natural sleep	3T	2000	4 × 4 × 4	5	scrubbing	data-specific template	SCA	SMN and VIS (exists as early as 2 weeks after birth)
		26 one-year-olds born prematurely or at full-term age	N/A	N/A									
		21 two-year-olds born prematurely or at full-term age	N/A	N/A									
4	Doria et al. (2010)	17 early preterm neonates scanned before TEA	25 weeks 2 days – 31 weeks 1 day	29 weeks 0 days – 32 weeks 1 day PMA	natural sleep	3T	1500	2.5 × 2.5 × 3.25	6.5	FD > 5 mm	data-specific template	ICA and SCA	1) In full-term neonates and preterm neonates scanned at TEA: VIS, AUD, SMN, motor, DMN, FPN, and ECN were completely present; 2) In early preterm neonates: AUD, dorsal visual stream and ECN were not found; 3) Before TEA, the DMN was incomplete.
		21 preterm neonates scanned before TEA	26 – 35 weeks	33 weeks 0 days – 36 weeks 4 days PMA	natural sleep (17/23) /under sedation								
		24 preterm neonates scanned at TEA	24 weeks 3 days – 35 weeks 3 days	39 weeks 3 days – 43 weeks 2 days PMA	under sedation								

		8 full-term neonates	38 – 41 weeks 4 days	39 weeks 1 day – 43 weeks 4 days PMA	natural sleep (6/8) /under sedation								
5	Smyser et al. (2010)	53 preterm neonates	23 weeks 2 days – 34 weeks 0 day	1) < 30 weeks PMA 2) 30 weeks PMA 3) 34.0 weeks PMA 4) 38.0 weeks PMA	natural sleep/resting quietly	3T	2910	2.4 × 2.4 × 2.4	10	scrubbing	Adult template	SCA	1) In preterm neonates and full-term neonates: motor-leg, motor-hand, motor-face, PCC, ACC, occipital, MPFC, LPFC, temporal, thalamus and cerebellum. 2) DMN precursor in full-term neonates.
		10 full-term newborns	N/A	Within 2—3 days of birth									
6	Alcauter et al. (2014)	112 preterm and full-term neonates	35 – 42 weeks	4 weeks 5 days ± 2 weeks 5 days after birth	natural sleep	3T	2000	4 × 4 × 4	5	scrubbing	data-specific template	SCA	1) Neonates: Adultlike SMN, AUD, medial visual, and occipital pole and SN; Incomplete lateral visual, DMN, and FPN. 2) The lateral VIS, DMN, FPN showed dramatic synchronization during the first year and had minor refinement during the second year.
		129 one-year-olds	N/A	1 year 32 days ± 35 days									
		92 two-year-olds	N/A	2 year 32 days ± 33 days									

7	Gao et al. (2009)	20 preterm and full-term neonates	35 – 42 weeks	3 weeks 3 days ± 1 week 5 days after birth	natural sleep	3T	2000	4 × 4 × 4	5	scrubbing	data-specific template	ICA	An incomplete DMN is present in 2-week-olds. More adultlike DMN were found in 1-year-olds and 2-year-olds.
		24 one-year-olds	N/A	1 year 1 month ± 1 month									
		27 two-year-olds	N/A	2 years 1 month ± 1 month									
8	Gao et al. (2013)	51 full-term and preterm neonates	35 – 42 weeks	3 weeks 2 days ± 1 week 5 days after birth	natural sleep	3T	2000	5 × 4 × 4	5	None	a subject not included in this study and scanned at 3 weeks	SCA	1) Neonates: incomplete DMN and DAN. 2) 1-year-olds: highly synchronized DMN and DAN.
		50 one-year-olds	N/A	1 year 1 month ± 1 month									
		46 two-year-olds	N/A	2 years ± 1 months									

9	Gao, Alcauter, Elton, et al. (2015)	65 full-term neonates	35 – 42 weeks	< 1 month (N = 45) 3 months (N = 34) 6 months (N = 33) 9 months (N = 29) 12 month (N = 35)	natural sleep	3T	2000	4 × 4 × 4	5	scrubbing	data-specific template and adult MNI template	SCA	1) Neonates: SMN, AUD, VN; incomplete lateral visual/parietal network, SN, DMN, FPN. 2) 1-year-olds: adultlike lateral visual/parietal network and DMN; incomplete SN and FPN
10	Gao, Alcauter, Smith, et al. (2015)	143 full-term neonates	36 – 42 weeks	4 weeks 5 days ± 2 weeks 5 days after birth (N = 112) 1 year old (N = 129) 2 years old (N = 92)	natural sleep	3T	2000	4 × 4 × 4	5	scrubbing	data-specific template	ICA	1) Neonates: VN and SMN; 2) The auditory/language, lateral visual/parietal, DMN, right FPN, SN, and left FPN were topologically incomplete and isolated in neonates but demonstrated consistent synchronization during the first 2 years of life.
11	Wylie et al. (2014)	12 full-term neonates	N/A	8 weeks 0 days ± 2 weeks 6 days after birth	under sedation	3T	2000	3.43 × 3.43 × 3.4	N/A	motion larger than 1 voxel	MNI template	ICA	DMN, VIS, AUD, SMN, basal ganglia, precuneus, visual spatial, language, ECN, anterior SN.

12	Damaraju et al. (2014)	4-month-old full-term infants	N/A	18 weeks 4 days ± 2 weeks 1 day after birth	natural sleep	3T	2000	thickness = 3.5 mm	8.3	despiking step	9-month MNI template (Altaye et al., 2008)	ICA	In both groups: sub-cortical, AUD, VIS, SMN, DMN, temporal, attentional and frontal network, cerebellum.
		9-month-old full-term infants		40 weeks 4 days ± 1 week 2 days after birth									
13	He and Parikh (2015)	27 preterm neonates scanned at TEA	26 weeks 6 days ± 2 weeks 0 days	39 weeks 4 days ± 1 week 3 days PMA	natural sleep	3 T	3000	slice thickness = 3 mm	5.2	scrubbing	neonate brain template (Kuklisova-Murgasova et al., 2011)	ICA	FPN, ECN, motor, SMN, medial visual, occipital visual and lateral visual areas.
14	He and Parikh (2016)	34 preterm neonates	≤ 32 weeks	32 weeks 4 days ± 1 week 0 days PMA (N = 19)	natural sleep	3 T	3000	slice thickness = 3 mm	5.2	scrubbing	neonate brain template (Kuklisova-Murgasova et al., 2011)	ICA	In all the three groups: The occipital visual, medial visual, lateral visual, AUD, motor, SMN, cerebellum, brainstem, DMN, ECN and FPN.
				39 weeks 2 days ± 1 week 2 days PMA (N = 22)									
				52 weeks 6 days ± 1 week 4 days PMA (N = 25)									

15	Ball et al. (2016)	105 preterm neonates scanned at TEA	30 (23 − 34) weeks	42 (39 − 48) weeks PMA	under sedation	3 T	1500	2.5 × 2.5 × 4	6.4	ICA + FIX clean up	preterm brain template (Serag et al., 2012)	ICA	For both groups: frontal, parietal, temporal, occipital cortex, basal ganglia and cerebellum.
		26 full-term neonates	39 (37 − 41) weeks	43 (39 − 46) weeks PMA									
16	Weinstein et al. (2016)	32 preterm neonates	29 weeks 0 days ± 2 weeks 5 days	37 weeks 4 days ± 1 week 4 days PMA	natural sleep	3 T	3000	slice thickness = 3 mm	N/A	None	None	SCA	Motor and VIS
17	Cui et al. (2017)	44 preterm neonates scanned before TEA	24 weeks 5 days – 32 weeks 2 days	32 weeks 1 day ± 1 week 5 days PMA (29 weeks 6 days – 35 weeks 4 days)	N/A	3 T	2000	4 × 4 × 4	N/A	None	Montreal Neurological Institute pediatric atlas	ICA	Medial visual, lateral visual, AUD, SN, motor, prefrontal network, brainstem and thalami, frontal cortical network and cerebellum.
18	Linke et al. (2018)	11 preterm neonates (No neuropathology)	27 weeks 4 days (25 – 34)	37 weeks 0 days PMA (35 − 42)	natural sleep with playing lullabies	1.5 T	1920	3 mm isotropic resolution	7	average >2 mm in two or more of the four fMRI runs	UNC neonatal brain template (Shi et al., 2011)	ICA	For both preterm scanned at TEA and full-term neonates: motor, AUD, VIS, ECN and DMN.
		19 preterm neonates (Neuropathology)	27 weeks 4 days (24 – 36)	37 weeks 4 days PMA (35 − 41)									

		3 full-term neonates (No neuropathology)	40 weeks 0 days (39 – 41)	40.5 (40 − 41) weeks PMA									
		7 full-term neonates (Neuropathology)	40 weeks 0 days (38 − 41)	41.0 (39 − 43) weeks PMA									
19	Rajasilta et al. (2020)	21 full-term neonates	39 weeks 6 days ± 1 week 1 day	3 weeks 5 days ± 1 week 0 days after birth	natural sleep	3T	2500	3 × 3 × 3	6	motion larger than 3 mm in multiple time points	UNC2 neonate T2 template (Shi et al., 2011)	ICA	VIS, AUD, thalamic, basal ganglia, cerebellar and brainstem, insular, SMN, motor, DMN, prefrontal, frontal, parietal and temporoparietal networks.
20	Eyre et al. (2021)	24 full-term neonates	38 weeks 6 days − 42 weeks 0 days)	43 weeks 4 days − 44 weeks 3 days	Natural sleep	3 T	392	2.16 × 2.16 × 2.15	15	scrubbing	Week-specific template	ICA	Lateral motor, medial motor, SMN, VIS, AUD, prefrontal, FPN, motor association, posterior parietal, temporoparietal, and visual association.

Abbreviations: GA, gestational age; PMA, postmenstrual age; ICA, Independent Component Analysis; SCA, Seed Correlation Analysis; FD, framewise displacement; TEA, term-equivalent age; SMN, sensorimotor network; VIS, visual network; DMN, default mode network; AUD, auditory network; FPN, frontoparietal network; ECN, executive network; SN, salience Network; ACC, anterior cingulate cortex; PCC, posterior cingulate cortex;

MPFC, medial prefrontal cortex; LPFC, lateral prefrontal cortex. The studies in bold are the most relevant to the current research, based on direct focus on the presence of the DMN/DAN/ECN and similar infant age range.

Table 6.2 Previous findings on the presence of the three high-order networks in infancy.

Studies	DMN	DAN	ECN
Fransson et al. (2007)	×	×	×
Fransson et al. (2009)	×	×	×
Lin et al. (2008)	-	-	-
Doria et al. (2010)	√	√(FPN)	√
Smyser et al. (2010)	√(precursor)	×	×
Alcauter et al. (2014)	√(incomplete)	√ (incomplete FPN)	×
Gao et al. (2009)	√(incomplete)	-	-
Gao et al. (2013)	√(incomplete)	√(incomplete)	×
Gao, Alcauter, Elton, et al. (2015)	√(incomplete)	√ (incomplete FPN)	×
Gao, Alcauter, Smith, et al. (2015)	√(incomplete)	√ (incomplete FPN)	×
Wylie et al. (2014)	√	×	√
Damaraju et al. (2014)	√	×	×
He and Parikh (2015)	×	√(FPN)	√
He and Parikh (2016)	√	√(FPN)	√
Ball et al. (2016)	×	×	×
Weinstein et al. (2016)	-	-	-
Cui et al. (2017)	×	×	×
Linke et al. (2018)	√	×	√
Rajasilta et al. (2020)	√	×	×
Eyre et al. (2021)	×	√(FPN)	×

Abbreviations: DMN, default mode network; DAN, dorsal attention network; ECN, executive network; FPN, frontoparietal network. "√" indicates that network was identified while "×" indicates not; "-" means that network was not investigated in that study. The studies in bold are the most relevant to the current research, based on direct focus on the presence of the DMN/DAN/ECN and similar infant age range.

Table 6.3 Regions of interests for the default mode network, dorsal attention network and executive control network (from Raichle (2011)).

Network	Index	ROI	MNI coordinates		
			x	*y*	*z*
Default Mode Network	1	Posterior cingulate/precuneus	0	-52	27
	2	Medial prefrontal	-1	54	27
	3	Left lateral parietal	-46	-66	30
	4	Right lateral parietal	49	-63	33
	5	Left inferior temporal	-61	-24	-9
	6	Right inferior temporal	58	-24	-9
Dorsal Attention Network	7	Left frontal eye field	-29	-9	54
	8	Right frontal eye field	29	-9	54
	9	Left posterior IPS	-26	-66	48
	10	Right posterior IPS	26	-66	48
	11	Left anterior IPS	-44	-39	45
	12	Right anterior IPS	41	-39	45
	13	Left MT	-50	-66	-6
	14	Right MT	53	-63	-6
Executive Control Network	15	Dorsal medial PFC	0	24	46
	16	Left anterior PFC	-44	45	0
	17	Right anterior PFC	44	45	0
	18	Left superior parietal	-50	-51	45
	19	Right superior parietal	50	-51	45

Abbreviations: IPS, Intraparietal sulcus; MT, Middle temporal area; PFC: Prefrontal cortex.

7. Appendix B – Supplementary materials in Chapter 3

7.1 Methods and Materials

7.1.1 UNC infant 0-1-2 atlas

The UNC infant 0-1-2 atlas was generated based on 95 infants scanned at 5 weeks, 1 year and 2 years after birth. The first release of UNC atlas (Shi et al., 2011) was generated by propagating the automated anatomical labelling (AAL) brain parcellations from adult to infant spaces based on structural similarity. To address the potential cancellation effects by averaging across heterogeneous BOLD signals within a given ROI when applying structural brain atlas in rs-fMRI studies, Shi et al., (2018) derived the first set of brain atlases by parcellating the infant brain into functionally homogeneous regions based on a novel hybrid iterative normalized cut approach. In the current study, we used the neonatal atlas from the recently released UNC infant atlas, which has 223 functionally homogenous regions.

For neonates, 223 regions of interest in MNI space provided by Shi et al., (2018) were transformed into neonate native space using the same registration procedure used in Chapter 2. Details on the procedure can be found in Chapter 2, Section 2.2.3. For adults, as the neonatal ROIs in MNI space provided by Shi et al., (2018) have a slightly different spatial resolution (FOV = 181 × 217 × 181 mm, spatial resolution of 1 mm isotropic) from the denoised HCP data (FOV = 91 × 109 × 91 mm, spatial resolution of 2 mm isotropic), we first aligning neonatal T1w image (with no dura and cerebellum) in MNI space to MNI T1w template (in 2 mm resolution) using non-linear registration (ANTs SyN) and then applying the warp file generated in the last step to ROIs with MNI T1w template (in resolution 2 mm) as a reference.

7.1.2 Traditional algorithms for calculating small worldness

The algorithm for calculating small-world properties proposed by Humphries and Gurney (2008) compares the observed clustering coefficient and characteristic path length with that of equivalent Erdos-Renyi random networks to get the small worldness (σ) of the observed network, which is given by the following equation

$$\sigma = \frac{\gamma}{\lambda} = \frac{\frac{C_{obs}}{C_{rand}}}{\frac{L_{obs}}{L_{rand}}}, \quad (1)$$

where *C* and *L* stand for clustering coefficient and characteristic path length respectively of the observed network (*obs*) and random network (rand). The equivalent random network has the same number of nodes and the same degree distribution as the observed network. According to this equation, the higher normalized *C* and lower normalized *L*, the higher σ.

7.1.3 Statistical analyses

Comparison of head motion

We investigated whether there is any significant difference in head motion between the four groups, the adults, full-term neonates, and preterm neonates at or before TEA. Independent sample *t*-tests were first applied to test the difference in the mean FD between the adults and each neonate group, and between the full-term neonates and each preterm neonate group separately.

Comparison of mean functional connectivity (FC)

GLMs were applied to test the difference in mean FC between the adults and each neonate group while controlling the mean FD value, given significantly lower FD in the adults relative to neonates (Figure 7.1). Independent sample *t*-tests were used to detect the difference in mean FC between full-term neonates and preterm neonates at TEA/before TEA, as no significant difference in FD was observed between neonate groups.

Comparison of functional connectivity at the nodal level

Independent-sample *t*-tests were conducted to detect the difference in FC patterns between the full-term neonates and preterm neonates at/before TEA. The FC matrices were standardized to z-scores to allow comparisons across subjects as the full-term neonates had significantly higher mean FC relative to the preterm neonate groups. Correction for the FDR was applied to all statistical results at a threshold of $p < 0.05$.

Comparison of small-world properties at the nodal level

Independent-sample *t*-tests were conducted to detect the difference in shortest path length patterns between the full-term neonates and preterm neonates at/before TEA. The path length matrices were standardized to z-scores to allow comparisons across subjects as they were calculated directly based on FC matrices. Group-wise comparisons in clustering coefficient at the nodal level were conducted between the full-term neonates and preterm neonates at/before TEA in GLMs including mean FC as a covariate. FDR correction was applied at a threshold of $p < 0.05$.

7.2 Results

7.2.1 Comparison of head motion

The adults had significantly lower mean FD relative to the full-term neonates (t (407.96) = -9.23, $p < 0.0001$), preterm neonates scanned at TEA (t (80.81) = -4.11, $p < 0.0001$), and preterm neonates scanned before TEA (t (84.82) = -4.80, $p < 0.0001$) (Figure 7.1). No significant differences were observed in mean FD between neonate groups.

Figure 7.1 about here please

7.2.2 Comparison of mean functional connectivity

GLMs were applied to compare the mean FC in the adults and each neonate group while controlling the mean FD. We observed a significant main effect of group for the comparison between the adults and full-term neonates (F (1, 451) = 10.99, $p = 0.001$), which was driven by significantly lower FC in the adults. GLM comparing the adults and preterm neonates at TEA also showed a significant main effect of groups (F (1, 245) = 42.64, $p < 0.0001$), driven by significantly higher mean FC in the adults. Similarly, GLM comparing the adults and preterm neonates before TEA showed a main effect of group (F (1, 243) = 17.66, $p < 0.0001$), again driven by higher mean FC in the adults (Figure 7.2a).

Independent t-tests were applied to compare the mean FC between the full-term neonates and preterm neonates at/before TEA. The full-term neonates had significantly higher mean FC relative to preterm neonates scanned at TEA (T (1, 126.84) = 9.96, $p < 0.0001$) and preterm neonates scanned before TEA (T (1, 346) = 7.11, $p < 0.0001$) (Figure 7.2b).

Figure 7.2 about here please

7.2.3 The effect of premature birth on nodal-level FC and small-world properties

Visual inspection of the connectivity matrices (Figure 7.3) suggested that each neonate group had less cohesive networks (lower within relative to between-network connectivity) across brain than the adult group. The sensorimotor networks were more adult-like relative to other networks in the neonate groups. The connectivity matrix in the preterm neonates at TEA resembled that in the full-term neonates. Networks in the preterm neonate before TEA were less differentiated/segregated relative to that in neonates at term or TEA.

Figure 7.3 about here please

Full-term neonates had significantly higher within- and between-network FC across the brain relative to preterm neonates before TEA (Figure 7.4a). By term-equivalent age, the functional connectivity maps in preterm neonates were like those in full-term neonates. However, we still observed significantly different within- and between-network FC between the full-term neonates and preterm neonates at TEA. Specifically, the full-term neonates had significantly higher FC within the default mode network but lower FC within the sensorimotor-hand network relative to the preterm neonates at TEA (Figure 7.4b). A similar pattern of results was observed when comparing shortest path length between the full-term neonates and preterm neonates (Figure 7.4).

Figure 7.4 about here please

When comparing nodal-level clustering coefficient, the full-term neonates showed a higher clustering coefficient in the right postcentral gyrus of sensory/somatomotor mouth network and lower clustering coefficient in the right precuneus of default mode network, when compared with preterm neonates before TEA (Figure 7.5). No significantly different clustering coefficient was observed in any nodes between the full-term neonates and preterm neonates at TEA.

Figure 7.5 about here please

7.2.4 Reproducibility of results

Adults versus neonates Higher small worldness, higher clustering coefficient and lower path length were consistently observed in the adults relative to preterm neonates before TEA across different algorithms and types of FC matrices (C3 in Figure 7.6) and parcellations (Figure 7.7 and Table 7.1). Using Power atlas, we consistently found significantly higher small worldness and higher clustering coefficient in adults relative to full-term neonates (C1 in Figure 7.6) and preterm neonates at TEA (C2 in Figure 7.6) across different algorithms and types of FC matrices. We did not observe any significant difference in small worldness between adults and those two neonate groups while using UNC atlas (Figure 7.7a). However, we observed significantly lower path length (Figure

7.7c) in adults relative to full-term neonates and significantly higher clustering coefficient in adults relative to preterm neonates at TEA (Figure 7.7b). These findings suggested the adults exhibited a more well-developed small-world architecture relative to neonates.

Figure 7.6, 7.7 and Table 7.1 about here please

Full-term versus preterm neonates Relative to preterm neonates before TEA, full-term neonates were consistently found to have higher small worldness and lower path length regardless of using different algorithms and types of FC matrices (C4 in Figure 7.6) and parcellations (Figure 7.8 and Table 7.2). In terms of the comparisons between full-term neonates and preterm neonates at TEA, full-term neonates consistently showed significantly higher clustering coefficient relative to preterm neonates at TEA (C5 in Figure 7.6; Figure 7.8). The only subtle inconsistency was observed in the comparison in small worldness. The marginal decrease in small-world propensity found in preterm neonates at TEA using the new algorithms was found to be significant using the commonly used algorithms (C5 in Figures 7.6 and Figure 7.8). Nevertheless, both results suggested a prematurity-related weaker functional small-world architecture in neonates at TEA.

Figure 7.8 about here please

Preterm neonates at TEA versus before TEA Lower path length was consistently observed in preterm neonates at TEA relative to the same neonates before TEA regardless of using

different algorithms and types of FC matrices (C6 in Figure 7.6) and parcellations (Figure 7.9 and Table 7.2), although some results did not survive multiple comparisons correction. Preterm neonates at TEA showed significantly higher small worldness relative to the same neonates before TEA using the new algorithm across different brain parcellations (Figure 7.9). However, we did not find any difference in small worldness between the two groups using the traditional algorithm (Figure 7.6).

Figure 7.9 and Table 7.2 about here please

7.3 Supplementary Figures and Legends

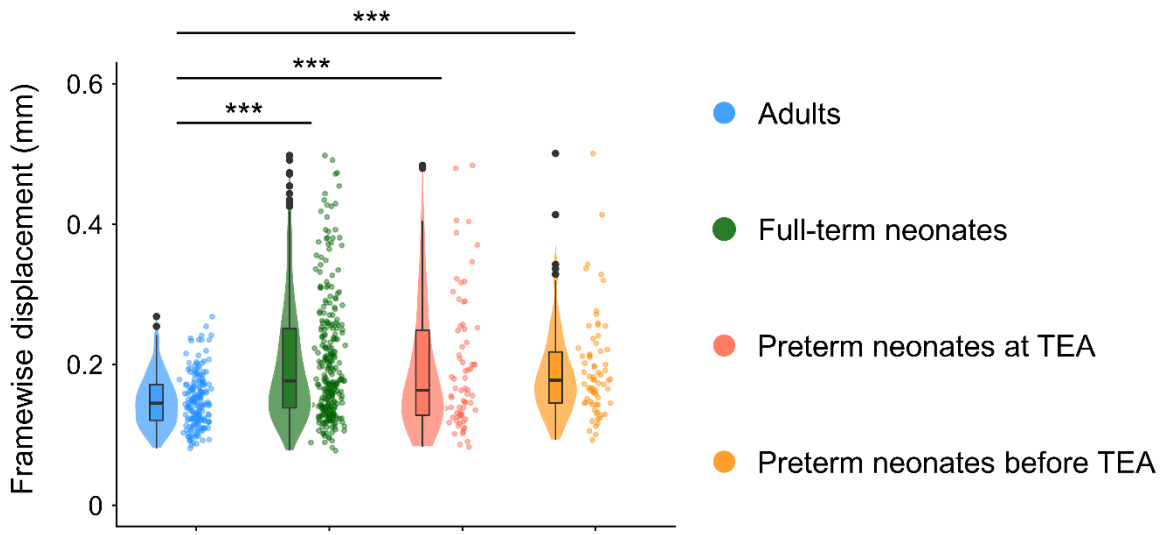

*Figure 7.1 Head motion in the adults and neonate groups after censoring. The violin plots show the distribution of the data. The line that divides the box into two parts represents the median of the data. The ends of the box represent the upper (Q3) and lower (Q1) quartiles of the data. The extreme lines of the boxplot show Q3 + 1.5 * interquartile to Q1 – 1.5 * interquartile range. The black dots beyond the extreme lines show potential outliers. Independent-sample t-tests were applied to detect the difference between every two groups. Abbreviations: TEA, term-equivalent age. *** = p < 0.0005.*

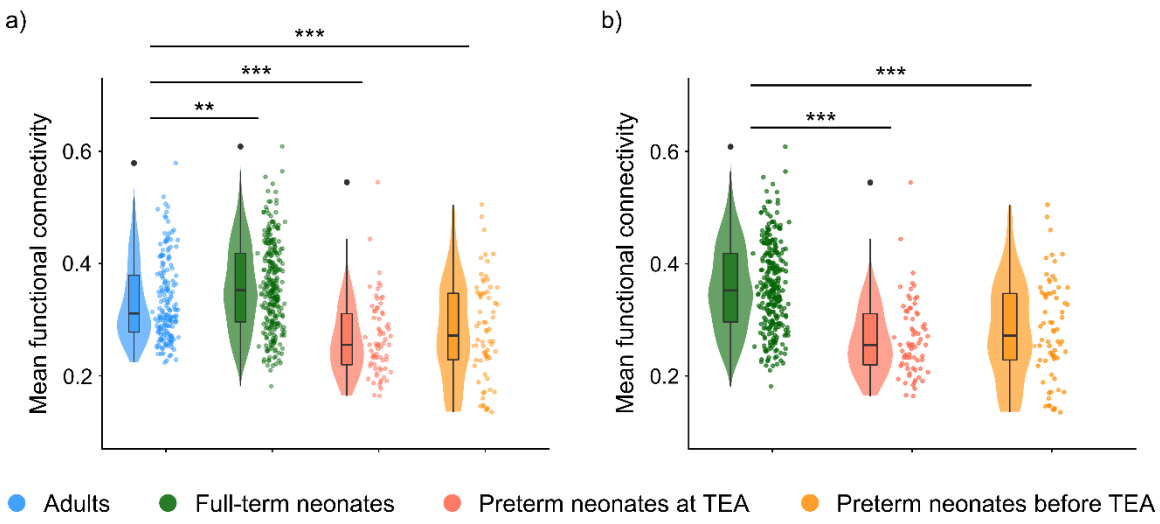

*Figure 7.2 Mean functional connectivity in adults and neonates. a) Comparisons between the adults and each neonate group. General linear models were applied to detect the difference in mean functional connectivity (FC) between the adults and each neonate group while controlling head motion. b) Comparisons between the full-term neonates and each preterm group. Independent sample t-tests were used to detect the difference in mean FC between full-term neonates and preterm neonates at TEA/before TEA, as no significant difference in FD was observed between neonate groups. The mean FC was calculated for each participant by averaging all positive edges. Abbreviations: TEA, term-equivalent age. *** = $p < 0.0005$; ** = $p < 0.005$.*

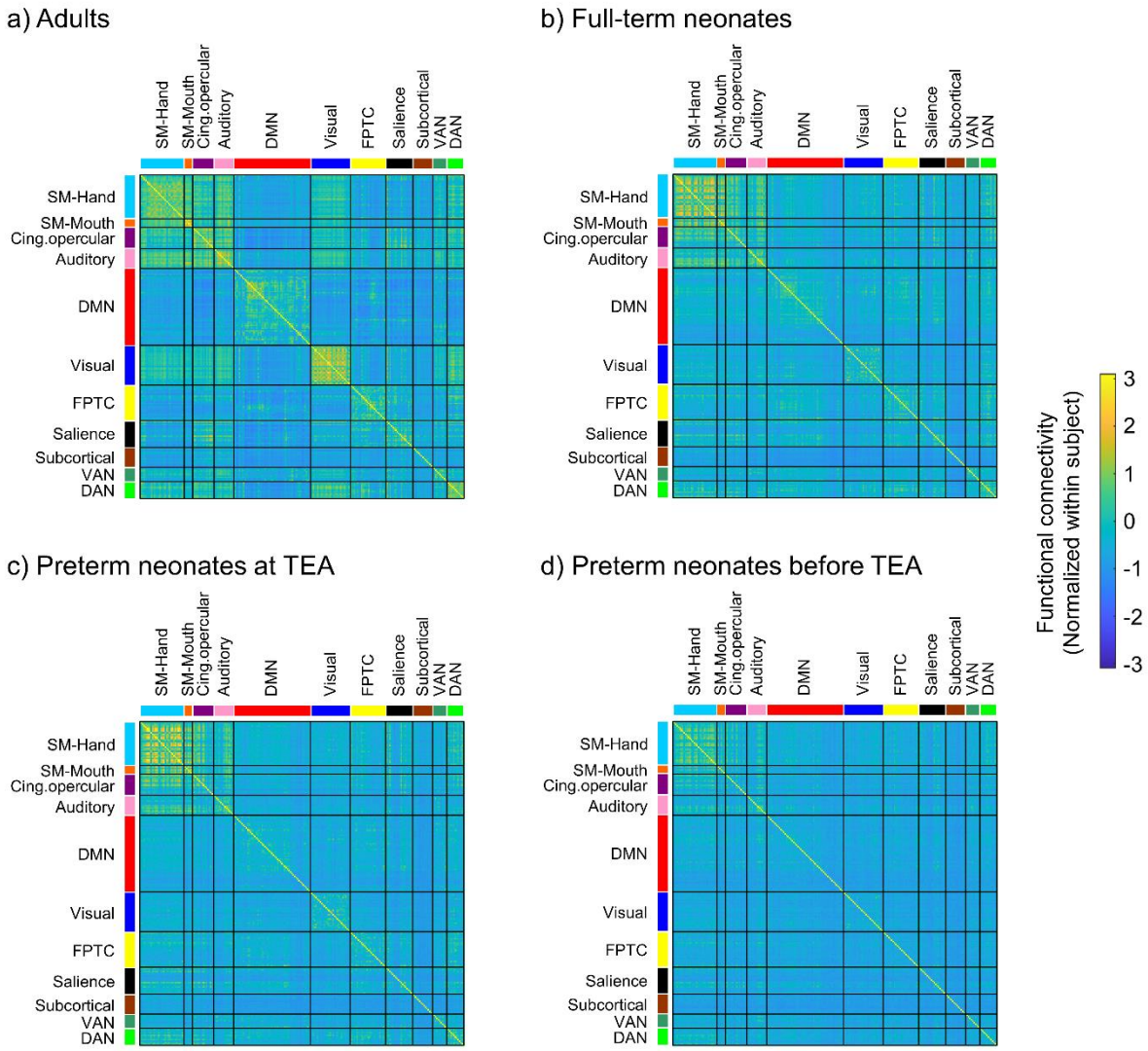

Figure 7.3 Functional connectivity in adults and neonate groups. a) adults, b) full-term neonates, c) preterm neonates scanned at TEA and d) preterm neonates scanned before TEA. The FC value presents here was normalized within each subject before being averaged within each group. Abbreviations: SM-Hand, sensory/somatomotor hand network; SM-Mouth, sensory/somatomotor mouth network; Cing. opercular, cingulo-opercular task control network; DMN, Default mode network; FPTC, frontoparietal task control network; VAN, ventral attention network; DAN, dorsal attention network.

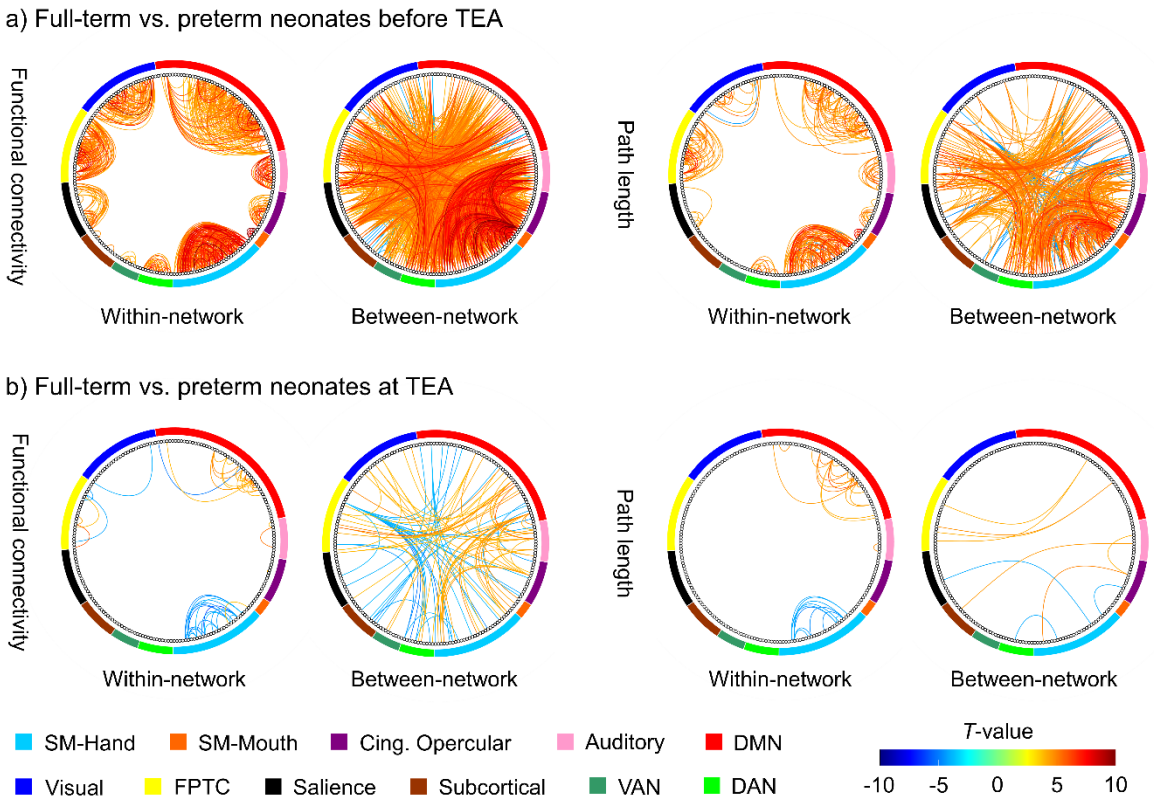

Figure 7.4 Differences in functional connectivity and path length between neonate groups. The lines in warm/cool colour represent higher/lower functional connectivity or shorter/longer path length in the full-term neonates relative to preterm groups. Correction for the false discovery rate was applied at a threshold of $p < 0.05$. Abbreviations: TEA, term-equivalent age; SM-Hand, sensory/somatomotor hand network; SM-Mouth, sensory/somatomotor mouth network; Cing. opercular, cingulo-opercular task control network; DMN, Default mode network; FPTC, frontoparietal task control network; VAN, ventral attention network; DAN, dorsal attention network.

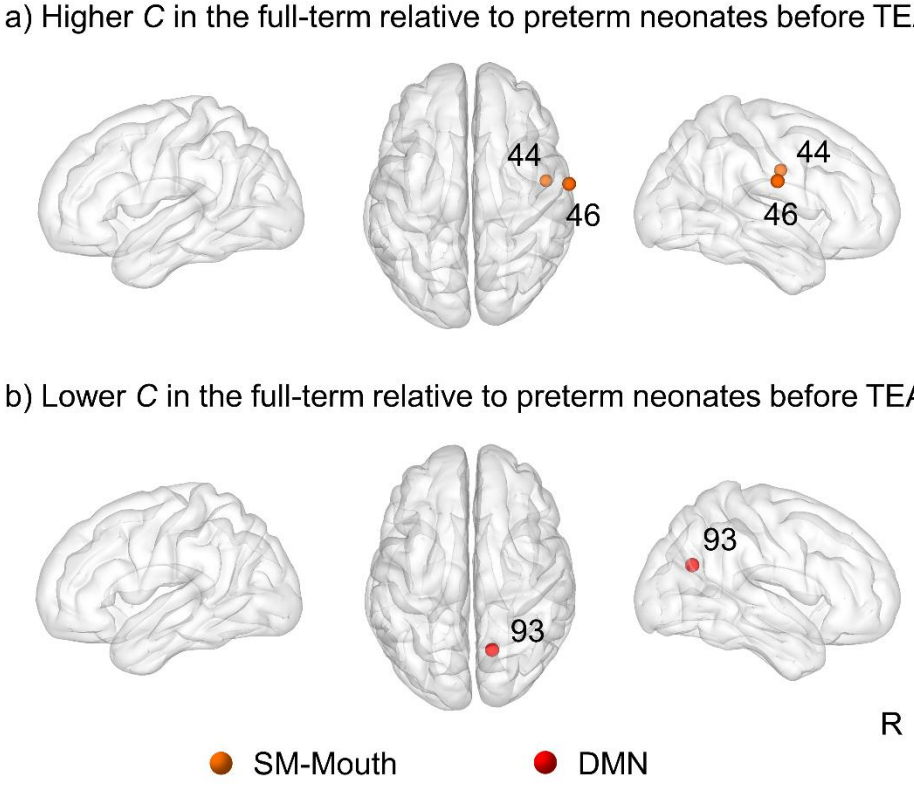

Figure 7.5 Effects of premature birth on nodal-level clustering coefficient. Nodes significantly showing a) higher or b) lower clustering coefficient in the full-term relative to preterm neonates before TEA. Correction for the false discovery rate was applied at a threshold of $p < 0.05$. Abbreviations: TEA, term-equivalent age; SM-Mouth, sensory/somatomotor mouth network; DMN, Default mode network; 44, node 44 (right postcentral gyrus); 46, node 46 (right postcentral gyrus); 93, node 93 (right precuneus); R, right.

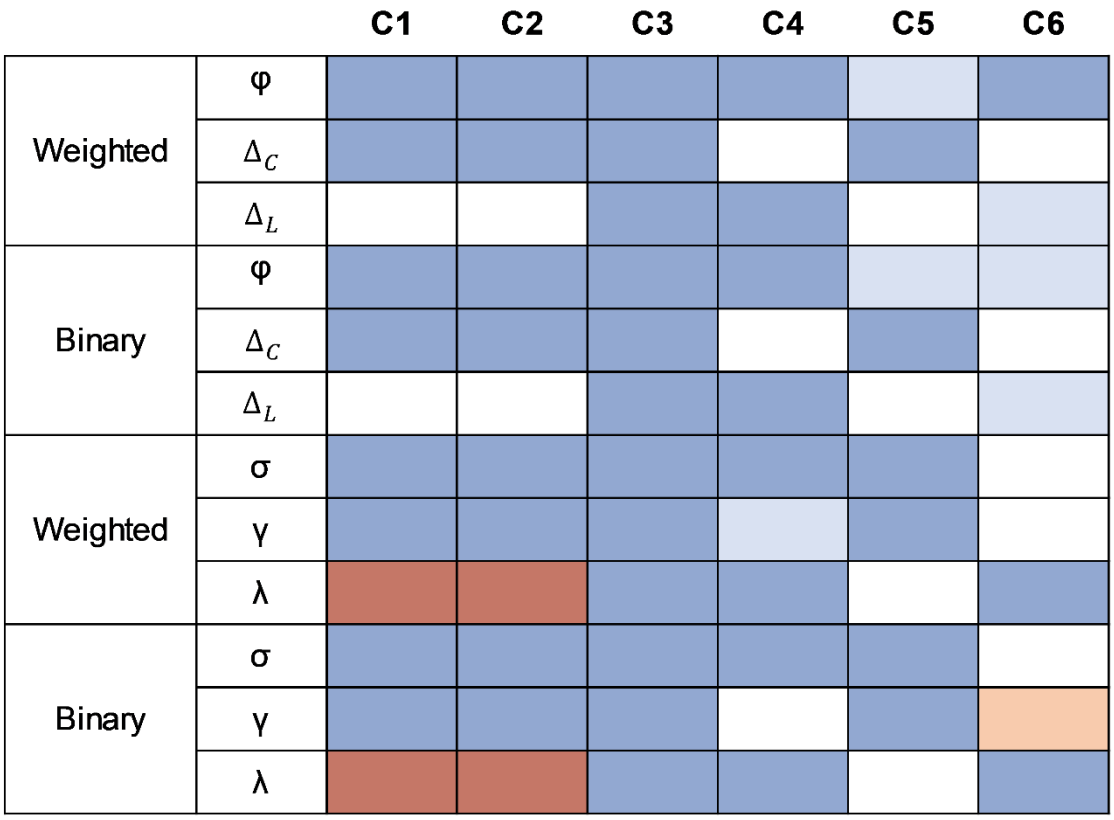

Figure 7.6 Consistency of results. φ/Δ_C/Δ_L are small-world propensity/normalized clustering coefficient/ characteristic path length calculated according to Muldoon et al., (2016). σ/γ/λ are small-worldness/normalized clustering coefficient/characteristic path length calculated according to Humphries and Gurney (2008). The blue/red colour indicates lower/higher small-worldness (φ/σ), lower/higher clustering coefficient (higher Δ_C/lower γ), longer/shorter path length (Δ_L/λ) in neonate groups relative to adults (C1 — C3), preterm neonate groups relative to full-term neonates (C4 and C5), or preterm neonates before TEA relative to preterm neonates at TEA (C6). The darker colour represents the results that survived FDR correction for multiple comparisons, and the lighter colour indicates p < 0.05 but did not survive the correction for multiple comparisons. Abbreviations: C1, comparison between the adults and full-term neonates; C2, comparison between the adults and preterm neonates at TEA; C3, comparison between the adults and preterm neonates before TEA; C4, comparison between the full-term neonates and preterm neonates before TEA; C5, comparison between the full-term neonates and preterm neonates at TEA; C6, comparison between preterm neonates scanned at TEA and the same neonates scanned before TEA; Binary, binary functional connectivity matrix; Weighted, weighted functional connectivity matrix.

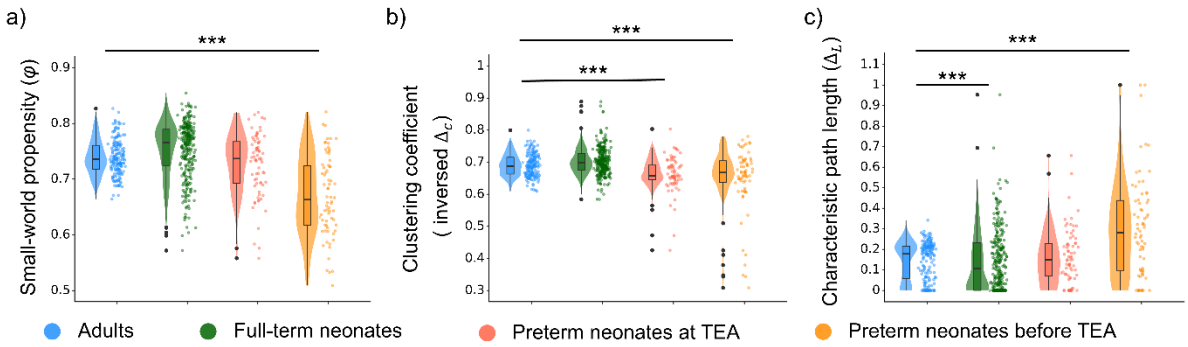

*Figure 7.7 The development of small-world architecture in the neonates relative to adults (UNC atlas). a) small-world propensity, b) clustering coefficient, and c) characteristic path length in the neonate groups relative to adults. Higher φ/inversed Δ_C/Δ_L represent higher small-world propensity, higher clustering coefficient and longer characteristic path length. The inversed Δ_C was calculated by 1 - Δ_C and for visualization purposes only and the statistical analyses were conducted using Δ_C. The violin plots show the distribution of the data. The line that divides the box into two parts represents the median of the data. The ends of the box represent the upper (Q3) and lower (Q1) quartiles of the data. The extreme lines of the boxplot show Q3 + 1.5 * interquartile to Q1 – 1.5 * interquartile range. The black dots beyond the extreme lines show potential outliers. Abbreviations: TEA, term-equivalent age. *** = p < 0.0005.*

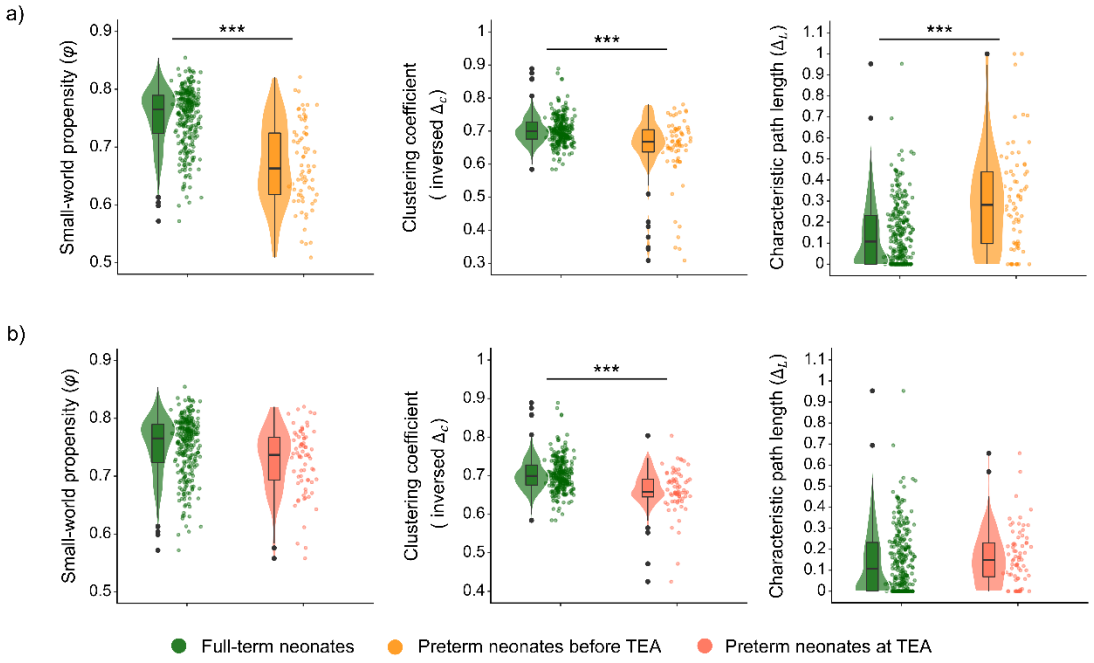

Figure 7.8 Effects of premature birth and neonate age on the development of small-world architecture (UNC atlas). a) small-world properties in the full-term neonates relative to preterm neonates before TEA; b) small-world properties in the full-term neonates relative to preterm neonates at TEA. Full-term neonates had significantly higher small-world propensity, higher clustering coefficient and lower normalized path length relative to preterm neonates before TEA, independent of mean functional connectivity. Full-term neonates had significantly higher clustering coefficient relative to preterm neonates at TEA. Higher φ/inversed Δ_C/Δ_L *represent higher small-world propensity, higher clustering coefficient and longer characteristic path length. The inversed* Δ_C *was calculated by 1 -* Δ_C *and for visualization purposes only and the statistical analyses were conducted using* Δ_C*. The violin plots show the distribution of the data. The line that divides the box into two parts represents the median of the data. The ends of the box represent the upper (Q3) and lower (Q1) quartiles of the data. The extreme lines of the boxplot show Q3 + 1.5 * interquartile to Q1 – 1.5 * interquartile range. The black dots beyond the extreme lines show potential outliers. Abbreviations: TEA, term-equivalent age. *** =* $p < 0.0005$.

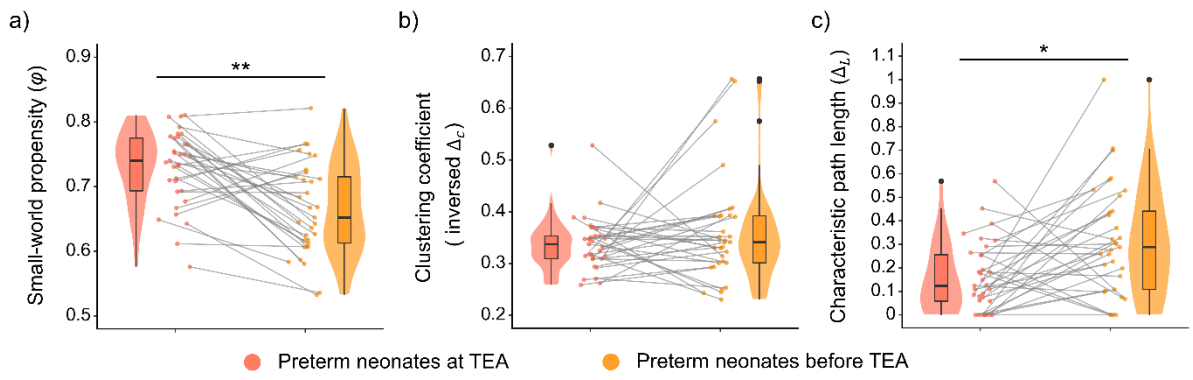

*Figure 7.9 The development of small-world architecture in preterm neonates up to term-equivalent age (UNC atlas). a) small-world propensity, b) clustering coefficient, and c) characteristic path length in the preterm neonates scanned at and before term-equivalent age. Significantly higher small-world propensity and lower path length were observed in the preterm neonates at TEA relative to the same neonates scanned before TEA. Higher φ/inversed Δ_C/Δ_L represent higher small-world propensity, higher clustering coefficient and longer characteristic path length. The inversed Δ_C was calculated by 1 - Δ_C and for visualization purposes only and the statistical analyses were conducted using Δ_C. The violin plots show the distribution of the data. The line that divides the box into two parts represents the median of the data. The ends of the box represent the upper (Q3) and lower (Q1) quartiles of the data. The extreme lines of the boxplot show Q3 + 1.5 * interquartile to Q1 – 1.5 * interquartile range. The black dots beyond the extreme lines show potential outliers. Abbreviations: TEA, term-equivalent age. ** = $p < 0.005$; * = $p < 0.05$.*

7.4 Supplementary Tables

Table 7.1 Comparison in small-world architecture in adults relative to neonates (UNC atlas)

Network properties	Comparisons	*F*-value (DF)	*p*-value
Small-world propensity	Adults vs. Full-term neonates	0.58 (1, 450)	0.447
	Adults vs. preterm neonates at TEA	2.50 (1, 244)	0.115
	Adults vs. preterm neonates before TEA	154.01 (1, 242)	< 0.0001 ***
Clustering coefficient	Adults vs. Full-term neonates	4.63 (1, 450)	0.032
	Adults vs. preterm neonates at TEA	18.49 (1, 244)	< 0.0001 ***
	Adults vs. preterm neonates before TEA	30.35 (1, 242)	< 0.0001 ***
Characteristic path length	Adults vs. Full-term neonates	15.28 (1, 450)	< 0.0001 ***
	Adults vs. preterm neonates at TEA	0.73 (1, 244)	0.394
	Adults vs. preterm neonates before TEA	49.76 (1, 242)	< 0.0001 ***

*Abbreviations: TEA, term-equivalent age; DF, degree of freedom; ***, $p < 0.0005$.*

Table 7.2 Comparison in small-world architecture between neonate groups (UNC atlas)

Network properties	Comparisons	*F*-value (DF)	*p*-value
Small worldness	Full-term vs. preterm neonates at TEA	2.14 (1, 346)	0.144
	Full-term vs. preterm neonates before TEA	124.29 (1, 344)	< 0.001 ***
	Preterm neonates at vs. before TEA	19.52 (1, 31.73)	0.001 **
Clustering coefficient	Full-term vs. preterm neonates at TEA	23.48 (1, 346)	< 0.001 ***
	Full-term vs. preterm neonates before TEA	27.65 (1, 344)	< 0.001 ***
	Preterm neonates at vs. before TEA	1.77 (1, 30.85)	0.193
Characteristic path length	Full-term vs. preterm neonates at TEA	2.83 (1, 346)	0.093
	Full-term vs. preterm neonates before TEA	41.29 (1, 344)	< 0.001 ***
	Preterm neonates at vs. before TEA	7.15 (1, 31.95)	0.012 *

*Abbreviations: TEA, term-equivalent age; DF, degree of freedom; ***, $p < 0.0005$; **, $p < 0.005$; *, $p < 0.05$.*

8. Appendix C – Supplementary materials in Chapter 4

8.1 Methods and Materials

8.1.1 Sample entropy of time course (TC)

To investigate whether neural entropy can be captured by dynamics of time course, we calculated sample entropy of TC in neonates. We first averaged the TC of each time window and then calculated the sample entropy of the mean TC across time windows for each participant.

8.1.2 Statistical analysis

Sample entropy of time course in neonates versus adults

To assess the development of sample entropy of TC, logistic regression models were applied with 'group' as the dependent variable ('1' = adults, '2' = full-term neonates/preterm neonates at TEA/before TEA), sample entropy of TC as the independent variable, and mean TC and mean FD as covariates.

Sample entropy of time course in preterm neonates versus full-term neonates

To assess the effects of premature birth on the entropy of TC, logistic regression models were applied with 'group' as the dependent variable ('1' = full-term neonates, '2' = preterm neonates at TEA/before TEA), sample entropy of TC as the independent variable, mean TC and mean FD as covariates.

The effect of neonate age on sample entropy of TC before TEA

To investigate the effects of neonate age (at scan) on the entropy of TC up to TEA, we used regression models to look at the association between sample entropy of TC and neonate age in preterm neonates before TEA. Specifically, we used sample entropy of TC as dependent variables, neonate age as independent variables, with mean TC and mean FD as covariates. Bonferroni correction for multiple comparisons was applied to all statistical results.

8.2 Results

8.2.1 Higher sample entropy of time course in full-term neonates relative to adults

Full-term neonates had significantly lower sample entropy of time course relative to adults (OR = 1.62E-23, 95% CI = [2.57E-29 2.81E-18], $p < 0.0001$) (Figure 8.1 and Table 8.3). Preterm neonates before TEA had significantly higher sample entropy of time course relative to adults (OR = 130702.57, 95% CI = [3.72 1.00 E+010], $p = 0.034$) (Figure 8.1 and Table 8.3), but this result did not survive multiple comparisons correction. No significant difference in sample entropy of time course between adults and preterm neonates at TEA was observed.

Figure 8.1 and Table 8.3 about here please

8.2.2 Higher sample entropy of time course in preterm neonates relative to full-term neonates

Preterm neonates at TEA showed significantly higher sample entropy of time course relative to full-term neonates (OR = 3.14E+21, 95% CI = [1.10E+16 3.39E+27], $p < 0.0001$) (Figure 8.2 and Table 8.4). Similarly, preterm neonates scanned before TEA had significantly higher sample entropy of time course relative to full-term neonates (OR = 1.64E+22, 95% CI = [6.95E+16 1.74E+28], $p < 0.0001$) (Figure 8.2 and Table 8.4).

Figure 8.2 and Table 8.4 about here please

8.2.3 Association between neonate age and sample entropy of TC

In preterm neonates before TEA, we found a significant negative association between neonate age and sample entropy of TC (β(SE) = -0.031 (0.010), $p = 0.005$) (Figure 8.3 and Table 8.5).

Figure 8.3 and Table 8.5 about here please

8.3 Supplementary Figures and Legends

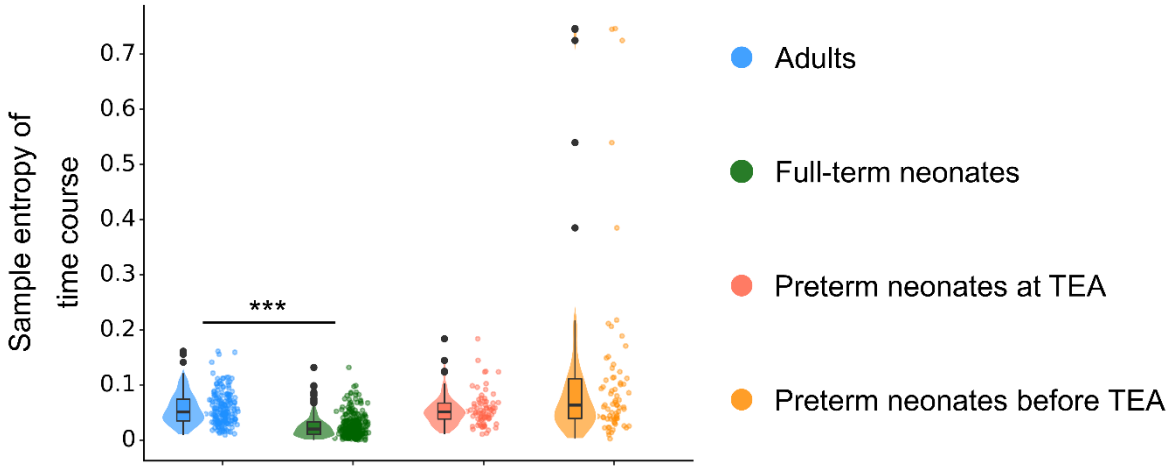

*Figure 8.1 Sample entropy of time course in adults relative to neonates (Power atlas). Significantly lower sample entropy of time course was found in the full-term neonates relative to adults. Abbreviations: TEA, term-equivalent age; ***, $p < 0.0005$.*

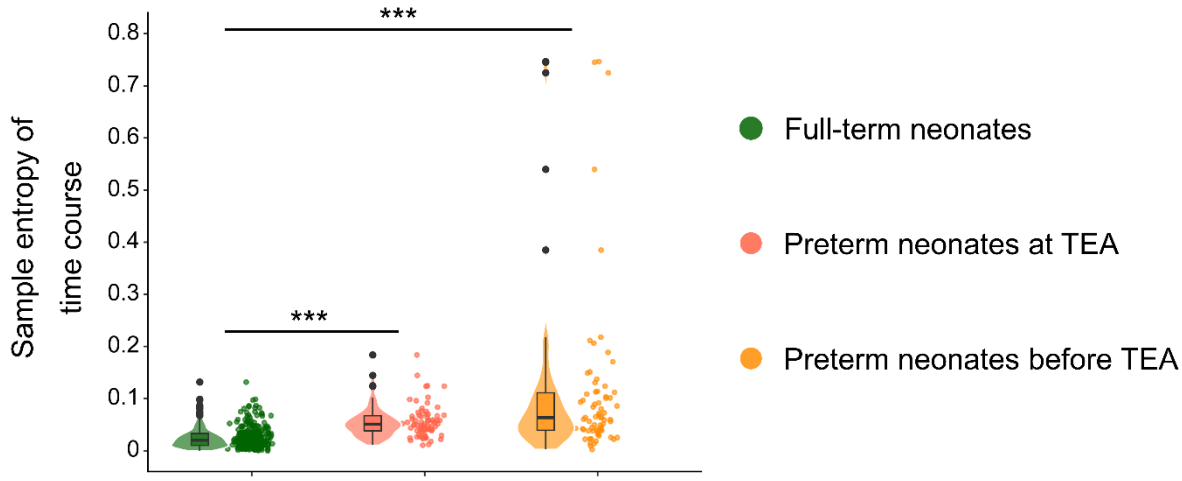

*Figure 8.2 Sample entropy of time course in full-term neonates relative to preterm neonates (Power atlas). Significantly higher sample entropy of time course was found in the preterm neonate groups relative to full-term neonates Abbreviations: TEA, term-equivalent age; ***, $p < 0.0005$.*

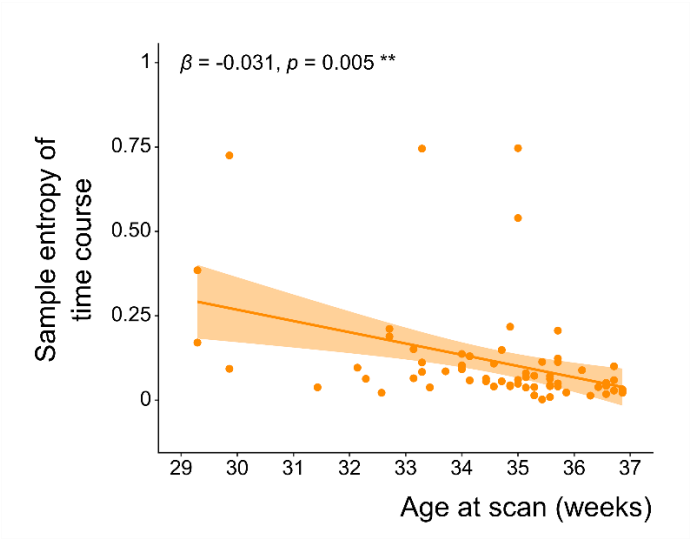

Figure 8.3 Association of neonate age with sample entropy of time course in preterm neonates before TEA (Power atlas). The x-axis displays neonates' postmenstrual age at scan, and the y-axis displays sample entropy of time course. A significant negative association between neonate age at scan and sample entropy of time course was observed in preterm neonates before TEA. Abbreviations: TEA, term-equivalent age.

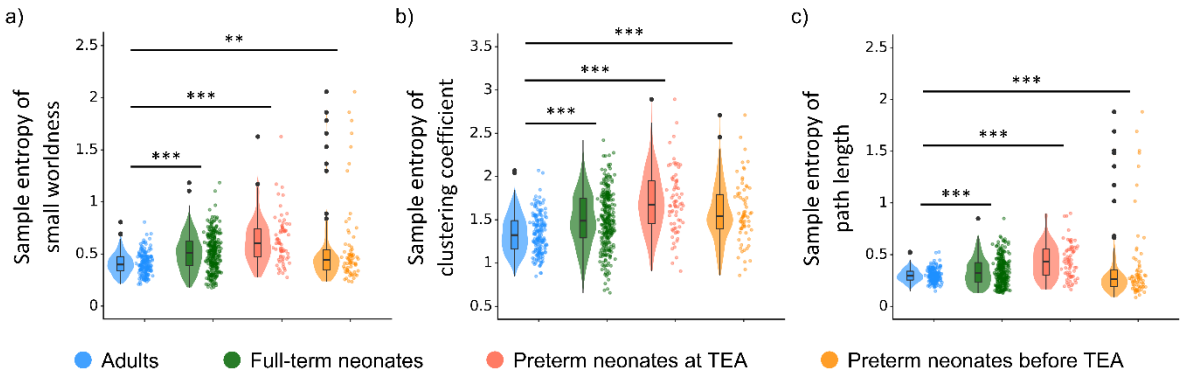

*Figure 8.4 Sample entropy of network properties in adults relative to neonates (UNC atlas). Sample entropy of a) small worldness, b) clustering coefficient, and c) path length in adults, full-term neonates, preterm neonates at TEA and preterm neonates before TEA. Significantly higher sample entropy of network properties was found in the neonate groups relative to adults. Abbreviations: ***, $p < 0.0005$; **, $p < 0.005$.*

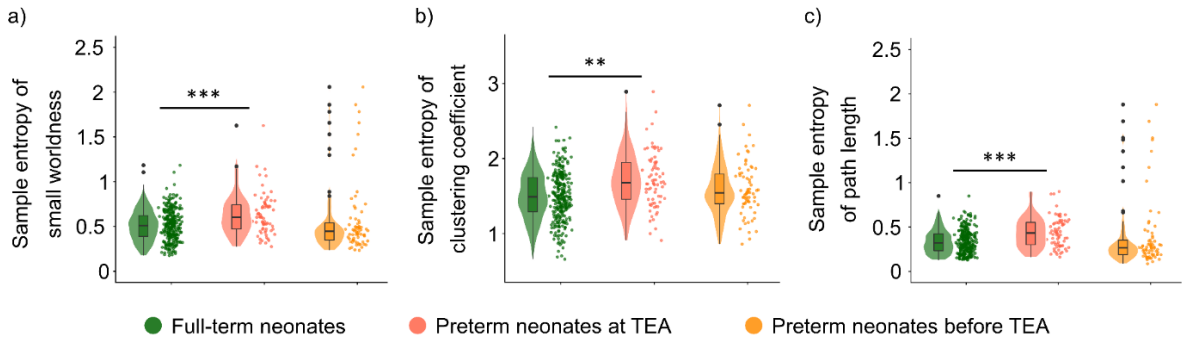

*Figure 8.5 Sample entropy of network properties in neonates (UNC atlas). Sample entropy of a) small worldness, b) clustering coefficient, and c) path length in neonates. Significantly higher sample entropy of network properties was found in preterm neonates at term-equivalent age relative to full-term neonates. Abbreviations: TEA, term-equivalent age; ***, $p < 0.0005$; **, $p < 0.005$.*

8.4 Supplementary Tables

Table 8.1 Association between neonate age and sample entropy of small worldness in preterm neonate before term-equivalent age (Power atlas)

Model summary	R^2	*F*	*p*
	0.71	39.67	< 0.0001 ***
DV	IV	*β*(SE)	*p*
Sample entropy of small worldness	Age at scan	-0.077 (0.037)	0.039
	Sample entropy of FC	0.603 (0.088)	< 0.0001 ***
	Small worldness	-4.881 (0.889)	< 0.0001 ***
	Mean FD	0.664 (0.865)	0.445

*Note: Unstandardized coefficient (β) and standard error (SE) were reported. DV, dependent variable; IV, independent variable; FC, functional connectivity; FD, frame-wised displacement; ***, p < 0.0005.*

Table 8.2 Association between neonate age and sample entropy of clustering coefficient in preterm neonate before term-equivalent age (Power atlas)

Model summary	R^2	*F*	*p*
	0.61	25.45	< 0.0001 ***
DV	IV	β(SE)	*p*
Sample entropy of clustering coefficient	Age at scan	-0.037 (0.027)	0.175
	Sample entropy of FC	0.096 (0.098)	0.331
	Clustering coefficient	2.402 (0.470)	< 0.0001 ***
	Mean FD	-0.334 (0.632)	0.599

*Note: Unstandardized coefficient (β) and standard error (SE) were reported. DV, dependent variable; IV, independent variable; FC, functional connectivity; FD, frame-wised displacement; ***, p < 0.0005.*

Table 8.3 Comparisons in sample entropy of time courses between adults and neonates (Power atlas)

Comparisons	Odds ratios (CI)	*p*-value
Adults vs. Full-term neonates	1.62E-23 [2.57E-29 2.81E-18]	< 0.0001 ***
Adults vs. preterm neonates at TEA	0.10 [7.37E-07 11655.22]	0.702
Adults vs. preterm neonates before TEA	130702.57 [3.72 1.0E+10]	0.034 *

*Abbreviations: CI, confidence interval; TEA, term-equivalent age; ***, p < 0.0005; *, p < 0.05.*

Table 8.4 Comparisons in sample entropy of time courses between full-term neonates and preterm neonates (Power atlas)

Comparisons	Odds ratios (CI)	*p*-value
Full-term neonates vs. Preterm neonates at TEA	3.14E+21 [1.10E+16 3.39E+27]	< 0.0001 ***
Full-term neonates vs. Preterm neonates before TEA	1.64E+22 [6.95E+16 1.74E+28]	< 0.0001 ***

*Abbreviations: CI, confidence interval; TEA, term-equivalent age; ***, p < 0.0005.*

Table 8.5 Association between neonate age and sample entropy of time course in preterm neonate before term-equivalent age (Power atlas)

Model summary	R^2	*F*	*p*
	0.25	7.35	< 0.0001 ***
DV	IV	*β*(SE)	*p*
Sample entropy of time course	Age at scan	-0.031 (0.010)	0.005 **
	Mean time course	-0.000 (0.000)	0.916
	Mean FD	0.693 (0.233)	0.004 **

*Note: Unstandardized coefficient (β) and standard error (SE) were reported. DV, dependent variable; IV, independent variable; FD, frame-wised displacement; **, p < 0.005.*

Table 8.6 Sample entropy of network properties in adults relative to neonates after resampling (Power atlas).

Network properties	Comparisons	SampEnt of network properties Odds ratios (CI)	*p*-value	SampEnt of FC Odds ratios (CI)	*p*-value
Small worldness	Adults vs. Full-term neonates	97.94 [19.16 573.43]	< 0.0001 ***	0.16 [0.08 0.31]	< 0.0001 ***
	Adults vs. preterm neonates at TEA	931.97 [35.02 38098.86]	< 0.0001 ***	0.56 [0.1 1.75]	0.327
	Adults vs. preterm neonates before TEA	1838.68 [29.41 300368.67]	0.001 **	0.26 [0.05 1.08]	0.084
Clustering coefficient	Adults vs. Full-term neonates	3.87 [1.47 10.46]	0.007 *	0.18 [0.10 0.32]	< 0.0001 ***
	Adults vs. preterm neonates at TEA	25.68 [4.44 194.43]	< 0.0001 ***	0.83 [0.30 2.38]	0.727
	Adults vs. preterm neonates before TEA	20.36 [4.68 99.90]	< 0.0001 ***	0.56 [0.25 1.19]	0.133
Path length	Adults vs. Full-term neonates	105.11 [18.71 661.76]	< 0.0001 ***	0.43 [0.26 0.68]	< 0.0001 ***
	Adults vs. preterm neonates at TEA	50018.60 [2695.16 1598538.01]	< 0.0001 ***	1.93 [0.81 4.76]	0.144
	Adults vs. preterm neonates before TEA	266889.90 [3651.82 47543593.56]	< 0.0001 ***	2.47 [0.75 8.96]	0.150

*Abbreviations: SampEnt, sample entropy; CI, confidence interval; FC, functional connectivity; TEA, term-equivalent age; ***, $p < 0.0005$; **, $p < 0.005$; *, $p < 0.05$.*

Table 8.7 Sample entropy of network properties in adults relative to neonates (UNC atlas).

Network properties	Comparisons	SampEnt of network properties Odds ratios (CI)	*p*-value	SampEnt of FC Odds ratios (CI)	*p*-value
Small worldness	Adults vs. Full-term neonates	891.37 [103.38 8985.96]	< 0.0001 ***	0.20 [0.10 0.38]	< 0.0001 ***
	Adults vs. preterm neonates at TEA	3477668.90 [69085.50 393082730.86]	< 0.0001 ***	1.11 [0.39 3.27]	0.843
	Adults vs. preterm neonates before TEA	188.37 [8.88 5563.16]	0.001 **	0.12 [0.04 0.29]	< 0.0001 ***
Clustering coefficient	Adults vs. Full-term neonates	55.66 [18.39 185.03]	< 0.0001 ***	0.14 [0.07 0.25]	< 0.0001 ***
	Adults vs. preterm neonates at TEA	238.92 [51.30 1406.54]	< 0.0001 ***	0.79 [0.33 1.87]	0.594
	Adults vs. preterm neonates before TEA	15.16 [3.52 72.67]	< 0.0001 ***	0.38 [0.19 0.75]	0.006 *
Path length	Adults vs. Full-term neonates	5078.35 [318.24 101367.05]	< 0.0001 ***	0.07 [0.03 0.14]	< 0.0001 ***
	Adults vs. preterm neonates at TEA	3442998.21 [54630.77 470942530. 10]	< 0.0001 ***	0.39 [0.13 1.20]	0.099
	Adults vs. preterm neonates before TEA	77.61 [11.26 930.99]	< 0.0001 ***	0.13 [0.05 0.29]	< 0.0001 ***

*Abbreviations: SampEnt, sample entropy; CI, confidence interval; FC, functional connectivity; TEA, term-equivalent age; ***, p < 0.0005; **, p < 0.005; *, p < 0.05.*

Table 8.8 Sample entropy of network properties in full-term neonates relative to preterm neonates (UNC atlas).

Network properties	Comparisons	SampEnt of network properties Odds ratios (CI)	*p*-value	SampEnt of FC Odds ratios (CI)	*p*-value
Small worldness	Full-term vs. preterm neonates at TEA	134.09 [20.74 1056.17]	< 0.0001 ***	5.89 [2.46 14.91]	< 0.0001 ***
	Full-term vs. preterm neonates before TEA	2.36 [0.45 14.08]	0.330	0.85 [0.36 1.96]	0.696
Clustering coefficient	Full-term vs. preterm neonates at TEA	5.65 [1.97 17.01]	0.002 **	5.01 [2.24 11.62]	< 0.0001 ***
	Full-term vs. preterm neonates before TEA	0.27 [0.08 0.85]	0.029	2.38 [1.15 5.03]	0.021
Path length	Full-term vs. preterm neonates at TEA	155.23 [15.93 1745.06]	< 0.0001 ***	7.42 [2.95 19.92]	< 0.0001 ***
	Full-term vs. preterm neonates before TEA	3.22 [0.67 16.38]	0.146	2.11 [0.95 4.75]	0.067

*Abbreviations: SampEnt, sample entropy; CI, confidence interval; FC, functional connectivity; TEA, term-equivalent age; ***, $p < 0.0005$; **, $p < 0.005$.*

Table 8.9 Association between neonate age and sample entropy of small worldness in preterm neonate before term-equivalent age (UNC atlas)

Model summary	R^2	*F*	*p*
	0.52	17.72	< 0.0001 ***
DV	IV	β(SE)	*p*
Sample entropy of small worldness	Age at scan	-0.003 (0.022)	0.882
	Sample entropy of FC	0.439 (0.066)	< 0.0001 ***
	Small worldness	-0.228 (0.634)	0.721
	Mean FD	0.465 (0.511)	0.366

*Note: Unstandardized coefficient (β) and standard error (SE) were reported. DV, dependent variable; IV, independent variable; FC, functional connectivity; FD, frame-wised displacement; ***, p < 0.0005.*

Table 8.10 Association between neonate age and sample entropy of clustering coefficient in preterm neonate before term-equivalent age (UNC atlas)

Model summary	R^2	*F*	*p*
	0.64	29.10	< 0.0001 ***
DV	IV	*β*(SE)	*p*
Sample entropy of clustering coefficient	Age at scan	-0.004 (0.016)	0.782
	Sample entropy of FC	0.215 (0.063)	0.001 **
	Clustering coefficient	1.759 (0.363)	< 0.0001 ***
	Mean FD	-0.469 (0.369)	0.208

*Note: Unstandardized coefficient (β) and standard error (SE) were reported. DV, dependent variable; IV, independent variable; FC, functional connectivity; FD, frame-wised displacement; ***, p < 0.0005; **, p < 0.005.*

Table 8.11. Association between neonate age and sample entropy of path length in preterm neonate before term-equivalent age (UNC atlas)

Model summary	R^2	*F*	*p*
	0.74	45.43	< 0.0001 ***
DV	IV	*β*(SE)	*p*
Sample entropy of path length	Age at scan	-0.045 (0.016)	0.006 *
	Sample entropy of FC	0.428 (0.044)	< 0.0001 ***
	Path length	-0.958 (0.181)	< 0.0001 ***
	Mean FD	-0.951 (0.348)	< 0.0001 ***

*Note: Unstandardized coefficient (β) and standard error (SE) were reported. DV, dependent variable; IV, independent variable; FC, functional connectivity; FD, frame-wised displacement; ***, p < 0.0005; *, p < 0.05.*

References

Achard, S., & Bullmore, E. (2007). Efficiency and cost of economical brain functional networks. *Plos Computational Biology*, *3*(2), e17. https://doi.org/10.1371/journal.pcbi.0030017

Acharya, R., Faust, O., Kannathal, N., Chua, T., & Laxminarayan, S. (2005). Non-linear analysis of EEG signals at various sleep stages. *Computer Methods and Programs in Biomedicine*, *80*(1), 37-45. https://doi.org/10.1016/j.cmpb.2005.06.011

Addabbo, M., Longhi, E., Marchis, I. C., Tagliabue, P., & Turati, C. (2018). Dynamic facial expressions of emotions are discriminated at birth. *PLoS one*, *13*(3). https://doi.org/10.1371/journal.pone.0193868

Alcauter, S., Lin, W., Smith, J. K., Short, S. J., Goldman, B. D., Reznick, J. S., Gilmore, J. H., & Gao, W. (2014). Development of thalamocortical connectivity during infancy and its cognitive correlations. *Journal of Neuroscience*, *34*(27), 9067-9075. https://doi.org/10.1523/JNEUROSCI.0796-14.2014

Allievi, A. G., Arichi, T., Tusor, N., Kimpton, J., Arulkumaran, S., Counsell, S. J., Edwards, A. D., & Burdet, E. (2016). Maturation of sensori-motor functional responses in the preterm brain. *Cerebral Cortex*, *26*(1), 402-413. https://doi.org/10.1093/cercor/bhv203

Altaye, M., Holland, S. K., Wilke, M., & Gaser, C. (2008). Infant brain probability templates for MRI segmentation and normalization. *Neuroimage*, *43*(4), 721-730. https://doi.org/10.1016/j.neuroimage.2008.07.060

Amsterdam, B. (1972). Mirror self-image reactions before age two. *Developmental Psychobiology*, *4*(5), 297-305. https://doi.org/10.1002/dev.420050403

Andrews-Hanna, J. R., Reidler, J. S., Huang, C., & Buckner, R. L. (2010). Evidence for the Default Network's Role in Spontaneous Cognition. *Journal of neurophysiology*, *104*(1), 322-335. https://doi.org/10.1152/jn.00830.2009

Ashwal, S., Cranford, R., & Bernat, J. (1994). The Multi-Society Task Force on PVS. Medical aspects of the persistent vegetative state. *N Engl J Med*, *330*, 1499-1508.

Bahrick, L. E., & Newell, L. C. (2008). Infant discrimination of faces in naturalistic events: Actions are more salient than faces. *Developmental psychology*, *44*(4), 983-996. https://doi.org/10.1037/0012-1649.44.4.983

Bai, Y., Xia, X., Kang, J., Yin, X., Yang, Y., He, J., & Li, X. (2016). Evaluating the Effect of Repetitive Transcranial Magnetic Stimulation on Disorders of Consciousness by Using TMS-EEG. *Frontiers in Neuroscience*, *10*, 473. https://doi.org/10.3389/fnins.2016.00473

Baird, B., Tononi, G., & LaBerge, S. (2022). Lucid dreaming occurs in activated rapid eye movement sleep, not a mixture of sleep and wakefulness. *Sleep*, *45*(4), zsab294. https://doi.org/doi.org/10.1093/sleep/zsab294

Baker, D. H. (2010). Visual consciousness: the binocular rivalry explosion. *Curr Biol*, *20*(15), R644-646. https://doi.org/10.1016/j.cub.2010.06.010

Ball, G., Aljabar, P., Arichi, T., Tusor, N., Cox, D., Merchant, N., Nongena, P., Hajnal, J. V., Edwards, A. D., & Counsell, S. J. (2016). Machine-learning to characterise neonatal functional connectivity in the preterm brain. *Neuroimage*, *124*, 267-275. https://doi.org/10.1016/j.neuroimage.2015.08.055

Ball, G., Aljabar, P., Zebari, S., Tusor, N., Arichi, T., Merchant, N., Robinson, E. C., Ogundipe, E., Rueckert, D., Edwards, A. D., & Counsell, S. J. (2014). Rich-club organization of the newborn human brain. *Proceedings of the National Academy of*

Sciences of the United States of America, *111*(20), 7456-7461. https://doi.org/10.1073/pnas.1324118111

Baranger, J., Demene, C., Frerot, A., Faure, F., Delanoe, C., Serroune, H., Houdouin, A., Mairesse, J., Biran, V., Baud, O., & Tanter, M. (2021). Bedside functional monitoring of the dynamic brain connectivity in human neonates. *Nature Communications*, *12*(1), 1080. https://doi.org/10.1038/s41467-021-21387-x

Bardin, J. C., Fins, J. J., Katz, D. I., Hersh, J., Heier, L. A., Tabelow, K., Dyke, J. P., Ballon, D. J., Schiff, N. D., & Voss, H. U. (2011). Dissociations between behavioural and functional magnetic resonance imaging-based evaluations of cognitive function after brain injury. *Brain*, *134*, 769-782. https://doi.org/10.1093/brain/awr005

Barrett, A. B., & Mediano, P. A. (2019). The Phi measure of integrated information is not well-defined for general physical systems. *Journal of Consciousness Studies*, *26*(1-2), 11-20.

Barttfeld, P., Uhrig, L., Sitt, J. D., Sigman, M., Jarraya, B., & Dehaene, S. (2015). Signature of consciousness in the dynamics of resting-state brain activity. *Proceedings of the National Academy of Sciences of the United States of America*, *112*(3), 887-892. https://doi.org/10.1073/pnas.1418031112

Bassett, D. S., & Bullmore, E. (2006). Small-world brain networks. *Neuroscientist*, *12*(6), 512-523. https://doi.org/10.1177/1073858406293182

Bassett, D. S., & Bullmore, E. T. (2017). Small-World Brain Networks Revisited. *Neuroscientist*, *23*(5), 499-516. https://doi.org/10.1177/1073858416667720

Bates, E., Bretherton, I., Camaioni, L., & Volterra, V. (1979). Cognition and communication from nine to thirteen months: Correlation findings. *The emergence of symbols: Cognition and communication in infancy*, 33-68.

Bates, E., Camaioni, L., & Volterra, V. (1975). The acquisition of performatives prior to speech. *Merrill-Palmer quarterly of behavior and development*, *21*(3), 205-226.

Batista-García-Ramó, K., & Fernández-Verdecia, C. I. (2018). What we know about the brain structure–function relationship. *Behavioral Sciences*, *8*(4), 39. https://doi.org/10.3390/bs8040039

Baum, G. L., Cui, Z., Roalf, D. R., Ciric, R., Betzel, R. F., Larsen, B., Cieslak, M., Cook, P. A., Xia, C. H., Moore, T. M., Ruparel, K., Oathes, D. J., Alexander-Bloch, A. F., Shinohara, R. T., Raznahan, A., Gur, R. E., Gur, R. C., Bassett, D. S., & Satterthwaite, T. D. (2020). Development of structure-function coupling in human brain networks during youth. *Proc Natl Acad Sci U S A*, *117*(1), 771-778. https://doi.org/10.1073/pnas.1912034117

Baumeister, R. F., Masicampo, E., & Vohs, K. D. (2011). Do conscious thoughts cause behavior? *Annual review of psychology*, *62*, 331-361. https://doi.org/10.1146/annurev.psych.093008.131126

Bayne, T. (2012). *The unity of consciousness*. Oxford University Press.

Bayne, T., Frohlich, J., Cusack, R., Moser, J., & Naci, L. (2023). Consciousness in the cradle: on the emergence of infant experience. *Trends in Cognitive Sciences*. https://doi.org/10.1016/j.tics.2023.08.018

Beckmann, C. F., DeLuca, M., Devlin, J. T., & Smith, S. M. (2005). Investigations into resting-state connectivity using independent component analysis. *Philosophical Transactions of the Royal Society B-Biological Sciences*, *360*(1457), 1001-1013. https://doi.org/10.1098/rstb.2005.1634

Beer, J. S. (2007). The default self: feeling good or being right? *Trends in Cognitive Sciences*, *11*(5), 187-189. https://doi.org/10.1016/j.tics.2007.02.004

Bekinschtein, T. A., Dehaene, S., Rohaut, B., Tadel, F., Cohen, L., & Naccache, L. (2009). Neural signature of the conscious processing of auditory regularities. *Proceedings of the National Academy of Sciences of the United States of America*, *106*(5), 1672-1677. https://doi.org/10.1073/pnas.0809667106

Bennett, J. (1978). Some remarks about concepts. *Behavioral and Brain Sciences*, *1*(4), 557-560. https://doi.org/10.1017/S0140525X00076573

Bhutta, A. T., Cleves, M. A., Casey, P. H., Cradock, M. M., & Anand, K. J. S. (2002). Cognitive and behavioral outcomes of school-aged children who were born preterm - A meta-analysis. *Jama-Journal of the American Medical Association*, *288*(6), 728-737. https://doi.org/10.1001/jama.288.6.728

Bidet-Ildei, C., Kitromilides, E., Orliaguet, J. P., Pavlova, M., & Gentaz, E. (2014). Preference for Point-Light Human Biological Motion in Newborns: Contribution of Translational Displacement. *Developmental psychology*, *50*(1), 113-120. https://doi.org/10.1037/a0032956

Biswal, B., Yetkin, F. Z., Haughton, V. M., & Hyde, J. S. (1995). Functional connectivity in the motor cortex of resting human brain using echo-planar MRI. *Magn Reson Med*, *34*(4), 537-541. https://doi.org/10.1002/mrm.1910340409

Blesa, M., Galdi, P., Cox, S. R., Sullivan, G., Stoye, D. Q., Lamb, G. J., Quigley, A. J., Thrippleton, M. J., Escudero, J., Bastin, M. E., Smith, K. M., & Boardman, J. P. (2021). Hierarchical Complexity of the Macro-Scale Neonatal Brain. *Cerebral Cortex*, *31*(4), 2071-2084. https://doi.org/10.1093/cercor/bhaa345

Blumensath, T., Jbabdi, S., Glasser, M. F., Van Essen, D. C., Ugurbil, K., Behrens, T. E., & Smith, S. M. (2013). Spatially constrained hierarchical parcellation of the brain with resting-state fMRI. *Neuroimage*, *76*, 313-324. https://doi.org/10.1016/j.neuroimage.2013.03.024

Boly, M., Coleman, M. R., Davis, M. H., Hampshire, A., Bor, D., Moonen, G., Maquet, P. A., Pickard, J. D., Laureys, S., & Owen, A. M. (2007). When thoughts become action: An fMRI paradigm to study volitional brain activity in non-communicative brain injured patients. *Neuroimage*, *36*(3), 979-992. https://doi.org/10.1016/j.neuroimage.2007.02.047

Boly, M., Perlbarg, V., Marrelec, G., Schabus, M., Laureys, S., Doyon, J., Pelegrini-Issac, M., Maquet, P., & Benali, H. (2012). Hierarchical clustering of brain activity during human nonrapid eye movement sleep. *Proceedings of the National Academy of Sciences of the United States of America*, *109*(15), 5856-5861. https://doi.org/10.1073/pnas.1111133109

Boly, M., Phillips, C., Tshibanda, L., Vanhaudenhuyse, A., Schabus, M., Dang-Vu, T. T., Moonen, G., Hustinx, R., Maquet, P., & Laureys, S. (2008). Intrinsic brain activity in altered states of consciousness - How conscious is the default mode of brain function? *Molecular and Biophysical Mechanisms of Arousal, Alertness, and Attention*, *1129*, 119-129. https://doi.org/10.1196/annals.1417.015

Bonhomme, V., Boveroux, P., Brichant, J. F., Laureys, S., & Boly, M. (2012). Neural correlates of consciousness during general anesthesia using functional magnetic resonance imaging (fMRI). *Arch Ital Biol*, *150*(2-3), 155-163. https://doi.org/10.4449/aib.v150i2.1242

Bouyssi-Kobar, M., Brossard-Racine, M., Jacobs, M., Murnick, J., Chang, T., & Limperopoulos, C. (2018). Regional microstructural organization of the cerebral cortex is affected by preterm birth. *Neuroimage-Clinical*, *18*, 871-880. https://doi.org/10.1016/j.nicl.2018.03.020

Bouyssi-Kobar, M., De Asis-Cruz, J., Murnick, J., Chang, T., & Limperopoulos, C. (2019). Altered Functional Brain Network Integration, Segregation, and Modularity in

Infants Born Very Preterm at Term-Equivalent Age. *Journal of Pediatrics*, *213*, 13-+. https://doi.org/10.1016/j.jpeds.2019.06.030

Boveroux, P., Vanhaudenhuyse, A., Bruno, M.-A., Noirhomme, Q., Lauwick, S., Luxen, A., Degueldre, C., Plenevaux, A., Schnakers, C., & Phillips, C. (2010). Breakdown of within-and between-network resting state functional magnetic resonance imaging connectivity during propofol-induced loss of consciousness. *The Journal of the American Society of Anesthesiologists*, *113*(5), 1038-1053. https://doi.org/10.1097/ALN.0b013e3181f697f5

Brewer, J. A., Worhunsky, P. D., Gray, J. R., Tang, Y.-Y., Weber, J., & Kober, H. (2011). Meditation experience is associated with differences in default mode network activity and connectivity. *Proceedings of the National Academy of Sciences*, *108*(50), 20254-20259. https://doi.org/10.1073/pnas.1112029108

Brown, R. (2015). The HOROR theory of phenomenal consciousness. *Philosophical Studies*, *172*, 1783-1794. https://doi.org/10.1007/s11098-014-0388-7

Bruce, E. N., Bruce, M. C., & Vennelaganti, S. (2009). Sample entropy tracks changes in EEG power spectrum with sleep state and aging. *Journal of clinical neurophysiology: official publication of the American Electroencephalographic Society*, *26*(4), 257. https://doi.org/10.1097/WNP.0b013e3181b2f1e3

Buckner, R. L., & Carroll, D. C. (2007). Self-projection and the brain. *Trends Cogn Sci*, *11*(2), 49-57. https://doi.org/10.1016/j.tics.2006.11.004

Burkhalter, A., Bernardo, K. L., & Charles, V. (1993). Development of local circuits in human visual cortex. *Journal of Neuroscience*, *13*(5), 1916-1931. https://doi.org/10.1523/JNEUROSCI.13-05-01916.1993

Buttelmann, D., Carpenter, M., & Tomasello, M. (2009). Eighteen-month-old infants show false belief understanding in an active helping paradigm. *Cognition*, *112*(2), 337-342. https://doi.org/10.1016/j.cognition.2009.05.006

Button, K. S., Ioannidis, J. P., Mokrysz, C., Nosek, B. A., Flint, J., Robinson, E. S., & Munafo, M. R. (2013). Power failure: why small sample size undermines the reliability of neuroscience. *Nature Reviews Neuroscience*, *14*(5), 365-376. https://doi.org/10.1038/nrn3475

Cai, L., Wang, J., Guo, Y., Lu, M., Dong, Y., & Wei, X. (2020). Altered inter-frequency dynamics of brain networks in disorder of consciousness. *J Neural Eng*, *17*(3), 036006. https://doi.org/10.1088/1741-2552/ab8b2c

Canales-Johnson, A., Billig, A. J., Olivares, F., Gonzalez, A., Garcia, M. D. C., Silva, W., Vaucheret, E., Ciraolo, C., Mikulan, E., Ibanez, A., Huepe, D., Noreika, V., Chennu, S., & Bekinschtein, T. A. (2020). Dissociable Neural Information Dynamics of Perceptual Integration and Differentiation during Bistable Perception. *Cerebral Cortex*, *30*(8), 4563-4580. https://doi.org/10.1093/cercor/bhaa058

Cao, M., He, Y., Dai, Z. J., Liao, X. H., Jeon, T. N., Ouyang, M. H., Chalak, L. N., Bi, Y. C., Rollins, N., Dong, Q., & Huang, H. (2017). Early Development of Functional Network Segregation Revealed by Connectomic Analysis of the Preterm Human Brain. *Cerebral Cortex*, *27*(3), 1949-1963. https://doi.org/10.1093/cercor/bhw038

Cao, M., Huang, H., & He, Y. (2017). Developmental Connectomics from Infancy through Early Childhood. *Trends in Neurosciences*, *40*(8), 494-506. https://doi.org/10.1016/j.tins.2017.06.003

Carhart-Harris, R. L. (2018). The entropic brain - revisited. *Neuropharmacology*, *142*, 167-178. https://doi.org/10.1016/j.neuropharm.2018.03.010

Carhart-Harris, R. L., & Friston, K. J. (2010). The default-mode, ego-functions and free-energy: a neurobiological account of Freudian ideas. *Brain*, *133*(Pt 4), 1265-1283. https://doi.org/10.1093/brain/awq010

Carhart-Harris, R. L., Leech, R., Erritzoe, D., Williams, T. M., Stone, J. M., Evans, J., Sharp, D. J., Feilding, A., Wise, R. G., & Nutt, D. J. (2013). Functional connectivity measures after psilocybin inform a novel hypothesis of early psychosis. *Schizophrenia Bulletin*, *39*(6), 1343-1351. https://doi.org/10.1093/schbul/sbs117

Carhart-Harris, R. L., Leech, R., Hellyer, P. J., Shanahan, M., Feilding, A., Tagliazucchi, E., Chialvo, D. R., & Nutt, D. (2014). The entropic brain: a theory of conscious states informed by neuroimaging research with psychedelic drugs. *Frontiers in Human Neuroscience*, *8*, 20. https://doi.org/10.3389/fnhum.2014.00020

Carp, J. (2012). On the plurality of (methodological) worlds: estimating the analytic flexibility of FMRI experiments. *Front Neurosci*, *6*, 149. https://doi.org/10.3389/fnins.2012.00149

Carruthers, P. (2003). *Phenomenal consciousness: A naturalistic theory*. Cambridge University Press.

Carskadon, M. A., & Dement, W. C. (2005). Normal human sleep: an overview. *Principles and practice of sleep medicine*, *4*(1), 13-23.

Carter, J. C., & Wrede, J. E. (2017). Overview of Sleep and Sleep Disorders in Infancy and Childhood. *Pediatric Annals*, *46*(4), E133-E138. https://doi.org/10.3928/19382359-20170316-02

Casali, A. G., Gosseries, O., Rosanova, M., Boly, M., Sarasso, S., Casali, K. R., Casarotto, S., Bruno, M. A., Laureys, S., Tononi, G., & Massimini, M. (2013). A theoretically based index of consciousness independent of sensory processing and behavior.

Science Translational Medicine, *5*(198), 198ra105. https://doi.org/10.1126/scitranslmed.3006294

Cavanna, F., Vilas, M. G., Palmucci, M., & Tagliazucchi, E. (2018). Dynamic functional connectivity and brain metastability during altered states of consciousness. *Neuroimage*, *180*(Pt B), 383-395. https://doi.org/10.1016/j.neuroimage.2017.09.065

Clare, L., Markova, I., Verhey, F., & Kenny, G. (2005). Awareness in dementia: A review of assessment methods and measures. *Aging Ment Health*, *9*(5), 394-413. https://doi.org/10.1080/13607860500142903

Cohen, J. D., McClure, S. M., & Yu, A. J. (2007). Should I stay or should I go? How the human brain manages the trade-off between exploitation and exploration. *Philosophical Transactions of the Royal Society B: Biological Sciences*, *362*(1481), 933-942. https://doi.org/10.1098/rstb.2007.2098

Cooney, J. W., & Gazzaniga, M. S. (2003). Neurological disorders and the structure of human consciousness. *Trends in Cognitive Sciences*, *7*(4), 161-165. https://doi.org/10.1016/S1364-6613(03)00058-5

Coppola, P., Spindler, L. R. B., Luppi, A. I., Adapa, R., Naci, L., Allanson, J., Finoia, P., Williams, G. B., Pickard, J. D., Owen, A. M., Menon, D. K., & Stamatakis, E. A. (2022). Network dynamics scale with levels of awareness. *Neuroimage*, *254*, 119128. https://doi.org/10.1016/j.neuroimage.2022.119128

Corbetta, M., & Shulman, G. L. (2002). Control of goal-directed and stimulus-driven attention in the brain. *Nature Reviews Neuroscience*, *3*(3), 201-215. https://doi.org/10.1038/nrn755

Cordes, D., Haughton, V. M., Arfanakis, K., Wendt, G. J., Turski, P. A., Moritz, C. H., Quigley, M. A., & Meyerand, M. E. (2000). Mapping functionally related regions

of brain with functional connectivity MR imaging. *American Journal of Neuroradiology*, *21*(9), 1636-1644.

Cristia, A., Minagawa, Y., & Dupoux, E. (2014). Responses to vocalizations and auditory controls in the human newborn brain. *PLoS one*, *9*(12), e115162. https://doi.org/10.1371/journal.pone.0115162

Crone, J. S., Lutkenhoff, E. S., Vespa, P. M., & Monti, M. M. (2020). A systematic investigation of the association between network dynamics in the human brain and the state of consciousness. *Neuroscience of Consciousness*, *2020*(1), niaa008. https://doi.org/10.1093/nc/niaa008

Cui, J., Tymofiyeva, O., Desikan, R., Flynn, T., Kim, H., Gano, D., Hess, C. P., Ferriero, D. M., Barkovich, A. J., & Xu, D. (2017). Microstructure of the Default Mode Network in Preterm Infants. *American Journal of Neuroradiology*, *38*(2), 343-348. https://doi.org/10.3174/ajnr.A4997

Cusack, R., Ball, G., Smyser, C. D., & Dehaene-Lambertz, G. (2016). A neural window on the emergence of cognition. *Year in Cognitive Neuroscience*, *1369*, 7-23. https://doi.org/10.1111/nyas.13036

Cusack, R., Linke, A. C., Zubiaurre-Elorza, L., Duffy, H., Herzmann, C., Stojanoski, B., Han, V. K., Lee, D. S., & Wild, C. (2017). Differences in the spatial and temporal patterns of head motion during MRI of adults and infants. *BioRxiv*, 114447. https://doi.org/10.1101/114447

Cusack, R., Wild, C. J., Zubiaurre-Elorza, L., & Linke, A. C. (2018). Why does language not emerge until the second year? *Hearing Research*, *366*, 75-81. https://doi.org/10.1016/j.heares.2018.05.004

D'Argembeau, A., Collette, F., Van der Linden, M., Laureys, S., Del Fiore, G., Degueldre, C., Luxen, A., & Salmon, E. (2005). Self-referential reflective activity and its

relationship with rest: a PET study. *Neuroimage*, *25*(2), 616-624. https://doi.org/10.1016/j.neuroimage.2004.11.048

Dai, R., Larkin, T. E., Huang, Z., Tarnal, V., Picton, P., Vlisides, P. E., Janke, E., McKinney, A., Hudetz, A. G., & Harris, R. E. (2023). Classical and non-classical psychedelic drugs induce common network changes in human cortex. *Neuroimage*, *273*, 120097. https://doi.org/10.1016/j.neuroimage.2023.120097

Dall'Orso, S., Fifer, W. P., Balsam, P. D., Brandon, J., O'Keefe, C., Poppe, T., Vecchiato, K., Edwards, A. D., Burdet, E., & Arichi, T. (2021). Cortical Processing of Multimodal Sensory Learning in Human Neonates. *Cerebral Cortex*, *31*(3), 1827-1836. https://doi.org/10.1093/cercor/bhaa340

Damaraju, E., Caprihan, A., Lowe, J. R., Allen, E. A., Calhoun, V. D., & Phillips, J. P. (2014). Functional connectivity in the developing brain: A longitudinal study from 4 to 9 months of age. *Neuroimage*, *84*, 169-180. https://doi.org/10.1016/j.neuroimage.2013.08.038

Damasio, A. R. (2000). A neurobiology for consciousness. *Neural Correlates of Consciousness*, 111-120. https://doi.org/10.7551/mitpress/4928.003.0010

Dasilva, M., Camassa, A., Navarro-Guzman, A., Pazienti, A., Perez-Mendez, L., Zamora-Lopez, G., Mattia, M., & Sanchez-Vivesa, M. V. (2021). Modulation of cortical slow oscillations and complexity across anesthesia levels. *Neuroimage*, *224*. https://doi.org/10.1016/j.neuroimage.2020.117415

Dayton Jr, G. O., & Jones, M. H. (1964). Analysis of characteristics of fixation reflexes in infants by use of direct current electrooculography. *Neurology*. https://doi.org/10.1212/WNL.14.12.1152

De Asis-Cruz, J., Bouyssi-Kobar, M., Evangelou, I., Vezina, G., & Limperopoulos, C. (2015). Functional properties of resting state networks in healthy full-term newborns. *Scientific reports*, *5*, 17755. https://doi.org/10.1038/srep17755

Decasper, A. J., & Fifer, W. P. (1980). Of Human Bonding - Newborns Prefer Their Mothers Voices. *science*, *208*(4448), 1174-1176. https://doi.org/10.1126/science.7375928

Deco, G., Jirsa, V. K., & McIntosh, A. R. (2011). Emerging concepts for the dynamical organization of resting-state activity in the brain. *Nat Rev Neurosci*, *12*(1), 43-56. https://doi.org/10.1038/nrn2961

Deco, G., Tononi, G., Boly, M., & Kringelbach, M. L. (2015). Rethinking segregation and integration: contributions of whole-brain modelling. *Nat Rev Neurosci*, *16*(7), 430-439. https://doi.org/10.1038/nrn3963

Dehaene-Lambertz, G., Dehaene, S., & Hertz-Pannier, L. (2002). Functional neuroimaging of speech perception in infants. *Science*, *298*(5600), 2013-2015. https://doi.org/10.1126/science.1077066

Dehaene, S., & Changeux, J. P. (2005). Ongoing spontaneous activity controls access to consciousness: a neuronal model for inattentional blindness. *PLoS Biology*, *3*(5), e141. https://doi.org/10.1371/journal.pbio.0030141

Dehaene, S., & Changeux, J. P. (2011). Experimental and theoretical approaches to conscious processing. *Neuron*, *70*(2), 200-227. https://doi.org/10.1016/j.neuron.2011.03.018

Dehaene, S., Changeux, J. P., & Naccache, L. (2011). The Global Neuronal Workspace Model of Conscious Access: From Neuronal Architectures to Clinical Applications. *Characterizing Consciousness: From Cognition to the Clinic*, 55-84. https://doi.org/10.1007/978-3-642-18015-6_4

Dehaene, S., Naccache, L., Le Clec, H. G., Koechlin, E., Mueller, M., Dehaene-Lambertz, G., van de Moortele, P. F., & Le Bihan, D. (1998). Imaging unconscious semantic priming. *Nature*, *395*(6702), 597-600. https://doi.org/10.1038/26967

Dehaene, S., Sergent, C., & Changeux, J. P. (2003). A neuronal network model linking subjective reports and objective physiological data during conscious perception. *Proceedings of the National Academy of Sciences of the United States of America*, *100*(14), 8520-8525. https://doi.org/10.1073/pnas.1332574100

Demertzi, A., Soddu, A., & Laureys, S. (2013). Consciousness supporting networks. *Current Opinion in Neurobiology*, *23*(2), 239-244. https://doi.org/10.1016/j.conb.2012.12.003

Demertzi, A., Tagliazucchi, E., Dehaene, S., Deco, G., Barttfeld, P., Raimondo, F., Martial, C., Fernandez-Espejo, D., Rohaut, B., Voss, H. U., Schiff, N. D., Owen, A. M., Laureys, S., Naccache, L., & Sitt, J. D. (2019). Human consciousness is supported by dynamic complex patterns of brain signal coordination. *Science advances*, *5*(2). https://doi.org/10.1126/sciadv.aat7603

Deng, F., Taylor, N., Owen, A. M., Cusack, R., & Naci, L. (2023). Responsiveness variability during anaesthesia relates to inherent differences in brain structure and function of the frontoparietal networks. *Human Brain Mapping*, *44*(6), 2142-2157. https://doi.org/10.1002/hbm.26199

Dereymaeker, A., Pillay, K., Vervisch, J., De Vos, M., Van Huffel, S., Jansen, K., & Naulaers, G. (2017). Review of sleep-EEG in preterm and term neonates. *Early Human Development*, *113*, 87-103. https://doi.org/10.1016/j.earlhumdev.2017.07.003

Diamond, A., & Goldman-Rakic, P. S. (1989). Comparison of human infants and rhesus monkeys on Piaget's AB task: evidence for dependence on dorsolateral prefrontal

cortex. *Experimental Brain Research*, *74*(1), 24-40. https://doi.org/10.1007/BF00248277

DiLorenzo, M. G., Pillai Riddell, R., Flora, D. B., & Craig, K. D. (2018). Infant Clinical Pain Assessment: Core Behavioral Cues. *The Journal of Pain*, *19*(9), 1024-1032. https://doi.org/10.1016/j.jpain.2018.03.016

Doria, V., Beckmann, C. F., Arichi, T., Merchant, N., Groppo, M., Turkheimer, F. E., Counsell, S. J., Murgasova, M., Aljabar, P., Nunes, R. G., Larkman, D. J., Rees, G., & Edwards, A. D. (2010). Emergence of resting state networks in the preterm human brain. *Proceedings of the National Academy of Sciences of the United States of America*, *107*(46), 20015-20020. https://doi.org/10.1073/pnas.1007921107

Dubois, J., Hertz-Pannier, L., Dehaene-Lambertz, G., Cointepas, Y., & Le Bihan, D. (2006). Assessment of the early organization and maturation of infants' cerebral white matter fiber bundles: a feasibility study using quantitative diffusion tensor imaging and tractography. *Neuroimage*, *30*(4), 1121-1132. https://doi.org/10.1016/j.neuroimage.2005.11.022

Duclos, C., Nadin, D., Mahdid, Y., Tarnal, V., Picton, P., Vanini, G., Golmirzaie, G., Janke, E., Avidan, M. S., Kelz, M. B., Mashour, G. A., & Blain-Moraes, S. (2021). Brain network motifs are markers of loss and recovery of consciousness. *Sci Rep*, *11*(1), 3892. https://doi.org/10.1038/s41598-021-83482-9

Duncan, J. (2010). The multiple-demand (MD) system of the primate brain: mental programs for intelligent behaviour. *Trends in Cognitive Sciences*, *14*(4), 172-179. https://doi.org/10.1016/j.tics.2010.01.004

Edelman, G. M. (2003). Naturalizing consciousness: a theoretical framework. *Proceedings of the National Academy of Sciences of the United States of America*, *100*(9), 5520-5524. https://doi.org/10.1073/pnas.0931349100

Elliott, R. (2003). Executive functions and their disorders: Imaging in clinical neuroscience. *British medical bulletin*, *65*(1), 49-59.

Ellis, C. T., Skalaban, L. J., Yates, T. S., Bejjanki, V. R., Cordova, N. I., & Turk-Browne, N. B. (2021). Evidence of hippocampal learning in human infants. *Current Biology*, *31*(15), 3358-+. https://doi.org/10.1016/j.cub.2021.04.072

Emberson, L. L., Boldin, A. M., Riccio, J. E., Guillet, R., & Aslin, R. N. (2017). Deficits in Top-Down Sensory Prediction in Infants At Risk due to Premature Birth. *Current Biology*, *27*(3), 431-436. https://doi.org/10.1016/j.cub.2016.12.028

Engemann, D. A., Raimondo, F., King, J. R., Rohaut, B., Louppe, G., Faugeras, F., Annen, J., Cassol, H., Gosseries, O., Fernandez-Slezak, D., Laureys, S., Naccache, L., Dehaene, S., & Sitt, J. D. (2018). Robust EEG-based cross-site and cross-protocol classification of states of consciousness. *Brain*, *141*(11), 3179-3192. https://doi.org/10.1093/brain/awy251

Eriksson, M., Storm, H., Fremming, A., & Schollin, J. (2008). Skin conductance compared to a combined behavioural and physiological pain measure in newborn infants. *Acta Paediatrica*, *97*(1), 27-30. https://doi.org/10.1111/j.1651-2227.2007.00586.x

Eyre, J. A., Miller, S., Clowry, G. J., Conway, E. A., & Watts, C. (2000). Functional corticospinal projections are established prenatally in the human foetus permitting involvement in the development of spinal motor centres. *Brain*, *123*, 51-64. https://doi.org/10.1093/brain/123.1.51

Eyre, M., Fitzgibbon, S. P., Ciarrusta, J., Cordero-Grande, L., Price, A. N., Poppe, T., Schuh, A., Hughes, E., O'Keeffe, C., Brandon, J., Cromb, D., Vecchiato, K., Andersson, J., Duff, E. P., Counsell, S. J., Smith, S. M., Rueckert, D., Hajnal, J. V., Arichi, T., . . . Edwards, A. D. (2021). The Developing Human Connectome

Project: typical and disrupted perinatal functional connectivity. *Brain*, *144*, 2199-2213. https://doi.org/10.1093/brain/awab118

Fair, D. A., Cohen, A. L., Dosenbach, N. U., Church, J. A., Miezin, F. M., Barch, D. M., Raichle, M. E., Petersen, S. E., & Schlaggar, B. L. (2008). The maturing architecture of the brain's default network. *Proceedings of the National Academy of Sciences of the United States of America*, *105*(10), 4028-4032. https://doi.org/10.1073/pnas.0800376105

Fair, D. A., Dosenbach, N. U. F., Church, J. A., Cohen, A. L., Brahmbhatt, S., Miezin, F. M., Barch, D. M., Raichle, M. E., Petersen, S. E., & Schlaggar, B. L. (2007). Development of distinct control networks through segregation and integration. *Proceedings of the National Academy of Sciences of the United States of America*, *104*(33), 13507-13512. https://doi.org/10.1073/pnas.0705843104

Farroni, T., Chiarelli, A. M., Lloyd-Fox, S., Massaccesi, S., Merla, A., Di Gangi, V., Mattarello, T., Faraguna, D., & Johnson, M. H. (2013). Infant cortex responds to other humans from shortly after birth. *Scientific reports*, *3*, 2851. https://doi.org/10.1038/srep02851

Faul, F., Erdfelder, E., Buchner, A., & Lang, A.-G. (2009). Statistical power analyses using G* Power 3.1: Tests for correlation and regression analyses. *Behavior research methods*, *41*(4), 1149-1160. https://doi.org/10.3758/BRM.41.4.1149

Fenn-Moltu, S., Fitzgibbon, S. P., Ciarrusta, J., Eyre, M., Cordero-Grande, L., Chew, A., Falconer, S., Gale-Grant, O., Harper, N., & Dimitrova, R. (2023). Development of neonatal brain functional centrality and alterations associated with preterm birth. *Cerebral Cortex*, *33*(9), 5585-5596. https://doi.org/10.1093/cercor/bhac444

Fenson, L., Dale, P. S., Reznick, J. S., Bates, E., Thal, D. J., Pethick, S. J., Tomasello, M., Mervis, C. B., & Stiles, J. (1994). Variability in early communicative development.

Monographs of the society for research in child development, i-185. https://doi.org/10.2307/1166093

Filippetti, M. L., Johnson, M. H., Lloyd-Fox, S., Dragovic, D., & Farroni, T. (2013). Body perception in newborns. *Curr Biol*, *23*(23), 2413-2416. https://doi.org/10.1016/j.cub.2013.10.017

Fitzgibbon, S. P., Harrison, S. J., Jenkinson, M., Baxter, L., Robinson, E. C., Bastiani, M., Bozek, J., Karolis, V., Grande, L. C., Price, A. N., Hughes, E., Makropoulos, A., Passerat-Palmbach, J., Schuh, A., Gao, J. L., Farahibozorg, S. R., O'Muircheartaigh, J., Ciarrusta, J., O'Keeffe, C., . . . Andersson, J. (2020). The developing Human Connectome Project (dHCP) automated resting-state functional processing framework for newborn infants. *Neuroimage*, *223*. https://doi.org/10.1016/j.neuroimage.2020.117303

Fleming, S. M., Dolan, R. J., & Frith, C. D. (2012). Metacognition: computation, biology and function. *Philos Trans R Soc Lond B Biol Sci*, *367*(1594), 1280-1286. https://doi.org/10.1098/rstb.2012.0021

Fox, M. D., Snyder, A. Z., Vincent, J. L., Corbetta, M., Van Essen, D. C., & Raichle, M. E. (2005). The human brain is intrinsically organized into dynamic, anticorrelated functional networks. *Proceedings of the National Academy of Sciences*, *102*(27), 9673-9678. https://doi.org/10.1073/pnas.0504136102

Frakes, W. B., & Baeza-Yates, R. (1992). *Information retrieval: data structures and algorithms*. Prentice-Hall, Inc.

França, L. G., Ciarrusta, J., Gale-Grant, O., Fenn-Moltu, S., Fitzgibbon, S., Chew, A., Falconer, S., Dimitrova, R., Cordero-Grande, L., & Price, A. N. (2022). Neonatal brain dynamic functional connectivity: impact of preterm birth and association with

early childhood neurodevelopment. *BioRxiv*, 2022.2011. 2016.516610. https://doi.org/10.1101/2022.11.16.516610

Frankenhuis, W. E., & Gopnik, A. (2023). Early adversity and the development of explore–exploit tradeoffs. *Trends in Cognitive Sciences*. https://doi.org/10.1016/j.tics.2023.04.001

Fransson, P. (2005). Spontaneous low-frequency BOLD signal fluctuations: An fMRI investigation of the resting-state default mode of brain function hypothesis. *Human Brain Mapping*, *26*(1), 15-29.

Fransson, P., Aden, U., Blennow, M., & Lagercrantz, H. (2011). The Functional Architecture of the Infant Brain as Revealed by Resting-State fMRI. *Cerebral Cortex*, *21*(1), 145-154. https://doi.org/10.1093/cercor/bhq071

Fransson, P., Skiöld, B., Engström, M., Hallberg, B., Mosskin, M., Åden, U., Lagercrantz, H., & Blennow, M. (2009). Spontaneous Brain Activity in the Newborn Brain During Natural Sleep-An fMRI Study in Infants Born at Full Term. *Pediatric Research*, *66*(3), 301-305. https://doi.org/10.1203/PDR.0b013e3181b1bd84

Fransson, P., Skiöld, B., Horsch, S., Nordell, A., Blennow, M., Lagercrantz, H., & Åden, U. (2007). Resting-state networks in the infant brain. *Proceedings of the National Academy of Sciences of the United States of America*, *104*(39), 15531-15536. https://doi.org/10.1073/pnas.0704380104

Frew, S., Samara, A., Shearer, H., Eilbott, J., & Vanderwal, T. (2022). Getting the nod: Pediatric head motion in a transdiagnostic sample during movie- and resting-state fMRI. *PLoS one*, *17*(4). https://doi.org/10.1371/journal.pone.0265112

Friederici, A. D. (2011). The Brain Basis of Language Processing: From Structure to Function. *Physiological Reviews*, *91*(4), 1357-1392. https://doi.org/10.1152/physrev.00006.2011

Friston, K. (2002). Beyond phrenology: what can neuroimaging tell us about distributed circuitry? *Annual review of neuroscience*, *25*(1), 221-250.

Froeliger, B., Garland, E. L., Kozink, R. V., Modlin, L. A., Chen, N.-K., McClernon, F. J., Greeson, J. M., & Sobin, P. (2012). Meditation-state functional connectivity (msFC): strengthening of the dorsal attention network and beyond. *Evidence-Based Complementary and Alternative Medicine*, *2012*. https://doi.org/10.1155/2012/680407

Frohlich, J., Moser, J., Sippel, K., Mediano, P. A., Preissl, H., & Gharabaghi, A. (2022). Sex differences in prenatal development of neural complexity in the human brain. *BioRxiv*, 2022.2011. 2021.517302. https://doi.org/10.1101/2022.11.21.517302

Fukushima, M., Betzel, R. F., He, Y., van den Heuvel, M. P., Zuo, X. N., & Sporns, O. (2018). Structure-function relationships during segregated and integrated network states of human brain functional connectivity. *Brain Structure & Function*, *223*(3), 1091-1106. https://doi.org/10.1007/s00429-017-1539-3

Gallagher, S. (2000). Philosophical conceptions of the self: implications for cognitive science. *Trends in Cognitive Sciences*, *4*(1), 14-21. https://doi.org/10.1016/S1364-6613(99)01417-5

Gao, W., Alcauter, S., Elton, A., Hernandez-Castillo, C. R., Smith, J. K., Ramirez, J., & Lin, W. L. (2015). Functional Network Development During the First Year: Relative Sequence and Socioeconomic Correlations. *Cerebral Cortex*, *25*(9), 2919-2928. https://doi.org/10.1093/cercor/bhu088

Gao, W., Alcauter, S., Smith, J. K., Gilmore, J. H., & Lin, W. L. (2015). Development of human brain cortical network architecture during infancy. *Brain Structure & Function*, *220*(2), 1173-1186. https://doi.org/10.1007/s00429-014-0710-3

Gao, W., Gilmore, J. H., Shen, D. G., Smith, J. K., Zhu, H. T., & Lin, W. L. (2013). The Synchronization within and Interaction between the Default and Dorsal Attention Networks in Early Infancy. *Cerebral Cortex*, *23*(3), 594-603. https://doi.org/10.1093/cercor/bhs043

Gao, W., Zhu, H. T., Giovanello, K. S., Smith, J. K., Shen, D. G., Gilmore, J. H., & Lin, W. L. (2009). Evidence on the emergence of the brain's default network from 2-week-old to 2-year-old healthy pediatric subjects. *Proceedings of the National Academy of Sciences of the United States of America*, *106*(16), 6790-6795. https://doi.org/10.1073/pnas.0811221106

Geng, X., Gouttard, S., Sharma, A., Gu, H., Styner, M., Lin, W., Gerig, G., & Gilmore, J. H. (2012). Quantitative tract-based white matter development from birth to age 2 years. *Neuroimage*, *61*(3), 542-557. https://doi.org/10.1016/j.neuroimage.2012.03.057

Giacino, J. T., Schnakers, C., Rodriguez-Moreno, D., Kalmar, K., Schiff, N., & Hirsch, J. (2009). Behavioral assessment in patients with disorders of consciousness: gold standard or fool's gold? *Coma Science: Clinical and Ethical Implications*, *177*, 33-48. https://doi.org/10.1016/S0079-6123(09)17704-X

Glasser, M. F., Sotiropoulos, S. N., Wilson, J. A., Coalson, T. S., Fischl, B., Andersson, J. L., Xu, J., Jbabdi, S., Webster, M., Polimeni, J. R., Van Essen, D. C., Jenkinson, M., & Consortium, W. U.-M. H. (2013). The minimal preprocessing pipelines for the Human Connectome Project. *Neuroimage*, *80*, 105-124. https://doi.org/10.1016/j.neuroimage.2013.04.127

Godwin, D., Barry, R. L., & Marois, R. (2015). Breakdown of the brain's functional network modularity with awareness. *Proceedings of the National Academy of*

Sciences of the United States of America, *112*(12), 3799-3804. https://doi.org/10.1073/pnas.1414466112

Goldenberg, R. L., Culhane, J. F., Iams, J. D., & Romero, R. (2008). Epidemiology and causes of preterm birth. *Lancet*, *371*(9606), 75-84. https://doi.org/10.1016/S0140-6736(08)60074-4

Goldenberg, R. L., Culhane, J. F., Iams, J. D., & Romero, R. (2008). Epidemiology and causes of preterm birth. *The lancet*, *371*(9606), 75-84.

Golkowski, D., Larroque, S. K., Vanhaudenhuyse, A., Plenevaux, A., Boly, M., Di Perri, C., Ranft, A., Schneider, G., Laureys, S., & Jordan, D. (2019). Changes in whole brain dynamics and connectivity patterns during sevoflurane-and propofol-induced unconsciousness identified by functional magnetic resonance imaging. *Anesthesiology*, *130*(6), 898-911. https://doi.org/10.1097/ALN.0000000000002704

Gopnik, A. (2007). Why babies are more conscious than we are. *Behavioral and Brain Sciences*, *30*(5-6), 503-504. https://doi.org/10.1017/S0140525x0700283x

Gopnik, A. (2009). *The philosophical baby: What children's minds tell us about truth, love & the meaning of life*. Random House.

Goupil, L., & Kouider, S. (2019). Developing a Reflective Mind: From Core Metacognition to Explicit Self-Reflection. *Current Directions in Psychological Science*, *28*(4), 403-408. https://doi.org/10.1177/0963721419848672

Gozdas, E., Parikh, N. A., Merhar, S. L., Tkach, J. A., He, L., & Holland, S. K. (2018). Altered functional network connectivity in preterm infants: antecedents of cognitive and motor impairments? *Brain Structure & Function*, *223*(8), 3665-3680. https://doi.org/10.1007/s00429-018-1707-0

Greicius, M. D., Krasnow, B., Reiss, A. L., & Menon, V. (2003). Functional connectivity in the resting brain: A network analysis of the default mode hypothesis.

Proceedings of the National Academy of Sciences of the United States of America, *100*(1), 253-258. https://doi.org/10.1073/pnas.0135058100

Gu, S., Satterthwaite, T. D., Medaglia, J. D., Yang, M., Gur, R. E., Gur, R. C., & Bassett, D. S. (2015). Emergence of system roles in normative neurodevelopment. *Proc Natl Acad Sci U S A*, *112*(44), 13681-13686. https://doi.org/10.1073/pnas.1502829112

Guarini, A., Sansavini, A., Fabbri, C., Alessandroni, R., Faldella, G., & Karmiloff-Smith, A. (2009). Reconsidering the impact of preterm birth on language outcome. *Early Human Development*, *85*(10), 639-645. https://doi.org/10.1016/j.earlhumdev.2009.08.061

Gusnard, D. A., & Raichle, M. E. (2001). Searching for a baseline: Functional imaging and the resting human brain. *Nature Reviews Neuroscience*, *2*(10), 685-694. https://doi.org/10.1038/35094500

Hagmann, P., Cammoun, L., Gigandet, X., Meuli, R., Honey, C. J., Wedeen, V. J., & Sporns, O. (2008). Mapping the structural core of human cerebral cortex. *PLoS Biology*, *6*(7), e159. https://doi.org/10.1371/journal.pbio.0060159

Hallquist, M. N., & Hillary, F. G. (2018). Graph theory approaches to functional network organization in brain disorders: A critique for a brave new small-world. *Network neuroscience*, *3*(1), 1-26. https://doi.org/10.1162/netn_a_00054

Hartley, C., Moultrie, F., Gursul, D., Hoskin, A., Adams, E., Rogers, R., & Slater, R. (2016). Changing Balance of Spinal Cord Excitability and Nociceptive Brain Activity in Early Human Development. *Current Biology*, *26*(15), 1998-2002. https://doi.org/10.1016/j.cub.2016.05.054

Haugg, A., Cusack, R., Gonzalez-Lara, L. E., Sorger, B., Owen, A. M., & Naci, L. (2018). Do Patients Thought to Lack Consciousness Retain the Capacity for Internal as

Well as External Awareness? *Frontiers in Neurology*, *9*. https://doi.org/10.3389/fneur.2018.00492

He, L. L., & Parikh, N. A. (2015). Aberrant Executive and Frontoparietal Functional Connectivity in Very Preterm Infants With Diffuse White Matter Abnormalities. *Pediatric Neurology*, *53*(4), 330-337. https://doi.org/10.1016/j.pediatrneurol.2015.05.001

He, L. L., & Parikh, N. A. (2016). Brain functional network connectivity development in very preterm infants: The first six months. *Early Human Development*, *98*, 29-35. https://doi.org/10.1016/j.earlhumdev.2016.06.002

Herzog, R., Mediano, P. A. M., Rosas, F. E., Lodder, P., Carhart-Harris, R., Perl, Y. S., Tagliazucchi, E., & Cofre, R. (2023a). A whole-brain model of the neural entropy increase elicited by psychedelic drugs. *Sci Rep*, *13*(1), 6244. https://doi.org/10.1038/s41598-023-32649-7

Herzog, R., Mediano, P. A. M., Rosas, F. E., Lodder, P., Carhart-Harris, R., Perl, Y. S., Tagliazucchi, E., & Cofre, R. (2023b). A whole-brain model of the neural entropy increase elicited by psychedelic drugs. *Scientific Reports*, *13*(1). https://doi.org/10.1038/s41598-023-32649-7

Hickok, G., & Poeppel, D. (2007). The cortical organization of speech processing. *Nature Reviews Neuroscience*, *8*(5), 393-402. https://doi.org/10.1038/nrn2113

Hoel, E. P., Albantakis, L., & Tononi, G. (2013). Quantifying causal emergence shows that macro can beat micro. *Proceedings of the National Academy of Sciences of the United States of America*, *110*(49), 19790-19795. https://doi.org/10.1073/pnas.1314922110

Hoptman, M. J., Zuo, X. N., D'Angelo, D., Mauro, C. J., Butler, P. D., Milham, M. P., & Javitt, D. C. (2012). Decreased interhemispheric coordination in schizophrenia: a

resting state fMRI study. *Schizophr Res*, *141*(1), 1-7. https://doi.org/10.1016/j.schres.2012.07.027

Horovitz, S. G., Braun, A. R., Carr, W. S., Picchioni, D., Balkin, T. J., Fukunaga, M., & Duyn, J. H. (2009). Decoupling of the brain's default mode network during deep sleep. *Proceedings of the National Academy of Sciences of the United States of America*, *106*(27), 11376-11381. https://doi.org/10.1073/pnas.0901435106

Howard, L. H., & Woodward, A. L. (2019). Human actions support infant memory. *Journal of Cognition and Development*, *20*(5), 772-789. https://doi.org/10.1080/15248372.2019.1664549

Howe, M. L., & Courage, M. L. (2004). Demystifying the beginnings of memory. *Developmental review*, *24*(1), 1-5. https://doi.org/10.1016/j.dr.2003.09.006

Howe, M. L., Courage, M. L., & Edison, S. C. (2003). When autobiographical memory begins. *Developmental review*, *23*(4), 471-494. https://doi.org/10.1016/j.dr.2003.09.001

Hu, H., Cusack, R., & Naci, L. (2022). Typical and disrupted brain circuitry for conscious awareness in full-term and preterm infants. *Brain Communications*, *4*(2), fcac071. https://doi.org/10.1093/braincomms/fcac071

Huang, H., Shu, N., Mishra, V., Jeon, T., Chalak, L., Wang, Z. J., Rollins, N., Gong, G., Cheng, H., & Peng, Y. (2015). Development of human brain structural networks through infancy and childhood. *Cerebral Cortex*, *25*(5), 1389-1404. https://doi.org/10.1093/cercor/bht335

Huang, Z., Zhang, J., Wu, J., Qin, P., Wu, X., Wang, Z., Dai, R., Li, Y., Liang, W., Mao, Y., Yang, Z., Zhang, J., Wolff, A., & Northoff, G. (2016). Decoupled temporal variability and signal synchronization of spontaneous brain activity in loss of

consciousness: An fMRI study in anesthesia. *Neuroimage*, *124*(Pt A), 693-703. https://doi.org/10.1016/j.neuroimage.2015.08.062

Huang, Z. R., Zhang, J., Wu, J. S., Mashour, G. A., & Hudetz, A. G. (2020). Temporal circuit of macroscale dynamic brain activity supports human consciousness. *Science advances*, *6*(11). https://doi.org/10.1126/sciadv.aaz0087

Humphries, M. D., & Gurney, K. (2008). Network 'small-world-ness': a quantitative method for determining canonical network equivalence. *PLoS one*, *3*(4), e0002051. https://doi.org/10.1371/journal.pone.0002051

Isler, J. R., Stark, R. I., Grieve, P. G., Welch, M. G., & Myers, M. M. (2018). Integrated information in the EEG of preterm infants increases with family nurture intervention, age, and conscious state. *PLoS one*, *13*(10), e0206237. https://doi.org/10.1371/journal.pone.0206237

Ito, T., Brincat, S. L., Siegel, M., Mill, R. D., He, B. Y. J., Miller, E. K., Rotstein, H. G., & Cole, M. W. (2020). Task-evoked activity quenches neural correlations and variability across cortical areas. *Plos Computational Biology*, *16*(8). https://doi.org/10.1371/journal.pcbi.1007983

Janjarasjitt, S., Scher, M. S., & Loparo, K. A. (2008). Nonlinear dynamical analysis of the neonatal EEG time series: The relationship between sleep state and complexity. *Clinical Neurophysiology*, *119*(8), 1812-1823. https://doi.org/10.1016/j.clinph.2008.03.024

Jennett, B., & Plum, F. (1972). Persistent vegetative state after brain damage. A syndrome in search of a name. *Lancet*, *1*(7753), 734-737. https://doi.org/10.1016/s0140-6736(72)90242-5

Johnson, M. H. (2001). Functional brain development in humans. *Nature Reviews Neuroscience*, *2*(7), 475-483. https://doi.org/10.1038/35081509

Johnson, M. H. (2003). Development of human brain functions. *Biological Psychiatry*, *54*(12), 1312-1316. https://doi.org/10.1016/s0006-3223(03)00426-8

Josipovic, Z., Dinstein, I., Weber, J., & Heeger, D. J. (2012). Influence of meditation on anti-correlated networks in the brain. *Frontiers in Human Neuroscience*, *5*, 183. https://doi.org/10.3389/fnhum.2011.00183

Kaffashi, F., Scher, M. S., Ludington-Hoe, S. M., & Loparo, K. A. (2013a). An analysis of the kangaroo care intervention using neonatal EEG complexity: A preliminary study. *Clinical Neurophysiology*, *124*(2), 238-246. https://doi.org/10.1016/j.clinph.2012.06.021

Kaffashi, F., Scher, M. S., Ludington-Hoe, S. M., & Loparo, K. A. (2013b). An analysis of the kangaroo care intervention using neonatal EEG complexity: a preliminary study. *Clinical Neurophysiology*, *124*(2), 238-246. https://doi.org/10.1016/j.clinph.2012.06.021

Kandeepan, S., Rudas, J., Gomez, F., Stojanoski, B., Valluri, S., Owen, A. M., Naci, L., Nichols, E. S., & Soddu, A. (2020). Modeling an auditory stimulated brain under altered states of consciousness using the generalized Ising model. *Neuroimage*, *223*, 117367. https://doi.org/10.1016/j.neuroimage.2020.117367

Kelly, A. C., Uddin, L. Q., Biswal, B. B., Castellanos, F. X., & Milham, M. P. (2008). Competition between functional brain networks mediates behavioral variability. *Neuroimage*, *39*(1), 527-537. https://doi.org/10.1016/j.neuroimage.2007.08.008

Kelly, D. J., Duarte, S., Meary, D., Bindemann, M., & Pascalis, O. (2019). Infants rapidly detect human faces in complex naturalistic visual scenes. *Developmental Science*, *22*(6), e12829. https://doi.org/10.1111/desc.12829

Keunen, K., Counsell, S. J., & Benders, M. J. N. L. (2017). The emergence of functional architecture during early brain development. *Neuroimage*, *160*, 2-14. https://doi.org/10.1016/j.neuroimage.2017.01.047

Kolmogorov, A. N. (1968). Three approaches to the quantitative definition of information. *International journal of computer mathematics*, *2*(1-4), 157-168.

Kostovic, I., & Jovanov-Milosevic, N. (2006). The development of cerebral connections during the first 20-45 weeks' gestation. *Seminars in Fetal & Neonatal Medicine*, *11*(6), 415-422. https://doi.org/10.1016/j.siny.2006.07.001

Kostovic, I., & Judas, M. (2006). Prolonged coexistence of transient and permanent circuitry elements in the developing cerebral cortex of fetuses and preterm infants. *Developmental Medicine and Child Neurology*, *48*(5), 388-393. https://doi.org/10.1017/S0012162206000831

Kostovic, I., & Judas, M. (2010). The development of the subplate and thalamocortical connections in the human foetal brain. *Acta Paediatrica*, *99*(8), 1119-1127. https://doi.org/10.1111/j.1651-2227.2010.01811.x

Kostovic, I., Judas, M., Rados, M., & Hrabac, P. (2002). Laminar organization of the human fetal cerebrum revealed by histochemical markers and magnetic resonance imaging. *Cerebral Cortex*, *12*(5), 536-544. https://doi.org/10.1093/cercor/12.5.536

Kostovic, I., Sedmak, G., & Judas, M. (2019). Neural histology and neurogenesis of the human fetal and infant brain. *Neuroimage*, *188*, 743-773. https://doi.org/10.1016/j.neuroimage.2018.12.043

Kotilahti, K., Nissila, I., Nasi, T., Lipiainen, L., Noponen, T., Merilainen, P., Huotilainen, M., & Fellman, V. (2010). Hemodynamic responses to speech and music in newborn infants. *Human Brain Mapping*, *31*(4), 595-603. https://doi.org/10.1002/hbm.20890

Kouider, S., Stahlhut, C., Gelskov, S. V., Barbosa, L. S., Dutat, M., de Gardelle, V., Christophe, A., Dehaene, S., & Dehaene-Lambertz, G. (2013). A Neural Marker of Perceptual Consciousness in Infants. *science*, *340*(6130), 376-380. https://doi.org/10.1126/science.1232509

Kovacs, A. M., Teglas, E., & Endress, A. D. (2010). The Social Sense: Susceptibility to Others' Beliefs in Human Infants and Adults. *science*, *330*(6012), 1830-1834. https://doi.org/10.1126/science.1190792

Kristen-Antonow, S., Sodian, B., Perst, H., & Licata, M. (2015). A longitudinal study of the emerging self from 9 months to the age of 4 years. *Frontiers in Psychology*, *6*. https://doi.org/10.3389/fpsyg.2015.00789

Kroger, J. K., Sabb, F. W., Fales, C. L., Bookheimer, S. Y., Cohen, M. S., & Holyoak, K. J. (2002). Recruitment of anterior dorsolateral prefrontal cortex in human reasoning: a parametric study of relational complexity. *Cerebral Cortex*, *12*(5), 477-485. https://doi.org/10.1093/cercor/12.5.477

Krsnik, Z., Majic, V., Vasung, L., Huang, H., & Kostovic, I. (2017). Growth of Thalamocortical Fibers to the Somatosensory Cortex in the Human Fetal Brain. *Frontiers in Neuroscience*, *11*. https://doi.org/10.3389/fnins.2017.00233

Kruskal, J. B. (1964). Nonmetric multidimensional scaling: a numerical method. *Psychometrika*, *29*(2), 115-129.

Kuklisova-Murgasova, M., Aljabar, P., Srinivasan, L., Counsell, S. J., Doria, V., Serag, A., Gousias, I. S., Boardman, J. P., Rutherford, M. A., Edwards, A. D., Hajnal, J. V., & Rueckert, D. (2011). A dynamic 4D probabilistic atlas of the developing brain. *Neuroimage*, *54*(4), 2750-2763. https://doi.org/10.1016/j.neuroimage.2010.10.019

Kumpulainen, V., Merisaari, H., Silver, E., Copeland, A., Pulli, E. P., Lewis, J. D., Saukko, E., Shulist, S. J., Saunavaara, J., & Parkkola, R. (2023). Sex differences,

asymmetry, and age-related white matter development in infants and 5-year-olds as assessed with tract-based spatial statistics. *Human Brain Mapping*, *44*(7), 2712-2725. https://doi.org/10.1002/hbm.26238

Laforge, G., Gonzalez-Lara, L. E., Owen, A. M., & Stojanoski, B. (2020). Individualized assessment of residual cognition in patients with disorders of consciousness. *Neuroimage-Clinical*, *28*, 102472. https://doi.org/10.1016/j.nicl.2020.102472

Lagercrantz, H. (2014). The emergence of consciousness: Science and ethics. *Seminars in Fetal and Neonatal Medicine*, *19*(5), 300-305. https://doi.org/10.1016/j.siny.2014.08.003

Lake, D. E., Richman, J. S., Griffin, M. P., & Moorman, J. R. (2002). Sample entropy analysis of neonatal heart rate variability. *Am J Physiol Regul Integr Comp Physiol*, *283*(3), R789-797. https://doi.org/10.1152/ajpregu.00069.2002

Lamme, V. A. (2006). Towards a true neural stance on consciousness. *Trends Cogn Sci*, *10*(11), 494-501. https://doi.org/10.1016/j.tics.2006.09.001

Lamme, V. A., & Roelfsema, P. R. (2000). The distinct modes of vision offered by feedforward and recurrent processing. *Trends in Neurosciences*, *23*(11), 571-579. https://doi.org/10.1016/s0166-2236(00)01657-x

Lau, H., & Rosenthal, D. (2011). Empirical support for higher-order theories of conscious awareness. *Trends in Cognitive Sciences*, *15*(8), 365-373. https://doi.org/10.1016/j.tics.2011.05.009

Laumann, T. O., Snyder, A. Z., Mitra, A., Gordon, E. M., Gratton, C., Adeyemo, B., Gilmore, A. W., Nelson, S. M., Berg, J. J., Greene, D. J., McCarthy, J. E., Tagliazucchi, E., Laufs, H., Schlaggar, B. L., Dosenbach, N. U. F., & Petersen, S. E. (2017). On the Stability of BOLD fMRI Correlations. *Cerebral Cortex*, *27*(10), 4719-4732. https://doi.org/10.1093/cercor/bhw265

Laureys, S. (2005). The neural correlate of (un)awareness: lessons from the vegetative state. *Trends Cogn Sci*, *9*(12), 556-559. https://doi.org/10.1016/j.tics.2005.10.010

Laureys, S., Owen, A. M., & Schiff, N. D. (2004). Brain function in coma, vegetative state, and related disorders. *Lancet Neurol*, *3*(9), 537-546. https://doi.org/10.1016/S1474-4422(04)00852-X

LeDoux, J. E., & Lau, H. (2020). Seeing consciousness through the lens of memory. *Current Biology*, *30*(18), R1018-R1022. https://doi.org/10.1016/j.cub.2020.08.008

Lee, G. M. H., Fattinger, S., Mouthon, A. L., Noirhomme, Q., & Huber, R. (2013). Electroencephalogram approximate entropy influenced by both age and sleep. *Frontiers in Neuroinformatics*, *7*. https://doi.org/10.3389/fninf.2013.00033

Lee, M., Sanz, L. R. D., Barra, A., Wolff, A., Nieminen, J. O., Boly, M., Rosanova, M., Casarotto, S., Bodart, O., Annen, J., Thibaut, A., Panda, R., Bonhomme, V., Massimini, M., Tononi, G., Laureys, S., Gosseries, O., & Lee, S. W. (2022). Quantifying arousal and awareness in altered states of consciousness using interpretable deep learning. *Nature Communications*, *13*(1), 1064. https://doi.org/10.1038/s41467-022-28451-0

Li, D., Vlisides, P. E., & Mashour, G. A. (2022a). Dynamic reconfiguration of frequency-specific cortical coactivation patterns during psychedelic and anesthetized states induced by ketamine. *Neuroimage*, *249*. https://doi.org/ARTN 118891 10.1016/j.neuroimage.2022.118891

Li, D., Vlisides, P. E., & Mashour, G. A. (2022b). Dynamic reconfiguration of frequency-specific cortical coactivation patterns during psychedelic and anesthetized states induced by ketamine. *Neuroimage*, *249*, 118891. https://doi.org/10.1016/j.neuroimage.2022.118891

Liang, W., Yu, Q., Wang, W., Dhollander, T., Suluba, E., Li, Z., Xu, F., Hu, Y., Tang, Y., & Liu, S. (2022). A comparative study of the superior longitudinal fasciculus subdivisions between neonates and young adults. *Brain Structure & Function*, *227*(8), 2713-2730. https://doi.org/10.1007/s00429-022-02565-z

Limperopoulos, C., Soul, J. S., Gauvreau, K., Huppi, P. S., Warfield, S. K., Bassan, H., Robertson, R. L., Volpe, J. J., & du Plessis, A. J. (2005). Late gestation cerebellar growth is rapid and impeded by premature birth. *Pediatrics*, *115*(3), 688-695. https://doi.org/10.1542/peds.2004-1169

Lin, W., Zhu, Q., Gao, W., Chen, Y., Toh, C.-H., Styner, M., Gerig, G., Smith, J., Biswal, B., & Gilmore, J. (2008). Functional connectivity MR imaging reveals cortical functional connectivity in the developing brain. *American Journal of Neuroradiology*, *29*(10), 1883-1889. https://doi.org/10.3174/ajnr.A1256

Linke, A. C., Wild, C., Zubiaurre-Elorza, L., Herzmann, C., Duffy, H., Han, V. K., Lee, D. S. C., & Cusack, R. (2018). Disruption to functional networks in neonates with perinatal brain injury predicts motor skills at 8 months. *Neuroimage-Clinical*, *18*, 399-406. https://doi.org/10.1016/j.nicl.2018.02.002

Lippé, S., Kovacevic, N., & McIntosh, A. R. (2009). Differential maturation of brain signal complexity in the human auditory and visual system. *Frontiers in Human Neuroscience*, *3*. https://doi.org/10.3389/neuro.09.048.2009

Liu, S., Brooks, N. B., & Spelke, E. S. (2019). Origins of the concepts cause, cost, and goal in prereaching infants. *Proceedings of the National Academy of Sciences*, *116*(36), 17747-17752. https://doi.org/10.1073/pnas.1904410116

Liu, X. L., Lauer, K. K., Ward, B. D., Roberts, C., Liu, S. Y., Gollapudy, S., Rohloff, R., Gross, W., Chen, G. Y., Xu, Z., Binder, J. R., Li, S. J., & Hudetz, A. G. (2017). Propofol attenuates low-frequency fluctuations of resting-state fMRI BOLD signal

in the anterior frontal cortex upon loss of consciousness. *Neuroimage*, *147*, 295-301. https://doi.org/10.1016/j.neuroimage.2016.12.043

Liu, Z. Q., Vazquez-Rodriguez, B., Spreng, R. N., Bernhardt, B. C., Betzel, R. F., & Misic, B. (2022). Time-resolved structure-function coupling in brain networks. *Commun Biol*, *5*(1), 532. https://doi.org/10.1038/s42003-022-03466-x

Lloyd-Fox, S., Begus, K., Halliday, D., Pirazzoli, L., Blasi, A., Papademetriou, M., Darboe, M. K., Prentice, A. M., Johnson, M. H., Moore, S. E., & Elwell, C. E. (2017). Cortical specialisation to social stimuli from the first days to the second year of life: A rural Gambian cohort. *Developmental cognitive neuroscience*, *25*, 92-104. https://doi.org/10.1016/j.dcn.2016.11.005

Lowe, M. J., Mock, B. J., & Sorenson, J. A. (1998). Functional connectivity in single and multislice echoplanar imaging using resting-state fluctuations. *Neuroimage*, *7*(2), 119-132. https://doi.org/10.1006/nimg.1997.0315

Luppi, A. I., Carhart-Harris, R. L., Roseman, L., Pappas, I., Menon, D. K., & Stamatakis, E. A. (2021a). LSD alters dynamic integration and segregation in the human brain. *Neuroimage*, *227*, 117653. https://doi.org/10.1016/j.neuroimage.2020.117653

Luppi, A. I., Carhart-Harris, R. L., Roseman, L., Pappas, I., Menon, D. K., & Stamatakis, E. A. (2021b). LSD alters dynamic integration and segregation in the human brain. *Neuroimage*, *227*. https://doi.org/ARTN 117653

10.1016/j.neuroimage.2020.117653

Luppi, A. I., Craig, M. M., Pappas, I., Finoia, P., Williams, G. B., Allanson, J., Pickard, J. D., Owen, A. M., Naci, L., Menon, D. K., & Stamatakis, E. A. (2019). Consciousness-specific dynamic interactions of brain integration and functional diversity. *Nature Communications*, *10*(1), 4616. https://doi.org/10.1038/s41467-019-12658-9

Luppi, A. I., Golkowski, D., Ranft, A., Ilg, R., Jordan, D., Menon, D. K., & Stamatakis, E. A. (2021). Brain network integration dynamics are associated with loss and recovery of consciousness induced by sevoflurane. *Human Brain Mapping*, *42*(9), 2802-2822. https://doi.org/10.1002/hbm.25405

Luppi, A. I., & Stamatakis, E. A. (2021). Combining network topology and information theory to construct representative brain networks. *Network neuroscience*, *5*(1), 96-124. https://doi.org/10.1162/netn_a_00170

Ma, X. L., Wu, X. S., & Shi, Y. (2020). Changes of Dynamic Functional Connectivity Associated With Maturity in Late Preterm Infants. *Frontiers in Pediatrics*, *8*. https://doi.org/ARTN 412

10.3389/fped.2020.00412

Margulies, D. S., Ghosh, S. S., Goulas, A., Falkiewicz, M., Huntenburg, J. M., Langs, G., Bezgin, G., Eickhoff, S. B., Castellanos, F. X., Petrides, M., Jefferies, E., & Smallwood, J. (2016). Situating the default-mode network along a principal gradient of macroscale cortical organization. *Proceedings of the National Academy of Sciences of the United States of America*, *113*(44), 12574-12579. https://doi.org/10.1073/pnas.1608282113

Marlow, N., Wolke, D., Bracewell, M. A., Samara, M., & Grp, E. S. (2005). Neurologic and developmental disability at six years of age after extremely preterm birth. *New England Journal of Medicine*, *352*(1), 9-19. https://doi.org/10.1056/NEJMoa041367

Martin, G. B., & Clark, R. D. (1982). Distress Crying in Neonates - Species and Peer Specificity. *Developmental psychology*, *18*(1), 3-9. https://doi.org/10.1037/0012-1649.18.1.3

Mashour, G. A., Roelfsema, P., Changeux, J. P., & Dehaene, S. (2020). Conscious Processing and the Global Neuronal Workspace Hypothesis. *Neuron*, *105*(5), 776-798. https://doi.org/10.1016/j.neuron.2020.01.026

Mateos, D. M., Erra, R. G., Wennberg, R., & Velazquez, J. L. P. (2018). Measures of entropy and complexity in altered states of consciousness. *Cognitive Neurodynamics*, *12*(1), 73-84. https://doi.org/10.1007/s11571-017-9459-8

Mediano, P. A. M., Rosas, F. E., Bor, D., Seth, A. K., & Barrett, A. B. (2022). The strength of weak integrated information theory. *Trends in Cognitive Sciences*, *26*(8), 646-655. https://doi.org/10.1016/j.tics.2022.04.008

Mehling, W. E., Gopisetty, V., Daubenmier, J., Price, C. J., Hecht, F. M., & Stewart, A. (2009). Body awareness: construct and self-report measures. *PLoS one*, *4*(5), e5614. https://doi.org/10.1371/journal.pone.0005614

Metzinger, T. (2020). Minimal phenomenal experience: Meditation, tonic alertness, and the phenomenology of "pure" consciousness. *Philosophy and the Mind Sciences*, *1*(I), 1-44.

Miskovic, V., MacDonald, K. J., Rhodes, L. J., & Cote, K. A. (2019). Changes in EEG multiscale entropy and power-law frequency scaling during the human sleep cycle. *Human Brain Mapping*, *40*(2), 538-551. https://doi.org/10.1002/hbm.24393

Monti, M. M., Lutkenhoff, E. S., Rubinov, M., Boveroux, P., Vanhaudenhuyse, A., Gosseries, O., Bruno, M. A., Noirhomme, Q., Boly, M., & Laureys, S. (2013). Dynamic change of global and local information processing in propofol-induced loss and recovery of consciousness. *Plos Computational Biology*, *9*(10), e1003271. https://doi.org/10.1371/journal.pcbi.1003271

Monti, M. M., Vanhaudenhuyse, A., Coleman, M. R., Boly, M., Pickard, J. D., Tshibanda, L., Owen, A. M., & Laureys, S. (2010). Willful Modulation of Brain Activity in

Disorders of Consciousness. *New England Journal of Medicine*, *362*(7), 579-589. https://doi.org/10.1056/NEJMoa0905370

Moser, J., Schleger, F., Weiss, M., Sippel, K., Semeia, L., & Preissl, H. (2021). Magnetoencephalographic signatures of conscious processing before birth. *Developmental cognitive neuroscience*, *49*, 100964. https://doi.org/10.1016/j.dcn.2021.100964

Muldoon, S. F., Bridgeford, E. W., & Bassett, D. S. (2016). Small-world propensity and weighted brain networks. *Scientific reports*, *6*(1), 22057. https://doi.org/10.1038/srep22057

Naccache, L., King, J. R., Sitt, J., Engemann, D., El Karoui, I., Rohaut, B., Faugeras, F., Chennu, S., Strauss, M., Bekinschtein, T., & Dehaene, S. (2015). Neural detection of complex sound sequences or of statistical regularities in the absence of consciousness? *Brain*, *138*(Pt 12), e395. https://doi.org/10.1093/brain/awv190

Naci, L., Cusack, R., Anello, M., & Owen, A. M. (2014). A common neural code for similar conscious experiences in different individuals. *Proceedings of the National Academy of Sciences of the United States of America*, *111*(39), 14277-14282. https://doi.org/10.1073/pnas.1407007111

Naci, L., Haugg, A., MacDonald, A., Anello, M., Houldin, E., Naqshbandi, S., Gonzalez-Lara, L. E., Arango, M., Harle, C., Cusack, R., & Owen, A. M. (2018). Functional diversity of brain networks supports consciousness and verbal intelligence. *Scientific reports*, *8*. https://doi.org/10.1038/s41598-018-31525-z

Naci, L., & Owen, A. M. (2022). Uncovering Consciousness and Revealing the Preservation of Mental Life in Unresponsive Brain-Injured Patients. *Seminars in Neurology*, *42*(3), 299-308. https://doi.org/10.1055/a-1892-1715

Naci, L., Sinai, L., & Owen, A. M. (2017). Detecting and interpreting conscious experiences in behaviorally non-responsive patients. *Neuroimage*, *145*(Pt B), 304-313. https://doi.org/10.1016/j.neuroimage.2015.11.059

Nagel, T. (1974). What is it Like to Be a Bat. *The Philosophical Review*, 435-450.

Nagel, T. (1980). What is it like to be a bat? In *The Language and Thought Series* (pp. 159-168). Harvard University Press.

Nakamura, Y., Uematsu, A., Okanoya, K., & Koike, S. (2022). The effect of acquisition duration on cerebral blood flow-based resting-state functional connectivity. *Human Brain Mapping*, *43*(10), 3184-3194. https://doi.org/10.1002/hbm.25843

Nelson, C. A. (2001). The development and neural bases of face recognition. *Infant and Child Development*, *10*(1-2), 3-18. https://doi.org/10.1002/icd.239

Nelson, T. O. (1996). Consciousness and metacognition. *American Psychologist*, *51*(2), 102-116. https://doi.org/10.1037/0003-066x.51.2.102

Nielsen, M., & Dissanayake, C. (2004). Pretend play, mirror self-recognition and imitation: a longitudinal investigation through the second year. *Infant Behavior & Development*, *27*(3), 342-365. https://doi.org/10.1016/j.infbeh.2003.12.006

Northoff, G., & Huang, Z. (2017). How do the brain's time and space mediate consciousness and its different dimensions? Temporo-spatial theory of consciousness (TTC). *Neuroscience & Biobehavioral Reviews*, *80*, 630-645.

Northoff, G., Tsuchiya, N., & Saigo, H. (2019). Mathematics and the Brain: A Category Theoretical Approach to Go Beyond the Neural Correlates of Consciousness. *Entropy*, *21*(12). https://doi.org/10.3390/e21121234

Nosarti, C., Reichenberg, A., Murray, R. M., Cnattingius, S., Lambe, M. P., Yin, L., MacCabe, J., Rifkin, L., & Hultman, C. M. (2012). Preterm Birth and Psychiatric

Disorders in Young Adult Life. *Archives of General Psychiatry*, *69*(6), 610-617. https://doi.org/10.1001/archgenpsychiatry.2011.1374

Nour, M. M., Evans, L., Nutt, D., & Carhart-Harris, R. L. (2016). Ego-Dissolution and Psychedelics: Validation of the Ego-Dissolution Inventory (EDI). *Front Hum Neurosci*, *10*, 269. https://doi.org/10.3389/fnhum.2016.00269

Ockleford, E. M., Vince, M. A., Layton, C., & Reader, M. R. (1988). Responses of neonates to parents' and others' voices. *Early Human Development*, *18*(1), 27-36. https://doi.org/10.1016/0378-3782(88)90040-0

Odegaard, B., Knight, R. T., & Lau, H. (2017). Should a Few Null Findings Falsify Prefrontal Theories of Conscious Perception? *Journal of Neuroscience*, *37*(40), 9593-9602. https://doi.org/10.1523/Jneurosci.3217-16.2017

Oizumi, M., Albantakis, L., & Tononi, G. (2014). From the Phenomenology to the Mechanisms of Consciousness: Integrated Information Theory 3.0. *Plos Computational Biology*, *10*(5). https://doi.org/10.1371/journal.pcbi.1003588

Omidvarnia, A., Fransson, P., Metsaranta, M., & Vanhatalo, S. (2014). Functional bimodality in the brain networks of preterm and term human newborns. *Cerebral Cortex*, *24*(10), 2657-2668. https://doi.org/10.1093/cercor/bht120

Onnela, J. P., Saramäki, J., Kertész, J., & Kaski, K. (2005). Intensity and coherence of motifs in weighted complex networks. *Physical Review E*, *71*(6). https://doi.org/10.1103/PhysRevE.71.065103

Owen, A. M., Coleman, M. R., Boly, M., Davis, M. H., Laureys, S., & Pickard, J. D. (2006). Detecting awareness in the vegetative state. *science*, *313*(5792), 1402-1402. https://doi.org/10.1126/science.1130197

Pandit, A. S., Expert, P., Lambiotte, R., Bonnelle, V., Leech, R., Turkheimer, F. E., & Sharp, D. J. (2013). Traumatic brain injury impairs small-world topology. *Neurology*, *80*(20), 1826-1833. https://doi.org/10.1212/WNL.0b013e3182929f38

Pandit, A. S., Robinson, E., Aljabar, P., Ball, G., Gousias, I. S., Wang, Z., Hajnal, J. V., Rueckert, D., Counsell, S. J., Montana, G., & Edwards, A. D. (2014). Whole-Brain Mapping of Structural Connectivity in Infants Reveals Altered Connection Strength Associated with Growth and Preterm Birth. *Cerebral Cortex*, *24*(9), 2324-2333. https://doi.org/10.1093/cercor/bht086

Papo, D., Zanin, M., Martinez, J. H., & Buldu, J. M. (2016). Beware of the Small-World Neuroscientist! *Frontiers in Human Neuroscience*, *10*, 96. https://doi.org/10.3389/fnhum.2016.00096

Parvizi, J., & Damasio, A. (2001). Consciousness and the brainstem. *Cognition*, *79*(1-2), 135-160. https://doi.org/10.1016/s0010-0277(00)00127-x

Pascalis, O., Fort, M., & Quinn, P. C. (2020). Development of face processing: are there critical or sensitive periods? *Current Opinion in Behavioral Sciences*, *36*, 7-12. https://doi.org/10.1016/j.cobeha.2020.05.005

Pedersen, M., Omidvarnia, A., Walz, J. M., Zalesky, A., & Jackson, G. D. (2017). Spontaneous brain network activity: Analysis of its temporal complexity. *Network neuroscience*, *1*(2), 100-115. https://doi.org/10.1162/NETN_a_00006

Pegg, J. E., Werker, J. F., & McLeod, P. J. (1992). Preference for infant-directed over adult-directed speech: Evidence from 7-week-old infants. *Infant behavior and development*, *15*(3), 325-345.

Perani, D., Saccuman, M. C., Scifo, P., Anwander, A., Spada, D., Baldoli, C., Poloniato, A., Lohmann, G., & Friederici, A. D. (2011). Neural language networks at birth (vol 108, pg 16056, 2011). *Proceedings of the National Academy of Sciences of the*

United States of America, *108*(45), 18566-18566. https://doi.org/10.1073/pnas.1116061108

Perner, J., Stummer, S., & Lang, B. (2023). Executive functions and theory of mind: Cognitive complexity or functional dependence? In *Developing theories of intention* (pp. 133-152). Psychology Press.

Petrides, M., & Pandya, D. N. (1984). Projections to the frontal cortex from the posterior parietal region in the rhesus monkey. *Journal of Comparative Neurology*, *228*(1), 105-116. https://doi.org/10.1002/cne.902280110

Plum, F. (1991). Coma and related global disturbances of the human conscious state. In *Normal and altered states of function* (pp. 359-425). Springer.

Plum, F., & Posner, J. B. (1982). *The diagnosis of stupor and coma* (Vol. 19). Oxford University Press, USA.

Poldrack, R. A., Baker, C. I., Durnez, J., Gorgolewski, K. J., Matthews, P. M., Munafo, M. R., Nichols, T. E., Poline, J. B., Vul, E., & Yarkoni, T. (2017). Scanning the horizon: towards transparent and reproducible neuroimaging research. *Nature Review Neuroscience*, *18*(2), 115-126. https://doi.org/10.1038/nrn.2016.167

Poppel, E., Held, R., & Frost, D. (1973). Residual visual function after brain wounds involving the central visual pathways in man. *Nature*, *243*(5405), 295-296. https://doi.org/10.1038/243295a0

Power, J. D., Barnes, K. A., Snyder, A. Z., Schlaggar, B. L., & Petersen, S. E. (2012). Spurious but systematic correlations in functional connectivity MRI networks arise from subject motion. *Neuroimage*, *59*(3), 2142-2154. https://doi.org/10.1016/j.neuroimage.2011.10.018

Power, J. D., Cohen, A. L., Nelson, S. M., Wig, G. S., Barnes, K. A., Church, J. A., Vogel, A. C., Laumann, T. O., Miezin, F. M., & Schlaggar, B. L. (2011). Functional

network organization of the human brain. *Neuron*, *72*(4), 665-678. https://doi.org/10.1016/j.neuron.2011.09.006

Power, J. D., Mitra, A., Laumann, T. O., Snyder, A. Z., Schlaggar, B. L., & Petersen, S. E. (2014). Methods to detect, characterize, and remove motion artifact in resting state fMRI. *Neuroimage*, *84*, 320-341. https://doi.org/10.1016/j.neuroimage.2013.08.048

Power, J. D., Plitt, M., Gotts, S. J., Kundu, P., Voon, V., Bandettini, P. A., & Martin, A. (2018). Ridding fMRI data of motion-related influences: Removal of signals with distinct spatial and physical bases in multiecho data. *Proceedings of the National Academy of Sciences of the United States of America*, *115*(9), E2105-E2114. https://doi.org/10.1073/pnas.1720985115

Preti, M. G., Bolton, T. A., & Van De Ville, D. (2017). The dynamic functional connectome: State-of-the-art and perspectives. *Neuroimage*, *160*, 41-54. https://doi.org/10.1016/j.neuroimage.2016.12.061

Pridmore, S., Turnier-Shea, Y., Rybak, M., & Pridmore, W. (2021). Transcranial Magnetic Stimulation (TMS) during pregnancy: A fetal risk factor. *Australasian Psychiatry*, *29*(2), 226-229. https://doi.org/10.1177/1039856221992636

Ptak, R. (2012). The frontoparietal attention network of the human brain: action, saliency, and a priority map of the environment. *Neuroscientist*, *18*(5), 502-515. https://doi.org/10.1177/1073858411409051

Qin, P. M., & Northoff, G. (2011). How is our self related to midline regions and the default-mode network? *Neuroimage*, *57*(3), 1221-1233. https://doi.org/10.1016/j.neuroimage.2011.05.028

Querleu, D., Lefebvre, C., Titran, M., Renard, X., Morillion, M., & Crepin, G. (1984). Reaction of the newborn infant less than 2 hours after birth to the maternal voice. *Journal de gynécologie, obstetrique et biologie de la reproduction*, *13*(2), 125-134.

Raichle, M. E. (2011). The restless brain. *Brain connectivity*, *1*(1), 3-12. https://doi.org/10.1089/brain.2011.0019

Rajasilta, O., Tuulari, J. J., Bjornsdotter, M., Scheinin, N. M., Lehtola, S. J., Saunavaara, J., Hakkinen, S., Merisaari, H., Parkkola, R., Lahdesmaki, T., Karlsson, L., & Karlsson, H. (2020). Resting-state networks of the neonate brain identified using independent component analysis. *Developmental Neurobiology*, *80*(3-4), 111-125. https://doi.org/10.1002/dneu.22742

Rakic, P. (1988). Specification of cerebral cortical areas. *science*, *241*(4862), 170-176. https://doi.org/10.1126/science.3291116

Rasmussen, E. (1992). Clustering algorithms. In R. B.-Y. William B. Frakes (Ed.), *Information retrieval: data structures and algorithms* (pp. 419–442). Prentice-Hall, Inc.

Ratnarajah, N., Rifkin-Graboi, A., Fortier, M. V., Chong, Y. S., Kwek, K., Saw, S. M., Godfrey, K. M., Gluckman, P. D., Meaney, M. J., & Qiu, A. (2013). Structural connectivity asymmetry in the neonatal brain. *Neuroimage*, *75*, 187-194. https://doi.org/10.1016/j.neuroimage.2013.02.052

Reid, V. M., Dunn, K., Young, R. J., Amu, J., Donovan, T., & Reissland, N. (2018). The Human Fetus Preferentially Engages with Face-like Visual Stimuli (vol 27, pg 1825, 2017). *Current Biology*, *28*(5), 824-824. https://doi.org/10.1016/j.cub.2018.02.025

Richards, J. E., & Casey, B. J. (2014). Development of sustained visual attention in the human infant. In *Attention and information processing in infants and adults* (pp. 30-60). Psychology Press.

Richman, J. S., & Moorman, J. R. (2000). Physiological time-series analysis using approximate entropy and sample entropy. *American journal of physiology-heart*

and circulatory physiology, *278*(6), H2039-2049. https://doi.org/10.1152/ajpheart.2000.278.6.H2039

Rigato, S., Menon, E., Johnson, M. H., Faraguna, D., & Farroni, T. (2011). Direct Gaze May Modulate Face Recognition in Newborns. *Infant and Child Development*, *20*(1), 20-34. https://doi.org/10.1002/icd.684

Ripley, B. D. (2007). *Pattern recognition and neural networks*. Cambridge university press.

Rochat, P. (2003). Five levels of self-awareness as they unfold early in life. *Consciousness and Cognition*, *12*(4), 717-731. https://doi.org/10.1016/S1053-8100(03)00081-3

Rochat, P., & Hespos, S. J. (1997). Differential rooting response by neonates: Evidence for an early sense of self. *Early Development & Parenting*, *6*(3-4), 105-112. https://doi.org/10.1002/(SICI)1099-0917(199709/12)6:3/4<105::AID-EDP150>3.0.CO;2-U

Romero, R., Dey, S. K., & Fisher, S. J. (2014). Preterm labor: one syndrome, many causes. *science*, *345*(6198), 760-765. https://doi.org/10.1126/science.1251816

Rose, J., Vassar, R., Cahill-Rowley, K., Guzman, X. S., Stevenson, D. K., & Barnea-Goraly, N. (2014). Brain microstructural development at near-term age in very-low-birth-weight preterm infants: an atlas-based diffusion imaging study. *Neuroimage*, *86*, 244-256. https://doi.org/10.1016/j.neuroimage.2013.09.053

Rosenthal, D. M. (2005). *Consciousness and mind*. Oxford University Press.

Rossi, S., Antal, A., Bestmann, S., Bikson, M., Brewer, C., Brockmöller, J., Carpenter, L. L., Cincotta, M., Chen, R., & Daskalakis, J. D. (2021). Safety and recommendations for TMS use in healthy subjects and patient populations, with updates on training, ethical and regulatory issues: Expert Guidelines. *Clinical Neurophysiology*, *132*(1), 269-306. https://doi.org/10.1016/j.clinph.2020.10.003

Rubinov, M., & Sporns, O. (2010). Complex network measures of brain connectivity: uses and interpretations. *Neuroimage*, *52*(3), 1059-1069. https://doi.org/10.1016/j.neuroimage.2009.10.003

Ruffman, T., Then, R., Cheng, C., & Imuta, K. (2019). Lifespan differences in emotional contagion while watching emotion-eliciting videos. *PLoS one*, *14*(1). https://doi.org/10.1371/journal.pone.0209253

Rushe, T. M. (2010). Language function after preterm birth. In *Neurodevelopmental outcomes of preterm birth* (pp. 176-184).

Saigal, S., & Doyle, L. W. (2008). An overview of mortality and sequelae of preterm birth from infancy to adulthood. *Lancet*, *371*(9608), 261-269. https://doi.org/10.1016/S0140-6736(08)60136-1

Salvador, R., Martínez, A., Pomarol-Clotet, E., Gomar, J., Vila, F., Sarró, S., Capdevila, A., & Bullmore, E. T. (2008). A simple view of the brain through a frequency-specific functional connectivity measure. *Neuroimage*, *39*(1), 279-289. https://doi.org/10.1016/j.neuroimage.2007.08.018

Samann, P. G., Wehrle, R., Hoehn, D., Spoormaker, V. I., Peters, H., Tully, C., Holsboer, F., & Czisch, M. (2011). Development of the brain's default mode network from wakefulness to slow wave sleep. *Cerebral Cortex*, *21*(9), 2082-2093. https://doi.org/10.1093/cercor/bhq295

Sarasso, S., Boly, M., Napolitani, M., Gosseries, O., Charland-Verville, V., Casarotto, S., Rosanova, M., Casali, A. G., Brichant, J. F., Boveroux, P., Rex, S., Tononi, G., Laureys, S., & Massimini, M. (2015). Consciousness and Complexity during Unresponsiveness Induced by Propofol, Xenon, and Ketamine. *Current Biology*, *25*(23), 3099-3105. https://doi.org/10.1016/j.cub.2015.10.014

Schacter, D. L. (1992). Priming and Multiple Memory-Systems - Perceptual Mechanisms of Implicit Memory. *Journal of Cognitive Neuroscience*, *4*(3), 244-256. https://doi.org/10.1162/jocn.1992.4.3.244

Schartner, M., Seth, A., Noirhomme, Q., Boly, M., Bruno, M. A., Laureys, S., & Barrett, A. (2015). Complexity of Multi-Dimensional Spontaneous EEG Decreases during Propofol Induced General Anaesthesia. *PLoS one*, *10*(8), e0133532. https://doi.org/10.1371/journal.pone.0133532

Schartner, M. M., Carhart-Harris, R. L., Barrett, A. B., Seth, A. K., & Muthukumaraswamy, S. D. (2017). Increased spontaneous MEG signal diversity for psychoactive doses of ketamine, LSD and psilocybin. *Scientific reports*, *7*, 46421. https://doi.org/10.1038/srep46421

Scheinost, D., Kwon, S. H., Shen, X. L., Lacadie, C., Schneider, K. C., Dai, F., Ment, L. R., & Constable, R. T. (2016). Preterm birth alters neonatal, functional rich club organization. *Brain Structure & Function*, *221*(6), 3211-3222. https://doi.org/10.1007/s00429-015-1096-6

Scher, M. S. (2008). Ontogeny of EEG-sleep from neonatal through infancy periods. *Sleep Medicine*, *9*(6), 615-636. https://doi.org/10.1016/j.sleep.2007.08.014

Scher, M. S., Waisanen, H., Loparo, K., & Johnson, M. W. (2005). Prediction of neonatal state and maturational change using dimensional analysis. *Journal of Clinical Neurophysiology*, *22*(3), 159-165. https://doi.org/10.1097/01.WNP.0000161258.92634.D6

Schmahmann, J. D., Schmahmann, J., & Pandya, D. (2009). *Fiber pathways of the brain*. OUP USA.

Schneider, F., Bermpohl, F., Heinzel, A., Rotte, M., Walter, M., Tempelmann, C., Wiebking, C., Dobrowolny, H., Heinze, H., & Northoff, G. (2008). The resting

brain and our self: self-relatedness modulates resting state neural activity in cortical midline structures. *Neuroscience*, *157*(1), 120-131. https://doi.org/10.1016/j.neuroscience.2008.08.014

Schroter, M. S., Spoormaker, V. I., Schorer, A., Wohlschlager, A., Czisch, M., Kochs, E. F., Zimmer, C., Hemmer, B., Schneider, G., Jordan, D., & Ilg, R. (2012). Spatiotemporal reconfiguration of large-scale brain functional networks during propofol-induced loss of consciousness. *Journal of Neuroscience*, *32*(37), 12832-12840. https://doi.org/10.1523/JNEUROSCI.6046-11.2012

Schuh, A., Makropoulos, A., Robinson, E. C., Cordero-Grande, L., Hughes, E., Hutter, J., Price, A. N., Murgasova, M., Teixeira, R. P. A., & Tusor, N. (2018). Unbiased construction of a temporally consistent morphological atlas of neonatal brain development. *BioRxiv*, 251512. https://doi.org/10.1101/251512

Seeley, W. W., Menon, V., Schatzberg, A. F., Keller, J., Glover, G. H., Kenna, H., Reiss, A. L., & Greicius, M. D. (2007). Dissociable intrinsic connectivity networks for salience processing and executive control. *Journal of Neuroscience*, *27*(9), 2349-2356. https://doi.org/10.1523/Jneurosci.5587-06.2007

Seeley, W. W., & Sturm, V. E. (2007). Self-representation and the frontal lobes. *The human frontal lobes: Functions and disorders*, 317-334.

Serag, A., Aljabar, P., Ball, G., Counsel, S. J., Boardman, J. P., Rutherford, M. A., Edwards, A. D., Hajnal, J. V., & Rueckert, D. (2012). Construction of a consistent high-definition spatio-temporal atlas of the developing brain using adaptive kernel regression. *Neuroimage*, *59*(3), 2255-2265. https://doi.org/10.1016/j.neuroimage.2011.09.062

Seth, A. (2009). Explanatory Correlates of Consciousness: Theoretical and Computational Challenges. *Cognitive Computation*, *1*(1), 50-63. https://doi.org/10.1007/s12559-009-9007-x

Seth, A. K., Izhikevich, E., Reeke, G. N., & Edelman, G. M. (2006). Theories and measures of consciousness: an extended framework. *Proc Natl Acad Sci U S A*, *103*(28), 10799-10804. https://doi.org/10.1073/pnas.0604347103

Shallice, T. (1988). *From neuropsychology to mental structure*. Cambridge University Press.

Shen, X., Tokoglu, F., Papademetris, X., & Constable, R. T. (2013). Groupwise whole-brain parcellation from resting-state fMRI data for network node identification. *Neuroimage*, *82*, 403-415. https://doi.org/10.1016/j.neuroimage.2013.05.081

Sherman, L. E., Rudie, J. D., Pfeifer, J. H., Masten, C. L., McNealy, K., & Dapretto, M. (2014). Development of the default mode and central executive networks across early adolescence: a longitudinal study. *Developmental cognitive neuroscience*, *10*, 148-159. https://doi.org/10.1016/j.dcn.2014.08.002

Shi, F., Salzwedel, A. P., Lin, W. L., Gilmore, J. H., & Gao, W. (2018). Functional Brain Parcellations of the Infant Brain and the Associated Developmental Trends. *Cerebral Cortex*, *28*(4), 1358-1368. https://doi.org/10.1093/cercor/bhx062

Shi, F., Yap, P.-T., Gao, W., Lin, W., Gilmore, J. H., & Shen, D. (2012). Altered structural connectivity in neonates at genetic risk for schizophrenia: a combined study using morphological and white matter networks. *Neuroimage*, *62*(3), 1622-1633. https://doi.org/10.1016/j.neuroimage.2012.05.026

Shi, F., Yap, P. T., Wu, G., Jia, H., Gilmore, J. H., Lin, W., & Shen, D. (2011). Infant brain atlases from neonates to 1- and 2-year-olds. *PLoS one*, *6*(4), e18746. https://doi.org/10.1371/journal.pone.0018746

Shimamura, A. P. (2000). Toward a cognitive neuroscience of metacognition. *Consciousness and Cognition*, *9*(2), 313-323. https://doi.org/10.1006/ccog.2000.0450

Shuffrey, L. C., Pini, N., Potter, M., Springer, P., Lucchini, M., Rayport, Y., Sania, A., Firestein, M., Brink, L., Isler, J. R., Odendaal, H., & Fifer, W. P. (2022). Aperiodic electrophysiological activity in preterm infants is linked to subsequent autism risk. *Developmental Psychobiology*, *64*(4). https://doi.org/10.1002/dev.22271

Simner, M. L. (1971). Newborn's response to the cry of another infant. *Developmental psychology*, *5*(1), 136.

Sitt, J. D., King, J. R., El Karoui, I., Rohaut, B., Faugeras, F., Gramfort, A., Cohen, L., Sigman, M., Dehaene, S., & Naccache, L. (2014). Large scale screening of neural signatures of consciousness in patients in a vegetative or minimally conscious state. *Brain*, *137*(Pt 8), 2258-2270. https://doi.org/10.1093/brain/awu141

Smith, V., Mitchelll, D. J., & Duncan, J. (2018). Role of the Default Mode Network in Cognitive Transitions. *Cerebral Cortex*, *28*(10), 3685-3696. https://doi.org/10.1093/cercor/bhy167

Smyser, C. D., Inder, T. E., Shimony, J. S., Hill, J. E., Degnan, A. J., Snyder, A. Z., & Neil, J. J. (2010). Longitudinal analysis of neural network development in preterm infants. *Cerebral Cortex*, *20*(12), 2852-2862. https://doi.org/10.1093/cercor/bhq035

Smyser, C. D., Snyder, A. Z., Shimony, J. S., Mitra, A., Inder, T. E., & Neil, J. J. (2016). Resting-State Network Complexity and Magnitude Are Reduced in Prematurely Born Infants. *Cerebral Cortex*, *26*(1), 322-333. https://doi.org/10.1093/cercor/bhu251

Soman, S. M., Vijayakumar, N., Thomson, P., Ball, G., Hyde, C., & Silk, T. J. (2023). Cortical structural and functional coupling during development and implications for

attention deficit hyperactivity disorder. *Transl Psychiatry*, *13*(1), 252. https://doi.org/10.1038/s41398-023-02546-8

Southgate, V., Chevallier, C., & Csibra, G. (2010). Seventeen-month-olds appeal to false beliefs to interpret others' referential communication. *Developmental Science*, *13*(6), 907-912. https://doi.org/10.1111/j.1467-7687.2009.00946.x

Spoormaker, V. I., Schröter, M. S., Gleiser, P. M., Andrade, K. C., Dresler, M., Wehrle, R., Sämann, P. G., & Czisch, M. (2010). Development of a large-scale functional brain network during human non-rapid eye movement sleep. *Journal of Neuroscience*, *30*(34), 11379-11387. https://doi.org/10.1523/JNEUROSCI.2015-10.2010

Sripada, C., Rutherford, S., Angstadt, M., Thompson, W. K., Luciana, M., Weigard, A., Hyde, L. H., & Heitzeg, M. (2020). Prediction of neurocognition in youth from resting state fMRI. *Mol Psychiatry*, *25*(12), 3413-3421. https://doi.org/10.1038/s41380-019-0481-6

Stevner, A. B. A., Vidaurre, D., Cabral, J., Rapuano, K., Nielsen, S. F. V., Tagliazucchi, E., Laufs, H., Vuust, P., Deco, G., Woolrich, M. W., Van Someren, E., & Kringelbach, M. L. (2019). Discovery of key whole-brain transitions and dynamics during human wakefulness and non-REM sleep. *Nature Communications*, *10*(1), 1035. https://doi.org/10.1038/s41467-019-08934-3

Stoecklein, S., Hilgendorff, A., Li, M., Forster, K., Flemmer, A. W., Galie, F., Wunderlich, S., Wang, D., Stein, S., Ehrhardt, H., Dietrich, O., Zou, Q., Zhou, S., Ertl-Wagner, B., & Liu, H. (2020). Variable functional connectivity architecture of the preterm human brain: Impact of developmental cortical expansion and maturation. *Proceedings of the National Academy of Sciences of the United States of America*, *117*(2), 1201-1206. https://doi.org/10.1073/pnas.1907892117

Sturm, V. E., Hua, A. Y., & Rosen, H. J. (2018). Self-awareness and frontal lobe networks. *The human frontal lobes: Functions and disorders*.

Sylvester, C. M., Kaplan, S., Myers, M. J., Gordon, E. M., Schwarzlose, R. F., Alexopoulos, D., Nielsen, A. N., Kenley, J. K., Meyer, D., Yu, Q., Graham, A. M., Fair, D. A., Warner, B. B., Barch, D. M., Rogers, C. E., Luby, J. L., Petersen, S. E., & Smyser, C. D. (2023). Network-specific selectivity of functional connections in the neonatal brain. *Cerebral Cortex*, *33*(5), 2200-2214. https://doi.org/10.1093/cercor/bhac202

Tagliazucchi, E., & Laufs, H. (2014). Decoding Wakefulness Levels from Typical fMRI Resting-State Data Reveals Reliable Drifts between Wakefulness and Sleep. *Neuron*, *82*(3), 695-708. https://doi.org/10.1016/j.neuron.2014.03.020

Tagliazucchi, E., Von Wegner, F., Morzelewski, A., Brodbeck, V., Borisov, S., Jahnke, K., & Laufs, H. (2013). Large-scale brain functional modularity is reflected in slow electroencephalographic rhythms across the human non-rapid eye movement sleep cycle. *Neuroimage*, *70*, 327-339. https://doi.org/10.1016/j.neuroimage.2012.12.073

Tagliazucchi, E., von Wegner, F., Morzelewski, A., Brodbeck, V., Jahnke, K., & Laufs, H. (2013). Breakdown of long-range temporal dependence in default mode and attention networks during deep sleep. *Proceedings of the National Academy of Sciences of the United States of America*, *110*(38), 15419-15424. https://doi.org/10.1073/pnas.1312848110

Takagi, K. (2018). Information-Based Principle Induces Small-World Topology and Self-Organized Criticality in a Large Scale Brain Network. *Front Comput Neurosci*, *12*, 65. https://doi.org/10.3389/fncom.2018.00065

Takagi, K. (2020). Principles of Mutual Information Maximization and Energy Minimization Affect the Activation Patterns of Large Scale Networks in the Brain.

Frontiers in Computational Neuroscience, *13*. https://doi.org/10.3389/fncom.2019.00086

Tan, T. L., & Cheong, S. A. (2017). Statistical complexity is maximized in a small-world brain. *PLoS one*, *12*(8). https://doi.org/10.1371/journal.pone.0183918

Telesford, Q. K., Joyce, K. E., Hayasaka, S., Burdette, J. H., & Laurienti, P. J. (2011). The ubiquity of small-world networks. *Brain connectivity*, *1*(5), 367-375. https://doi.org/10.1089/brain.2011.0038

Telford, E. J., Cox, S. R., Fletcher-Watson, S., Anblagan, D., Sparrow, S., Pataky, R., Quigley, A., Semple, S. I., Bastin, M. E., & Boardman, J. P. (2017). A latent measure explains substantial variance in white matter microstructure across the newborn human brain. *Brain Structure & Function*, *222*(9), 4023-4033. https://doi.org/10.1007/s00429-017-1455-6

Termenon, M., Jaillard, A., Delon-Martin, C., & Achard, S. (2016). Reliability of graph analysis of resting state fMRI using test-retest dataset from the Human Connectome Project. *Neuroimage*, *142*, 172-187. https://doi.org/10.1016/j.neuroimage.2016.05.062

Thomason, M. E., Brown, J. A., Dassanayake, M. T., Shastri, R., Marusak, H. A., Hernandez-Andrade, E., Yeo, L., Mody, S., Berman, S., Hassan, S. S., & Romero, R. (2014). Intrinsic functional brain architecture derived from graph theoretical analysis in the human fetus. *PLoS one*, *9*(5), e94423. https://doi.org/10.1371/journal.pone.0094423

Thomason, M. E., Grove, L. E., Lozon, T. A., Vila, A. M., Ye, Y. Q., Nye, M. J., Manning, J. H., Pappas, A., Hernandez-Andrade, E., Yeo, L. M., Mody, S., Berman, S., Hassan, S. S., & Romero, R. (2015). Age-related increases in long-range connectivity in fetal functional neural connectivity networks in utero.

Developmental cognitive neuroscience, *11*, 96-104. https://doi.org/10.1016/j.dcn.2014.09.001

Toker, D., Pappas, I., Lendner, J. D., Frohlich, J., Mateos, D. M., Muthukumaraswamy, S., Carhart-Harris, R., Paff, M., Vespa, P. M., & Monti, M. M. (2022). Consciousness is supported by near-critical slow cortical electrodynamics. *Proceedings of the National Academy of Sciences*, *119*(7), e2024455119. https://doi.org/doi.org/10.1073/pnas.2024455119

Tononi, G. (2004). An information integration theory of consciousness. *BMC Neurosci*, *5*, 42. https://doi.org/10.1186/1471-2202-5-42

Tononi, G. (2008). Consciousness as integrated information: a provisional manifesto. *The Biological Bulletin*, *215*(3), 216-242.

Tononi, G., Boly, M., Massimini, M., & Koch, C. (2016). Integrated information theory: from consciousness to its physical substrate. *Nature Reviews Neuroscience*, *17*(7), 450-461. https://doi.org/10.1038/nrn.2016.44

Tononi, G., & Edelman, G. M. (1998). Consciousness and complexity. *science*, *282*(5395), 1846-1851. https://doi.org/10.1126/science.282.5395.1846

Tononi, G., & Koch, C. (2008). The neural correlates of consciousness: an update. *Ann N Y Acad Sci*, *1124*, 239-261. https://doi.org/10.1196/annals.1440.004

Tononi, G., & Sporns, O. (2003). Measuring information integration. *BMC neuroscience*, *4*, 1-20. https://doi.org/10.1186/1471-2202-4-31

Triantafyllou, C., Hoge, R. D., Krueger, G., Wiggins, C. J., Potthast, A., Wiggins, G. C., & Wald, L. L. (2005). Comparison of physiological noise at 1.5 T, 3 T and 7 T and optimization of fMRI acquisition parameters. *Neuroimage*, *26*(1), 243-250. https://doi.org/10.1016/j.neuroimage.2005.01.007

Truzzi, A., & Cusack, R. (2023). The development of intrinsic timescales: A comparison between the neonate and adult brain. *Neuroimage*, *275*, 120155. https://doi.org/10.1016/j.neuroimage.2023.120155

Turk, E., van den Heuvel, M. I., Benders, M. J., de Heus, R., Franx, A., Manning, J. H., Hect, J. L., Hernandez-Andrade, E., Hassan, S. S., Romero, R., Kahn, R. S., Thomason, M. E., & van den Heuvel, M. P. (2019). Functional Connectome of the Fetal Brain. *Journal of Neuroscience*, *39*(49), 9716-9724. https://doi.org/10.1523/Jneurosci.2891-18.2019

Uda, S., Matsui, M., Tanaka, C., Uematsu, A., Miura, K., Kawana, I., & Noguchi, K. (2015). Normal development of human brain white matter from infancy to early adulthood: a diffusion tensor imaging study. *Developmental Neuroscience*, *37*(2), 182-194. https://doi.org/10.1159/000373885

van den Heuvel, M., Mandl, R., Luigjes, J., & Hulshoff Pol, H. (2008). Microstructural organization of the cingulum tract and the level of default mode functional connectivity. *Journal of Neuroscience*, *28*(43), 10844-10851. https://doi.org/10.1523/JNEUROSCI.2964-08.2008

van den Heuvel, M. P., de Lange, S. C., Zalesky, A., Seguin, C., Yeo, B. T., & Schmidt, R. (2017). Proportional thresholding in resting-state fMRI functional connectivity networks and consequences for patient-control connectome studies: Issues and recommendations. *Neuroimage*, *152*, 437-449. https://doi.org/10.1016/j.neuroimage.2017.02.005

van den Heuvel, M. P., Kersbergen, K. J., de Reus, M. A., Keunen, K., Kahn, R. S., Groenendaal, F., de Vries, L. S., & Benders, M. J. N. L. (2015). The Neonatal Connectome During Preterm Brain Development. *Cerebral Cortex*, *25*(9), 3000-3013. https://doi.org/10.1093/cercor/bhu095

Van Essen, D. C., Smith, S. M., Barch, D. M., Behrens, T. E. J., Yacoub, E., Ugurbil, K., & Consortium, W.-M. H. (2013). The WU-Minn Human Connectome Project: An overview. *Neuroimage*, *80*, 62-79. https://doi.org/10.1016/j.neuroimage.2013.05.041

Vanderwal, T., Kelly, C., Eilbott, J., Mayes, L. C., & Castellanos, F. X. (2015). Inscapes: A movie paradigm to improve compliance in functional magnetic resonance imaging. *Neuroimage*, *122*, 222-232. https://doi.org/10.1016/j.neuroimage.2015.07.069

Vandormael, C., Schoenhals, L., Hüppi, P. S., Filippa, M., & Tolsa, C. B. (2019). Language in Preterm Born Children: Atypical Development and Effects of Early Interventions on Neuroplasticity. *Neural Plasticity*, *2019*. https://doi.org/10.1155/2019/6873270

Vanhatalo, S., & Kaila, K. (2006). Development of neonatal EEG activity: From phenomenology to physiology. *Seminars in Fetal & Neonatal Medicine*, *11*(6), 471-478. https://doi.org/10.1016/j.siny.2006.07.008

Vanhaudenhuyse, A., Demertzi, A., Schabus, M., Noirhomme, Q., Bredart, S., Boly, M., Phillips, C., Soddu, A., Luxen, A., Moonen, G., & Laureys, S. (2011). Two distinct neuronal networks mediate the awareness of environment and of self. *Journal of Cognitive Neuroscience*, *23*(3), 570-578. https://doi.org/10.1162/jocn.2010.21488

Varley, T. F., Carhart-Harris, R., Roseman, L., Menon, D. K., & Stamatakis, E. A. (2020). Serotonergic psychedelics LSD & psilocybin increase the fractal dimension of cortical brain activity in spatial and temporal domains. *Neuroimage*, *220*, 117049. https://doi.org/10.1016/j.neuroimage.2020.117049

Varley, T. F., Luppi, A. I., Pappas, I., Naci, L., Adapa, R., Owen, A. M., Menon, D. K., & Stamatakis, E. A. (2020). Consciousness & Brain Functional Complexity in

Propofol Anaesthesia. *Sci Rep*, *10*(1), 1018. https://doi.org/10.1038/s41598-020-57695-3

Vatansever, D., Manktelow, A., Sahakian, B. J., Menon, D. K., & Stamatakis, E. A. (2018). Default Mode Network Engagement Beyond Self-Referential Internal Mentation. *Brain connectivity*, *8*(4), 245-253. https://doi.org/10.1089/brain.2017.0489

Vogelsang, L., Gilad-Gutnick, S., Ehrenberg, E., Yonas, A., Diamond, S., Held, R., & Sinha, P. (2018). Potential downside of high initial visual acuity. *Proc Natl Acad Sci U S A*, *115*(44), 11333-11338. https://doi.org/10.1073/pnas.1800901115

Wang, J., Ren, Y., Hu, X., Nguyen, V. T., Guo, L., Han, J., & Guo, C. C. (2017). Test-retest reliability of functional connectivity networks during naturalistic fMRI paradigms. *Human Brain Mapping*, *38*(4), 2226-2241. https://doi.org/10.1002/hbm.23517

Watts, D. J., & Strogatz, S. H. (1998). Collective dynamics of 'small-world' networks. *Nature*, *393*(6684), 440-442. https://doi.org/10.1038/30918

Waxman, J. A., Pillai Riddell, R. R., Tablon, P., Schmidt, L. A., & Pinhasov, A. (2016). Development of Cardiovascular Indices of Acute Pain Responding in Infants: A Systematic Review. *Pain Research and Management*, *2016*, 8458696. https://doi.org/10.1155/2016/8458696

Weinstein, M., Ben-Sira, L., Moran, A., Berger, I., Marom, R., Geva, R., Gross-Tsur, V., Leitner, Y., & Bashat, D. B. (2016). The motor and visual networks in preterm infants: An fMRI and DTI study. *Brain Research*, *1642*, 603-611. https://doi.org/10.1016/j.brainres.2016.04.052

Weiskopf, N., Hutton, C., Josephs, O., & Deichmann, R. (2006). Optimal EPI parameters for reduction of susceptibility-induced BOLD sensitivity losses: A whole-brain

analysis at 3 T and 1.5 T. *Neuroimage*, *33*(2), 493-504. https://doi.org/10.1016/j.neuroimage.2006.07.029

Weiskrantz, L., Warrington, E. K., Sanders, M. D., & Marshall, J. (1974). Visual capacity in the hemianopic field following a restricted occipital ablation. *Brain*, *97*(4), 709-728. https://doi.org/10.1093/brain/97.1.709

Wen, X., Zhang, H., Li, G., Liu, M., Yin, W., Lin, W., Zhang, J., & Shen, D. (2019). First-year development of modules and hubs in infant brain functional networks. *Neuroimage*, *185*, 222-235. https://doi.org/10.1016/j.neuroimage.2018.10.019

Werker, J. F., Gilbert, J. H., Humphrey, K., & Tees, R. C. (1981). Developmental aspects of cross-language speech perception. *Child development*, *52*(1), 349-355. https://doi.org/10.2307/1129249

Wicker, B., Ruby, P., Royet, J. P., & Fonlupt, P. (2003). A relation between rest and the self in the brain? *Brain Research Reviews*, *43*(2), 224-230. https://doi.org/10.1016/j.brainresrev.2003.08.003

Wielek, T., Del Giudice, R., Lang, A., Wislowska, M., Ott, P., & Schabus, M. (2019). On the development of sleep states in the first weeks of life. *PLoS one*, *14*(10), e0224521. https://doi.org/10.1371/journal.pone.0224521

Wild, C. J., Linke, A. C., Zubiaurre-Elorza, L., Herzmann, C., Duffy, H., Han, V. K., Lee, D. S. C., & Cusack, R. (2017). Adult-like processing of naturalistic sounds in auditory cortex by 3-and 9-month old infants. *Neuroimage*, *157*, 623-634. https://doi.org/10.1016/j.neuroimage.2017.06.038

Wimmer, H., & Perner, J. (1983). Beliefs about beliefs: Representation and constraining function of wrong beliefs in young children's understanding of deception. *Cognition*, *13*(1), 103-128. https://doi.org/10.1016/0010-0277(83)90004-5

Woodward, A. L. (1998). Infants selectively encode the goal object of an actor's reach. *Cognition*, *69*(1), 1-34. https://doi.org/10.1016/S0010-0277(98)00058-4

Woolgar, A., Parr, A., Cusack, R., Thompson, R., Nimmo-Smith, I., Torralva, T., Roca, M., Antoun, N., Manes, F., & Duncan, J. (2010). Fluid intelligence loss linked to restricted regions of damage within frontal and parietal cortex. *Proceedings of the National Academy of Sciences of the United States of America*, *107*(33), 14899-14902. https://doi.org/10.1073/pnas.1007928107

Wylie, K. P., Rojas, D. C., Ross, R. G., Hunter, S. K., Maharajh, K., Cornier, M.-A., & Tregellas, J. R. (2014). Reduced brain resting-state network specificity in infants compared with adults. *Neuropsychiatric disease and treatment*, 1349-1359. https://doi.org/10.2147/NDT.S63773

Yates, T. S., Ellis, C. T., & Turk-Browne, N. B. (2023). Functional networks in the infant brain during sleep and wake states. *Cerebral Cortex*, *33*(21), 10820-10835. https://doi.org/10.1093/cercor/bhad327

Yates, T. S., Skalaban, L. J., Ellis, C. T., Bracher, A. J., Baldassano, C., & Turk-Browne, N. B. (2022). Neural event segmentation of continuous experience in human infants. *Proceedings of the National Academy of Sciences of the United States of America*, *119*(43), e2200257119. https://doi.org/10.1073/pnas.2200257119

Yeo, B. T., Tandi, J., & Chee, M. W. (2015). Functional connectivity during rested wakefulness predicts vulnerability to sleep deprivation. *Neuroimage*, *111*, 147-158. https://doi.org/10.1016/j.neuroimage.2015.02.018

Zhang, D., Ding, H., Liu, Y., Zhou, C., Ding, H., & Ye, D. (2009). Neurodevelopment in newborns: a sample entropy analysis of electroencephalogram. *Physiological Measurement*, *30*(5), 491-504. https://doi.org/10.1088/0967-3334/30/5/006

Zhang, H., Shen, D. G., & Lin, W. L. (2019). Resting-state functional MRI studies on infant brains: A decade of gap-filling efforts. *Neuroimage*, *185*, 664-684. https://doi.org/10.1016/j.neuroimage.2018.07.004

Zhang, X., Liu, J., Yang, Y., Zhao, S., Guo, L., Han, J., & Hu, X. (2022). Test-retest reliability of dynamic functional connectivity in naturalistic paradigm functional magnetic resonance imaging. *Human Brain Mapping*, *43*(4), 1463-1476. https://doi.org/10.1002/hbm.25736

Zhou, X., Vyas, S., Ning, J., & Moulson, M. C. (2022). Naturalistic Face Learning in Infants and Adults. *Psychological Science*, *33*(1), 135-151. https://doi.org/10.1177/09567976211030630

Zuo, X. N., Di Martino, A., Kelly, C., Shehzad, Z. E., Gee, D. G., Klein, D. F., Castellanos, F. X., Biswal, B. B., & Milham, M. P. (2010). The oscillating brain: Complex and reliable. *Neuroimage*, *49*(2), 1432-1445. https://doi.org/10.1016/j.neuroimage.2009.09.037